厚生労働科学研究費補助金
難治性疾患等克服研究事業
(難治性疾患克服研究事業)

致死性骨異形成症の診断と予後に関する研究

平成２４年度　総括・分担研究報告書

研究代表者　澤井英明

平成２５（２０１３）年３月

厚生労働科学研究費補助金研究報告書目次

Ⅰ．総括研究報告

厚生労働科学研究費補助金(難治性疾患克服研究事業)
総括研究報告書

致死性骨異形成症の診断と予後に関する研究

研究代表者　澤井英明　兵庫医科大学産科婦人科准教授

研究要旨　致死性骨異形成症（疾患区分（１７）奇形症候群）は稀な先天性骨系統疾患で、2 人／10 万分娩程度とされるが、正確な統計はなく、日本の症例数の概略も不明であった。本研究事業の H22 年度 feasibility study で、全国 1 次調査として症例数と概要を明らかにし、73 例（うち生産 51 例、死産 4 例、流産 15 例）を把握した。結果は致死性という名称にもかかわらず、周産期死亡率は 56%であった。周産期死亡を起こさなかった 24 例のうち 16 例は 1 年以上生存しており、これは生産児の 31%にあたる。H23 年度は長期生存例の発達や経過を明らかする 2 次調査を開始し平成 24 年度にデータ収集を終了した。この結果によると致死性骨異形成症はその名称とは異なり、周産期致死性とは必ずしも言えず、またこの疾患名が患児を育てている家族にとって違和感のある名称であることが明らかとなった。平成 23 年度に致死性骨異形成症という名称が実情に合わないとして名称の変更を提起し、平成 24 年度にタナトフォリック骨異形成症への変更が日本整形外科学会において承認された。本疾患は妊娠中の胎児の四肢長幹骨の著明な短縮が特徴で、早期診断は妊娠管理や分娩形式の決定など周産期管理に重要である。しかし現在は四肢長幹骨の正常値のデータがないため、超音波検査での四肢長幹骨の標準値作成プロジェクトを開始し、データ収集を完了し、平成 24 年度に一部の超音波断層装置に装備できる状態にすることができた。診断方法として近年は３次元胎児ヘリカル CT が導入されたが、胎児被爆、撮影条件、確定診断で重視すべき所見など、未解決の問題が山積しているので、放射線科医と技師による胎児 CT サブグループを結成し、撮影条件や症例数などの全国で調査し、2 次調査として、適応や撮影ガイドラインの作成を開始した。胎児骨系統疾患に詳しい各領域専門医の集まり「胎児骨系統疾患フォーラム」を基盤として、効率的な疾患の診断・登録を行い、臨床医を支援する仕組みを開始した。また平成 24 年度には文部科学省と厚生労働省の共同プロジェクトである「疾患特異的 iPS 細胞を活用した難病研究」に研究班として参画することで、今後の治療に貢献すべく、倫理的な課題を克服し、骨の再生医療や細胞バンクへの取組を開始した。すでに致死性骨異形成症やⅡ型コラーゲン異常症の検体の提供を行った。

研究分担者氏名　所属機関名及び所属機関における職名
室月　淳　宮城県立こども病院産科・部長
山田崇弘　北海道大学病院産科・助教
堤　誠司　山形大学医学部産科婦人科・講師
佐藤秀平　青森県立中央病院総合周産期母子医療センター産科・センター長
林　聡　　東京マザークリニック・院長
篠塚憲男　胎児医学研究所臨床研究・代表
高橋雄一郎　独立行政法人国立病院機構長良医療センター産科・医長
佐世正勝　山口県立総合医療センター総合周産期母子医療センター・センター長
沼部博直　京都大学大学院医学研究科社会健康医学系専攻医療倫理学・准教授
鬼頭浩史　名古屋大学医学部附属病院整形外科・講師
宮嵜　治　国立成育医療研究センター放射線診療部・医長
緒方　勤　国立成育医療研究センター研究所小児思春期発育研究部臨床・分子遺伝学・部長
池川志郎　理化学研究所ゲノム医科学研究センター・チームリーダー
妻木範行　京都大学 iPS 細胞研究所（CiRA）・教授
芳賀信彦　東京大学医学部附属病院リハビリテーション科・教授

A. 研究目的

致死性骨異形成症 thanatophoric dysplasia: TD は線維芽細胞増殖因子受容体３(Fibroblast growth factor receptor 3: FGFR3)遺伝子変異によって生じる先天性骨系統疾患で、胎児は出生後早期に死亡するとされている。周産期致死性とされる骨系統疾患ではもっとも頻度が高いとされているが、日本では実際の患者数や出生頻度は不明である。また、その名称にもかかわらず実際には長期生存例の症例報告も散見される。

（１）全国調査による致死性骨異形成症の出生後の経過についてのデータの収集：

全国の医療機関の産科、小児科、整形外科のうち骨系統疾患の管理が可能と考えられる施設を対象に、全国調査（一次調査）として症例数とその予後についての概要の調査を実施し、患者数、周産期死亡率や出生後の児の生存の状況、そして長期生存の可能性を把握した。ついで二次調査として、児の身体的および精神的な発達の状況を把握する目的で、これらの調査を一次調査で協力を取り付けた施設に依頼して実施する。

致死性骨異形成症の分娩形式を決定するための正確な出生前診断の手法の確立と新生児管理に重要な予後の実際の情報の取得を目的として、以下の研究も行う。

（２）インターネット利用による胎児の骨系統疾患を診断支援するための症例検討システムの構築：

セキュリティの充実したウェブ閲覧型システムを構築して臨床医の診断の支援を行う。

（３）過去の症例検討のとりまとめ：

胎児骨系統疾患に詳しい各領域横断的専門医のグループ「胎児骨系統疾患フォーラム」でメールによる検討を行った骨系統疾患症例の整理と分析を行い、診断の指針の作成に役立つようにとりまとめる。

（４）妊娠期間中の胎児の診断指針の作成：

致死性骨異形成症の診断は出生後については、レントゲン所見と遺伝子診断による診断がほぼ確立している。したがって妊娠期間中に判明した骨格異常の胎児診断としてどのような所見に注目してどのような検査を行うべきかという指針の作成を行うために下記の事業を行う。

（ア）超音波検査：正常の胎児の四肢長幹骨の標準値作成プロジェクトを行って、日本人での標準値を得る。

（イ）胎児ＣＴ：全国調査を行って、胎児ＣＴの症例数の把握と、標準的な撮影方法と見方の指針

の作成を行う。

（ウ）遺伝子診断：遺伝子診断により確定診断をできる体制づくりを支援する。

（５）地域診断支援システムの構築：

日本全国を一定地域ごとに分担して胎児骨系統疾患の妊娠例に遭遇した産婦人科医から相談を受けられるような体制づくりを行い、臨床医療に成果を還元する。

（６）臨床医への情報提供：

所定の研究報告書を作成するのみならず、胎児骨系統疾患をまとめた書物を発刊して、臨床医に情報提供を行う。

（７）社会への還元：

公開シンポジウムの開催や致死性骨異形成症についてホームページによる情報発信を行って成果を社会に還元する。

（８）再生医療と細胞バンク：

現在は致死性骨異形成症の治療は呼吸管理以外にはほとんど方法がない。また一般に骨系統疾患には根治的治療法はなく、骨延長術などの対症療法に限られる。そこで平成 24 年度には文部科学省と厚生労働省の共同プロジェクトである「疾患特異的 iPS 細胞を活用した難病研究」に研究班として参画することで、根治的治療を目的として iPS 細胞をはじめとした再生医療の実現のために患者細胞を提供することとした。

B. 研究方法

（１）全国調査による患者数等の疾患に関する基本的なデータの収集：

骨系統疾患の診断、児や母の管理が可能と考えられる施設として、総合周産期母子センターと地域周産期母子センター、大学病院の産科 381 施設、小児科 394 施設、整形外科 381 施設を対象にアンケート調査を行った。産科に対しては人工妊娠中絶を含めて、周産期の死産や生産の患児の状況を調査した。小児科に対しては出生児の予後の調査を重視して、出生直後の呼吸管理を中心とした介入的な処置により、その後の生命予後が改善されるかどうかも検討するために、より詳細な記録をとることとした。そして小児科については１年以上の長期生存例を経験している医師についてはインタビュー調査のための 2 次調査の依頼を行った。また整形外科については、本疾患が整形外科的管理を必要とするまで成長するかどうかを調査した。

（２）（３）（５）（６）（７）（８）詳細はC．研究結果に記載した。

（４）妊娠期間中の胎児の診断指針の作成：

（ア）超音波検査：正常の胎児の四肢長幹骨の標準値作成プロジェクトとして研究分担者の産科医の所属する施設が中心となって、超音波検査の際に胎児の大腿骨、脛骨・腓骨、上腕骨、橈骨・尺骨の測定を行い、標準値を算出する。

（イ）胎児ＣＴ：全国調査として胎児ＣＴの撮影経験のある３施設の放射線科医・技師を中心に胎児ＣＴサブグループを結成し、撮影条件の調査用紙を作成し、全国の施設でこれまで胎児ＣＴの学会報告のある施設に対して、症例数の把握と撮影条件の調査を行う。

（ウ）遺伝子診断：関西と関東に各１施設の遺伝子診断が実施可能な施設を整備する。

（倫理面への配慮）

本研究においては、全体の研究計画について、研究代表者の所属する兵庫医科大学において倫理委員会の承認を得ている。また個別の研究分担者が行う研究については、診断指針の作成など全体の研究計画に承認されたことで十分と見なされる研究を除いて、各施設において倫理委員会の承認を得ている。

C. 研究結果

（１）全国調査による患者数等の疾患に関する基本的なデータの収集：

産科 127 施設（33.2％）、小児科 186 施設（47.2%）、整形外科 115 施設（30.2%）より回答

を得た。報告された TD の症例数は合計 85 例で、うち産科から 53 例、小児科から 30 例，整形外科から 2 例であった。重複しない 73 例についてデータの解析を行った。このうち流産が 15 例、死産が 4 例、生産が 51 例、不明が 3 例であった。生産児 51 例中 27 例は 7 日以内に死亡しており、周産期死亡率は 56%であった。一方で周産期死亡を起こさなかった 24 例中には 1 年以上の生存も 16 例あり、生産児 51 例の 31%に達した。なお、生産児のうち呼吸管理実施例（24 例）では全例周産期死亡を起こさなかった。一方で呼吸管理非実施例（25 例）では全例 2 日以内に死亡していた。

これらの情報を提供していただいた施設に対して、さらに詳しい身体的・精神的な発達のデータを依頼すべく現在調査用紙を作成中である。

（２）インターネット利用による胎児の骨系統疾患を診断支援するための症例登録・検討システムの構築：

システムは兵庫医科大学の協力により同大学にサーバーを設置して、運営することとし、システムの構築をすでに完了し、ウェブ上に匿名化して症例の経過と画像をアップして、専門家グループで討議して症例を登録して、診断を支援するシステムを構築した。

（３）過去の症例検討のとりまとめ：

上記のウェブ上のシステム構築までの段階で全国の症例を検討した 3,500 通のメールの内容の解析と症例（108 症例以上）の分析を行っている。

（４）妊娠期間中の胎児の診断指針の作成：

（ア）超音波検査については胎児の四肢長幹骨の標準値作成のためのデータ収集を目的として、宮城県立こども病院を中心に 9 施設で実施し 700 例以上の症例を集めて分析中した。

（イ）胎児ＣＴについては全国で胎児ＣＴを実施している施設 17 施設を対象に、詳細な胎児ＣＴの撮影条件とこれまでの撮影対象疾患を調査して胎児 CT の撮影条件特に被曝量との関係から我が国の現状を把握した。

（ウ）遺伝子診断は慶応大学と大阪市立総合医療センターにて FGFR3 遺伝子診断が実施できるような体制を構築した。また全国規模で遺伝子診断のできるラボや研究施設のリストアップをおこなった。

（５）地域診断支援システムの構築：

研究班の研究分担者の属する施設を中心に、北海道、東北、東京、神奈川、東海、近畿、中国、四国、九州において中心的なセンター施設を選定した。

（６）臨床医への情報提供：

研究班でホームページ www.thanatophoric.com を作成し骨系統疾患の情報を提供し、診断や治療に取り組む産科医や小児科医などからの問い合わせを受け付ける体制を作った。すでに地域の病院や患者家族から数件の問い合わせがあり、上記の地域診断支援システムに紹介して対応した。また平成 24 年 12 月 2 日（日）に本研究班会議と共催して、これらの医師を対象に第５回胎児骨系統疾患フォーラムを開催し、致死性骨異形成症を含めた胎児骨系統疾患の新生児管理について集中的な情報提供と討議を行った。

（７）社会への還元：

上記ホームページに患者家族向けの情報を提供している。

（８）致死性骨異形成症の２名の患者から線維芽細胞を埼玉県立小児医療センターの細胞バンクに寄贈し、ここを通じて細胞株を樹立し京都大学 iPS 細胞研究所に送付することとした。またⅡ型コラーゲン異常症についても提供した。

D. 考察

（１）全国調査による患者数等の疾患に関する基本的なデータの収集：現在研究実施中である。

（２）インターネット利用による胎児の骨系統疾患を診断支援するための症例登録・検討システムの構築：従来から行っているメーリングリストによる症例検討システムに加えて、日本産科婦人科

学会周産期委員会の胎児骨系統疾患小委員会と協力して、全国の拠点となる県を選定して、症例登録事業を開始している。

（３）過去の症例検討のとりまとめ：前記の症例検討の結果をとりまとめる作業を並行して実施している。

（４）妊娠期間中の胎児の診断指針の作成：

（ア）超音波のデータについては解析が終了しており、結果がまとまっている。現在投稿論文を作成中であるが、データはすでに一部の超音波機器メーカーのプログラムに組み込んでもらっている。

（イ）胎児ＣＴについては各施設の標準的な照射線量についてのデータが揃ったため、今後は胎児ＣＴの標準的な撮影条件の提示を行うと同時に、今後は撮影条件だけではなくて、どのような疾患が疑われる場合やどのような週数で実施するかを含めたガイドラインを作成したい。

（ウ）遺伝子診断については全国規模の遺伝子検査解析ラボ一覧を積極的に活用していきたい。

（５）地域診断支援システムの構築：

日本産科婦人科学会の胎児骨系統疾患小委員会とも協力して体制整備を進めている。

（６）臨床医への情報提供（７）社会への還元：

ホームページの利用と講演会等を通じてこうした機会を提供していることが必要である。

E. 結論

平成２４年度は日本で初めての致死性骨異形成症の全国調査を行い、引き続き二次調査として出生後の身体的および精神的な発達の状態を調べてデータを収集した。他のプロジェクトについても上記のように概ね完了した。

F. 健康危険情報

特になし

G. 研究発表

１．論文発表

Tsutsumi S, Maekawa A, Obata M, Morgan T, Robertson SP, Kurachi H. A Case of Boomerang Dysplasia with a Novel Causative Mutation in Filamin B: Identification of Typical Imaging Findings on Ultrasonography and 3D-CT Imaging. Fetal Diagn Ther. 2012

Yamada T, Takagi M, Nishimura G, Akaishi R, Furuta I, Morikawa M, Yamada T, Cho K, Sawai H, Ikegawa S, Hasegawa T, Minakami H. Recurrence of osteogenesis imperfecta due to maternal mosaicism of a novel COL1A1 mutation. Am J Med Genet A. 2012 Nov;158A(11):2969-71.

Wada R, Sawai H, Nishimura G, Isono K, Minagawa K, Takenobu T, Harada K, Tanaka H, Ishikura R, Komori S. Prenatal diagnosis of Kniest dysplasia with three-dimensional helical computed tomography. J Matern Fetal Neonatal Med. 24:1181-1184.2011

Numabe H, Sawai H, Yamagata Z, Muto K, Kosaki R, Yuki K, Kosaki K. Reproductive success in patients with Hallermann-Streiff syndrome. Am J Med Genet A. 2011 Sep;155A(9):2311-3.

Watanabe A, Karasugi T, Sawai H, Naing BT, Ikegawa S, Orimo H, Shimada T. Prevalence of c.1559delT in ALPL, a common mutation resulting in the perinatal (lethal) form of hypophosphatasia in Japanese and effects of the mutation on heterozygous carriers. J Hum Genet. 2011 56:166-168

Yamada T, Nishimura G, Nishida K, Sawai H,

Omatsu T, Kimura T, Nishihara H, Shono R, Shimada S, Morikawa M, Mizushima M, Yamada T, Cho K, Tanaka S, Shirato H, Minakami H. Prenatal diagnosis of short-rib polydactyly syndrome type 3 (Verma-Naumoff type) by three-dimensional helical computed tomography. J Obstet Gynaecol Res. 2011 37:151-155

Daniel PB, Morgan T, Alanay Y, Bijlsma E, Cho TJ, Cole T, Collins F, David A, Devriendt K, Faivre L, Ikegawa S, Jacquemont S, Jesic M, Krakow D, Liebrecht D, Maitz S, Marlin S, Morin G, Nishikubo T, Nishimura G, Prescott T, Scarano G, Shafeghati Y, Skovby F, Tsutsumi S, Whiteford M, Zenker M, Robertson SP. Disease-associated mutations in the actin-binding domain of filamin B cause cytoplasmic focal accumulations correlating with disease severity. Hum Mutat. 2011 [Epub ahead of print]

Sasaki A, Sawai H, Masuzaki H, Hirahara F, Sago H. Low prevalence of genetic prenatal diagnosis in Japan. Prenat Diagn. 2011 Oct;31(10):1007-9.

西村玄、室月淳、澤井英明　編　骨系統疾患　出生前診断と周産期管理　メジカルビュー

２．学会発表

澤井英明　致死性骨異形成症の全国調査から　第56回日本人類遺伝学会　平成23年11月9日～12日　幕張

西山深雪、澤井英明、小杉眞司　羊水染色体分析の検査前後の妊婦への情報提供に関する調査　第56回日本人類遺伝学会　平成23年11月9日～12日　幕張

山田崇弘、高木優樹、西村玄、赤石理奈、古田伊都子、小嶋崇史、石川聡司、武田真光、西田竜太郎、森川守、山田俊、長和俊、澤井英明、池川志郎、長谷川奉延、水上尚典　COL1A1のモザイク変異によるII型骨形成不全症の再発例

胎児骨系統疾患における II 型コラーゲン異常症の遺伝子変異の解析　澤井英明、和田龍、武信尚史、原田佳世子、岡本陽子、三村博子、管原由恵　第56回日本人類遺伝学会　平成23年11月9日～12日　幕張

H. 知的所有権の取得状況

1.特許取得

なし

2.実用新案登録

なし

3.その他

なし

Ⅱ．分担研究報告

致死性骨異形成症の診断と予後に関する研究
重度胸郭形成不全を伴う第 14 染色体父性ダイソミー症候群の発症機序解明

研究分担者　緒方勤
浜松医科大学　小児科　教授

研究要旨
本年度は、昨年度に引き続き、周産期致死性骨系統疾患の 1 つである第 14 染色体父親性ダイソミー症候群について以下研究を行い、 (1) 母性発現遺伝子 RTL1as が microRNA として RTL1 発現を抑制すること、(2)ヒト DIO3 がインプリンティングされないこと、(3) 胎盤組織の特徴が遺伝子発現パターンを反映すること、(4) 出産年齢解析が第一減数分裂時の不分離を介する R/PE type-upd(14)pat 発症のリスクファクターであることが示された。これらのデータは、microRNA を用いた本症候群の治療や、高齢出産を避けることで upd(14)pat 発症を予防しうることを示唆するものである。

A．研究目的

第 14 染色体父親性ダイソミー症候群は、ベル型・コートハンガー型と形容される胸郭形成不全、臍帯ヘルニア・腹直筋離開などの腹壁異常、前額部突出・長い人中などの特徴的顔貌などの個体症状と共に、羊水過多、胎盤過形成などの胎盤症状を示す稀な疾患である。本症候群は、胸郭形成不全が重度の呼吸障害を生じる新生児期の致死性骨系統疾患の一つである。

本症候群の存在は、まず第 14 染色体父性ダイソミー(upd(14)pat)の同定に由来する。すなわち、第 14 染色体長腕遠位部にはインプリンティング領域が存在し、父親由来アレルからのみ発現する父性発現遺伝子、母親由来アレルからのみ発現する母性発現遺伝子が存在し、これらのインプリンティング遺伝子の発現異常が本症候群を招くことが判明した。われわれは、このインプリンティング領域について、世界で初めて以下のことを明らかとしている。 (1) このインプリンティング領域にはメチル化可変領域 (Differentially Methylated Region: DMR)が存在すること、(2) 生殖細胞形成期に確立される IG-DMR が胎盤におけるインプリンティングセンターとして機能すること、(3) 受精後初期発生段階に確立される MEG3-DMR が個体におけるインプリンティングセンターとして機能すること、(4) IG-DMR のメチル化パターンが MEG3-DMR のメチル化パターンを制御すること、(5) 臨床症状を招く主因が、父性発現遺伝子 RTL1 の過剰発現である。これらの成果は、世界的に高く評価されている。

そして、昨年度、われわれは、この(upd(14)pat)について、(1) レントゲン画像診断基準の作成、(2) 胎児診断の可能性とそれに基づく適切な早期申請時からの治療介入、(3) 現在までに遺伝子診断された患者 26 例の分子遺伝学的データに基づく遺伝子診断法フローチャートの構築、という成果を挙げた。この研究過程において、われわれは本邦において 35 例の同様の症状を呈する患者を集積している。そして、同様の表現型が、upd(14)pat のみならず、インプリンティング領域の微小欠失やエピ変異でも生じることを見出し、このような表現型を第 14 染色体父親性ダイソミー症候群と命名した。

本研究年度においては、この第 14 染色体父親性ダイソミー症候群において、(1) 母性発現遺伝子 RTL1as が microRNA として RTL1 発現を抑制するか否か、(2) DIO3 がインプリンティング遺伝子であるか否か、(3) 胎盤組織像の特徴、(4) 高齢出産が upd(14)pat の発症リスクとなるか否か、という未解明の課題について取り組んだ。

B．研究方法

出生前診断により新鮮な胎盤を入手できた本症候群の 2 例と、既に胎便を集積されている症例を主に解析した。

（倫理面への配慮）

遺伝子解析にあたっては、ヒトゲノム・遺伝子解析研究に関する倫理指針を遵守し、検体の収集を含めた研究計画については、国立成育医療センター、および各検体の収集施設において予め倫理委員会の承認を得ている。検体は、書面によるインフォームド・コンセントを取得後に収集している。

C．研究結果

(1) 母性発現遺伝子 RTL1as が microRNA として RTL1 発現を抑制するか否か

Upd(14)pat 患者 2 例とコントロール 3 例の新鮮胎盤を用いて定量的発現解析を行った。生データでは、父性発現遺伝子 DLK1 と RTL1 はコントロール胎盤よりも過剰発現を示し、母性発現遺伝子は RTL1as にコードされる miR433 と miR127 を含めて発現消失を示した（図 1A）。そして、DLK1 発現量と組織所見に基づき、各遺伝子発現細胞あたりの父性発現遺伝子を補正して算出した結果、DLK1 は父性ダイソミー状態に一致して 2 倍の発現量を呈したが、RTL1 は父性ダイソミー状態では説明できない約 5 倍の発現量を示した。

(2) DIO3 がインプリンティング遺伝子であるか否か

上記の解析において、父性発現遺伝子 DIO3 発現量は、生データではコントロール胎盤よりも過剰であったが、補正後はコントロール胎盤と同じく 1 倍であった（図 1A, B）。

(3) 胎盤組織像の特徴

Upd(14)pat 患者 2 例の新鮮胎盤、既報のインプリンティング領域の欠失による第 14 染色体父親性ダイソミー症候群患者のフルマリン処理胎盤、コントロールの新鮮胎盤を用いて検討した。光顕と電顕では末梢絨毛の血管内皮細胞の腫大と血管壁細胞の肥大化が、免疫染色では末梢絨毛の血管内皮細胞の腫大と血管壁細胞に限する DLK1、RTL1、DIO3 タンパク発現と遺伝子発現量に比例した DLK1 と RTL1、特に RTL1 タンパクの発現増加が認められた（図 2）。

(4) 高齢出産が upd(14)pat の発症リスクとなるか否か

- Upd(14)pat は、trisomy rescue（TR）、monosomy rescue（MR）、gamete complementation（GC）、post-zygotic mitotic error（PE）により発症し、このうち高齢出産は、減数第一分裂時の不分離により産生される nullisomic oocyte を介する MR と GC に影響すると考えられる（図 3）。すなわち、父性ダイソミーのうち、MR/PE type-upd(14)pat の発症に高齢出産が関わりうると考えられる。このため、われわれは、既に遺伝的発症原因を明らかとした 26 例中、IG-DMR と MEG3-DMR を含む微小欠失患者 3 例、IG-DMR のみの欠失患者 1 例、MEG3-DMR のみの欠失患者 1 例、 TR/GC type-upd(14) pat 患者 5 例、MR/PE type-upd(14)pat 患者 11 例、PE 特異的部分的ホモダイソミー患者 1 例、エピ変異患者 4 例において、出産年齢を比較した。その結果、35 歳以上の高齢出産は、MR/PE type-upd(14)pat に集中して認められた（図 4）。さらに、高齢出産の頻度は、MR/PE type-upd(14)pat で 6/11、それ以外の原因で 2/15 と、MR/PE type-upd(14)pat において有意に高く（P=0.034）、出産年齢中央値は、MR/PE type-upd(14)pat で 36.0、それ以外の原因で 29.5 と、MR/PE type-upd(14)pat において有意に高かった（P=0.045）。

D．考察

本研究の遺伝子発現解析と組織学的解析データは、以下のことを示唆する。(1) 母性発現遺伝子 RTL1as が microRNA として RTL1 発現を抑制することを示す。(2) マウス Dio3 が部分的にインプリンティングされることと異なり、ヒト DIO3 はインプリンティングされない。(3) 胎盤組織の特徴は遺伝子発現パターンを反映し、絨毛末端に本症候群の異常が存在する。これは、世界で初めてのデータであり、microRNA を用いた本症候群の治療の道を示すものである。

さらに、出産年齢解析は、第一減数分裂時の不分離を伴い易い高齢出産が R/PE type-upd(14)pat 発症のリスクファクターであることを示すものである。これは、既にわれわれが報告した disomic oocyte を介する TR/GC[M1] type-upd(15)mat が、高

齢出産により有意に増加していることに一致するものであり、高齢出産を避けることが upd(14)pat 発症の予防になりうることを示唆するものである。なお、upd(14)pat 症候群では、nullisomic oocyte が第一減数分裂時の不分離と第二減数分裂時の不分離のいずれの時期に形成されたかを鑑別することは不可能である（図 3）。したがって、今回の MR/PE type-upd(14)pat グループには、高齢出産が影響する第一減数分裂時の不分離に起因する upd(14)pat のみならず、高齢出産が影響しない第二減数分裂時の不分離に起因する upd(14)pat や PE による upd(14)pat が含まれていると考えられる。

Ｅ．結論

本研究により、(1) 母性発現遺伝子 RTL1as が microRNA として RTL1 発現を抑制すること、(2) ヒト DIO3 がインプリンティングされないこと、(3) 胎盤組織の特徴が遺伝子発現パターンを反映すること、(4) 出産年齢解析が第一減数分裂時の不分離を介する R/PE type-upd(14)pat 発症のリスクファクターであること示すものである。これらのデータは、microRNA を用いた本症候群の治療や、高齢出産を避けることで upd(14)pat 発症を予防しうることを示唆するものである。

Ｆ．健康危険情報

なし

Ｇ．研究発表

１．論文発表

1. Kagami M, Kato F, Matsubara K, Sato T, Nishimura G, Ogata T*: Relative frequency of underlying genetic causes for the development of UPD(14)pat-like phenotype. *Eur J Hum Genet* 20 (9): 928–932, 2012.
2. Fuke-Sato T, Yamazawa K, Nakabayashi K, Matsubara K, Matsuoka K, Hasegawa T, Dobashi K, Ogata T*: Mosaic upd(7)mat in a patient with Silver-Russell syndrome: correlation between phenotype and mosaic ratio in the body and the placenta. *Am J Med Genet A* 158A (2): 465–468, 2012.
3. Hiura H, Okae H, Miyauchi N, Sato F, Sato A, Van De Pette M, John RM, Kagami M, Nakai K, Soejima H, Ogata T, Arima T*: Characterization of DNA methylation errors in patients with imprinting disorders conceived by assisted reproduction technologies. *Hum Reprod* 27 (8): 2541–2548, 2012.
4. Kagami M, Matsuoka K, Nagai T, Yamanaka M, Kurosawa K, Suzumori N, Sekita Y, Miyado M, Matsubara K, Fuke T, Kato F, Fukami M, Ogata T*: Paternal uniparental disomy 14 and related disorders: placental gene expression analyses and histological examinations. *Epigenetics* 7 (10): 1142–1150, 2012.
5. Nagasaki K*, Tsuchuya S, Saitoh A, Ogata T, Fukami M: Neuromuscular symptoms in a patient with familial pseudohypoparathyroidism type Ib diagnosed by methylation-specific multiplex ligation-dependent probe amplification. *Endocr J* (accepted).
6. Fuke T, Mizuno S, Nagai T, Hasegawa T, Horikawa R, Miyoshi Y, Muroya K, Kondoh T, Numakura C, Sato S, Nakabayashi K, Tayama C, Hata K, Sano S, Matsubara K, Kagami M, Tamazawa K, Ogata T*: Molecular and clinical studies in 138 Japanese patients with Silver-Russell syndrome. *PLoS One* (accepted).
7. Ayabe T, Matsubara K, Ogata T, Ayabe A, Murakami N, Nagai T, Fukami M*: Birth seasonality in Prader-Willi syndrome resulting from chromosome 15 microdeletion. *Am J Med Genet A* (accepted).
8. Matsubara K, Ogata T*: Advanced maternal age at childbirth and the development of uniparental disomy. A commentary on the proportion of uniparental disomy is increased in Prader-Willi syndrome due to an advanced maternal childbearing age in Korea. J Hum Genet. 2013 Jan 31. doi: 10.1038/jhg.2013.4. [Epub ahead of print]

２．学会発表

省略

Ｈ．知的財産権の出願・登録状況

１．特許取得

なし

２．実用新案登録

なし

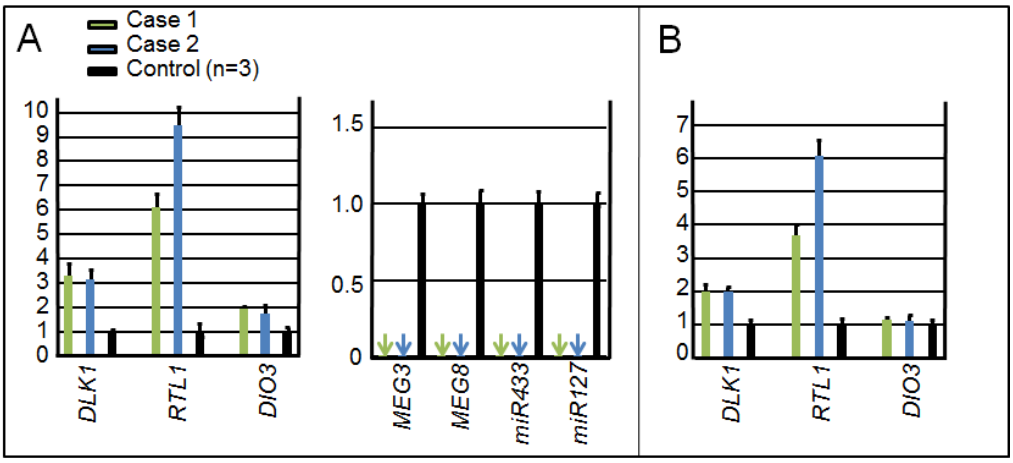

図 1. 胎盤を用いた遺伝子発現量解析

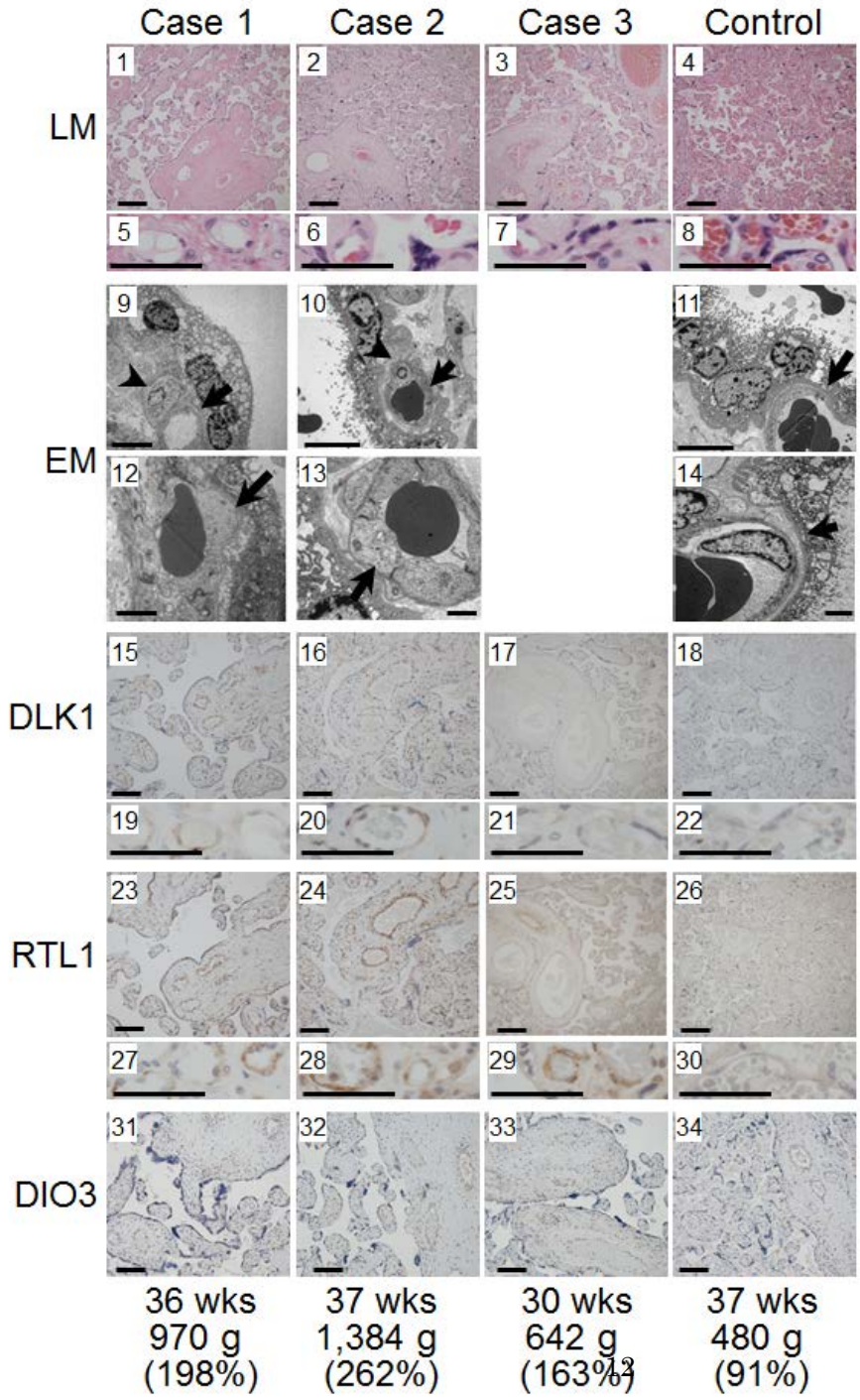

図 2. 胎盤を用いた組織学的解析

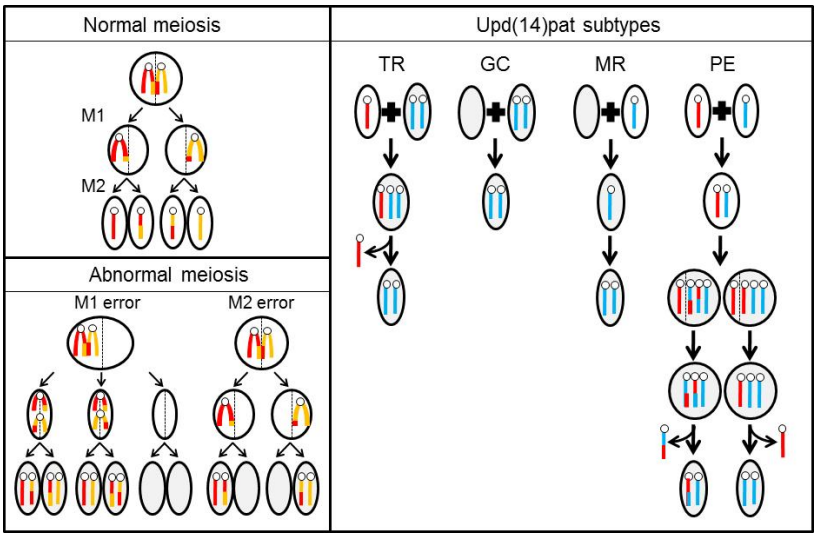

図 3. 正常および異常減数分裂時と第 14 染色体父性ダイソミー(upd(14)pat)発症機序を示す模式図。第一減数分裂（M1）あるいは第二減数分裂（M2）時の不分離でヌリソミーの卵子が形成される。このうち、M1 エラーは高齢出産で増加する。Upd(14)pat は、TR: trisomy rescue; GC: gamete complementation; MR: monosomy rescue; PE: postzygotic mitotic error で形成される．このうち GC, PE は極めて稀であり、TR, MR が upd(14)pat 発症原因の大多数をしめる。そして、MR では、高齢出産がリスク因子となる nullisomic oocytes が関与する。

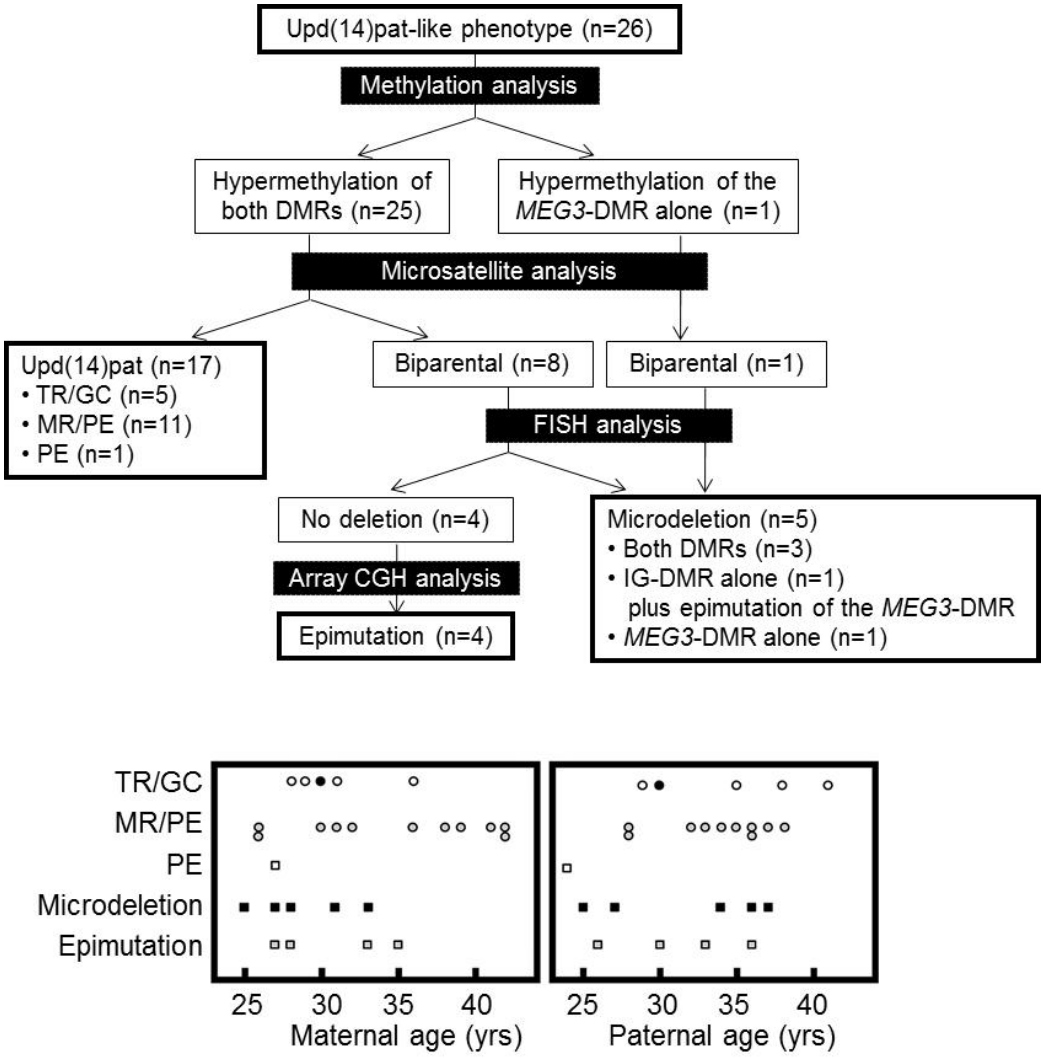

図 4. 第 14 染色体父性ダイソミー症候群患者 26 例における発症原因の分類（上）と出生時両親年齢の分布（下）。

厚生労働科学研究費補助金（難治性疾患克服研究事業）
研究分担報告書

致死性骨異形成症の診断と予後に関する研究

研究分担者　池川　志郎
理化学研究所・ゲノム医科学研究センター
骨関節疾患研究チーム・チームリーダー

研究要旨

致死性骨異形成症は頻度の高い骨系統疾患で、その正確な診断と、それに基づく的確な治療は、新生時期の遺伝性骨関節疾患の医療上の大きな課題である。しかし、致死性骨異形成症には多くの類似疾患が存在し、従来の臨床所見、X 線所見に頼った方法では、診断は非常に困難である。診断能の向上のためには、類似疾患を含めた包括的な遺伝子レベルでの診断システムを確立する必要がある。そのような遺伝子診断システムの構築のために、致死性骨異形成症、及びその類似疾患の DNA 解析を行なった。臨床家の協力の下に、致死性骨異形成症、及びその類似疾患の表現型の詳細なデータ（臨床像、X 線像）と DNA を収集した。*FGFR3* を含む既知の疾患遺伝子に変異が疑われる場合は、それらの変異解析を行ない、変異が同定された患者については、表現型データとの対応を検討した。その結果、1）致死性骨異形成症類似疾患のひとつ opsismodysplasia の原因遺伝子が *INPPL1* であることを明らかにした。2）短体幹症の原因遺伝子の PAPSS2 であることを明らかにした。これらの新規の疾患遺伝子を加えた致死性骨異形成症の遺伝子診断システムを構築中である。

共同研究者

Dai Jin（理化学研究所・ゲノム医科学研究センター・骨関節疾患研究チーム）

A. 研究目的

致死性骨異形成症は多くの類似疾患が存在するため、正確な診断が困難である。その確定診断のためには、遺伝子レベルでの診断システムを構築する必要がある。致死性骨異形成症の遺伝子診断法の確立のために、致死性骨異形成症、及びその類似疾患の DNA 解析を行う。

B. 研究方法

胎児骨系統疾患フォーラムを中心とする臨床家の協力の下に、致死性骨異形成症、及びその類似疾患の表現型の詳細なデータ（臨床像、X 線像）と genomic DNA を収集した。*FGFR3* を含む既知の疾患遺伝子に変異が疑われる場合は、DNA sequence 解析をはじめとする遺伝子
解析を行ない、変異の同定を試みた。変異が同定された

患者については、表現型のデータとの対応を検討した。

（倫理面への配慮）

本研究の遂行にあったっては、ヒトゲノム・遺伝子解析研究に関する倫理指針（平成 13 年 3 月 29 日文部科学省・厚生労働省・経済産業省告示第 1 号）に従っている。検体の収集を含めた研究計画については、理化学研究所、及び各検体の収集施設において予め倫理委員会の承認を得ている。検体は、書面によるインフォームド・コンセントを取得後に収集している。

C. 研究結果

1) 致死性骨異形成症類似疾患のひとつ opsismodysplasia の原因遺伝子が INPPL1(1)であることを明らかにした。新規の遺伝子の欠出変異を同定した。(Iida *et al.* J Hum Genet, 2013)。

2) 常染色体劣性型の短体幹症(brachyolmia)の原因遺伝子が PAPSS2 であることを明らかにした(Miyake *et al.* J Med Genet, 2012)。この疾患の詳細な臨床像、X 線像を明らかにした (Hum Mutat、投稿中)。

D. 考察

致死性骨異形成症には多くの類似疾患が存在する。変異を同定した例について、表現型の再評価を行ったが、胎児期、新生児時期の表現型の臨床像、X 線像のデータからは、それがいかに詳細なものであっても、致死性骨異形成症の診断、鑑別診断には多くの困難が伴い、類似疾患を正確に鑑別する事は困難であると考えられる。包括的な遺伝子診断が、その解決のための最も現実的な方法であると考えられる。

E. 結論

致死性骨異形成症の正確な診断のためには、類似疾患を含めた遺伝子レベルでの診断法を確立する必要がある。

F. 健康危険情報

なし

G. 研究発表

1. 論文発表

1. Iida A, Okamoto N, Miyake N, Nishimura G, Minami S, Sugimoto T, Nakashima M, Tsurusaki Y, Saitsu H, Shiina M, Ogata K, Watanabe S, Ohashi H, Matsumoto N, Ikegawa S. Exome sequencing identifies a novel INPPL1 mutation in opsismodysplasia. J Hum Genet. 2013 Apr 4. doi: 10.1038/jhg.2013.25. [Epub ahead of print]
2. Semba K, Araki K, Matsumoto K, Suda H, Ando T, Sei A, Mizuta H, Takagi K, Nakahara M, Muta M, Yamada G, Nakagata N, Iida A, Ikegawa S, Nakamura Y, Araki M, Abe K, Yamamura K. Ectopic expression of Ptf1a induces spinal defects, urogenital defects, and anorectal malformations in Danforth's short tail mice. PLoS Genet. 2013 9(2):e1003204
3. Yamada T, Takagi M, Nishimura G, Akaishi R, Furuta I, Morikawa M, Yamada T, Cho K, Sawai H, Ikegawa S, Hasegawa T, Minakami H. Recurrence of osteogenesis imperfecta due to maternal mosaicism of a novel COL1A1 mutation. Am J Med Genet A. 158A(11):2969-71, 2012.
4. Cho TJ, Lee KE, Lee SK, Song SJ, Kim KJ, Jeon D, Lee G, Kim HN, Lee HR, Eom HH, Lee ZH, Kim OH, Park WY, Park SS, Ikegawa S, Yoo WJ, Choi IH, Kim JW. A single recurrent mutation in the 5'-UTR of IFITM5 causes osteogenesis imperfecta Type V. Am J Hum Genet. 91(2):343-8, 2012.

5. Miyake N, Elcioglu NH, Iida A, Isguven P, Dai J, Murakami N, Takamura K, Cho TJ, Kim OH, Hasegawa T, Nagai T, Ohashi H, Nishimura G, Matsumoto N, Ikegawa S. PAPSS2 mutations cause autosomal recessive brachyolmia. J Med Genet. 49(8):533-8, 2012.
6. Cho TJ, Matsumoto K, Fano V, Dai J, Kim OH, Chae JH, Yoo WJ, Tanaka Y, Matsui Y, Takigami I, Monges S, Zabel B, Shimizu K, Nishimura G, Lausch E, Ikegawa S. TRPV4-pathy manifesting both skeletal dysplasia and peripheral neuropathy: A report of three patients. Am J Med Genet A. 158A(4):795-802, 2012.
7. Daniel PB, Morgan T, Alanay Y, Bijlsma E, Cho TJ, Cole T, Collins F, David A, Devriendt K, Faivre L, Ikegawa S, Jacquemont S, Jesic M, Krakow D, Liebrecht D, Maitz S, Marlin S, Morin G, Nishikubo T, Nishimura G, Prescott T, Scarano G, Shafeghati Y, Skovby F, Tsutsumi S, Whiteford M, Zenker M, Robertson SP. Disease-associated mutations in the actin-binding domain of filamin B cause cytoplasmic focal accumulations correlating with disease severity. Hum Mutat. 33(4):665-73, 2012.
8. Sasagawa S, Takemori H, Uebi T, Ikegami D, Hiramatsu K, Ikegawa S, Yoshikawa H, Tsumaki N. SIK3 is essential for chondrocyte hypertrophy during skeletal development in mice. Development. 139(6):1153-63, 2012.

2. 学会発表

(招待講演のみ)

1. 池川志郎. 遺伝性疾患の原因遺伝子をみつけるには:骨の病気を例に. 遺伝医学研究会協賛セミナー. 東京. 2012 年 5 月 10 日.
2. Ikegawa S. Genomic study of Bone and joint diseases - Where we were, and where we are going. Nature Genetics China. Hangzhou. May 19, 2012
3. Ikegawa S. Rare Diseases and Common Problems: Lessons from One to the other. 6th Annual Introductory Course on Skeletal Dysplasias. Lousanne. Jul. 5, 2012
4. 池川志郎. 股関節疾患と遺伝 - 大腿骨頭壊死症を中心に -. 第 4 回股関節疾患研究会. 福岡. 2012 年 8 月 10 日.
5. Ikegawa S. Skeletal Dysplasia in Mice and Human. 22nd Annual Scientific Meeting/1st Asia-Pacific Bone and Mineral Research Meeting. Perth. Sep 3, 2012
6. 池川志郎. 骨・関節疾患のゲノム解析:パーソナルゲノム時代の疾患研究. 日本人類遺伝学会 第 57 回大会. 東京. 2012 年 10 月 26 日.
7. 池川志郎. 小児整形外科疾患の遺伝子解析. 第 27 回 日本整形外科学会基礎学術集会. 名古屋. 2012 年 10 月 27 日.
8. Ikegawa S. Genomic study of bone and joint diseases - where we were, and where we are going. 12th Annual Meeting of East Asian Union of Human Genetics Societies. Seoul. Nov 29, 2012
9. 池川志郎. 運動器疾患のゲノム解析ー遺伝子から分子病態へ. 京都大学再生医科学研究所・生体分子設計学分野セミナー. 京都. 2013 年 1 月 31 日.
10. 池川志郎. 日常の臨床の現場で遭遇する関節の遺伝病:家族歴、聞いていますか? 第 12 回 久留米関節セミナー. 久

留米. 2013 年 2 月 10 日.

H. 知的財産権の出願・登録状況
(予定を含む。)

1. 特許取得

B3GALT6 異常症の遺伝子診断(出願)

2. 実用新案登録

なし

3. その他

厚生労働科学研究費補助金（難治性疾患克服研究事業）
研究分担報告書

致死性骨異形成症の診断と予後に関する研究

胎児超音波計測による長管骨長の基準値作成
（多施設共同観察研究）

研究分担者	室月　淳	宮城県立こども病院　部長
	澤井英明	兵庫医科大学　准教授
	山田崇弘	北海道大学　助教
	堤　誠司	山形大学　講師
	佐藤秀平	青森県立中央病院　センター長
	篠塚憲男	胎児医学研究所　代表
	高橋雄一郎	長良医療センター　医長
	佐世正勝	山口県立総合医療センター　センター長

研究要旨　超音波断層法による胎児の長管骨（すなわち大腿骨 femur、脛骨 tibia、腓骨 fibula、上腕骨 humerus、尺骨 ulna、橈骨 radius）の長さについての日本人の基準値をつくり、胎児骨系統疾患などの骨病変の診断に有用な基礎資料を作成する多施設共同研究である。なお大腿骨長については日本超音波医学会によりすでに基準値がつくられているが､それ以外の胎児の脛骨､腓骨、上腕骨、尺骨、橈骨の長さの基準値は、過去に海外では発表されており、本邦ではそれらが参考にされている。しかし長管骨の発達には人種差があり、日本人で決められた大腿骨長と欧米のそれを比べると、妊娠末期となると 10mm 近い差が認められている。

胎児骨系統疾患は骨の全身の発達成熟に何らかの異常を呈する遺伝子病である。胎児骨系統疾患は、ほとんどが子宮内か出生直後に死亡する生命予後がきわめて悪いものから、成長後の低身長が唯一の症状である予後良好のものまで非常に多彩である。胎児期に骨短縮を認める疾患は 100 種類以上あるといわれているが、ひとつひとつの疾患の発症頻度が低いため、胎児期に長管骨の短縮を認める場合、その診断に難渋することが多い。日本人胎児の長管骨の基準値を作成することにより、骨系統疾患の正確な診断の一助とする。

A. 研究目的

胎児の長管骨、すなわち大腿骨 femur、脛骨 tibia､腓骨 fibula､上腕骨 humerus､尺骨 ulna、橈骨 radius の長さについての日本人の基準値をつくり、胎児骨系統疾患などの骨病変の診断の基礎資料を作成する。

大腿骨長（以下の図 FL）については日本超音波医学会によりすでに基準値がつくら

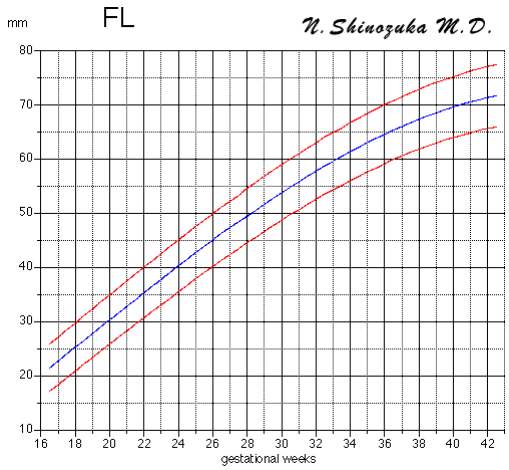

れている。

それ以外の胎児の脛骨、腓骨、上腕骨、尺骨、橈骨の長さの基準値は、過去にQueenan（1980）、Farrant（1981）、Jeanty (1984)、Merz (1987)などが発表しており、本邦では今でもJeantyやMerzの値が用いられている。しかし長管骨の発達には人種差があるのは自然であり、日本人で決められた大腿骨長と欧米のそれを比べると、妊娠末期となると10mm近い差が認められている。実際にJenatyやMerzの基準値は、臨床上の印象よりかけ離れた評価が出てくることがしばしばである。

胎児骨系統疾患は骨の全身の発達成熟に何らかの異常を呈する遺伝子病である。胎児骨系統疾患は、ほとんどが子宮内か出生直後に死亡する生命予後がきわめて悪いものから、成長後の低身長が唯一の症状である予後良好のものまで非常に多彩である。胎児期に骨短縮を認める疾患は100種類以上あるといわれているが、ひとつひとつの疾患の発症頻度が低いため、胎児期に長管骨の短縮を認める場合、その診断に難渋することが多い。日本人胎児の長管骨の基準値を作成することにより、骨系統疾患の正確な診断の一助とする。

B. 研究方法

試験タイプ：多施設共同観察試験

【対象】

1. 妊娠16週0日より妊娠40週6日まで
2. 16歳以上45歳未満
3. 単胎である
4. 妊娠初期にCRL計測により分娩予定日が決められている
5. 明らかな胎児奇形や発育遅延を認めない
6. 妊娠高血圧症や妊娠糖尿病などの母体合併症を認めない
7. 試験参加について本人から文書で同意が得られている

【方法】

1. 妊婦健康診査時に胎児の長管骨（大腿骨、脛骨、腓骨、上腕骨、尺骨、橈骨）の長さを計測して記録する。
2. 胎児期の長管骨はしばしば骨幹の部分しか骨化していない。その骨化部分を両端まで画面上に描出し、いちばん長いところを計測する。
3. 下腿の脛骨、腓骨、前腕の尺骨、橈骨は、それぞれ混同されて計測されることがあるので注意する。区別するために、最初に同一画面上に両方の骨を一緒に描出する。
4. 下腿では脛骨は腓骨より常に長い。腓骨は脛骨より外側に位置し、脛骨より若干薄く描出される。脛骨がより近位側に位置し、遠位側では脛骨、腓骨ともほぼ同じレベルにある。
5. 前腕では尺骨は橈骨より長い。尺骨はより近位側に位置し、より遠位側にあるのが橈骨である。
6. 長管骨の計測は画像に描出しやすい方で左右どちらでも構わない。胎児がうつ伏せか仰向けでない限り両側の長管骨をすべて描出することは難しいし、また時間的にも無駄である。

7. 胎児の計測データは、出生後に出生児の体重、身長、頭囲、腹囲のデータをあわせて事務局の宮城県立こども病院（室月　淳）に報告する。

（胎児）
妊婦
↓
ＩＣ（研究分担者）
↓
計測
↓
データ
↓
匿名化、本学のとりまとめ　澤井
↓
登録事務局
　～宮城県立こども病院～
↓
統計処理　～胎児医学研究所～
↓
公表

8. 統計処理などは共同研究者である胎児医学研究所・篠塚憲男に委託する。

【登録数と研究期間】
登録数：一施設100計測で合計1,000計測を目標とした。
予定研究期間：平成22年年6月（倫理委員会承認後）より平成23年3月31日。
　宮城県立こども病院を中心に 9 施設で実施した。

【問い合わせ先】
適格基準など臨床的判断を要するもの：事務局（宮城県立こども病院　室月　淳）
記録用紙（CRF）記入など：胎児医学研究所（篠塚憲男）。
研究者などの登録など：事務局　宮城県立こども病院（室月　淳）。

C. 研究結果

超音波計測をおこなった正期産正常体重出生児のデータ。

分布の正規性を検討

　平均 f(x)　±　標準偏差　g(x) で　基準化する。

症例

	計測数	AFD	出生	±	体重	±	症例数	計測/症例
山口医療	183	167	39w2d	8.2	2989	343	89	
久留米大	468	462	39w4d	10	3046	338	108	
瀬戸	289	283	39w1d	7.2	2961	333	264	
春日井市民	107	103	39w6d	9.7	3062	276	103	
北大	99	96	39w0d	9.7	2972	333	32	
長良医療	31	31	37w6d	12.3	2924	428	31	
順天浦安	111	111	38w4d	10.8	2889	247	15	
宮城こども	61	54	39w2d	7.1	3067	278	38	
愛媛県中	328	326	39W3D	13.7	3047	416	51	
全体	1677	1633	39w1d	9.3	2995	344	731	2.29

施設間の計測値の解析

施設間（測定者間のばらつき）ＦＬ計測で解析

	25w	30w	36w
愛媛県中	44.4±2.5	53.9 ±2.5	65.8 ±2.7
北大		55.0 ±3.4	65.6 ±2.1
順天浦安	43.3±2.6	54.8 ±1.9	65.2 ±1.9
春日井	43.9±2.5		66.6 ±3.4
久留米大	43.9±1.4	55.1 ±2.3	65.7 ±2.3
宮城こども	45.5±0.7	54.3 ±2.1	63.0 ±3.5
長良	55.0 ±1.0	65.3 ±3.0	
瀬戸	42.8±2.21	54.6 ±1.7	64.0±2.6
山口医療	43.7±2.4	52.8 ±3.4	64.1±2.5

	ulna/HL	tibia/FL
愛媛県中	0.95±0.05	0.89±0.07
北大	0.96±0.06	0.89±0.04
順天浦安	0.95±0.05	0.90±0.04
春日井	0.95±0.05	0.89±0.04
久留米	0.95±0.05	0.89±0.04
宮城こども	0.96±0.04	0.90±0.04
長良医療	0.96±0.03	0.88±0.03
瀬戸	0.94±0.07	0.89±0.05
山口医療	0.95±0.09	0.89±0.03

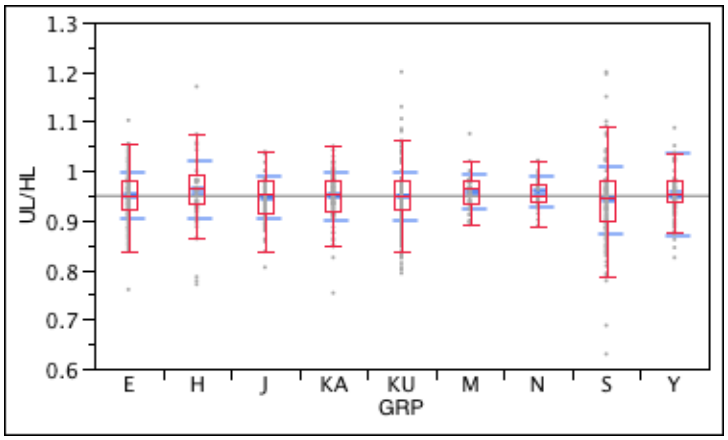

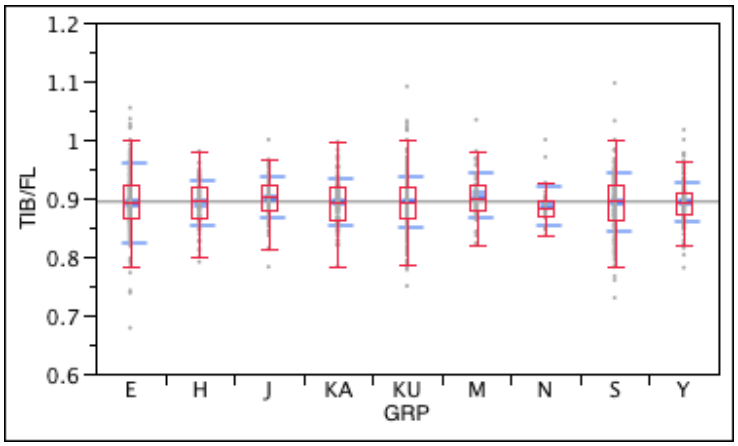

	RL/UL	tibia/FL
愛媛県中	0.89±0.05	0.96±0.03
北大	0.89±0.04	0.94±0.04
順天浦安	0.91±0.04	0.96±0.03
春日井	0.89±0.04	0.97±0.02
久留米	0.90±0.05	0.97±0.03
宮城こども	0.89±0.04	0.97±0.03
長良医療	0.88±0.04	0.98±0.03
瀬戸	0.91±0.04	0.94±0.03
山口医療	0.88±0.03	0.97±0.02

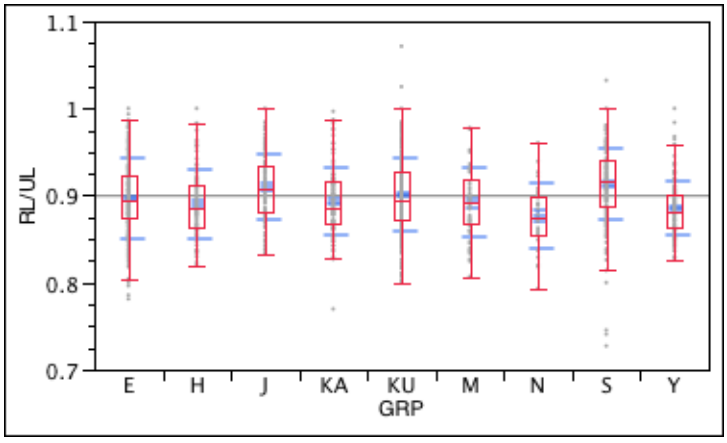

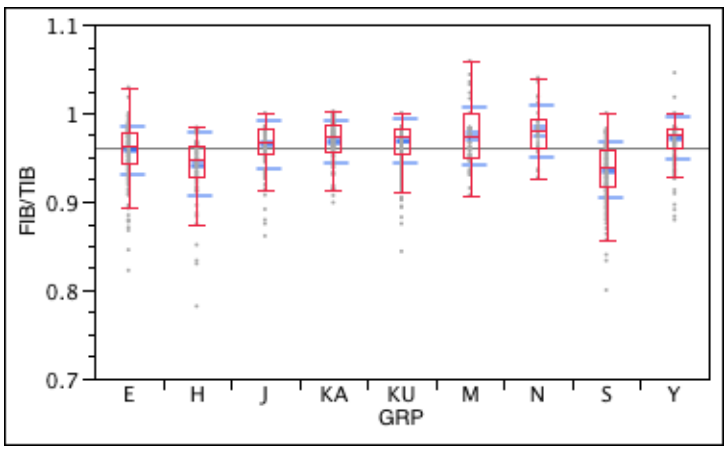

Ulna/radius と fibula/tibia の計測に関しては施設間にややばらつきがみられるが、FL や HL にくらべて計測がやや煩雑なことを表していると思われる． 超音波の計測精度を含め、統計的には無視しうる範囲のばらつきと考える。

FL

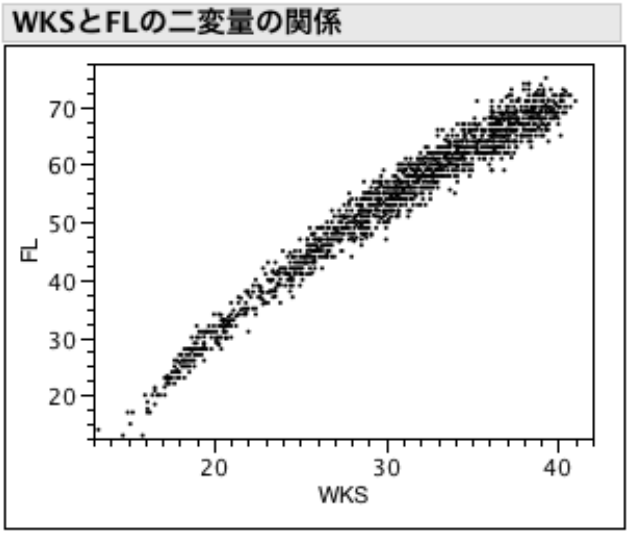

FL (Mean) =-25.89 + 0.37899* g + 4.3304*g*g*0.0001-2.0255*g*g*g*0.000001

FL(SD) =0.795 + 0.006658 * g

g =day

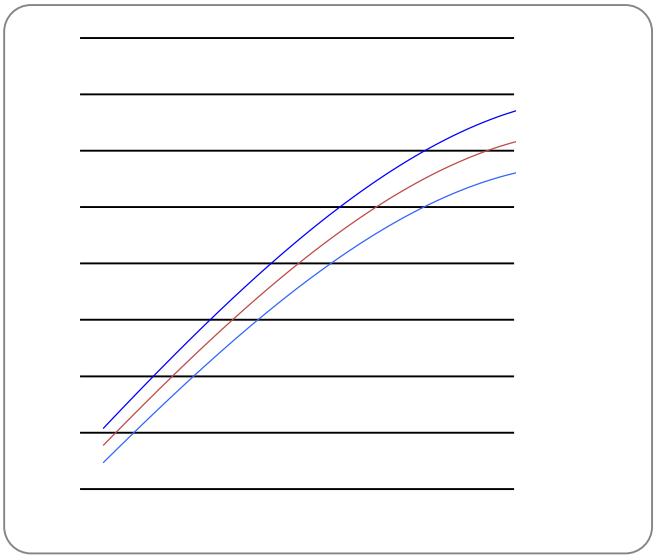

厚生労働科学研究費補助金（難治性疾患克服研究事業）
分担研究報告書

致死性骨異形成症の iPS 細胞作成に関する研究

研究分担者　京都大学 iPS 細胞研究所　細胞誘導制御学分野　教授　妻木範行

研究要旨

多くの骨系統疾患では病態が不明で、治療薬は存在しない。その理由の一つは、骨系統疾患の病変部、すなわち骨、軟骨が入手困難で、これらを用いた研究が行えないことによる。そこで将来の病態解明と治療薬探索に資することを目標に，患者皮膚線維芽細胞から等を作製し軟骨細胞を培養にて誘導することを行った。

共同研究者
澤井英明（兵庫医科大学　産科婦人科学）
室月淳（東北大学　発達成育医学講座胎児医学分野）
池川志郎（理化学研究所　統合生命医科学研 究センター　骨関節疾患研究チーム）

A. 研究目的

最近の研究により、いくつかの骨系統疾患については、原因遺伝子変異が明らかにされてきた。例えば、軟骨細胞外マトリックスであるＩＩ型コラーゲンの遺伝子や、軟骨細胞分化にかかわる増殖因子のレセプターである線維芽細胞増殖因子（FGF）受容体の遺伝子の変異が見つかっている。しかし、原因遺伝子がわかったとしても、多くの骨系統疾患では病態が不明で、治療薬は存在しない。ヒトの疾患細胞の中でどのような機序が働くことによって、症状が現れているかは、殆どわかっていない。その理由の一つは、骨系統疾患の病変部、すなわち骨、軟骨が入手困難で、これらを用いた研究が行えないことによる。そこで，本研究ではこれらの疾患に対して、疾患 iPS 細胞を用いたアプローチを行う。即ち、骨系統疾患患者の皮膚細胞から iPS 細胞を作成し、iPS 細胞から軟骨細胞を分化誘導する。その細胞を用いて、病態の解析を試み、治療薬の探索に役立てることを目標に研究を行う。

B. 研究方法

致死性骨異形成症および II 型コラーゲン病患者の皮膚を採取し、埼玉県立小児医療センターへ送付して線維芽細胞を樹立する。その線維芽細胞を京都大学 iPS 細胞研究所に導入し、iPS 細胞および軟骨細胞様細胞を直接誘導によって作製する。iPS 細胞は、エピソマールベクターを用いて作成し、軟骨細胞様細胞への誘導はレトロウイルスを用いて行う。

（倫理面への配慮）

骨系系統疾患患者から皮膚細胞を入手して iPS 細胞を作製、または軟骨細胞様細胞を直接誘導することについて、京都大学および埼玉県立小児医療センターの倫理委員会の審査を受け、承認を得た。

C. 研究結果

致死性骨異形成症 3 症例と II 型コラーゲン病 6 症例から線維芽細胞を入手した。うち、致死性骨異形成症 2 症例と II 型コラーゲン病 3 症例について、iPS 細胞を樹立し

ている。また、II 型コラーゲン病 2 症例について、軟骨細胞様細胞を直接誘導している。

D. 考察

致死性骨異形成症および II 型コラーゲン病において、iPS 細胞技術を用いて患者の線維芽細胞由来の iPS 細胞及び軟骨細胞様細胞を培養にて誘導することが可能になった。このことは今後、病態の解析と治療薬の探索に貢献すると考える。

E. 結論

致死性骨異形成症および II 型コラーゲン病において、患者の線維芽細胞由来の iPS 細胞及び軟骨細胞様細胞を培養にて誘導した。

F. 健康危険情報

無し

G. 研究発表

1. 論文発表

無し

2. 学会発表

1. 妻木範行、皮膚線維芽細胞から軟骨細胞様細胞へのダイレクト・リプログラミング、第 33 回日本炎症・再生医学会、博多、7/5-6
2. 妻木範行、カレントコンセプト：軟骨細胞リプログラミングによる関節軟骨疾患の治療戦略、第 30 回日本骨代謝学会、東京
3. 妻木範行、Meet the Expert: 軟骨マトリックス転写活性を指標にした、細胞リプログラミングによる軟骨細胞誘導、第 30 回日本骨代謝学会、東京、7/19-21
4. Tsumaki N, Regulation of differentiation and cell reprogramming of chondrocytes、Cold Spring Harbor Asia Conference, Bone and Cartilage 、Suzhou Dushu, China、6/11-15
5. Tsumaki N, Generation of induced chondrogenic cells directly from dermal fibroblast culture by defined factors、Internatinal Conference on Bone Morphogenetic Protein、Lake Tahoe, CA, USA、6/19-23
6. 妻木範行、再生医療の最前線－軟骨疾患をターゲットとして一、第 46 回日本小児内分泌学会学術集会、大阪、2012/9/27-29
7. 岡田稔、In vivo and In vitro Modeling of Type II Collagenopathy using Cell Reprogramming Technologies、第 13 回運動器科学研究会、京都市、2012/9/14-15
8. 妻木範行、細胞リプログラミング技術による軟骨疾患治療、日本整形外科学会 基礎学術集会 シンポジウム、名古屋市、2012/10/26-27
9. 岡田稔、妻木範行、細胞リプログラミング技術を用いた II 型コラーゲン病疾患モデルの解析、第 9 回 Skeletal Research Meeting、京都市、2012/11/10
10. 妻木範行、細胞リプログラミング技術を用いた軟骨疾患モデリング、第 5 回胎児骨系統疾患フォーラム、仙台市、2012/12/2
11. Okada, M.; Tsumaki, N.; Chondrogenic differentiation of human induced pluripotent stem cells, International Society for Stem Cell Research 10th annual meeting, Yokohama, 6/13-16

H. 知的財産権の出願・登録状況

無し

3. 特許取得

無し

4. 実用新案登録

無し

3. その他

無し

致死性骨異形成症の診断と予後に関する研究

研究分担者 芳賀 信彦 東京大学リハビリテーション科教授

研究要旨

2010 年版骨系統疾患国際分類の和訳に関する検討経過を振り返った。関連 3 学会から構成される WG で検討した結果、「致死性骨異形成症」を「タナトフォリック骨異形成症」、「窒息性胸郭異形成症」を「呼吸不全性胸郭異形成症」に変更した。

研究分担者
鬼頭　浩史（名古屋大学医学系研究科整形外科学）
室月　淳（宮城県立こども病院産科）

研究協力者
西村　玄（東京都立小児総合医療ｾﾝﾀｰ診療放射線科）

Ａ．研究目的

骨系統疾患には数多くの疾患が含まれ、その表現型、病態は多様である。これら多くの疾患を整理する目的で、1969 年に世界各国の専門家が集まり命名法、分類に関する話し合いが行われ、公表された。以後新しい疾患が加わり、また病態が解明されるに従い数回の改定を重ね、前回 2006 年の分類では疾患数は約 370 に上った。一方、日本整形外科学会の骨系統疾患委員会（2007 年より身障福祉・義肢装具等委員会と統合し小児整形外科委員会に改組）では 1983 年版の国際分類から和訳作業を続け、2006 年版の和訳は日整会誌、日本小児科学会雑誌に報告した。最新の 2010 年版国際分類は 2011 年に公表された。この間、産科医療の進歩により骨系統疾患の出生前診断が広く行われるようになってきたこと、また小児医療の進歩により全身管理を含めた小児科医による骨系統疾患の診療の幅が広がってきたことから、今回は日本整形外科学会小児整形外科委員会のもとに骨系統疾患国際分類和訳作業ワーキンググループ（WG）を立ち上げ、日本産科婦人科学会、日本小児科学会からもメンバーを推薦していただき和訳作業を行った。本研究の目的は、その和訳作業の経過を報告し、特に従来致死性・重症とされていた疾患の和訳に関する検討経過を明らかにすることである。

Ｂ．研究方法

平成 24 年 3 月 21 日に開催された第 1 回 WG 会合の議事録、ならびにその後のメール審議の経過を振り返った。

（倫理面への配慮）

本研究は患者の臨床情報を扱わない研究であり、倫理委員会への申請等は不要と考えた。

Ｃ．研究結果

2010 年版国際分類には 40 グループ 456 疾患が収められており、2006 年版の 37 グループ 372 疾患から大きく増えているが、対象疾患の考え方は 2006 年版と同じであ

る。316 の疾患（全体の 69%）で 226 の遺伝子との関連が明らかになっている。

和訳作業を行うことに関しては、平成 23 年 11 月に来日していた Andrea Superti-Furga（2010 年版国際分類の last author）に和訳作業の意義に関して芳賀が説明し、口頭で承諾を得た。その後日本産科婦人科学会、日本小児科学会に協力を呼びかけて WG に参加する会員の推薦を受け、7 名から構成される WG を立ち上げた。

平成 24 年 3 月に第 1 回 WG 会合を行い、その後はメールを用いて作業を進めた。この中でまず、基本的に 2006 年版までの和訳作業の方針を踏襲することとした。これを箇条書きにすると以下のようになる。

① 直訳を心掛ける。
② 日整会用語集に従うが、小児科用語集（日本小児科学会）、日本医学会医学用語辞典（日本医学会）等も参考にする。
③ dysplasia の和訳については、Stickler 骨異形成症のように Stickler 異形成症とすると骨疾患であることが分からなくなる場合には「骨異形成症」とし、多発性骨端異形成症のように骨疾患であることが明らかな場合には「異形成症」とする。
④ malformation を「奇形」ではなく「形態異常」、anomaly を「奇形」ではなく「異常」と訳す。
⑤ polydactyly など手指と足趾を合わせて指す用語の場合、日整会用語集のように「多指（趾）症」とせず「多指症」と訳す。
⑥ 人名の表記は原文のままとする。

以上に加えて、従来致死性・重症とされていた疾患の和訳を検討した。これは本研究班から thanatophoric dysplasia のこれまでの和訳である「致死性骨異形成症」について、以下の理由から再検討して欲しいとの要望が寄せられたためである。

① 医学的には必ずしも致死性ではなく、疾患名が実情を反映していないこと。
② 妊娠中に胎児が「致死性骨異形成症」の診断または疑いとされた場合に、両親がまだ生まれていない我が子に対して妊娠中から否定的な印象を抱く懸念があること。
③ 長期生存児の家族にとって、日々接している我が子の病名が「致死性･･･」ではやりきれない思いを抱かせること。
④ thanatophoric は古代ギリシア語を語源とし英語の意味は death bearing や lethal とされているが、米国では疾患名はあくまで thanatophoric dysplasia であり、古代ギリシア語を英語に翻訳しているわけではない。日本のように「致死性」と自国語に翻訳すると、その意味が患者家族に外国語のままよりも直裁的で強く伝わること。

以上を慎重に検討した結果、thanatophoric dysplasia については「タナトフォリック骨異形成症」の和訳を当てはめることに決定した。一方で、低フォスファターゼ症や骨形成不全症の分類の中にある lethal については、純粋な英単語であるとの認識から「致死性」の訳語を残すことにした。また、2006 年版まで窒息性胸郭異形成症と訳していた asphyxiating thoracic dysplasia については、「窒息性」という言葉の持つイメージを考慮し、今回は「呼吸不全性胸郭異形成症」の訳語を当てはめることにした。なお、やはり古代ギリシア語を語源とする言葉が用いられている疾患、例えば diastrophic dysplasia（捻曲性骨異形成症）や metatropic dysplasia

（変容性骨異形成症）については、和文の疾患名になじみが深いことから今回は訳語を変更しないことにした。

以上の方針に従い最終決定した和訳を別表に示す。(巻末に添付)

Ｄ．考察

今回の和訳作業は、初めて日本整形外科学会、日本産科婦人科学会、日本小児科学会のメンバーから構成される WG で行った。これにより、疾患数が前回の国際分類より大きく増えたものの、順調に作業を行うことができた。

中でも、従来致死性・重症とされていた疾患の和訳に関して十分な検討を行い、その結果、「致死性骨異形成症」を「タナトフォリック骨異形成症」、「窒息性胸郭異形成症」を「呼吸不全性胸郭異形成症」に変更した。これはこれまでに行われてきた国際分類の和訳作業の中ではきわめてまれな対応であり、学術的な意義のみならず、社会的なインパクトも大きいものと考える。

Ｅ．結論

2010 年版骨系統疾患国際分類の和訳に関する検討経過を報告した。この中で、従来致死性・重症とされていた疾患の和訳を検討した。その結果、「致死性骨異形成症」を「タナトフォリック骨異形成症」、「窒息性胸郭異形成症」を「呼吸不全性胸郭異形成症」に変更した。

Ｆ．健康危険情報

該当なし

Ｇ．研究発表

１．論文発表

1) Taketomi S, Hiraoka H, Nakagawa T, Miyamoto Y, Kuribayashi S, Fukuda A, Takeda H, Fukai A, Hirota J, Nakajima K, Haga N, Nakamura K: Osteochondral autograft for medial femoral condyle chondral lesions in a patient with multiple epiphyseal dysplasia: long-term result. J Orthop Sci 17: 507-511, 2012

2) Susami T, Mori Y, Tamura K, Ohkubo K, Nagahara K, Takahashi N, Uchino N, Uwatoko K, Haga N, Takato T: Facial morphology and occlusion of a patient with fibrodysplasia ossificans progressiva (FOP): Follow-up from 8 to 21 years of age. Spec Care Dentist 32: 165-170, 2012

3) Jiao S, Zhang Y, Ma W, Haga N: FOP in China and Japan: an overview from domestic literatures. Am J Med Genet Part A 161A: 892-893, 2013

２．学会発表

1) 山川陽子、鈴木竜洋、工藤孝弘、染谷朋之介、春名英典、鈴木光幸、青柳陽、清水俊明、片桐岳信、芳賀信彦: 本邦初の遺伝子異常を認めた進行性骨化性線維異形成症(FOP)の一女児例. 第 115 回日本小児科学会学術集会, 2012.4.20-22, 福岡

2) 滝川一晴、矢吹さゆみ、松岡夏子、芳賀信彦: 多発性軟骨性外骨腫症の足関節外反に対するスクリューを用いた脛骨遠位内側部分骨端線閉鎖術の治療成績. 第 85 回日本整形外科学会, 2012.5.17-20, 京都

3) 芳賀信彦: 2010 国際分類和訳作業を通して(講演).第 24 回日本整形外科学会骨系統疾患研究会, 2012.12.1, 福岡

4) Haga N, Nakahara Y, Ogata N: Ambulation and its Support in Patients with Fibrodysplasia Ossificans Progressiva. The 14th Congress of the

International Society for Prosthetics and Orthotics, 2013.2.4-7, Hyderabad (India)

H．知的財産権の出願・登録状況

該当なし

症例の収集と診断の支援システム構築

研究分担者	室月　淳	宮城県立こども病院　部長
	澤井英明	兵庫医科大学　准教授
	山田崇弘	北海道大学　助教
	堤　誠司	山形大学　講師
	佐藤秀平	青森県立中央病院　センター長
	林　聡	国立成育医療研究センター　医長
	篠塚憲男	胎児医学研究所　代表
	高橋雄一郎	長良医療センター　医長
	佐世正勝	山口県立総合医療センター　センター長
	鬼頭浩史	名古屋大学　講師
	沼部博直	京都大学　准教授
	宮崎　治	国立成育医療研究センター　医長
	緒方　勤	浜松医科大学　教授
	池川志郎	理化学研究所ゲノム医科学研究センター　チームリーダー
	妻木範行	京都大学 iPS 細胞研究所（CiRA）　教授
	芳賀信彦	東京大学　教授
研究協力者	西村　玄	東京都立小児総合医療センター　部長

研究要旨　本研究は出生前に超音波検査で指摘された骨系統疾患疑いの胎児に対してどのように診断をアプローチし、その後の妊娠管理をどのように行い、分娩方式はどのようにして決定し、新生児管理に結びつけるかについて広範な専門集団が支援するシステムを構築するものである。具体的には１）インターネット利用による胎児の骨系統疾患を診断支援するための症例検討システムの構築、２）セキュリティの充実したウェブ閲覧型システムを構築して臨床医の診断の支援、３）過去の症例検討のとりまとめ、４）地域ごとの診断支援システムの構築、５）臨床医への情報提供、６）一般の妊婦や罹患児を持つ家族への情報提供といったシステム化されたフローを構築することである。

A. 研究目的

本研究は出生前に超音波検査で指摘された骨系統疾患疑いの胎児に対してどのように診断をアプローチし、その後の妊娠管理をどのように行い、分娩方式はどのようにして決定し、新生児管理に結びつけるかについて広範な専門集団が支援するシステムを構築するものである。

B. 研究方法

１）インターネット利用による胎児の骨系統疾患を診断支援するための症例検討システムの構築は、システムを兵庫医科大学の協力により同大学にサーバーを設置して、運営する。また専門システム開発業者とともにシステムの設計を行う。

２）上記システムを用いて、実際に臨床医から問合せのあった症例の検討を行う。

３）過去の症例検討のとりまとめは、」上記のウェブ上のシステム構築までの段階で全国の症例を検討した 2,800 通以上のメールの内容の解析と症例の分析を行う。

４）地域ごとに胎児骨系統疾患に詳しい産科の専門家を配置し、地域の医療機関からの相談に乗る体制を構築する。

５）胎児骨系統疾患フォーラムと共同で臨床医への情報提供を目的に、講演会を開催し、またホームページでの情報提供を行う。

６）一般の妊婦や罹患児を持つ家族への情報提供をホームページを作成して行う。

C. 研究結果

１）システムの構築をすでに完了して、試行したが、一部改変を必要とするため現在は作業中である。今年度中にはウェブ上に匿名化して症例の経過と画像をアップして症例登録を行い、専門家グループで討議して診断を支援するシステムが運用開始できる予定である。

２）来年度から完全な形での運用を開始予定である。

３）過去の症例をとりまとめて日本周産期学会にて発表した。

４）研究班の研究分担者の属する施設を中心に、北海道、東北、東京、神奈川、東海、近畿、中国、四国、九州においてセンター施設を選定した。

５）平成 23 年 11 月 13 日（日）と平成 24 年 12 月 2 日（日）に本研究班会議と胎児骨系統疾患フォーラムが共催して、一般臨床医を含めた医師を対象に第４回胎児骨系統疾患フォーラムを開催し、致死性骨異形成症を含めた胎児骨系統疾患の新生児管理について集中的な情報提供と討議を行った。

また、本研究班で致死性骨異形成症のホームページ www.thanatophoric.com を作成し骨系統疾患の情報を提供し、診断や治療に取り組む産科医や小児科医などからの問い合わせを受け付ける体制を作った。すでに地域の病院（産科）や患者家族から複数件の問い合わせがあり、上記の地域診断支援システムに紹介して対応した。

６）ホームページにおいて情報発信を行っている。

D. 考察

本研究においては今年度で個別に体制はほぼ完成した。引き続き情報を更新して行きたいと考えている。

E. 結論

出生前に超音波検査で指摘された骨系統疾患疑いの胎児に対してどのように診断をアプローチし、その後の妊娠管理をどのように行い、分娩方式はどのようにして決定し、新生児管理に結びつけるかについて広範な専門集団が支援するシステムを構築した。また患者家族が情報を得ることができるウェブサイトも構築した。

F. 健康危険情報

なし

G. 研究発表

なし

H. 知的財産権の出願・登録状況　なし

胎児骨系統疾患の出生前診断と周産期ケアのガイドライン作成に関する小委員会　平成 24 年度活動報告

研究分担者　　**室月　淳、篠塚憲男，佐世正勝，林聡，山田崇弘**
研究代表者　　**澤井英明，**

日本産科婦人科学会周産期委員会（平成 25 年 2 月 1 日，砂防会館）

1.　メンバー

室月淳（小委員長），澤井英明，篠塚憲男，佐世正勝，林聡，山田崇弘，望月純子

2.　1 年間の活動

3 月 21 日（水）　骨系統疾患国際分類和訳作業ワーキンググループ会議（日整会事務局，東京）

5 月 25 日（金）　第 1 回小委員会（日産婦周産期委員会，東京ステーションコンファランス）

12 月 1 日（日）　第 2 回小委員会（第 5 回胎児骨系統疾患フォーラム，仙台市情報産業プラザ）

厚生労働科学研究費補助金（澤井班）班会議

2 月 2 日（金）　第 3 回小委員会（日産婦周産期委員会，砂防会館）

3.　報告・承認事項

(1)「産科婦人科用語集･用語解説集」における骨系統疾患関連の改訂（資料 1）→【終了】

(2)　骨系統疾患国際分類（2010 年版）の和訳作業　→【ほぼ終了】

・3 月 21 日和訳作業ワーキンググループ打ち合わせ会（日本整形外科学会事務局），以後，メールでの検討作業

・thanatophoric dysplasia → タナトフォリック骨異形成症

・hypophosphatasia perinatal lethal type　→　低フォスファターゼ症周産期型→従来のとおり

・asphyxiating thoracic dysplasia → ①呼吸不全性胸郭異形成症

・「2010 年版骨系統疾患国際分類の和訳」ができあがったら論文として日本整形外科学会誌に発表（資料 2），日産婦理事会の承認の上で日産婦誌でも公表をめざす

・「産科婦人科用語集・用語解説集」を初め，「日本医学会医学用語辞典」（日本医学会），「先天異常用語集」（日本先天異常学会）などにも用語統一の働きかけを行う

(3) 長管骨基準値作成 →【ほぼ終了】

・Dr 篠塚の解析報告（資料 3）

・日本人の超音波基本計測値の基準化において報告された方法を用い，胎児長長幹骨の基準値を作成した．具体的には正期産・正常体重出生児（AFD）のデータを用い，理想的な子宮内環境において発育は正規分布するという仮定に基づき，基準値を平均 f(x)　±　標準偏差　g(x) で数値化した．平均値の回帰式は妊娠日数 g を変数とし、

stepwise を用い 3 次までの変数に対して，Mallows の CP index および AIC を変数選択の基準とし，回帰式を作成、基準値を設定した
・研究データ協力施設(宮城県立こども病院，北海道大学，順天堂大学浦安病院,長良医療センター,山口県立総合医療センター,愛媛県立病院,春日井市民病院，久留米大学，兵庫医科大学)
・作成終了し公表，論文化，超音波機器へのプログラム搭載をめざす

(4) 骨系統疾患の疾患遺伝子および解説可能施設の情報収集 →【継続】
・データベースの作成およびコンサルテーションシステムの確立
・胎児骨系統疾患フォーラムが受け皿？

(5) 骨系統疾患症例登録システム →【ほぼ手つかず】
・厚労科研澤井班の症例登録システムの導入

(6) 胎児 CT の適応ガイドライン作成 →【継続】
・日本産科婦人科学会と日本医学放射線学会によるワーキンググループ
　→理事会承認
・胎児 CT の適応の検討，推奨プロトコールの作成などを検討する

【資料 2】論文の表紙

表題）2010 年版骨系統疾患国際分類の和訳
The Japanese Translation of “Nosology and Classification of Genetic Skeletal Disorders: 2010 Revision”

著者所属）
1)日本整形外科学会 小児整形外科委員会，2)東京大学大学院医学系研究科リハビリテーション医学分野，3)札幌医科大学医学部整形外科，4)名古屋大学大学院医学系研究科整形外科学教室，5)静岡県立こども病院整形外科，6)日本小児科学会，7)岡山済生会総合病院小児科，8)東京都立小児総合医療センター診療放射線科，9)日本産科婦人科学会,10)宮城県立こども病院産科,11)東北大学大学院医学系研究科胎児医学分野

著者氏名）
日本整形外科学会 小児整形外科委員会 骨系統疾患和訳作業ワーキンググループ
芳賀信彦 1,2、射場浩介 1,3、鬼頭浩史 1,4、滝川一晴 1,5、田中弘之 6,7、西村玄 1,8、室月淳 9,10,11、

キーワード）和訳、遺伝性骨疾患、骨系統疾患、国際分類
Japanese Translation, Genetic skeletal disorders, Skeletal dysplasia, Nosology and classification

（資料 1)「産科婦人科用語集・用語解説集」における骨系統疾患関連の改訂

1. 不適切な用語の削除
・「小人症」,「侏儒」を削除（差別的なニュアンスがあるため現在では使用されない）
・「胎児軟骨発育不全[症]」,「軟骨異栄養症」,「軟骨発育不全[症]」を削除
（chondrodystrophy という語が現在では使用されないため）
・p236「胎児軟骨発育不全[症]」とその解説を削除する
（chondrodystrophy という概念がすでにないこと，achondroplasia との混同が認められること）

2. 用語の一部修正
・「骨形成不全[症] (E)osteogenesis imperfecta, dysosteogenesis, dystosis (D)Osteopsathyrose, Osteogenesis imperfecta」→「骨形成不全症 (E)osteogenesis imperfecta」
・「骨軟骨異形成 (E)osteochondrodysplasia」→「骨軟骨異形成症 (E)osteochondrodysplasia」
・「achondroplasia 軟骨発育不全[症]」→「achondroplasia 軟骨無形成症」
・「osteochondrodysplasia 骨軟骨異形成」→「osteochondrodysplasia 骨軟骨異形成症」
・「osteogenesis imperfecta 骨形成不全[症]」→「osteogenesis imperfecta 骨形成不全症」

3. 新たな用語の追加
・「用語解説」に追加する用語とその解説

骨形成不全症 osteogenesis imperfecta

易骨折性，青色強膜，歯牙形成不全症，難聴，関節弛緩などを示す一群の骨系統疾患である．骨系統疾患の中では最も頻度の高いものの一つである．骨折はしばしば胎児期から発症する．成人期
以降に X 線検査等で偶然発見されるような軽症型から，周産期に死亡する重症型までさまざまな予後を示す．多くはⅠ型コラーゲン遺伝子(*COL1A1, COL1A2* の２つが存在する）の優性変異によって発症する．別の原因遺伝子による常染色体劣性遺伝も存在する．非罹患両親からの同胞再発例がしばしば認められため遺伝カウンセリング上の問題となるが，両親が上記の常染色体劣性の遺伝子異常の保因者の場合や，両親のどちらかが Ⅰ 型コラーゲン遺伝子変異の性腺モザイクの場合などが知られている．画像診断上の特徴としては，長管骨の骨折や彎曲像，肋骨の数珠様変形，頭蓋骨の膜性骨化不全などが重要である．

骨系統疾患　skeletal dysplasia, bone dysplasia

骨系統疾患は骨格の成長・発達・分化の異常をきたす疾患の総称である．主病変は骨や軟骨にあり，X 線上の形態変化を伴う．全身性の異常で，発達とともに病変の進行が認められる骨軟骨異形成症 osteochondrodysplasia と，頭蓋，四肢，脊椎など骨格の特定の部位に形態異常が限局する異骨症 dysostosis のふたつに大別される．最新の骨系統疾患国際分類（2010 年）では，40 グループ 456 疾患名が挙げられている．骨系統疾患はひとつひとつはきわめてまれであるが，全体としては千人にひとりの発生率で頻度は高い．胎児骨系統疾患 fetal skeletal dysplasia は，出生時にすでに症状が出現している骨系統疾患である．骨系統疾患の全体の半数以上を占めると推定され，出生前診断や周産期管理の対象となっている．なお過去には dwarfism の訳として小人症，侏儒ということばが臨床で使われてきたが，差別的な印象を与えるので現在は使用されな い．

致死性骨異形成症 thanatophoric dysplasia

胎児期から発症する重症型の骨系統疾患である．4 番染色体短腕上にある線維芽細胞増殖因子受容体 3（FGFR3）遺伝子の変異が原因である．変異は優性で，FGFR3 の機能が過剰に亢進し，成長軟骨の形成が阻害される．出生児（死産を含む）の 1/20,000～1/50,000 程度で認められる．主な特徴は長管骨（特に上腕骨と大腿骨）の著明な短縮で，肋骨の短縮による胸郭低形成により出生前は羊水過多，出生後は重度の呼吸障害を来す．巨大頭蓋と前頭部突出を示し，顔面は比較的低形成である．出生後のＸ線所見から，大腿骨が彎曲（受話器様変形）し頭蓋骨の変形のない１型と，大腿骨の彎曲は少なく頭蓋骨がクローバー葉様に変形した２型に分類される．従来は周産期致死性とされてきたが，近年の呼吸管理の進歩により数多くの長期生存例が報告されており，もはや致死性ということばはそぐわなくなっている．

軟骨無形成症 achondroplasia

四肢短縮型の骨系統疾患で，頻度は約 1～2 万出生に 1 人程度とされる．知的障害はなく生命予後も良好である．低身長や，前額部の突出，鼻根部の陥凹，顔面正中部の低形成などによる特徴的な顔貌といった臨床像を呈する。出生時の低身長は目立たないこともあり出生前後にはしばしば見逃されるが，生後 1 年以内に低身長を初めとした特徴的所見が明らかになる．超音波検査による非特異的な所見として妊娠 22 週以降の長幹骨短縮，大きめな児頭大横径（BPD），三尖手(trident hand)がある．胎児 CT を併用することにより診断的所見である大腿骨近位部の帯状透亮像が確認できる．原因は 4 番染色体短腕上にある線維芽細胞増殖因子受容体 3（FGFR3）遺伝子の変異である．常染色体優性の遺伝形式をとるが，約 80%は散発性で，父親側の精子の突然変異がほとんどである．軟骨無形成症の患者同士の子どもの 25%に生じるホモ接合体は重症型で出生後早期に死亡することが多い．

低フォスファターゼ症　hypophosphatasia

組織非特異的（骨，肝臓，腎臓由来）アルカリフォスファターゼ tissue nonspecific alkaline phosphatase（TNSALP）の機能低下により骨化不全や歯のミネラル化異常を来す疾患である．1 番染色体短腕上にある TNSALP 遺伝子変異が原因である．遺伝形式の多くは常染色体劣性，一部は常染色体優性を示す．症状の程度はさまざまで，重症度により周産期型，乳児型，小児型，成人型，歯限局型に区別される．最重症型の周産期型では骨化がほとんど認められず，四肢短縮と柔らかく容易に変形する比較的大きな頭蓋，胸郭低形成が特徴であり，出生直後より呼吸不全をきたし早期に死亡することも多い．臍帯血や末梢血の血清 ALP 値は極めて低い．周産期型は欧米に比べ日本人の発症頻度は高く，日本人にのみ報告されている特異的な遺伝子変異（1559delT）によるものであり，両親が近親婚でなくてもホモ接合体の罹患者もまれではない．

GW	HL	HL-SD	UL	UL-SD	RL	RL-SD	TIB	TIB-SD	FIB	FIB-SD
16-0	18.5	1.8	16.3	1.8	14.3	1.5	15.6	1.6	13.9	1.6
17-0	21.3	1.9	19.3	1.9	17.2	1.6	18.6	1.7	17.0	1.7
18-0	23.9	1.9	22.1	1.9	19.9	1.7	21.5	1.7	20.0	1.7
19-0	26.5	2.0	24.7	2.0	22.4	1.7	24.3	1.8	22.9	1.8
20-0	29.0	2.0	27.2	2.0	24.7	1.8	27.0	1.9	25.6	1.9
21-0	31.3	2.1	29.6	2.1	26.9	1.9	29.6	1.9	28.1	1.9
22-0	33.6	2.1	31.8	2.1	29.0	2.0	32.0	2.0	30.6	2.0
23-0	35.8	2.1	34.0	2.2	30.9	2.1	34.4	2.0	32.9	2.0
24-0	37.9	2.2	36.0	2.3	32.7	2.1	36.7	2.1	35.1	2.1
25-0	39.9	2.2	37.9	2.3	34.4	2.2	38.9	2.2	37.3	2.2
26-0	41.8	2.3	39.7	2.4	35.9	2.3	40.9	2.2	39.3	2.2
27-0	43.6	2.3	41.4	2.4	37.4	2.4	42.9	2.3	41.2	2.3
28-0	45.3	2.4	43.1	2.5	38.8	2.5	44.8	2.4	43.0	2.4
29-0	47.0	2.4	44.6	2.5	40.1	2.5	46.7	2.4	44.8	2.4
30-0	48.6	2.5	46.1	2.6	41.4	2.6	48.4	2.5	46.5	2.5
31-0	50.1	2.5	47.5	2.7	42.6	2.7	50.1	2.5	48.1	2.5
32-0	51.5	2.6	48.9	2.7	43.8	2.8	51.7	2.6	49.6	2.6
33-0	52.9	2.6	50.3	2.8	44.9	2.8	53.2	2.7	51.1	2.7
34-0	54.2	2.6	51.5	2.8	46.0	2.9	54.7	2.7	52.5	2.7
35-0	55.4	2.7	52.8	2.9	47.1	3.0	56.0	2.8	53.9	2.8
36-0	56.6	2.7	54.1	2.9	48.2	3.1	57.4	2.8	55.2	2.8
37-0	57.7	2.8	55.3	3.0	49.3	3.2	58.6	2.9	56.5	2.9
38-0	58.8	2.8	56.5	3.0	50.5	3.2	59.8	3.0	57.7	3.0
39-0	59.8	2.9	57.7	3.1	51.6	3.3	61.0	3.0	59.0	3.0
40-0	60.7	2.9	58.9	3.2	52.8	3.4	62.1	3.1	60.2	3.1
41-0	61.6	3.0	60.2	3.2	54.1	3.5	63.2	3.2	61.3	3.2

致死性骨異形成症の発達調査

研究代表者　兵庫医科大学　准教授　澤井英明
研究協力者　兵庫医科大学　大学院生　潮田まり子
兵庫医科大学　認定遺伝カウンセラー　守井見奈

研究要旨　全国 1 次調査として症例数と概要を明らかにし、73 例（うち生産 51 例、死産 4 例、流産 15 例）を把握した。結果は致死性という名称にもかかわらず、周産期死亡率は 56%であった。周産期死亡を起こさなかった 24 例のうち 16 例は 1 年以上生存しており、これは生産児の 31%にあたる。H23 年度は長期生存例の発達や経過を明らかする 2 次調査を開始し平成 24 年度にデータ収集を終了した。この結果によると致死性骨異形成症はその名称とは異なり、周産期致死性とは必ずしも言えず、またこの疾患名が患児を育てている家族にとって違和感のある名称であることが明らかとなった。

症例 1　TD I
調査協力者　担当医師・母親

遺伝子変異　742C>T
生年月日　H2.5.28
調査時年齢　22 歳 4 か月
性別　男
出生時父親年齢　31 歳/母親年齢 29 歳
出生時週数　36 週 5 日
出生前診断　超音波のみ
　　四肢短縮・胸郭低形成・羊水過多
分娩方法　帝王切開
アプガースコア　4 点/1 分、6 点/5 分
体重 2798g
身長・頭周囲長　不明
レントゲン所見　TD 所見
蘇生処置　有（詳細不明）
合併奇形　裂手

＜呼吸管理法＞
出生直後は不明
出生後 2 時間より人工換気（SIMV）
生後 6 か月までは啼泣の度にチアノーゼあり bagging が頻回に必要
月齢 8 に気管切開施行
1 歳 1 か月　長時間の自己抜管にて心停止および低酸素状態
現在もレスピレーターに依存し、自発呼吸は認めず

＜栄養方法＞
完全経管栄養管理（経鼻胃チューブ）
月齢 8 の時に離乳食を始めたが、咀嚼・嚥下ともにうまくいかず。
卵アレルギーあり
最終的に離乳食はうまくいかず、中止となる。

＜合併症＞

無酸素脳症（自己抜管による）
四肢麻痺（低酸素脳症に起因するものと考えられる）
痙攣（足クローヌス、目の上転、舌をだす）
てんかん（脳波異常あり）
呼吸器感染症
気管部肉芽形成（カニューラのサイズアップにより対応）
便秘
黒色表皮腫（全身）1 歳ころより認めていた
褥瘡
胃潰瘍（NICU 在室時のみ）
浮腫（1 歳時）原因不明。水分制限およびラシックスにて改善
ITP（7 歳児）プレドニン著効し 1 か月で治癒

＜精神・運動発達＞
発達遅延あり
四肢麻痺あり寝たきり
人に向かってにこにこ笑いかける
人を求めて泣く
嫌な時は表情が変化しているようにも感じ取れる
有意語ではないあーあーという発語のみ（11 歳時に声変わりあり）

＜歯牙＞
正常な発達
永久歯あり

＜身体発育＞

＜両親の心情＞
＞出生前
出生前より異常を指摘され、非常に動揺した。
生存の可能性は低いといわれ、人工呼吸器の使用をするかを聞かれた。
しかし、二人の間に生まれてくる子供であり、出生前に出生後の方針を決める事はできなかった。出生後に何もしないのは見殺しにするような気持ちになると思った。
最終的には死ぬために生まれてきたわけではないから、挿管を希望した。
蘇生を希望した事が正しい選択であったかはわからないが、ほっとした。
＞出生後
病名を聞いたときは致死性に加えて、手足も短いということでショックであった。
致死性という名前から、常にタイムリミットを感じながら過ごしている。
しかし 22 年が経過し、病名に違和感を感じている。
＞その他
入院中に院内学級に参加して、卒業までできた。
学校に行くときは表情が変化していき、楽しい時間もある。
致死性という名前は生きている事自体が悪いといわれているみたいであり、チャンスがないような感じがする。
病気だからあきらめるわけではなく、チャンスも与えてほしい。
生きていく中で、この子も成長しているのです。
＞遺伝子検査を受けるにあたって
自分がうつしてしまった病気ではないかと心配であった。
遺伝子検査をしてはっきりとした病名を知ることができ、逆に安心した。
何か解決するわけではなかったが、心が楽

になった。
自分の子供だけが特殊な病気になったのではなく、他にも同じ病気の人がいるんだと知ることができてよかった。

症例 2　TD I
調査協力者　担当医師

遺伝子変異　検査未
生年月日　H17.3.30
調査時年齢　7 歳 7 か月
性別　女
出生時父親年齢　35 歳/母親年齢 34 歳
出生時週数　40 週 3 日
出生前診断　有
分娩方法　経膣分娩（吸引分娩）
アプガースコア　8 点/1 分、4 点/5 分　啼泣あり
体重 2978g
身長 38 ㎝
頭周囲長 38 ㎝
身長・頭周囲長　不明
レントゲン所見　TD 所見
蘇生処置　有（出生直後から吸引→マスク換気→挿管）
合併奇形　無

＜呼吸管理＞
出生時　HFO
生後 12 日　IMV
生後 2.5 か月　SIMV(LTV)
日齢 51　気管切開（肺低形成で抜管困難であるため）
3.5 歳より在宅に向けて準備
2011.3 月に退院
自己抜管なし

＜栄養方法＞
普通食摂取
食欲もあり、咀嚼も問題なし
食べ物の好き嫌いあり
誤嚥のエピソードもなし

＜合併症＞
痙攣（年 1 回程度の短時間の強直性痙攣、治療は行っていない）
脳波異常なし
急性呼吸窮迫症候群
便秘
黒色表皮腫　年月とともに増加
　　全体的に浅黒いが、関節部が目立つ
大後頭孔狭窄（1 歳児に解除術施行）
水頭症（脳実質委縮、脳室拡大）

＜精神・運動発達＞
車いす（補助具あり）使用にて移動可
運動面　3 歳頃から動きが活発になってきた
　　手足をよく動かす
　　背中でずりばいで移動（体が回転する）
精神面　笑う
　　簡単な指示がわかる
　　簡単なルールがわかる（我慢をしている様子がある）
　　音楽に合わせてタンバリンを鳴らす
　　人の区別をしている（お気に入りの看護師さんだと表情が違う）

欲求（空腹時）をあーあーという言葉で表現する
食事が楽しみである

＜歯芽＞
正常発育
乳歯および永久歯あり

＜リハビリテーション＞
月 2 回

症例 3
調査協力者　母親

遺伝子検査　未
生年月日　H16.5.8
調査時年齢　8 歳 7 か月
性別　男
出生時父親年齢　34 歳/母親年齢 31 歳
出生時週数　35 週 2 日
出生前診断　超音波のみ（27 週時）
四肢短縮・胸郭低形成・羊水過多
分娩方法　帝王切開（胎児適応）
アプガースコア　1 点/1 分、2 点/5 分
体重 2783g
身長 35 ㎝
頭周囲長 32.3 ㎝
胸囲 27.9 ㎝
レントゲン所見　情報なし
蘇生処置　有（出生直後より気管内挿管）
合併奇形　無

＜呼吸管理＞
出生直後より著しい呼吸障害の為、気管内挿管の上人工換気開始。肺低形成、遷延性肺高血圧のため HFO 管理開始。酸素化が悪いため NO 吸入療法開始（3 日間）。
生後一か月で自発呼吸は安定するも、呼気陽圧が必要であり、終末呼気陽圧人工換気を使用。
日齢 131 気管切開
現在在宅にてレジェンドエア使用中

＜栄養管理＞
日齢 144　経口哺乳開始
2 歳時に喘息症状出現し、その後哺乳意欲消失となり経口哺乳は中止となる。
経鼻胃チューブでの経管栄養を行っていたが、誤嚥性肺炎を認めたため、胃瘻造設。

＜合併症＞
痙攣（熱上昇があるとおこりやすい、強直性痙攣）
脳波異常なし
呼吸器感染症
便秘
黒色表皮腫（全体的に浅黒いが、額および足が特に著明）
大後頭孔狭窄（手術は脳外科に不可能と言われている）

＜その他＞
猿線あり

＜リハビリテーション＞
現在は施行せず
入院中は関節リハを行っていた。
リハビリで手足の動きはました

＜精神・運動発達＞

手足の動きあり
あやすと笑う
顔をしかめる
人の区別はできている印象（家族）

＜歯芽＞
乳歯と永久歯あり

＜在宅療法＞
訪問看護 5 回/週
往診 1 回/週

症例 4
調査協力者　担当医師・両親

遺伝子変異　Arg248Cys
生年月日　H22.11. 2
調査時年齢　2 歳
性別　男
出生時父親年齢　37 歳/母親年齢 37 歳
出生時週数　37 週 5 日
出生前診断　有（CT）
分娩方法　帝王切開（胎児適応）
アプガースコア　6 点/1 分、8 点/5 分
体重 2800g
身長 39 ㎝
頭周囲長 37.5 ㎝
レントゲン所見　TD 所見
蘇生処置　有（出生直後から）
合併奇形　無

＜呼吸管理＞
HFO および SIMV を交互に
日齢 97　気管切開
日齢 131　在宅用呼吸器（トリロジー）
無気肺のエピソードあり
日齢 479　院内用呼吸器
自発呼吸と人工呼吸器の換気が合いにくいため、現在はトリロジーX にて管理中

＜栄養方法＞
離乳食摂取
呼吸機能の事を考慮して、水分制限を行っている

＜リハビリテーション＞
生後 1 か月より呼吸リハ開始
7 か月～1 歳 6 か月　ミルク経口量アップと離乳食の導入目的で ST 開始
ST→言語聴覚りは、嚥下状態の把握
現在作業療法開始
＜合併症＞
痙攣（4 か月より顔面半側痙攣）
脳波異常
てんかん
呼吸器感染症
洞性除脈
便秘
黒色表皮腫
甲状腺機能低下（治療はなし）
無気肺（H24,2 月）
大後頭孔狭窄
水頭症経度

＜精神・運動発達＞
介助をするとぼーろを手でつかみ、口元にもっていく
対立動作は不可
手足の動きあり
笑う

簡単な指示はわかる
自分の気もちをジェスチャーで伝える（いやいや、ちょうだい）
人見知りあり（人の区別ありそう）

＜歯芽＞
乳歯あり

＜その他＞
移動時ようのバギーあり（補助具装着）

症例 5
調査協力者　担当医師

遺伝子検査　Arg248Cys
生年月日　H23.8.9
調査時年齢　1 歳 5 か月
性別　男
出生時父親年齢　歳/母親年齢歳
出生時週数　38 週 2 日
出生前診断　無
分娩方法　経膣分娩
アプガースコア　2 点/1 分、6 点/5 分
体重 2528g
身長 37 ㎝
頭周囲長 37 ㎝
レントゲン所見　TD 様所見
蘇生処置　有（出生直後から酸素投与）
合併奇形　無

＜呼吸管理＞
HFO
生後 38 日　気管切開
生後 107 日　在宅呼吸器導入
生後 178 日　在宅へ
汎用人工呼吸器レジェンドエアー（エアロックス社）
努力呼吸があるのに 1 回換気量が増えるエピソードがあるので PIP 設定が難しい
本人の呼吸 flow を器械が感知しにくい

＜栄養管理＞
経鼻栄養から開始
現在経鼻（ミルク、白湯）+離乳食（1～2 回/日）+経口（ミルク、イオン飲料、果汁）

＜リハビリテーション＞
呼吸リハ　1 回/週
保育士訪問　1～2 回/月
歯科衛生士訪
＜合併症＞
痙攣（間代性、眼球変位）
脳波異常なし
呼吸器感染症
便秘
黒色表皮腫（全体的に浅黒いが、足が特に著明）
褥瘡
遷延性肺高血圧（出生後 7 日間 NO 使用）
気管支内肉芽
右鼠径ヘルニア

<精神・運動発達＞
追視
音のする方を見る
なん語
笑う
泣く
顔をしかめる
人見知りあり
人に来てもらいたいときは鈴を鳴らす

手ではらいのける

＜その他＞
猿線あり

＜リハビリテーション＞
現在は施行せず
入院中は関節リハを行っていた。
リハビリで手足の動きはました

＜精神・運動発達＞
手足の動きあり
あやすと笑う
顔をしかめる
人の区別はできている印象（家族）

＜歯芽＞
乳歯と永久歯あり

＜在宅療法＞
訪問看護 5 回/週
往診 1 回/週

症例 6

調査協力者　担当医師・母親

遺伝子検査　未
生年月日　H21．10.30
調査時年齢　3 歳 2 ヶ月
性別　男
出生時父親年齢　昭和 54 年生/母親年齢 昭和 55 年生
出生時週数　38 週 0 日
出生前診断　超音波および CT
四肢短縮・胸郭低形成・羊水過多
分娩方法　経膣分娩（C/S のリスクよりも母体の安全性のため）
アプガースコア　8 点/1 分、9 点/5 分
体重 2362g
身長 40 ㎝
頭周囲長 36 ㎝
胸囲 26 ㎝
レントゲン所見　情報なし
蘇生処置　有（酸素投与）
合併奇形　無

＜呼吸管理＞
看取り予定であり、最初は酸素投与のみであったが 24 時間経過後も自発呼吸および酸素投与にて生存していたため、積極的な医療介入となる。
nasalCPAP および酸素投与を行っていたが、急変時の気道維持が困難である事から気管切開を日齢 187 で施行（在宅療法に向けての意味合いもある）
生後 320 日に呼吸不全をおこしたため、呼吸器導入（フィリップス LTV1200）
現在在宅でクリーンエア VEILA 使用

＜栄養管理＞
VG チューブにて経管栄養
シリンジ・カップフィーディングでミルクや水分摂取は可能
経口での離乳食摂取も可能だが、本人が離乳食を嫌がる。
赤ちゃんせんべいは自分でつかんで摂取可能

＜リハビリテーション＞

H25．5.16 か訪問リハビリテーション開始

＜合併症＞
難聴（補聴器装着）
脳波異常
てんかん（痙攣は不明）
浮腫（時々認める）
呼吸器感染症
便秘
水頭症
大後頭孔狭窄（手術は脳外科に不可能と言われている）
鼠径ヘルニア（手術施行）

＜精神・運動発達＞
手足の動きあり
寝返りあり

あやすと笑う
顔をしかめる
人の区別はできている印象（家族）
自分の意思を伝える（母に来てほしいときの合図）
眠たくなると自分でガーゼを顔の上にのせる
わざとチューブを抜く
お姉ちゃんが踊っていると、体全体を動かして真似をしている
足を上げてしばらくの間拳上したままにできる

＜歯芽＞
乳歯あり

発達状況のまとめ

歯牙	体幹運動	四肢	言語	有意語	笑う	嫌がる	指示理解	気持ちを伝える	ベビーサイン	人見知り	人の区別
永久歯	なし	なし	あ～	なし	あり		なし	なし	なし		
乳歯+永久歯	背尻ばい	あり	あ～	なし	あり	あり	±				あり
5番2本	尻もぞもぞ	あり	あ～	なし	あり	あり	±	あり	あり	あり	±
乳歯+永久歯（1本）	なし	あり（軽度）		なし	あり	あり	なし				
乳歯	寝返り	あり		なし	あり	あり	なし	あり	あり	あり	あり

出生児の状況

出生年月日	調査時年齢	性別	分娩様式	適応	出生時体重	身長	頭囲	胸囲	出生週数	出生前診断	診断方法	確定診断	AS	蘇生処置	蘇生時期
H2.5.28	22歳5か月	男	帝王切開	CPD	2798				36週5日	あり	エコー	なし	4点6点	あり	出生直後（挿管）
H17.3.30	7歳7か月	女	経腟分娩		2978	38	38		40週3日	あり			8・4	あり	出生直後（挿管）
H22.11.2	2歳0ヶ月	男	帝王切開	胎児適応					37週5日	あり	CT	なし	6/8挿管あり	あり	出生直後（挿管）
H16.5.8	8歳7か月	男	帝王切開	胎児適応	2783g	35	32.3	27.9	35週2日	あり	US	なし	1点2点	あり	出生直後（挿管）
H21.10.30	3歳2か月	男	経腟分娩		2362g	40	36		38週0日	あり	US,CT	なし	8点9点	なし（酸素のみ）	生直後（酸素のみ）
H23.8.9	1歳5か月	男	経腟分娩		2528g	37	37		38週2日	なし	なし	なし	2点6点	あり	出生直後（酸素）

合併症

膀胱機能異	肝機能異常	消化管機能	便秘	イレウス	糖尿病	褥瘡	骨折	甲状腺機能低下	無気肺	大孔頭狭窄	水頭症	四肢麻痺	奇形	鼠径ヘルニア	浮腫
なし	なし	なし	あり	なし	なし	あり	なし	なし		あり	軽度	あり	裂手	なし	
なし	なし	なし	あり	なし	なし	なし	なし	なし		あり（OPE）	軽度	なし	なし	なし	
なし	なし	なし	あり	なし	なし	なし	なし	あり	あり	あり	軽度	なし	なし	なし	
なし	なし	なし	あり	なし	なし	なし	なし	なし	なし	あり	軽度	なし	なし	なし	
なし	なし	なし	あり	なし	なし	なし	なし	なし	なし	あり	軽度	なし	なし	あり	時々あり
なし	なし	なし	あり	なし	なし	あり	なし	なし	なし			なし	なし	あり	

家族状況

父年齢（出生時年齢）	母年齢	兄弟	家族歴	出生前対応	社会福祉サービス	愛情形成
31	29	姉・妹	なし	医療者サイド	あり	あり
35	34	姉	なし	医療者再度		あり
S48（37）	S48（38）	なし	なし	医療者サイド	あり	あり
34	31	妹	なし	最善	あり	あり
s54	S55（29）	姉	なし	看取り	あり	あり
			なし	出生前診断なし		あり

栄養状況

経鼻	直母	離乳食	普通食	アレルギー	おやつ	食欲求
あり		なし	なし	あり（小麦・卵・米）	なし	なし
			あり	なし		あり
あり	あり	あり（つぶし食）	未	なし	ぼーろ	
あり	なし	なし	なし	なし		なし
あり	なし	なし	なし	なし	せんべい	あり
あり		あり（つぶし食）	なし	なし	果汁、イオン飲料	

遺伝子検査

検査	検査の時期	変異	その他
あり	出生後	Arg248Cys	
なし	なし	なし	
あり	出生後	Arg248Cys	
なし			
なし			検査予定あり
あり		Arg248Cys	

リハビリテーション

リハビリテーション	内容
あり（現在はなし）	理学療法（関節）、呼吸リハ、現在は施行なし
あり	2回/回
あり	理学療法（関節・呼吸）、作業療法、嚥下リハ
なし	
あり	理学療法
あり	呼吸リハ、保育士訪問

計測値

生後日数	0	30	90	180	485	720	720									
体重(g)	2362	2452	2816	3050	3594	4515	4515									
頭囲(cm)	36	36.5	36.4	39.3	44	45.5	45.5									
身長(cm)	40	40	43.5	45.7	45.8	51	51									
胸囲(cm)	26	27.7	28.6	28.9	30.5	34.2	34.2									
生後日数	0	30	57	90	120	150	240	510								
体重(g)	2528	2515	2776	3250	3481	3950	4510	4856								
右上肢								12.5								
右下肢								10								
左上肢								11.5								
左下肢								12								
頭位周囲	37	38		40.5	41.4	42.8	42	48.6								
身長	37	40														
胸囲	26	27						34.6								
生後月数	0	6	12	24	36	48	72	96								
体重	2783	3765	3755	4715	5120	4870	5280									
身長	35	44	45.7	52.1	49	53	52	55								
頭囲	32.3	43.5	45.3	49	49.5	51		53								
胸囲	27.9	30.5	30.5			29.5		33								
生後日数	0	55	56	198	237	245	273	304	406	461	580	598	612	644	675	725
体重	2800	3152		3332	3620			3946		4396		4410				4450
身長	39		40	44	44			47		49					50.5	
頭囲	37.5		40.5	42.3	44.4					44			44	46	46.5	
胸囲	28.5		28.5		28		30.5		30.5						30.5	
右上肢						8.5	8.5	10.5		10	11.5			11	11	
右下肢						9.5	10	11.5		12	13.5			14	14	
左上肢						8.5	8.5	11.5		10	11			11	11	
左下肢						9	10	11		13	13			14	14	
生後日数	0	189	365	730	1095	2190	2555	2735								
体重	2978	4162	4450	5760	5930	8170	9470	9920								
身長	38	44.5	48	51.6		58.8	61.5	62.6								
頭囲	38	45	47.8	51		54.4	55.4	54.8								
胸囲		35	34													

Ⅲ．研究成果の刊行に関する一覧表

Japanese Congenital Cytomegalovirus Infection Immunoglobulin Fetal Therapy Study Group. Yamada H, Morizane M, Tanimura K, Morioka I, Ebina Y, Matsuda H, Yoshida M, Wakamatsu H, Furuya K, Murotsuki J, Saito S, Kawabata I, Takahashi Y, Ueda T, Sato Y, Kamitomo M, Maruyama Y, Hirano H, Yamada T, Minakami H, Yaegashi N, Minematsu T, Matsuoka R, Banzai M, Ikenoue T. A trial of immunoglobulin fetal therapy for symptomatic congenital cytomegalovirus infection. 2012 Sep;95(1-2):73-9. J Reprod Immunol

Taketomi S, Hiraoka H, Nakagawa T, Miyamoto Y, Kuribayashi S, Fukuda A, Takeda H, Fukai A, Hirota J, Nakajima K, Haga N, Nakamura K: Osteochondral autograft for medial femoral condyle chondral lesions in a patient with multiple epiphyseal dysplasia: long-term result. J Orthop Sci 17: 507-511, 2012

Susami T, Mori Y, Tamura K, Ohkubo K, Nagahara K, Takahashi N, Uchino N, Uwatoko K, Haga N, Takato T: Facial morphology and occlusion of a patient with fibrodysplasia ossificans progressiva (FOP): Follow-up from 8 to 21 years of age. Spec Care Dentist 32: 165-170, 2012

Jiao S, Zhang Y, Ma W, Haga N: FOP in China and Japan: an overview from domestic literatures. Am J Med Genet Part A 161A: 892-893, 2013

Tsutsumi S, Maekawa A, Obata M, Morgan T, Robertson SP, Kurachi H. A Case of Boomerang Dysplasia with a Novel Causative Mutation in Filamin B: Identification of Typical Imaging Findings on Ultrasonography and 3D-CT Imaging. Fetal Diagn Ther. 2012

Yamada T, Takagi M, Nishimura G, Akaishi R, Furuta I, Morikawa M, Yamada T, Cho K, Sawai H, Ikegawa S, Hasegawa T, Minakami H. Recurrence of osteogenesis imperfecta due to maternal mosaicism of a novel COL1A1 mutation. Am J Med Genet A. 2012 Nov;158A(11):2969-71.

Kagami M, Kato F, Matsubara K, Sato T, Nishimura G, Ogata T*: Relative frequency

of underlying genetic causes for the development of UPD(14)pat-like phenotype. Eur J Hum Genet 20 (9): 928-932, 2012.

Fuke-Sato T, Yamazawa K, Nakabayashi K, Matsubara K, Matsuoka K, Hasegawa T, Dobashi K, Ogata T*: Mosaic upd(7)mat in a patient with Silver-Russell syndrome: correlation between phenotype and mosaic ratio in the body and the placenta. Am J Med Genet A 158A (2): 465-468, 2012.

Hiura H, Okae H, Miyauchi N, Sato F, Sato A, Van De Pette M, John RM, Kagami M, Nakai K, Soejima H, Ogata T, Arima T*: Characterization of DNA methylation errors in patients with imprinting disorders conceived by assisted reproduction technologies. Hum Reprod 27 (8): 2541-2548, 2012.

Kagami M, Matsuoka K, Nagai T, Yamanaka M, Kurosawa K, Suzumori N, Sekita Y, Miyado M, Matsubara K, Fuke T, Kato F, Fukami M, Ogata T*: Paternal uniparental disomy 14 and related disorders: placental gene expression analyses and histological examinations. Epigenetics 7 (10): 1142-1150, 2012.

Nagasaki K*, Tsuchuya S, Saitoh A, Ogata T, Fukami M: Neuromuscular symptoms in a patient with familial pseudohypoparathyroidism type Ib diagnosed by methylation-specific multiplex ligation-dependent probe amplification. Endocr J (accepted).

Fuke T, Mizuno S, Nagai T, Hasegawa T, Horikawa R, Miyoshi Y, Muroya K, Kondoh T, Numakura C, Sato S, Nakabayashi K, Tayama C, Hata K, Sano S, Matsubara K, Kagami M, Tamazawa K, Ogata T*: Molecular and clinical studies in 138 Japanese patients with Silver-Russell syndrome. PLoS One (accepted).

Ayabe T, Matsubara K, Ogata T, Ayabe A, Murakami N, Nagai T, Fukami M*: Birth seasonality in Prader-Willi syndrome resulting from chromosome 15 microdeletion. Am J Med Genet A (accepted).

Matsubara K, Ogata T*: Advanced maternal age at childbirth and the development of uniparental disomy. A commentary on the proportion of uniparental disomy is increased in Prader-Willi syndrome due to an advanced maternal childbearing age in Korea. J Hum Genet. 2013 Jan 31. doi: 10.1038/jhg.2013.4.

Iida A, Okamoto N, Miyake N, Nishimura G, Minami S, Sugimoto T, Nakashima M, Tsurusaki Y, Saitsu H, Shiina M, Ogata K, Watanabe S, Ohashi H, Matsumoto N, Ikegawa S. Exome sequencing identifies a novel INPPL1 mutation in opsismodysplasia. J Hum Genet. 2013 Apr 4. doi: 10.1038/jhg.2013.25. [Epub ahead of print]

Semba K, Araki K, Matsumoto K, Suda H, Ando T, Sei A, Mizuta H, Takagi K, Nakahara M, Muta M, Yamada G, Nakagata N, Iida A, Ikegawa S, Nakamura Y, Araki M, Abe K, Yamamura K. Ectopic expression of Ptf1a induces spinal defects, urogenital defects, and anorectal malformations in Danforth's short tail mice. PLoS Genet. 2013 9(2):e1003204

Yamada T, Takagi M, Nishimura G, Akaishi R, Furuta I, Morikawa M, Yamada T, Cho K, Sawai H, Ikegawa S, Hasegawa T, Minakami H. Recurrence of osteogenesis imperfecta due to maternal mosaicism of a novel COL1A1 mutation. Am J Med Genet A. 158A(11):2969-71, 2012.

Cho TJ, Lee KE, Lee SK, Song SJ, Kim KJ, Jeon D, Lee G, Kim HN, Lee HR, Eom HH, Lee ZH, Kim OH, Park WY, Park SS, Ikegawa S, Yoo WJ, Choi IH, Kim JW. A single recurrent mutation in the 5'-UTR of IFITM5 causes osteogenesis imperfecta Type V. Am J Hum Genet. 91(2):343-8, 2012.

Miyake N, Elcioglu NH, Iida A, Isguven P, Dai J, Murakami N, Takamura K, Cho TJ, Kim OH, Hasegawa T, Nagai T, Ohashi H, Nishimura G, Matsumoto N, Ikegawa S. PAPSS2 mutations cause autosomal recessive brachyolmia. J Med Genet. 49(8):533-8, 2012.

Cho TJ, Matsumoto K, Fano V, Dai J, Kim OH, Chae JH, Yoo WJ, Tanaka Y, Matsui Y, Takigami I, Monges S, Zabel B, Shimizu K, Nishimura G, Lausch E, Ikegawa S. TRPV4-pathy manifesting both skeletal dysplasia and peripheral neuropathy: A report of three patients. Am J Med Genet A. 158A(4):795-802, 2012.

Daniel PB, Morgan T, Alanay Y, Bijlsma E, Cho TJ, Cole T, Collins F, David A, Devriendt K, Faivre L, Ikegawa S, Jacquemont S, Jesic M, Krakow D, Liebrecht D, Maitz S, Marlin S, Morin G, Nishikubo T, Nishimura G, Prescott T, Scarano G, Shafeghati Y, Skovby F, Tsutsumi S, Whiteford M, Zenker M, Robertson SP. Disease-associated mutations in the actin-binding domain of filamin B cause cytoplasmic focal accumulations correlating with disease severity. Hum Mutat. 33(4):665-73,

2012.

Sasagawa S, Takemori H, Uebi T, Ikegami D, Hiramatsu K, Ikegawa S, Yoshikawa H, Tsumaki N. SIK3 is essential for chondrocyte hypertrophy during skeletal development in mice. Development. 139(6):1153-63, 2012.

Ⅳ．研究成果の刊行物・別冊

Osteochondral autograft for medial femoral condyle chondral lesions in a patient with multiple epiphyseal dysplasia: long-term result

Shuji Taketomi, Hisatada Hiraoka, Takumi Nakagawa, Yoshinari Miyamoto, So Kuribayashi, Akira Fukuda, Hideki Takeda, Atsushi Fukai,

Journal of Orthopaedic Science
Official Journal of the Japanese Orthopaedic Association

ISSN 0949-2658
Volume 17
Number 4

J Orthop Sci (2012) 17:507-511
DOI 10.1007/s00776-011-0096-5

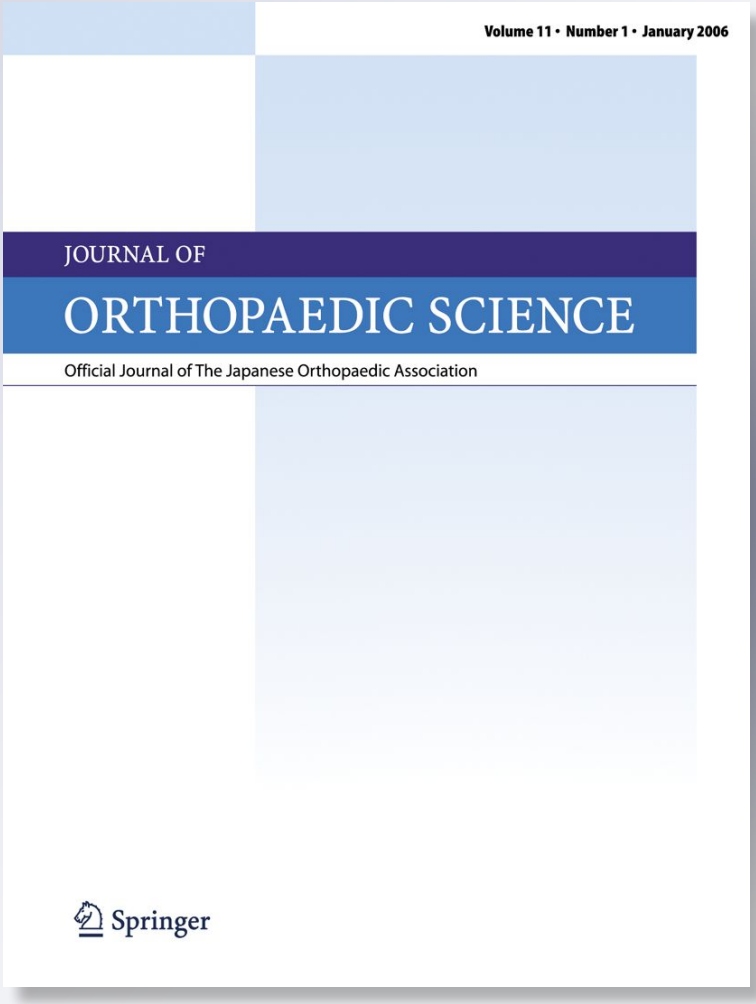

Springer

J Orthop Sci (2012) 17:507–511
DOI 10.1007/s00776-011-0096-5

CASE REPORT

Osteochondral autograft for medial femoral condyle chondral lesions in a patient with multiple epiphyseal dysplasia: long-term result

Shuji Taketomi · Hisatada Hiraoka · Takumi Nakagawa · Yoshinari Miyamoto · So Kuribayashi · Akira Fukuda · Hideki Takeda · Atsushi Fukai · Jinso Hirota · Kohei Nakajima · Nobuhiko Haga · Kozo Nakamura

Received: 20 October 2010 / Accepted: 12 April 2011 / Published online: 11 May 2011

Introduction

Multiple epiphyseal dysplasia (MED) is a form of osteochondrodysplasia characterized by abnormal epiphyseal growth and assumed to be a clinical condition of extracellular matrix abnormality [1]. Osteoarthritis and chondral lesions, for example osteochondritis dissecans (OCD), are among the clinical expressions of MED [2, 3]. It is possible for osteoarthritic changes of the knee to develop easily even in young patients with MED [4]. Total knee arthroplasty (TKA) and correction osteotomy have been performed for severe deformity and destruction of the knee in MED patient [4, 5].

Osteochondral autograft has been performed for patients with localized full-thickness cartilage damage of weight-bearing surfaces of the knee and other synovial joints [6, 7]. The surgical technique of an osteochondral autograft for the knee involves harvesting small osteochondral grafts from the minimum-weight-bearing periphery of the patellofemoral joint and transplanting these to prepared defect sites on the weight-bearing surfaces [8]. Good results of such transplantation for osteochondral defects of knee have been reported [7, 9]. The clinical result after osteochondral autograft in patients with MED, however, remains to be clarified. We experienced a patient with MED who underwent an osteochondral autograft for localized chondral lesions of bilateral medial femoral condyles (MFC) in order to preserve the articular surface and joint function. Here we report results of the 10-year follow up of this procedure; to our knowledge, this is the first report of an osteochondral autograft for chondral lesions of the knee in a patient with MED.

S. Taketomi (✉) · T. Nakagawa · Y. Miyamoto · S. Kuribayashi · A. Fukuda · H. Takeda · A. Fukai · J. Hirota · K. Nakajima · K. Nakamura
Department of Orthopaedic Surgery, Faculty of Medicine, The University of Tokyo, 7-3-1 Hongo, Bunkyo-ku, Tokyo 113-0033, Japan
e-mail: takeos-tky@umin.ac.jp

H. Hiraoka
Department of Orthopaedic Surgery, Saitama Medical Center, Saitama Medical University, 1981 Kamoda-Tsujido, Kawagoe, Saitama 350-8550, Japan

N. Haga
Department of Rehabilitation, Faculty of Medicine, The University of Tokyo, 7-3-1 Hongo, Bunkyo-ku, Tokyo 113-0033, Japan

Report of the case

A 38-year-old woman, 150 cm tall and weighing 51 kg with no history of trauma visited our hospital. She suffered from bilateral knee pain after walking a long distance, while descending stairs, and while standing. She had tenderness in the medial joint space of both knees at palpation, but the knees were not swollen. The extension and flexion of the knees was 0 and 150° bilaterally. Visual analog scale (VAS) for activities of daily living (0 mm: not satisfied, 100 mm: very satisfied) was 20 mm for the right knee and 50 mm for the left knee. She had no remarkable family history or past history.

Radiographs showed a loose body in the right knee, a shallow femoral trochlear groove in the bilateral knees, and flattening of the bilateral MFC (Fig. 1). The femorotibial angle of each knee was 178°. T1-weighted magnetic resonance imaging (MRI) with fat suppression showed an irregular joint surface corresponding to the articular cartilage of bilateral MFC (Fig. 2). Radiograph of the hip joints showed flattening of the femoral heads and short necks

(Fig. 3a). There was slight irregularity of the end plate in the radiograph of the thoraco-lumbar spine (Fig. 3b). Based on the radiographic findings, this case was diagnosed as the Ribbing type (mild form) of MED with chondral lesions in bilateral knees.

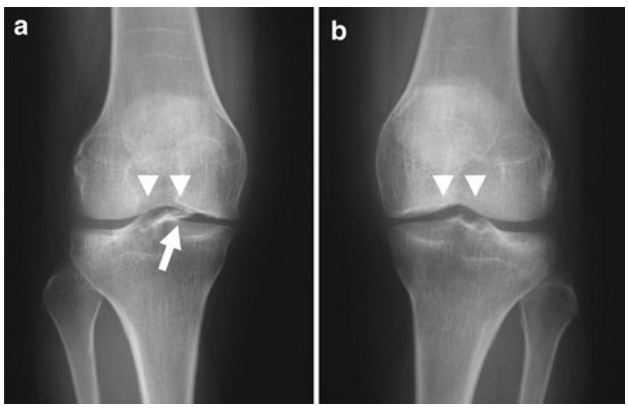

Fig. 1 Anteroposterior radiographs of both knees showed a shallow femoral trochlear groove (*arrowheads*) and flattening of the medial femoral condyle. **a** Radiograph of the right knee showing a loose body (*arrow*). **b** Radiograph of the left knee

Arthroscopy on both knees was performed. The articular cartilage of the bilateral MFC was detached from the subchondral bone. The cartilage defects extended down more than 50% of the cartilage depth but not through to the subchondral bone (Fig. 4). According to the International Cartilage Repair Society (ICRS) scoring system [10], the chondral lesions were Grade 3. There were 2 loose bodies (10 mm and 3 mm in diameter, respectively) in the right knee joint and these were excised.

Osteochondral autograft was performed for the left knee and for the right knee 22 months later, using the Osteochondral Autograft Transfer System (OATS^{TM}; Arthrex, Naples, FL, USA). Osteochondral autograft using this system involves obtaining small cylindrical osteochondral grafts from the minimum-weight-bearing periphery of the femoral condyles at the level of the patellofemoral joint and transplanting these to the recipient sites on the weight-bearing surfaces. Sizes of the lesions were 20 × 15 mm in the left MFC, and 20 × 10 mm in the right MFC. For the left knee, 6 osteochondral plugs 6 mm in diameter were harvested from the minimum-weight-bearing periphery of the ipsilateral patella-femoral joint and transplanted to the

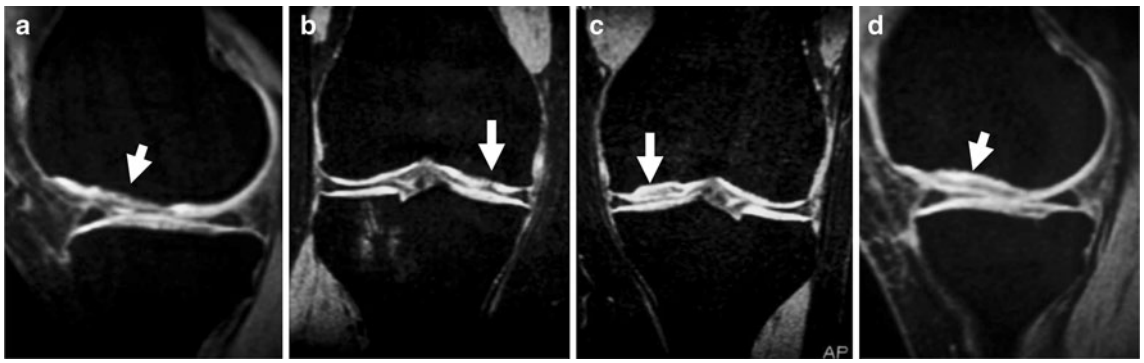

Fig. 2 T1-weighted magnetic resonance imaging (MRI) with fat suppression showed an irregular joint surface corresponding to the articular cartilage of the bilateral medial femoral condyle (*arrows*). **a** Coronal MRI of the right knee. **b** Sagittal image of the right knee. **c** Sagittal image of the left knee. **d** Coronal image of the left knee

Fig. 3 **a** Radiograph of the hip joints showed flattening of the femoral head and short neck. **b** There was slight irregularity of the end plate in the radiograph of the thoraco-lumbar spine

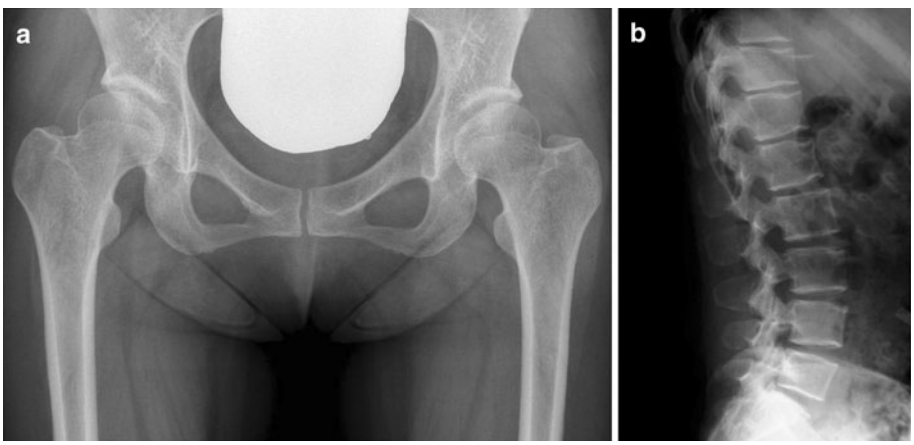

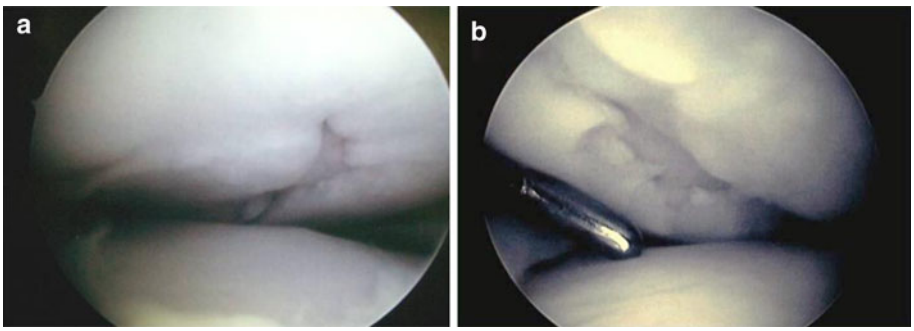

Fig. 4 Arthroscopy showed the chondral lesions of the medial femoral condyle of both knees. **a** Chondral lesion in the right knee. **b** Chondral lesion in the left knee

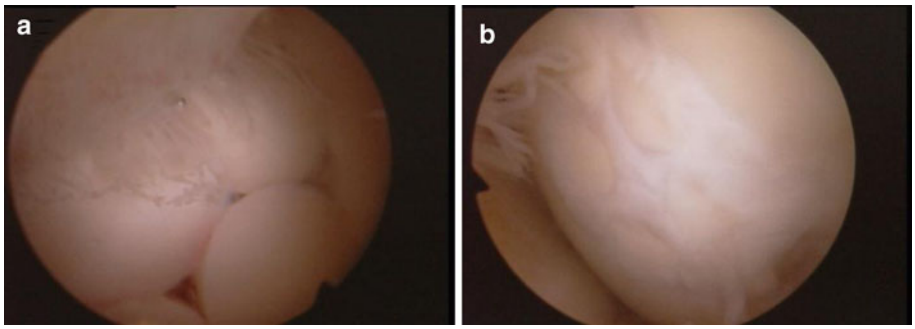

Fig. 5 **a** Intraoperative arthroscopic image of the recipient site of the right knee after osteochondral autograft. **b** Second-look arthroscopic image of the recipient site of the left knee 24 months after the surgery. The gaps surrounding the grafts were filled with fibrous cartilage-like tissue and the surface of the grafted area was totally smooth

chondral defect of the MFC. For the right knee, 4 osteochondral plugs 7 mm in diameter were transplanted to the chondral defect of the MFC (Fig. 5a). Bone plugs harvested from the host site were transplanted to the recipient site in exchange.

Postoperatively, passive range of motion exercise of the operated knee was allowed 3 days after the surgery, partial weight-bearing was allowed 2 weeks after the surgery, and full weight-bearing was allowed 12 weeks after the surgery.

Twenty-two months after the surgery, second-look arthroscopy was performed for the left knee at the same time as the osteochondral transplantation for the right knee. The gaps surrounding the grafts were filled with fibrous cartilage-like tissue and the surface of the grafted area was totally smooth. Palpation with a probe showed no instability of the grafts and the same elasticity as normal cartilage. According to ICRS cartilage repair assessment [10], the cartilage repair was graded as Grade I (12/12 points, normal) (Fig. 5b).

Ten years after the surgery on the left knee and 8 years after that on the right, the patient walked without limitation with no pain and had full range of motion in both knees. Radiographs at final follow up showed no apparent progression of osteoarthritis in either knee (Fig. 6). T1-weighted MRI with fat suppression 10 years after surgery of the right knee and 8 years after surgery of the left knee showed smooth cartilage surface and the same signal intensity of the grafted bone as the surrounding bone in the MFC (Fig. 7). VAS for activities of daily living was 90 mm for the right knee and 87 mm for the left knee.

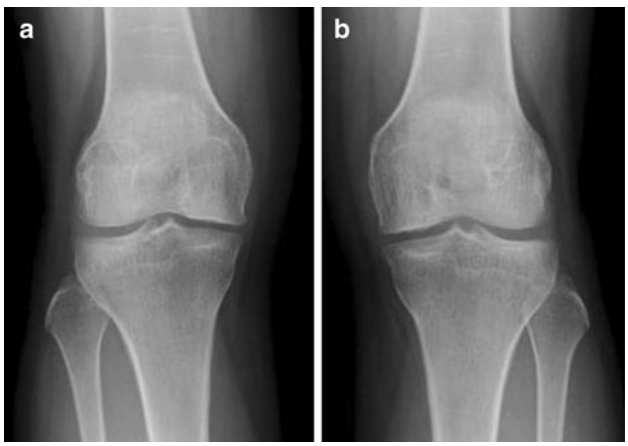

Fig. 6 Radiographs showed no apparent progression of osteoarthritis in the bilateral knee. The medial joint spaces were preserved. **a** Anteroposterior radiograph 8 years after surgery of the right knee. **b** Anteroposterior radiograph 10 years after surgery of the left knee

The patient was informed that data from the case would be submitted for publication, and gave her consent.

Discussion

MED is a form of osteochondrodysplasia characterized by abnormal epiphyseal growth with almost normal findings in the spine [1]. Classically, MED has been divided into the severe form (Fairbank type) [11] and the mild form (Ribbing type) [2]. Diagnostic criteria of MED are not

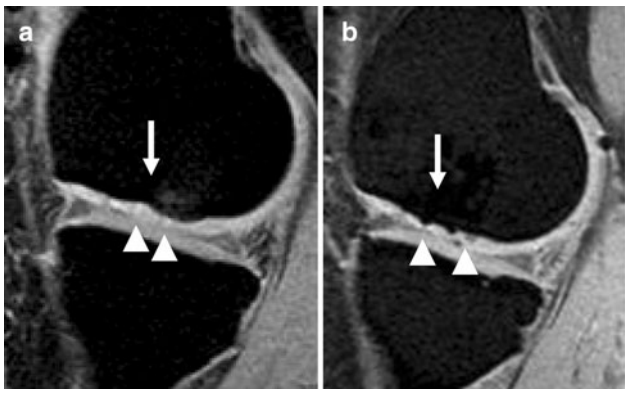

Fig. 7 T1-weighted MRI with fat suppression after the surgery showed a smooth cartilage surface (*arrowheads*) and the same signal intensity of the grafted bone as the surrounding bone in the medial femoral condyle (*arrows*). **a** Sagittal image of the right knee. **b** Sagittal image of the left knee

clear and diagnosis of MED for a patient after epiphyseal closure is often difficult. According to Eguchi, MED is diagnosed radiographically when there are abnormalities of the epiphysis in more than two joints with almost normal findings in the spine [12]. It was known that, although there are typical changes on the radiograph of the knee joint before epiphyseal closure, the changes are no longer discernible in the adult [13]. According to Miura et al. [4] after epiphyseal closure the most characteristic finding in the knee is a shallow femoral trochlear groove.

The radiographs of this patient showed a shallow femoral trochlear groove and slight osteoarthritis (subchondral sclerosis) in the knee despite her young age. They also showed flattening of the femoral heads and almost normal findings of the thoraco-lumbar spine with only slight irregularity of the end plate. The patient was therefore diagnosed with the Ribbing type (mild form) of MED. Although we did not have genetic evidence and obvious family history of the patient, it was possible to diagnose the patient with MED radiographically. Genetic screening is not indispensable to diagnosis of MED, because MED is not caused by a specific gene. According to Jakkula et al. [14] mutation analysis resulted in identification of 6 known genes in only 34% of patients and patients with MED had family history in only 40% of patients. Early osteoarthritis of the knee occurs in many patients of MED. It has been reported that gene mutations, for example of the cartilage oligomeric matrix protein (COMP) gene or matrilin3 (MATN3) can be the cause [15, 16]. Therefore, it is speculated that early osteoarthritic change or chondral lesions, for example OCD, occur because of abnormalities of the extracellular matrix.

Osteochondral autograft is one of the surgical procedures performed for patients with localized full-thickness cartilage defect in weight bearing synovial joints [6–9, 17], and has been used on OCD and traumatic cartilage defect. Hangody and Füles reported 10-year follow up results of autologous osteochondral grafting in the knee. According to them, results for 92% of patients after femoral condylar osteochondral transplantation were shown to be good to excellent [7]. There is concern about fragility of the extracellular matrix of the donor graft when performing osteochondral autografts in patients with MED. Thus, TKA and correction osteotomy have usually been performed for deformity and destruction of the knee [4, 5]. Our patient was young, her activity level was high, the alignment of the bilateral knees was almost normal, and the diagnosis was the mild form (Ribbing type) of MED. Although the cartilage defect was full-thickness in the weight-bearing area, the lesion was localized and no other degenerative lesion was observed inside the knee. Concomitant high tibial valgus osteotomy has been one option for reducing stress to the medial compartment and transplanted grafts. However, there was concern that the valgus alignment after the osteotomy might progress in future and, as a result, could have an adverse effect on the hip joints or ankle joints. No report was found of surgical treatment for early stage chondral lesion of the knee in a patient with MED, nor any report of osteochondral autograft for a chondral lesion with MED. Taking these risks and the lower invasiveness of the procedure into account, the osteochondral autograft alone was chosen for treatment of the chondral defects in this patient.

The long-term clinical and radiographical results of the patient were excellent, although an attentive and further long-term follow up is required because results of osteochondral autograft for a chondral lesion with MED have not previously been clear. In conclusion, osteochondral autograft can be one of the viable options for treating a regional chondral lesion of the knee even in a patient with MED. Careful preoperative assessment of the clinical features of the knee and the adjacent joints including hip and ankle joints is mandatory before performing this procedure.

Conflict of interest The authors declare that they have no conflict of interest in relation to the contents of this manuscript.

References

1. Haga N, Nakamura K, Takikawa K, Manabe N, Ikegawa S, Kimizuka M. Stature and severity in multiple epiphyseal dysplasia. J Pediatr Orthop. 1998;18:394–7.
2. Ribbing S. The hereditary multiple epiphyseal disturbance and its consequences for the aetiogenesis of local malacians. Particularly the osteochondrosis dissecans. Acta Orthop Scand. 1955;24:286–99.
3. Versteylen RJ, Zwemmer A, Lorié CAM, Schuur KH. Multiple epiphyseal dysplasia complicated by severe osteochondritis

dissecans of the knee. Incidence in two families. Skeletal Radiol. 1988;17:407–12.
4. Miura H, Noguchi Y, Matsuyasu H, Nagamine R, Urabe K, Matsuda S, Iwamoto Y. Clinical features of multiple epiphyseal dysplasia expressed in the knee. Clin Orthop Relat Res. 2000;380:184–90.
5. Sebik A, Sebik B, Kutluay E, Kuyurtar F, Ademoglu Y. The orthopaedic aspects of multiple epiphyseal dysplasia. Int Orthop. 1998;22:417–21.
6. Hangody L, Feczkó P, Bartha L, Bodó G, Kish G. Mosaicplasty for the treatment of articular defects of the knee and ankle. Clin Orthop Relat Res. 2001;391S:328–36.
7. Hangody L, Füles P. Autologous osteochondral mosaicplasty for treatment of full-thickness defects of weight-bearing joints: 10 years of experimental and clinical experience. J Bone Joint Surg Am. 2003;85A(suppl 2):25–32.
8. Hangody L, Ráthonyi GK, Duska Z, Vásárhelyi G, Füles P, Módis L. Autologous osteochondral mosaicplasty. Surgical technique. J Bone Joint Surg Am. 2004;86A(Suppl 1):65–72.
9. Jakob RP, Franz T, Gautier E, Mainil-Varlet P. Autologous osteochondral grafting in the knee: indication, results, and reflections. Clin Orthop Relat Res. 2002;401:170–84.
10. Brittberg M, Winalski CS. Evaluation of cartilage injuries and repair. J Bone Joint Surg Am. 2003;85A(suppl 2):58–69.
11. Fairbank T. Dysplasia epiphysialis multiplex. Br J Surg. 1947;34:225–32.
12. Eguchi M Hip problems in multiple epiphyseal dysplasia. In: Itami Y, Nishino A editors. Constitutional Disease of Bone, Orthopaedic MOOK; 1982. p. 82–104 (in Japanese).
13. Unger S, Bonafé L, Superti-Furga A. Multiple epiphyseal dysplasia: clinical and radiographic features, differential diagnosis and molecular basis. Best Pract Res Clin Rheumatol. 2008;22:19–32.
14. Jakkula E, Mäkitie O, Czarny-Ratacjzak M, Jackson GC, Damignani R, Susic M, Briggs MD, Cole WG, Ala-Kokko L. Mutations in the known genes are not the major cause of MED; distinctive phenotypic entities among patients with no identified mutations. Eur J Hum Genet. 2005;13:292–301.
15. Briggs MD, Hoffman SM, King LM, Olsen AS, Mohrenweiser H, Leroy JG, Mortier GR, Rimoin DL, Lachman RS, Gaines ES, Cekleniak JA, Knowlton RG, Cohn DH. Pseudochondroplasia and multiple epiphyseal dysplasia is due to mutations in the cartilage oligomeric matrix protein gene. Nat Genet. 1995;10:330–6.
16. Chapman KL, Mortier GR, Chapman K, Loughlin J, Grant ME, Briggs MD. Mutations in the region encoding the von Willebrand factor A domain of matrilin-3 are associated with multiple epiphyseal dysplasia. Nat Genet. 2001;28:393–6.
17. Magnussen RA, Dunn WR, Carey JL, Spindler KP. Treatment of focal articular cartilage defects in the knee: a systematic review. Clin Orthop Relat Res. 2008;466:952–62.

Epigenetics 7:10, 1142–1150; October 2012; © 2012 Landes Bioscience

Paternal uniparental disomy 14 and related disorders

Placental gene expression analyses and histological examinations

Masayo Kagami,[1] Kentaro Matsuoka,[2] Toshiro Nagai,[3] Michiko Yamanaka,[4] Kenji Kurosawa,[5] Nobuhiro Suzumori,[6] Yoichi Sekita,[7] Mami Miyado,[1] Keiko Matsubara,[1] Tomoko Fuke,[1] Fumiko Kato,[1,8] Maki Fukami[1] and Tsutomu Ogata[1,8,*]

[1]Department of Molecular Endocrinology; National Research Institute for Child Health and Development; Tokyo, Japan; [2]Departments of Pathology; National Center for Child Health and Development; Tokyo, Japan; [3]Department of Pediatrics; Dokkyo University School of Medicine; Koshigaya, Japan; [4]Department of Integrated Women's Health; St. Luke's International Hospital; Tokyo, Japan; [5]Division of Medical Genetics; Kanagawa Children's Medical Center; Yokohama, Japan; [6]Department of Obstetrics and Gynecology; Nagoya City University Graduate School of Medicine; Nagoya, Japan; [7]Department of Pathology; Graduate School of Medicine; Osaka University, Osaka, Japan; [8]Department of Pediatrics; Hamamatsu University School of Medicine; Hamamatsu, Japan

Keywords: Upd(14)pat, microdeletion, placenta, expression dosage, histopathology, imprinting

Abbreviations: *PEGs*, paternally expressed genes; *MEGs*, maternally expressed genes; DMRs, differentially methylated regions; IG-DMR, *DLK1-MEG3* intergenic DMR; *RTL1as*, *RTL1* antisense; upd(14)pat, paternal uniparental disomy 14; BWS, Beckwith-Wiedemann syndrome; q-PCR, quantitative real-time PCR; CGH, oligoarray comparative genomic hybridization; LM, light microscopic; EM, electron microscopic; IHC, immunohistochemical

Although recent studies in patients with paternal uniparental disomy 14 [upd(14)pat] and other conditions affecting the chromosome 14q32.2 imprinted region have successfully identified underlying epigenetic factors involved in the development of upd(14)pat phenotype, several matters, including regulatory mechanism(s) for *RTL1* expression, imprinting status of *DIO3* and placental histological characteristics, remain to be elucidated. We therefore performed molecular studies using fresh placental samples from two patients with upd(14)pat. We observed that *RTL1* expression level was about five times higher in the placental samples of the two patients than in control placental samples, whereas *DIO3* expression level was similar between the placental samples of the two patients and the control placental samples. We next performed histological studies using the above fresh placental samples and formalin-fixed and paraffin-embedded placental samples obtained from a patient with a maternally derived microdeletion involving *DLK1*, the-IG-DMR, the *MEG3*-DMR and *MEG3*. Terminal villi were associated with swollen vascular endothelial cells and hypertrophic pericytes, together with narrowed capillary lumens. DLK1, RTL1 and DIO3 proteins were specifically identified in vascular endothelial cells and pericytes, and the degree of protein staining was well correlated with the expression dosage of corresponding genes. These results suggest that *RTL1as*-encoded microRNA functions as a repressor of *RTL1* expression, and argue against *DIO3* being a paternally expressed gene. Furthermore, it is inferred that DLK1, DIO3 and, specially, RTL1 proteins, play a pivotal role in the development of vascular endothelial cells and pericytes.

Introduction

Human chromosome 14q32.2 region carries a cluster of imprinted genes including protein coding paternally expressed genes (*PEGs*) such as *DLK1* and *RTL1* (alias *PEG11*) and non-coding maternally expressed genes (*MEGs*) such as *MEG3* (alias *GTL2*) and *RTL1as* (*RTL1* antisense encoding microRNAs).[1,2] The 14q32.2 imprinted region also harbors two differentially methylated regions (DMRs), i.e., the germline-derived primary *DLK1-MEG3* intergenic DMR (IG-DMR) and the postfertilization-derived secondary *MEG3*-DMR.[1,2] Both DMRs are hypermethylated after paternal transmission and hypomethylated after maternal transmission in the body, whereas in the placenta the IG-DMR alone remains as a DMR and the *MEG3*-DMR is rather hypomethylated.[2] We have previously revealed that the hypomethylated IG-DMR and *MEG3*-DMR of maternal origin function as imprinting control centers in the placenta and the body, respectively, and that the IG-DMR functions hierarchically as an upstream regulator for the methylation pattern of the *MEG3*-DMR on the maternally inherited chromosome in the body, but not in the placenta.[3]

*Correspondence to: Tsutomu Ogata; Email: tomogata@hama-med.ac.jp
Submitted: 06/21/12; Revised: 08/20/12; Accepted: 08/22/12
http://dx.doi.org/10.4161/epi.21937

Consistent with these findings, paternal uniparental disomy 14 [upd(14)pat] results in a unique phenotype characterized by facial abnormality, small bell-shaped thorax with coat hanger appearance of the ribs, abdominal wall defects, placentomegaly and polyhydramnios.[2,4] We have studied multiple patients with upd(14)pat and related conditions, such as epimutations of the maternally derived DMRs and various types of microdeletions involving the maternally inherited imprinted region, suggesting that markedly increased *RTL1* expression is the major underlying factor for the development of upd(14)pat-like phenotype.[2] The notion of excessive *RTL1* expression is primarily based on the following mouse data indicating a trans-acting repressor function of *Rtl1as*-encoded microRNAs for *Rtl1* expression: (1) targeted deletion of the maternally derived IG-DMR causes maternal to paternal epigenotypic switch of the imprinted region, with ~4.5 times rather than ~2 times of *Rtl1* expression as well as ~2 times of *Dlk1* expression and nearly absent *Megs* expression, in the presence of two functional copies of *Pegs* and no functional copy of *Megs*[5] and; (2) targeted deletion of the maternally derived *Rtl1as* results in 2.5–3.0 times of *Rtl1* expression, in the presence of a single functional copy of *Rtl1*.[6] Similarly, in the human, typical upd(14)pat phenotype is observed in patients with epimutations that are likely associated with markedly increased *RTL1* expression because of the combination of two functional copies of *RTL1* and no functional copy of *RTL1as*, whereas relatively mild upd(14)pat-like phenotype is found in patients with maternally inherited microdeletions involving *RTL1as* that are likely accompanied by moderately elevated *RTL1* expression because of the combination of a single functional copy of *RTL1* and no functional copy of *RTL1as*.[2]

Human imprinting disorders are usually associated with placental abnormalities. For example, Beckwith-Wiedemann syndrome (BWS) and upd(14)pat are associated with placentomegaly,[4,7] and Silver-Russell syndrome is accompanied by hypoplastic placenta.[8] Similarly, mouse imprinting aberrations also usually affect placental growth and development.[9] In agreement with this, virtually all the imprinted genes studied to date are expressed in the placenta and play a pivotal role in the placental growth and development,[10] although placental structure is more or less different between placental animals.[11]

However, several matters remain to be clarified in upd(14)pat and related conditions. For example, it is unknown whether human *RTL1* expression is actually elevated in the absence of functional *RTL1as*-encoded microRNAs. It is also unknown whether *DIO3* is a *PEG*, although mouse *Dio3* has been shown to undergo partial imprinting.[12] In this regard, while we examined fresh blood cells, cultured skin fibroblasts and formalin-fixed and paraffin-embedded placental and body samples obtained from patients with upd(14)pat-like phenotype, precise assessment of *RTL1* and *DIO3* expression levels was impossible because of extremely low *RTL1* and *DIO3* expression levels in fresh blood cells and cultured skin fibroblasts and poor quality of RNAs extracted from paraffin-embedded tissues.[2,3] In addition, while cSNP genotyping has demonstrated paternal *DLK1* and *RTL1* expression and maternal *MEG3* expression in the body and the placenta,[2,3] no informative cSNP data showing paternal *DIO3* expression have been obtained.[2,3] Furthermore, although standard light microscopic (LM) examinations have been performed using formalin-fixed and paraffin-embedded placental samples, fine placental histopathological studies, such as electron microscopic (EM) examinations and immunohistochemical (IHC) examinations, remain to be performed.

To examine these unresolved matters, fresh placental tissues are highly useful, because precise quantitative real-time PCR (q-PCR) analyses and EM studies can be performed with fresh placentas. Thus, we performed q-PCR analyses and EM studies, as well as IHC studies with RTL1 antibodies produced by ourselves and commercially available DLK1 and DIO3 antibodies, using fresh placental samples obtained from two previously reported patients with prenatally diagnosed upd(14)pat.[13,14] We also performed IHC studies using formalin-fixed and paraffin-embedded placental samples obtained from a previously reported patient with a microdeletion involving *DLK1*, but not *RTL1* and *DIO3*,[2] to compare the placental protein expression levels between upd(14)pat and the microdeletion. Furthermore, we also studied a hitherto unreported patient with an unbalanced translocation involving the 14q32.2 imprinted region, to obtain additional data regarding the *RTL1-RTL1as* interaction and the primary factor for the development of upd(14)pat phenotype.

Results

Patients and samples. This study consisted of three previously reported patients with typical body and placental upd(14)pat phenotype and a normal karyotype (cases 1–3),[2,13-15] and a new patient with various non-specific features and a 46,XX,der(17)t(14;17)(q31;p13) karyotype accompanied by three copies of the distal 14q region and a single copy of the terminal 17p region (case 4) . Clinical phenotypes of cases 1–4 are summarized in **Table S1**. In brief, cases 1 and 2 were suspected to have upd(14)pat phenotype including bell-shaped thorax by prenatal ultrasound studies performed for polyhydroamnios, and were confirmed to have upd(14)pat by microsatellite analysis after birth. Case 3 was found to have typical upd(14)pat phenotype during infancy and was shown to have a maternally derived microdeletion affecting the chromosome 14q32.2 imprinted region. Case 4 had growth failure, developmental delay, multiple non-specific anomalies, and omphalocele. There was no history of polyhydramnios or placentomegaly. Thus, except for omphalocele, case 4 had no upd(14)pat-like phenotype. The parental karyotype was normal, indicating a de novo occurrence of the unbalanced translocation.

We obtained fresh placental samples immediately after birth from prenatally diagnosed cases 1 and 2 for molecular studies using genomic DNA and RNA, and fresh leukocyte samples from cases 1, 2 and 4 and their parents for molecular studies using genomic DNA. The fresh placental samples of cases 1 and 2 were also utilized for histopathological examinations, together with formalin-fixed and paraffin-embedded placental samples of case 3. For controls, we obtained three fresh placentas at 37 weeks of gestation, and fresh leukocytes from three adult subjects; for molecular studies using placentas, we prepared pooled samples

consisting of an equal amount of DNA or RNA extracted from each placenta.

Molecular studies in cases 1 and 2. We performed microsatellite analysis for 19 loci on chromosome 14 and bisulfite sequencing for the IG-DMR (CG4 and CG6) and the *MEG3*-DMR (CG7), using placental and leukocyte genomic DNA samples; while microsatellite analysis had been performed for 15 loci in case 1 and 16 loci in case 2, only leukocyte genomic DNA samples were examined in the previous study.[15] Consequently, we identified two peaks for *D14S609* and single peaks for the remaining loci in case 1 (the combination of paternal heterodisomy and isodisomy), and single peaks for all the examined loci in case 2 (apparently full paternal isodisomy) (**Table S2**). Furthermore, no trace of maternally inherited peak was identified in both placental and leukocyte genomic DNA samples (**Fig. 1**). Bisulfite sequencing showed that both the IG-DMR and the *MEG3*-DMR were markedly hypermethylated in the leukocytes of cases 1 and 2, whereas in the placental samples the IG-DMR was obviously hypermethylated and the *MEG3*-DMR was grossly hypomethylated to an extent similar to that identified in control placentas (**Fig. 2**). Furthermore, q-PCR analysis for placental RNA samples revealed that *DLK1*, *RTL1*, and *DIO3* expression levels were 3.3 times, 6.1 times and 1.9 times higher in the placental samples of case 1 than in the control placental samples, respectively, and were 3.1 times, 9.4 times and 1.7 times higher in the placental samples of case 2 than in the control placental samples, respectively (**Fig. 3A**). By contrast, the expressions of all *MEGs* examined were virtually absent in the placental samples of cases 1 and 2. PCR products were sufficiently obtained after 30 cycles for the fresh placental as well as leukocyte samples, consistent with high quality of DNA and RNA obtained from fresh materials.

Molecular studies in case 3. Detailed molecular findings have already been reported previously.[2] In brief, microsatellite analysis revealed biparentally derived homologs of chromosome 14, and a deletion analysis demonstrated a maternally inherited 108,768 bp microdeletion involving *DLK1*, the IG-DMR, the *MEG3*-DMR, and *MEG3*, but not affecting *RTL1*/*RTL1as*. Since loss of the DMRs causes maternal to paternal epigenotypic alteration,[2] it is predicted that case 3 has a single functional copy of *DLK1* and two functional copies of *RTL1* and *DIO3*, as well as no functional copy of *RTL1as* and other *MEGs*. Bisulfite sequencing showed that both the IG-DMR and the *MEG3*-DMR were markedly hypermethylated in leukocytes, whereas in the formalin-fixed and paraffin-embedded placental samples the IG-DMR was obviously hypermethylated and the *MEG3*-DMR was comprised of roughly two-thirds of hypermethylated clones and roughly one-third of hypomethylated clones. In addition, RT-PCR analysis for such placental samples indicated positive *PEGs* (especially *RTL1*) expression and absent *MEGs* expression. For the formalin-fixed and paraffin-embedded placental samples, PCR products could be obtained only after 35 cycles, because of poor quality (severe degradation) of DNA and RNA.

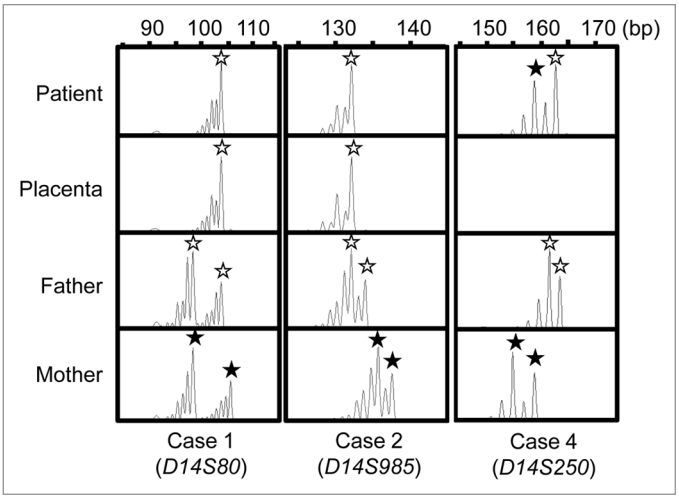

Figure 1. Representative results of microsatellite analysis, using leukocyte genomic DNA samples of the patient and the parents and placental genomic DNA samples. In cases 1 and 2, one of the two paternal peaks is inherited by the patients and the placentas, and no trace of maternal peaks is identified. In case 4, both paternally and maternally derived peaks are found in the patient, with the paternally derived long peak being larger than the maternally inherited short peak.

Molecular findings in case 4. We examined the presence or absence of the 14q32.2 imprinted region on the der(17) chromosome (**Fig. 4**). Oligoarray comparative genomic hybridization (CGH) indicated three copies of a ~19.6 Mb 14q31–qter region, and FISH analysis for four segments around the chromosome 14q32.2 imprinted region delineated positive signals on the der(17) chromosome as well as on the normal chromosome 14 homologs. This demonstrated the presence of the 14q32.2 imprinted region on the der(17) chromosome. In addition, similar oligoarray CGH and FISH analysis revealed loss of a ~455 kb region from the distal chromosome 17p (**Fig. S1**).

Thus, we investigated the parental origin of the translocated 14q distal region. Microsatellite analysis for *D14S250* and *D14S1007* on the translocated 14q distal region delineated biparentally derived two peaks, with paternally derived long PCR products showing larger peaks than maternally derived short PCR products (**Fig. 1**; **Table S2**). Since short products are usually more easily amplified than long products, this indicated paternal

Figure 2 (See opposite page). Bisulfite sequencing analysis of the IG-DMR (CG4 and CG6) and the *MEG3*-DMR (CG7), using leukocyte and placental genomic DNA samples. Filled and open circles indicate methylated and unmethylated cytosines at the CpG dinucleotides, respectively. Upper part: structure of CG4, CG6, and CG7. Pat, paternally derived chromosome; Mat, maternally derived chromosome. The PCR products for CG4 (311 bp) harbor 6 CpG dinucleotides and a G/A SNP (*rs12437020*), those for CG6 (428 bp) carry 19 CpG dinucleotides and a C/T SNP (*rs10133627*) and those for CG7 (168 bp) harbor 7 CpG dinucleotides. Lower part: the results of cases 1, 2, 4 and a control subject. Each horizontal line indicates a single subcloned allele. The control data represent the methylation patterns obtained with a leukocyte genomic DNA sample extracted from a single subject heterozygous for the G/A SNP (*rs12437020*) (body) and those obtained with a pooled DNA sample consisting of an equal amount of genomic DNA extracted from three control placentas homozygous for that SNP.

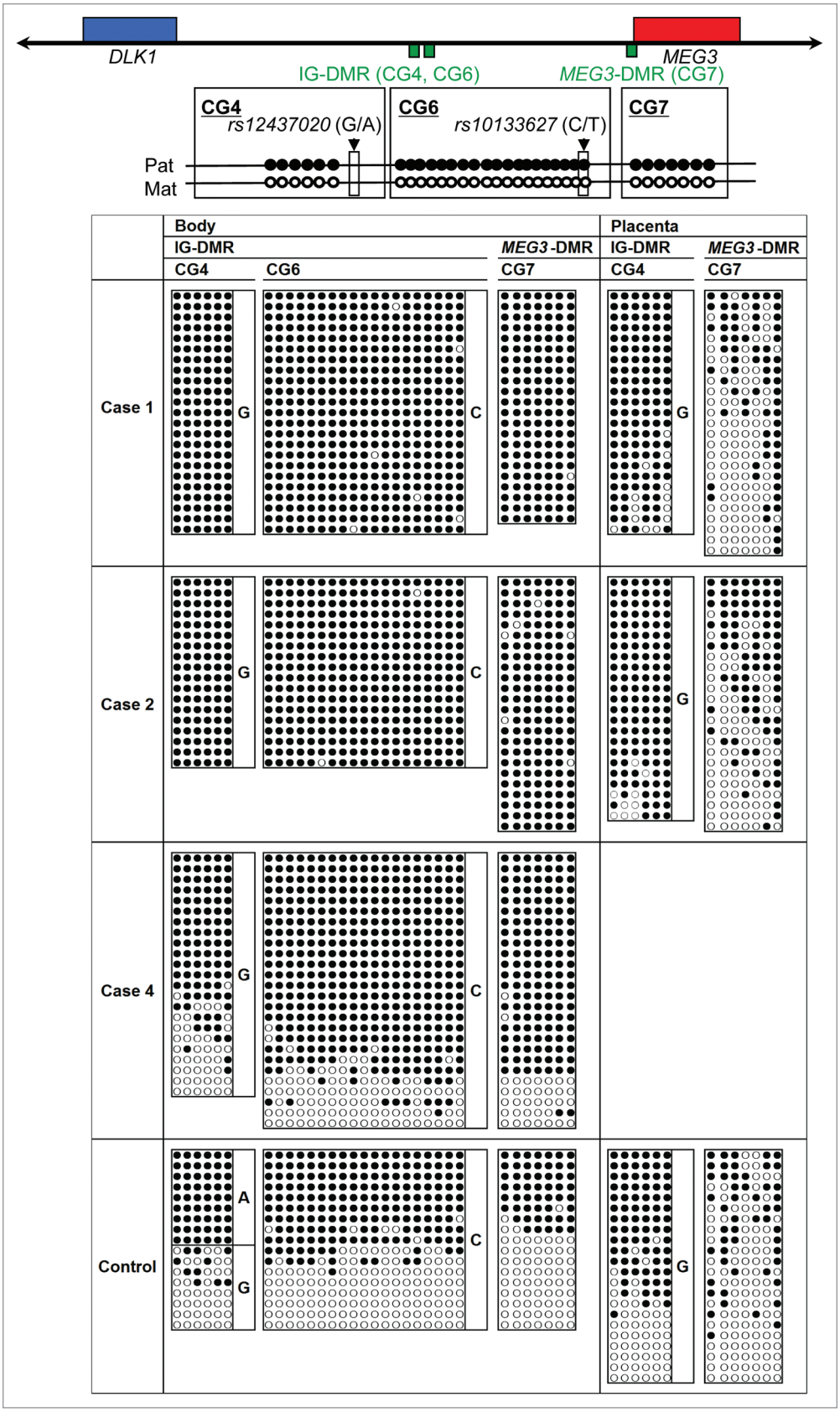

Figure 2. For figure legend, see page 1144.

origin of the der(17) chromosome harboring the chromosome14q32.2 imprinted region. Consistent with this, bisulfite sequencing showed moderate hypermethylation of the IG-DMR and the *MEG3*-DMR (**Fig. 2**).

Placental histopathological studies. We performed LM and EM studies, and IHC examinations (**Fig. 5**). LM examinations showed proliferated chorionic villi in cases 1–3. Capillary lumens were irregularly dilated with thickened endothelium in the stem to intermediate villi, but not in the terminal villi. Immature villi were present in case 3, probably because of 30 weeks of gestational age. Chorangioma was also identified in case 3. There was no villous chorangiosis, edematous change of villous stroma, or mesenchymal dysplasia characterized by grapelike vesicles in cases 1–3. Although the terminal villi exhibited no definitive abnormalities in the LM studies, EM examinations revealed swelling of vascular endothelial cells and hypertrophic change of pericytes in the terminal villi, together with narrowed capillary lumens, in cases 1 and 2.

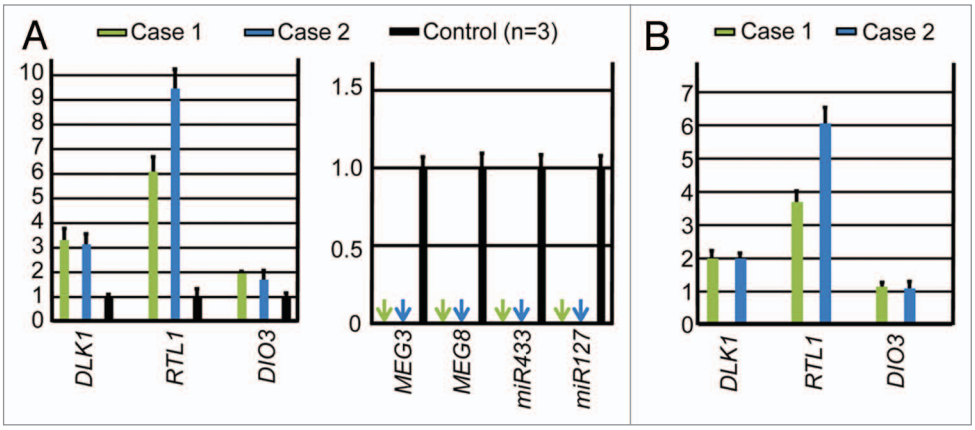

Figure 3. Quantitative real-time PCR analysis using placental samples. For a control, a pooled RNA sample consisting of an equal amount of total RNA extracted from three fresh control placentas was utilized. (A) Relative mRNA expression levels for *DLK1*, *RTL1*, and *DIO3* against *GAPDH* (mean ± SE) and lack of *MEGs* expression (indicated by arrows) (*miR433* and *miR127* are encoded by *RTL1as*) in the placental samples of cases 1 and 2. (B) Relative mRNA expression levels for *DLK1*, *RTL1*, and *DIO3* against *GAPDH* (mean ± SE), in the equal amount of expression positive placental cells (vascular endothelial cells and pericytes) of cases 1 and 2 (corrected for the difference in the relative proportion of expression positive cells between the placental samples of cases 1 and 2 and the control placental samples, on the assumption that the *DLK1* expression level is "simply doubled" in the expression positive placental cells of case 1 and 2).

IHC examinations identified RTL1, DLK1 and DIO3 protein expressions in the vascular endothelial cells and pericytes of chorionic villi, but not in the cytotrophoblasts, syncytiotrophoblasts, and stromal cells, in the placentas of cases 1–3 and in the control placenta. The PEGs protein expression level was variable in the control placenta, with moderate DLK1 expression, high RTL1 expression, and low DIO3 expression. Furthermore, DLK1 protein expression was apparently stronger in the placentas of cases 1 and 2 than in the placenta of case 3 and the control placenta, RTL1 protein expression was obviously stronger in the placentas of cases 1–3 than in the control placenta, and DIO3 protein expression was apparently similar between the placentas of cases 1–3 and the control placenta.

Discussion

We studied placental samples obtained from cases 1–3 with typical body and placental upd(14)pat phenotype. In this regard, the microsatellite data suggest that upd(14)pat with heterodisomic and isodisomic loci in case 1 was caused by trisomy rescue or gamete complementation, and that upd(14)pat with isodisomic loci alone in case 2 resulted from monosomy rescue or postzygotic mitotic error, although it is possible that heterodisomic locus/loci remained undetected in case 2.[15] Notably, there was no trace of a maternally inherited locus indicative of the presence of trisomic cells or normal cells with biparentally inherited chromosome 14 homologs in the placentas as well as in the leukocytes of cases 1 and 2. In addition, the microdeletion of case 3 has been shown to be inherited from the mother with the same microdeletion.[2] These findings imply that the placental tissues as well as the leukocytes of cases 1–3 almost exclusively, if not totally, consisted of cells with upd(14)pat or those with the microdeletion.

The q-PCR analysis was performed for the fresh placental samples of cases 1 and 2. In this context, two matters should be pointed out. First, the proportion of vascular endothelial cells and pericytes expressing *DLK1*, *RTL1*, and *DIO3* would be somewhat variable among samples, because only a small portion of the placenta was analyzed. This would be relevant to the some degree of difference in the expression levels between the placental samples of cases 1 and 2. Second, the relative proportion of vascular endothelial cells and pericytes expressing *DLK1*, *RTL1*, and *DIO3* would be higher in the placental samples of cases 1 and 2 than in the control placental samples, because the placentas of cases 1 and 2 were accompanied by proliferation of the chorionic villi with such expression positive cells. Thus, it would be inappropriate to perform a simple comparison of relative expression levels against *GAPDH* between the placental samples of cases 1 and 2 and the control placental samples. Indeed, although a complex regulatory mechanism(s), as implicated for the *RTL1* expression,[1,2] is unlikely to be operating for the *DLK1* expression, the relative *DLK1* expression level was 3.3 times and 3.1 times, not 2 times, higher in the placental samples of cases 1 and 2 than in the control placental samples, respectively (**Fig. 3A**). Assuming that *DLK1* expression level is simply doubled in expression positive cells of cases 1 and 2, it is predicted that the relative proportion of such expression positive cells is 1.65 times (3.3 ÷ 2.0) and 1.55 times (3.1 ÷ 2.0) larger in the placental samples of cases 1 and 2 than in the control placental samples, respectively. Thus, the expression level against *GAPDH* in the equal

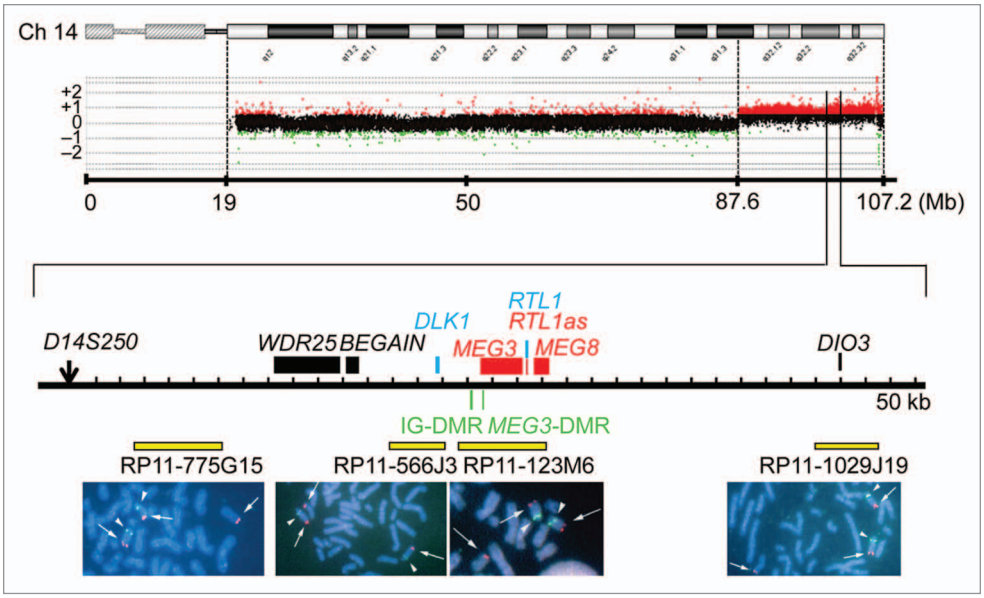

Figure 4. Array CGH and FISH analysis for the distal chromosome 14 region in case 4. In CGH analysis, the black, the red, and the green dots denote signals indicative of the normal, the increased (> +0.5), and the decreased (< –1.0) copy numbers, respectively. In FISH analysis, red signals (arrows) are derived from the probes detecting the various parts of the 14q32.2 imprinted region (the physical positions are indicated with yellow bars), and the green signals (arrowheads) are derived from an RP11–566I2 probe for 14q11.2 used as an internal control.

amount of expression positive cells is estimated as 3.69 times (6.1 ÷ 1.65) increased for *RTL1* and 1.15 times (1.9 ÷ 1.65) increased for *DIO3* in case 1, and as 6.06 times (9.4 ÷ 1.55) increased for *RTL1* and 1.09 times (1.7 ÷ 1.55) increased for *DIO3* in case 2 (**Fig. 3B**).

Thus, the expression data are summarized as follows (**Fig. 6**). First, it is inferred that the relative *RTL1* expression level is markedly (~5 times) increased in the expression positive cells of the placentas with upd(14)pat, as compared with the control placentas. This degree of elevation is grossly similar to that identified in the body of mice with the targeted deletion of the maternally derived IG-DMR (~4.5 times).[5] Such a markedly increased *RTL1* expression would be explained by assuming that *RTL1as*-encoded microRNAs (e.g., *miR433* and *miR127*) function as a repressor for *RTL1* expression through the RNAi mechanism, as has been indicated for the mouse *Rtl1-Rtl1as* interaction.[16,17] Second, it is unlikely that *DIO3* is solely expressed from the paternally inherited allele, although it remains to be determined whether *DIO3* undergoes partial imprinting like mouse *Dio3*[12] or completely escapes imprinting. In either case, the results would explain why patients with upd(14)pat and upd(14)mat lack clinically recognizable thyroid disorders,[2] although *DIO3* plays a critical role in the inactivation of thyroid hormones.[18]

This study provides further support for a critical role of excessive *RTL1* expression in the development of upd(14)pat phenotype (**Fig. 6**). Indeed, markedly (~5 times) increased *RTL1* expression is shared in common by cases 1–3 with typical upd(14)pat body and placental phenotype. In this context, it is notable that case 4 had no clinically recognizable upd(14)pat body and placental phenotype, except for omphalocele. This would imply that a single copy of *RTL1as* can almost reduce the *RTL1* expression dosage below the threshold level for the development of upd(14)pat phenotype by exerting a trans-acting repressor effect on the two functional copies of *RTL1*. By contrast, the relevance of *DLK1* to upd(14)pat phenotype is unlikely, because case 3 exhibited typical upd(14)pat phenotype in the presence of a single functional copy of *DLK1*, and case 4 showed no upd(14)pat phenotype except for omphalocele in the presence of two functional copies of *DLK1*. Similarly, if *DIO3* were more or less preferentially expressed from paternally inherited allele, the relevance of *DIO3* to upd(14)pat phenotype would also remain minor, if any. Case 4 had no upd(14)pat phenotype except for omphalocele in the presence of with two copies of *DIO3* of paternal origin. It should be pointed out, however, that the absence of *MEGs* expression may have a certain effect on the development of upd(14)pat phenotype.

The placental histological examinations revealed several informative findings. First, DLK1, RTL1, and DIO3 proteins were specifically identified in vascular endothelial cells and pericytes of chorionic villi in the control placenta, with RTL1 protein being most strongly expressed. These results, together with abnormal LM and EM findings of such cells in cases 1–3, suggest that these proteins, especially RTL1 protein, plays a pivotal role in the development of endothelial cells and pericytes. In this regard, it may be possible that the endothelial thickening and resultant narrowing the capillary lumens in the terminal villi have resulted in the dilatation of the stem to intermediate portions of the chorionic villi.

Second, the degree of protein staining was well correlated with the expression dosage of corresponding genes. In this regard, since characteristic macroscopic and microscopic placental features were identified in cases 1–3 who shared markedly elevated RTL1 protein expression, this is consistent with the notion that upd(14)pat phenotype is primarily caused by the markedly

elevated *RTL1* expression.[2] Indeed, DLK1 protein expression was not exaggerated in case 3 with typical upd(14)pat phenotype, and DIO3 protein expression was not enhanced in cases 1–3. It may be possible, however, that the abnormality of placental structures may have resulted in a difference in immunostaining without an actual change in gene expression. This point awaits further investigations.

Third, villous chorangiosis, stromal expansion, and mesenchymal dysplasia were not identified in the placental samples of cases 1–3, although such a lesion(s) may have existed in non-examined portions. Notably, such lesions are frequently observed in placentas of patients with BWS.[19-21] Thus, while both upd(14)pat and BWS are associated with placentomegaly and polyhydroamnios, characteristic histological findings appear to be different between upd(14)pat and BWS.

This study would also provide useful information on the methylation patterns of the *MEG3*-DMR in the placenta. Our previous studies using formalin-fixed and paraffin-embedded placental samples revealed that roughly two-thirds of clones were hypermethylated and the remaining roughly one-third of clones were hypomethylated in case 3 as well as in the previously reported patients with upd(14)pat (not cases 1 and 2) and epimutation (hypermethylation of the IG-DMR and the *MEG3*-DMR of maternal origin), and that roughly one-third of clones were hypermethylated and the remaining roughly two-thirds of clones were hypomethylated in control placental samples (see Fig. S2C in ref. 2). However, this study showed that the *MEG3*-DMR was grossly hypomethylated in the fresh placental samples of cases 1 and 2, with an extent similar to that identified in the fresh control placental samples. In this regard, it is notable that PCR products could be obtained only after 35 cycles for the formalin-fixed and paraffin-embedded placental samples and were sufficiently obtained after 30 cycles for the fresh placental samples. Thus, several specific clones may have been selectively amplified in the previous study. Furthermore, it may be possible that efficacy of bisulfite treatment (conversion of unmethylated cytosine into uracils and subsequently thymines) may be insufficient for the formalin-fixed and paraffin-embedded placental samples. Thus, it appears that the present data denote precise methylation patterns of the *MEG3*-DMR in the placenta.

In summary, the present study provides useful clues for the clarification of regulatory mechanism for the *RTL1* expression, imprinting status of *DIO3* and characteristic placental histological findings in patients with upd(14)pat and related conditions. Further studies will help improve our knowledge about upd(14)pat and related conditions.

Methods

Ethical approval. This study was approved by the Institutional Review Board Committees of each investigator, and performed after obtaining written informed consent.

Primers. Primers utilized in this study are summarized in **Table S3**.

Sample preparation for molecular studies. Genomic DNA samples were obtained from leukocytes using FlexiGene DNA Kit (Qiagen) and from placental samples using ISOGEN (Nippon Gene). Transcripts of *DLK1, MEG3, RTL1*, *MEG8* and *DIO3* were isolated with ISOGEN (Nippon Gene), and *microRNAs* were extracted with mirVana™ miRNA Isolation Kit (Ambion). After DNase treatment, cDNA samples for *DLK1, MEG3, MEG8* and *DIO3* were prepared with oligo(dT) primers from 1 μg of RNA using Superscript III Reverse Transcriptase (Invitrogen), and those of *microRNAs* were synthesized from 300 ng of RNA using TaqMan MicroRNA Reverse Transcription Kit (Applied Biosystems). For *RTL1*, 3'-RACE was utilized to prevent amplification of *RTL1as*; cDNA was synthesized from 1 μg of RNA using Superscript III Reverse Transcriptase with a long primer hybridizing to poly A site and introducing the adaptor sequence. Lymphocyte metaphase spreads for FISH analysis were prepared from leukocytes using colcemide (Invitrogen).

Molecular studies. Microsatellite analysis for 19 loci on chromosome 14, methylation analysis for the IG-DMR and

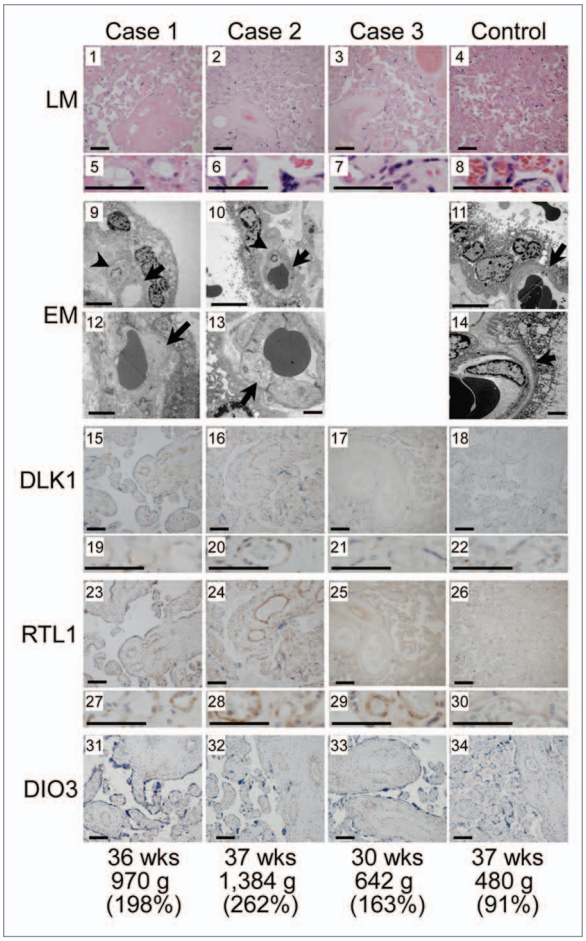

Figure 5. Histological examinations. LM, light microscopic examinations; EM, electron microscopic examinations; DLK1, RTL1 and DIO3, immunohistochemical examinations for the corresponding proteins. The arrows and arrowheads in the EM findings indicate endothelial cells and pericytes, respectively. Scale bars represent 100 μm for 1–4, 15–18, 23–26 and 31–34, 50 μm for 5–8, 19–22 and 27–30, 5 μm for 9–11 and 2 μm for 12–14. Gestational age, placental weight, and % placental weight assessed by the gestational age-matched Japanese references for placental weight[4,22] are described.

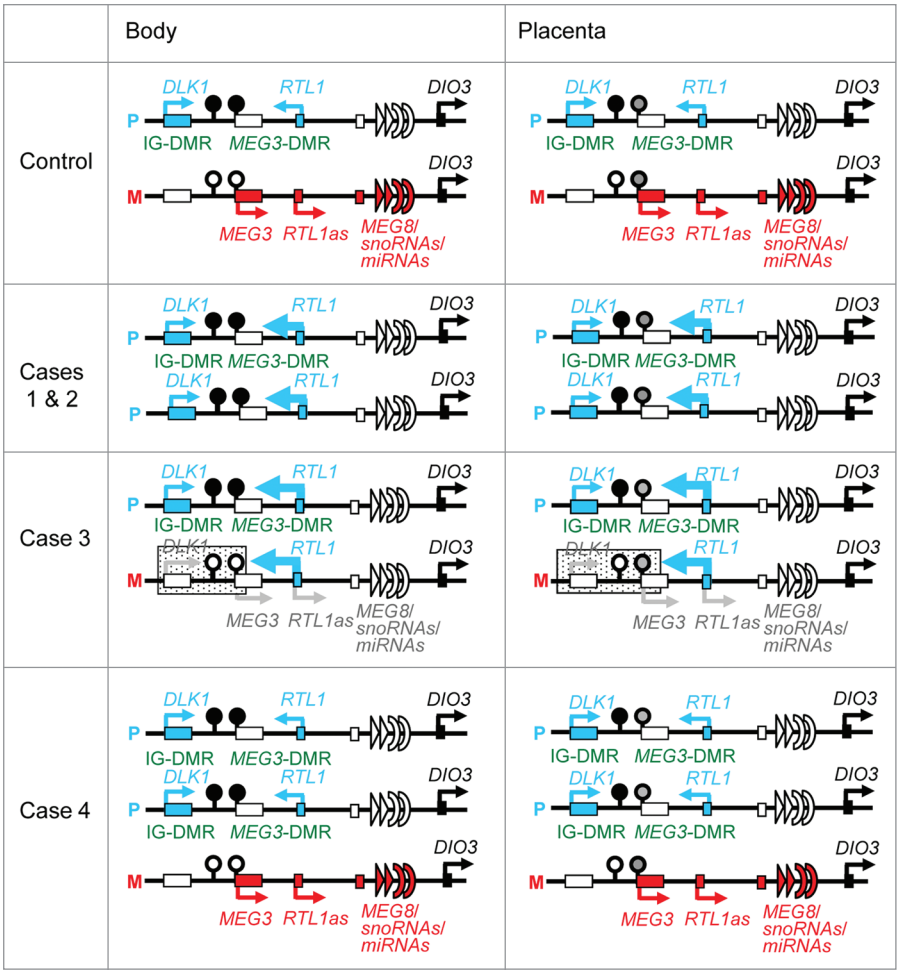

Figure 6. Schematic representation of the chromosome 14q32.2 imprinted region in a control subject, cases 1 and 2 with upd(14)pat, case 3 with a microdeletion (indicated by stippled rectangles), and case 4 with two copies of the imprinted region of paternal origin and a single copy of the imprinted region of maternal origin. This figure has been constructed using the present results and the previous data.[2,3] P, paternally derived chromosome; M, maternally derived chromosome. Filled and open circles represent hypermethylated and hypomethylated DMRs, respectively; since the *MEG3*-DMR is grossly hypomethylated and regarded as non-DMR in the placenta, it is painted in gray. *PEGs* (*DLK1* and *RTL1*) are shown in blue, *MEGs* (*MEG3*, *RTL1as*, *MEG8*, *snoRNAs* and *miRNAs*) in red, a probably non-imprinted gene (*DIO3*) in black, and non-expressed genes in white. Thick arrows for *RTL1* in cases 1–3 represent increased *RTL1* expression that is ascribed to loss of functional microRNA-containing *RTL1as* as a repressor for *RTL1*.

the *MEG3*-DMR, and FISH analyses for the 14q32.2 region were performed as described previously.[2,3] For FISH analysis of 17p13.3, a 17p sub-telomere probe and an RP11–411G7 probe for the 17p13.3 region were utilized, together with a CEP17 probe for the 17p11.1 region utilized as an internal control. The 17p sub-telomere probe was detected according to the manufacture's protocol, the RP11–411G7 probe was labeled with digoxigenin and detected by rhodamine anti-digoxigenin, and the CEP17 control probe was labeled with biotin and detected by avidin conjugated to fluorescein isothiocyanate. Quantitative real-time PCR analysis was performed on an ABI PRISM 7000 (Applied Biosystems) using TaqMan real-time PCR probe primer mixture for the following genes (assay No: Hs00171584 for *DLK1,* Hs00292028 for *MEG3*, Hs00419701 for *MEG8* and Hs00704811 for *DIO3*; assay ID: 001028 for *miR433* and 000452 for *miR127*). For *RTL1*, q-PCR analysis was performed with a forward primer hybridized to the sequence of *RTL1* and a reverse primer hybridized to the adaptor sequence. Fifty nanongrams of cDNA in a 50 μl reaction mixture contacting 2 × KOD FX buffer (Toyobo), 2.0 mM dNTP mixture (Toyobo), KOD FX (Toyobo), SYBR Green I (Invitrogen), and primer set for *RTL1* were subjected to the ABI PRISM 7000. Data were normalized against *GAPDH* (catalog No: 4326317E) for *DLK1, MEG3*, *MEG8*, *RTL1*, and *DIO3*, and against *RNU48* (assay ID: 0010006) for *microRNAs*. The expression studies were performed three times for each sample. Oligoarray CGH was performed using 1 × 1M format Human Genome Array (Catalog No G4447A) (Agilent Technologies).

Histopathogical analysis. Placental samples were fixed with 20% buffered formaldehyde at room temperature and embedded in paraffin wax according to standard protocols for LM examinations. Then, sections of 3 μm thick were stained with hematoxylin-eosin. For EM examinations, fresh placental tissues were fixed with phosphate-buffered 2.5% glutaraldehyde, postfixed in 1% osmium tetroxide, and embedded in Epon 812 (catalog No. R3245, TAAB). Semithin sections were stained with 1% methylene blue, and ultrathin sections were double-stained with uranyl acetate and lead citrate. Subsequently, they were examined with a Ninhon Denshi JEM-1230 electron microscope.

For IHC analysis, sections of 3 μm thick were prepared by the same methods utilized for the LM examinations, and were examined with rabbit anti human DLK1 polyclonal antibody at 1:100 dilutions (catalog No 10636-1-AP, ProteinTech Group), rabbit anti human RTL1 polyclonal antibody at 1:200 dilutions, and rabbit anti human DIO3 polyclonal antibody at 1:50 dilutions (catalog No ab102926, abcam); anti human RTL1 polyclonal antibody was produced by immunizing rabbits with the synthesized RTL1 peptide (NH2-RGFPRDPSTESG-COOH) in this study. Sections were dewaxed in xylene and rehydrated through graded ethanol series and, subsequently, incubated in 10% citrate buffer (pH 6.0) for 40 min in a 98°C water bath, for antigen retrieval. Endogenous peroxidase activity was quenched with 1% H_2O_2 and 100% methanol for 20 min. To prevent non-specific background staining, sections are incubated with Protein Block Serum-Free (Dako corporation) for 10 min at room temperature. Then, sections were incubated overnight with primary antibody at 4°C

and, subsequently, treated with the labeled polymer prepared by combining amino acid polymers with peroxidase and anti- rabbit polyclonal antibody (Histofine Simple Stain MAX PO MULTI, Nichirei). Peroxidase activities were visualized by diaminobenzidine staining, and the nuclei were stained with hematoxylin.

Disclosure of Potential Conflicts of Interest

No potential conflicts of interest were disclosed.

Acknowledgments

This work was supported by Grants-in-Aid for Scientific Research (A) (22249010) and Research (B) (21028026) from the Japan Society for the Promotion of Science (JSPS), by Grants-in-Aid for Scientific Research on Innovative Areas (22132004-A04) from the Ministry of Education, Culture, Sports, Science and Technology (MEXT), by Grants for Research on Intractable Diseases (H22–161) from the Ministry of Health, Labor and Welfare (MHLW), by Grant for National Center for Child Health and Development (23A-1), and by Grant from Takeda Science Foundation and from Novartis Foundation.

Supplemental Materials

Supplemental materials may be found here:
www.landesbioscience.com/journals/epigenetics/article/21937

References

1. da Rocha ST, Edwards CA, Ito M, Ogata T, Ferguson-Smith AC. Genomic imprinting at the mammalian Dlk1-Dio3 domain. Trends Genet 2008; 24:306-16; PMID:18471925; http://dx.doi.org/10.1016/j.tig.2008.03.011.
2. Kagami M, Sekita Y, Nishimura G, Irie M, Kato F, Okada M, et al. Deletions and epimutations affecting the human 14q32.2 imprinted region in individuals with paternal and maternal upd(14)-like phenotypes. Nat Genet 2008; 40:237-42; PMID:18176563; http://dx.doi.org/10.1038/ng.2007.56.
3. Kagami M, O'Sullivan MJ, Green AJ, Watabe Y, Arisaka O, Masawa N, et al. The IG-DMR and the MEG3-DMR at human chromosome 14q32.2: hierarchical interaction and distinct functional properties as imprinting control centers. PLoS Genet 2010; 6:e1000992; PMID:20585555; http://dx.doi.org/10.1371/journal.pgen.1000992.
4. Kagami M, Yamazawa K, Matsubara K, Matsuo N, Ogata T. Placentomegaly in paternal uniparental disomy for human chromosome 14. Placenta 2008; 29:760-1; PMID:18619672; http://dx.doi.org/10.1016/j.placenta.2008.06.001.
5. Lin SP, Youngson N, Takada S, Seitz H, Reik W, Paulsen M, et al. Asymmetric regulation of imprinting on the maternal and paternal chromosomes at the Dlk1-Gtl2 imprinted cluster on mouse chromosome 12. Nat Genet 2003; 35:97-102; PMID:12937418; http://dx.doi.org/10.1038/ng1233.
6. Sekita Y, Wagatsuma H, Nakamura K, Ono R, Kagami M, Wakisaka N, et al. Role of retrotransposon-derived imprinted gene, Rtl1, in the feto-maternal interface of mouse placenta. Nat Genet 2008; 40:243-8; PMID:18176565; http://dx.doi.org/10.1038/ng.2007.51.
7. Lage JM. Placentomegaly with massive hydrops of placental stem villi, diploid DNA content, and fetal omphaloceles: possible association with Beckwith-Wiedemann syndrome. Hum Pathol 1991; 22:591-7; PMID:1864589; http://dx.doi.org/10.1016/0046-8177(91)90237-J.
8. Yamazawa K, Kagami M, Nagai T, Kondoh T, Onigata K, Maeyama K, et al. Molecular and clinical findings and their correlations in Silver-Russell syndrome: implications for a positive role of IGF2 in growth determination and differential imprinting regulation of the IGF2-H19 domain in bodies and placentas. J Mol Med (Berl) 2008; 86:1171-81; PMID:18607558; http://dx.doi.org/10.1007/s00109-008-0377-4.
9. Georgiades P, Watkins M, Burton GJ, Ferguson-Smith AC. Roles for genomic imprinting and the zygotic genome in placental development. Proc Natl Acad Sci U S A 2001; 98:4522-7; PMID:11274372; http://dx.doi.org/10.1073/pnas.081540898.
10. Fowden AL, Sibley C, Reik W, Constancia M. Imprinted genes, placental development and fetal growth. Horm Res 2006; 65(Suppl 3):50-8; PMID:16612114; http://dx.doi.org/10.1159/000091506.
11. Georgiades P, Ferguson-Smith AC, Burton GJ. Comparative developmental anatomy of the murine and human definitive placentae. Placenta 2002; 23:3-19; PMID:11869088; http://dx.doi.org/10.1053/plac.2001.0738.
12. Tsai CE, Lin SP, Ito M, Takagi N, Takada S, Ferguson-Smith AC. Genomic imprinting contributes to thyroid hormone metabolism in the mouse embryo. Curr Biol 2002; 12:1221-6; PMID:12176332; http://dx.doi.org/10.1016/S0960-9822(02)00951-X.
13. Yamanaka M, Ishikawa H, Saito K, Maruyama Y, Ozawa K, Shibasaki J, et al. Prenatal findings of paternal uniparental disomy 14: report of four patients. Am J Med Genet A 2010; 152A:789-91; PMID:20186803; http://dx.doi.org/10.1002/ajmg.a.33247.
14. Suzumori N, Ogata T, Mizutani E, Hattori Y, Matsubara K, Kagami M, et al. Prenatal findings of paternal uniparental disomy 14: Delineation of further patient. Am J Med Genet A 2010; 152A:3189-92; PMID:21108407; http://dx.doi.org/10.1002/ajmg.a.33719.
15. Kagami M, Kato F, Matsubara K, Sato T, Nishimura G, Ogata T. Relative frequency of underlying genetic causes for the development of UPD(14)pat-like phenotype. Eur J Hum Genet 2012; 20:928-32; PMID:22353941; http://dx.doi.org/10.1038/ejhg.2012.26.
16. Seitz H, Youngson N, Lin SP, Dalbert S, Paulsen M, Bachellerie JP, et al. Imprinted microRNA genes transcribed antisense to a reciprocally imprinted retrotransposon-like gene. Nat Genet 2003; 34:261-2; PMID:12796779; http://dx.doi.org/10.1038/ng1171.
17. Davis E, Caiment F, Tordoir X, Cavaillé J, Ferguson-Smith A, Cockett N, et al. RNAi-mediated allelic trans-interaction at the imprinted Rtl1/Peg11 locus. Curr Biol 2005; 15:743-9; PMID:15854907; http://dx.doi.org/10.1016/j.cub.2005.02.060.
18. Köhrle J. Thyroid hormone transporters in health and disease: advances in thyroid hormone deiodination. Best Pract Res Clin Endocrinol Metab 2007; 21:173-91; PMID:17574002; http://dx.doi.org/10.1016/j.beem.2007.04.001.
19. Kraus FT, Redline RW, Gersell DJ, Nelson DM, Dicker JM. Disorders of placental Development. Placental Pathology (Atlas of Noutumor Pathology). Washington, DC: American Registry of Pathology, 2004:59-68.
20. Fox HE, Sebire NJ. The placenta in abnormalities and disorders of the fetus. Pathology of the Placenta. Third edition, Philadelphia, PA: SAUNDERS, 2007:262-3.
21. Parveen Z, Tongson-Ignacio JE, Fraser CR, Killeen JL, Thompson KS. Placental mesenchymal dysplasia. Arch Pathol Lab Med 2007; 131:131-7; PMID:17227114.
22. Nakayama M. Placental pathology. Tokyo, Igaku Shoin, 2002:106-7 (in Japanese).

RESEARCH LETTER

AMERICAN JOURNAL OF medical genetics PART A

Recurrence of Osteogenesis Imperfecta Due to Maternal Mosaicism of a Novel *COL1A1* Mutation

Takahiro Yamada,[1]* Masaki Takagi,[2] Gen Nishimura,[3] Rina Akaishi,[1] Itsuko Furuta,[1] Mamoru Morikawa,[1] Takashi Yamada,[1] Kazutoshi Cho,[1] Hideaki Sawai,[4] Shiro Ikegawa,[5] Tomonobu Hasegawa,[2] and Hisanori Minakami[1]

[1]Department of Obstetrics and Gynecology, Hokkaido University Graduate School of Medicine, Sapporo, Japan

[2]Department of Pediatrics, Keio University School of Medicine, Tokyo, Japan

[3]Department of Radiology, Tokyo Metropolitan Children's Medical Center, Tokyo, Japan

[4]Department of Obstetrics and Gynecology, Hyogo College of Medicine, Nishinomiya, Japan

[5]Laboratory for Bone and Joint Diseases, Center for Genomic Medicine, RIKEN, Tokyo, Japan

Manuscript Received: 4 May 2012; Manuscript Accepted: 5 July 2012

TO THE EDITOR:

The lethal form of osteogenesis imperfecta (type II OI, OMIM #166210) is a common skeletal dysplasia that occurs during the perinatal period. Most cases are sporadic and attributable to heterozygous mutations of type 1 collagen genes (*COL1A1* and *COL1A2*). Therefore, type II OI is not likely to occur in siblings with normal parents; however, the occurrence of type II OI has been reported in 7–8% of siblings [Byers et al., 1988]. This is attributed in part to the autosomal recessive (AR) inheritance of OI because several genes encoding the enzymes involved in collagen post-translational modifications cause type II OI as AR traits [Barnes et al., 2006; Morello et al., 2006; Cabral et al., 2007; van Dijk et al., 2009; Lapunzina et al., 2010]. The occurrence of type II OI in siblings is also attributed to parental mosaics of type 1 collagen gene mutations [Byers et al., 1988; Cohen-Solal et al., 1991]. Indeed, several reports have described fatal outcomes from mosaic mutations in OI [Cohn et al., 1990; Constantinou et al., 1990; Wallis et al., 1990; Mottes et al., 1993; Cohen-Solal et al., 1994].

Here, we report on a family with recurrence of type II OI due to a *COL1A1* mosaic mutation in the mother. A 25-year-old Japanese woman reported a therapeutic abortion of her first pregnancy at 20 weeks of gestation due to shortening and bending of the long bones in her fetus. Neither tissue specimens nor radiographic images were obtained from the terminated fetus. She was referred to us at 17 weeks of gestation of her second pregnancy because bowing and shortening of the femora were found again in her second fetus. The mother was short in height (147 cm, −2.2 SD), but had no history of bone fracture and no clinical features of OI, such as blue sclera, hearing impairment, and abnormal tooth development. Her marriage was not consanguineous. Ultrasonography revealed a fetal biparietal diameter of 40.1 mm (+0.70 SD); lengths of the curved femur and humerus of 16.2 mm (−3.1 SD) and 14.2 mm (−3.8 SD), respectively; a narrowed thorax with short ribs; defective calvarial ossification evidenced by easy skull compression with an ultrasound probe (Fig. 1A); and unusually well-defined cerebral gyri.

After genetic counseling with a tentative diagnosis of severe OI, the mother underwent a termination of the pregnancy at 19 weeks of gestation. Postmortem radiographs revealed beaded ribs, shortened broad and crumpled long bones, and nonossified calvaria, which warranted a diagnosis of type IIA OI (Fig. 1B). The parents did not permit an autopsy, but they gave consent for genetic examination of the umbilical cord blood and fetal skin sampled at the termination.

We extracted genomic DNA from the umbilical cord blood of the affected fetus and the peripheral blood of the unaffected parents by

How to Cite this Article:
Yamada T, Takagi M, Nishimura G, Akaishi R, Furuta I, Morikawa M, Yamada T, Cho K, Sawai H, Ikegawa S, Hasegawa T, Minakami H. 2012. Recurrence of osteogenesis imperfecta due to maternal mosaicism of a novel *COL1A1* mutation.
Am J Med Genet Part A 158A:2969–2971.

Grant sponsor: Ministry of Health, Labour and Welfare of Japan; Grant numbers: H23-Nanchi-Ippan-123, H22-Nanchi-Ippan-194, Jitsuyoka (Nanbyo)-Ippan-014 (23300102).
Takahiro Yamada and Masaki Takagi contributed equally to this work.
*Correspondence to:
Takahiro Yamada, M.D., Ph.D., Department of Obstetrics and Gynecology, Hokkaido University Graduate School of Medicine, N15W7, Kita-ku, Sapporo 060-8638, Japan. E-mail: taka0197@med.hokudai.ac.jp
Article first published online in Wiley Online Library (wileyonlinelibrary.com): 17 September 2012
DOI 10.1002/ajmg.a.35602

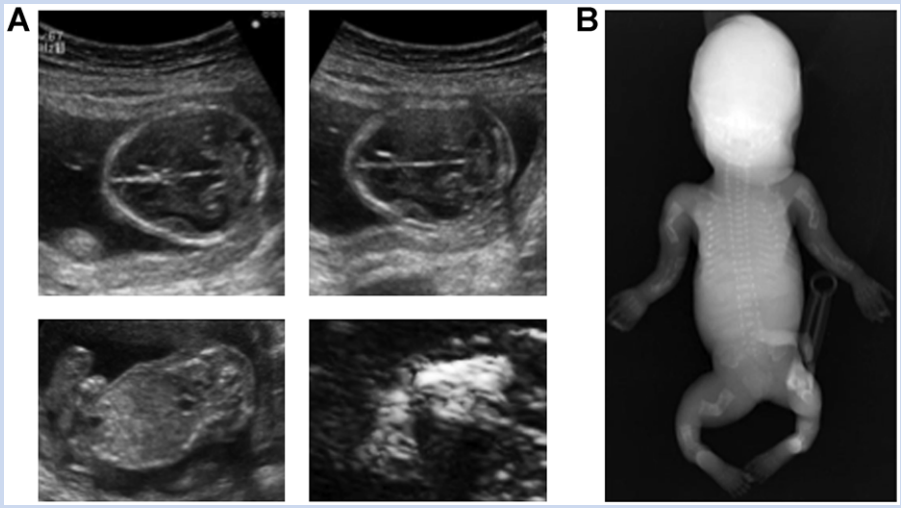

FIG. 1. A: Prenatal ultrasonography of the affected second fetus. Upper panels: Easily compressed unossified calvaria. The shape of the calvaria was easily changed before (left image) and after (right image) the compression. Lower left panel: Coronal view of the narrow thorax with short ribs. Lower right panel: Highly curved femur of the affected fetus. B: A postmortem radiograph of the fetus showing beaded ribs, shortened broad and crumpled long bones, and nonossified calvaria.

using a QIAamp DNA Mini Kit (Qiagen, Tokyo, Japan). We analyzed all coding exons and flanking introns of *COL1A1*, *COL1A2*, *LEPRE1*, *CRTAP*, and *PPIB* by polymerase chain reaction (PCR) of the genomic DNA and direct sequencing. A heterozygous mutation c.1054_1056 + 2 del AAGGT was found in *COL1A1* (Fig. 2A). Because the deletion involved the consensus splice donor site, a reverse transcription-PCR (RT-PCR) was performed using the fetus's RNA to check for a splicing abnormality. RNA was extracted from the fetal skin using an RNeasy Mini Kit (Qiagen). The cDNAs were subjected to PCR amplification using primers (5′-AAA TGG AGC TCC TGG TCA GA-3′ and 5′-AGG AGC ACC AGC AAT ACC AG-3′) encompassing exons 13–19. Sequencing of the RT-PCR products showed an insertion of 255 bp in intron 16, resulting in an in-frame insertion of 84 amino acids (Fig. 2B). *COL1A1* sequencing of the PCR products of the parents' genomic DNA from their blood samples revealed the same mutation in the mother, but not in the father. The electropherographic signal intensity of the mutant allele was low in the mother, suggesting a mosaic mutation (data not shown). The mosaic rate of this mutation was examined by subcloning of PCR products from genomic DNAs of various tissues; the ratio (mutant:wild-type) was 13:37 in blood, 16:34 in hair roots, and 8:42 in nails.

The mother became pregnant 3 months after the termination of her second pregnancy. A molecular examination of the chorionic villus sample excluded the *COL1A1* mutation (data not shown). She gave birth to an unaffected baby at 39 weeks of gestation. The mother underwent skeletal survey and dual energy X-ray absorptiometry for the lumbar spine (L2–L4) postpartum. Her bone mineral density was slightly low (0.865 g/cm^2; *Z*-score, −1.3), but still within the normal range. Radiographic examination revealed no abnormality suggestive of OI.

The unique *COL1A1* mutation reported here was predicted to cause mis-splicing and consequently to create an elongated procollagen protein. This elongated procollagen would presumably interfere the triple helix formation of collagen and hence is responsible for the lethal phenotypes of the affected siblings. This speculation is consistent with our current understanding of the pathogenesis of severe OI, which is believed to involve a dominant negative mechanism. As with the mother of fetus investigated in the current report, mosaic parents are sometimes asymptomatic or only mildly affected, if at all [Cohn et al., 1990; Constantinou et al., 1990; Wallis et al., 1990; Wijsman, 1991]. The mother showed only mildly short stature and mildly decreased bone density in the lumbar spine. The mosaic state of the mutation in the mother was 16–32% in the tissue examined. This observation was consistent with results of previous reports; a patient with 20% mosaic mutations in the blood and hair roots was asymptomatic [Cohn et al., 1990], while patients with 50% mutations in fibroblasts and 27% mutations in the blood were symptomatic [Wallis et al., 1990], and those with 25% mutations in fibroblasts and blood were also mildly symptomatic [Constantinou et al., 1990].

A molecular analysis to determine the mosaic state is important for familial recurrence. A genetic test, which confirms the mode of inheritance, followed by precise genetic counseling based on the recurrence rate estimation by mosaic rate, is particularly important in the management of severe perinatal OI.

ACKNOWLEDGMENTS

This study was supported by a Grant-in-Aid for Scientific Research from the Ministry of Health, Labour and Welfare of Japan, H23-Nanchi-Ippan-123 (to H.S., S.I.), H22-Nanchi-Ippan-194 (to T.H.) and Jitsuyoka (Nanbyo)-Ippan-014 (23300102) (to T.H.).

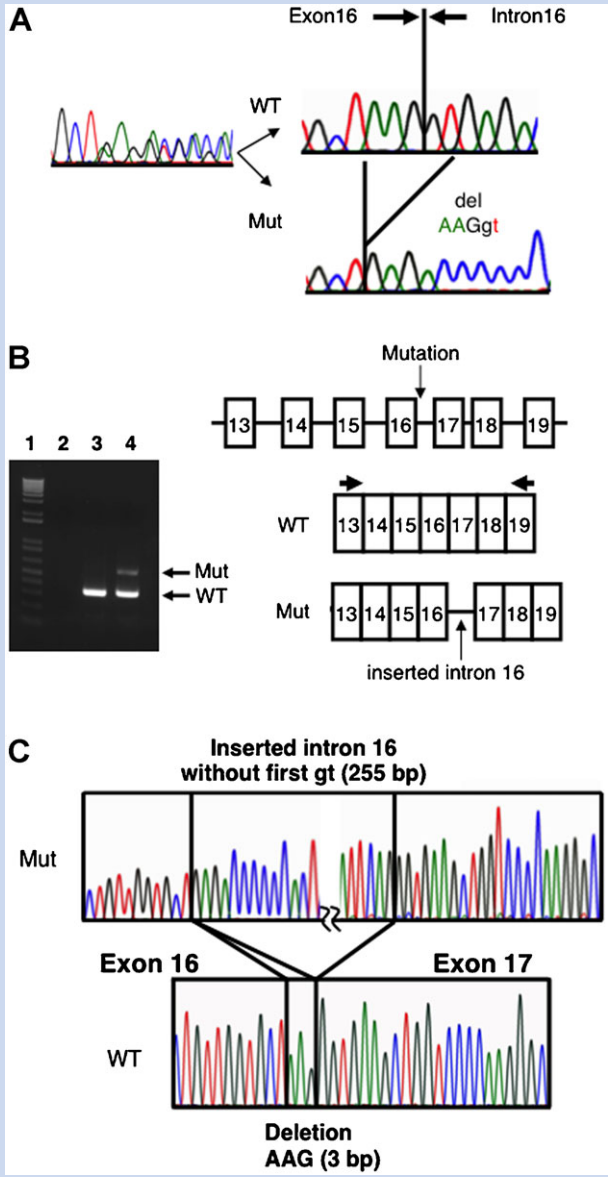

FIG. 2. ***COL1A1*** **mutation in the affected second fetus. A: Left: Direct sequencing of genomic DNA. The electropherograms of the wild-type (WT) and mutant (Mut) alleles were overlapping. Right: Subcloning revealed an AAGgt deletion in the junction of exon 16 and intron 16. B: RT-PCR of the mRNA from the fetal skin. Left: PCR products of WT (346 bp) and Mut (598 bp) are shown. Lanes 1: Marker, 2: Negative control, 3: Control cDNA, 4: Patient cDNA. Right: RT-PCR was performed using a primer set at exons 13 and 19 (arrows). C: cDNA sequence of the mutation. In the WT allele, intron 16 (257 bp) had been spliced out. The Mut allele had 5 bp deletion; "AAG" are the last 3 bp of exon 16 and "GT" are the first 2 bp of intron 16. The deletion of the splice donor site of intron 16 resulted in contiguous transcription to exon 16. The contiguous intron 16 was 255 bp long.**

REFERENCES

Barnes AM, Chang W, Morello R, Cabral WA, Weis M, Eyre DR, Leikin S, Makareeva E, Kuznetsova N, Uveges TE, Ashok A, Flor AW, Mulvihill JJ, Wilson PL, Sundaram UT, Lee B, Marini JC. 2006. Deficiency of cartilage-associated protein in recessive lethal osteogenesis imperfecta. N Engl J Med 355:2757–2764.

Byers PH, Tsipouras P, Bonadio JF, Starman BJ, Schwartz RC. 1988. Perinatal lethal osteogenesis imperfecta (OI type II): A biochemically heterogeneous disorder usually due to new mutations in the genes for type I collagen. Am J Hum Genet 42:237–428.

Cabral WA, Chang W, Barnes AM, Weis M, Scott MA, Leikin S, Makareeva E, Kuznetsova NV, Rosenbaum KN, Tifft CJ, Bulas DI, Kozma C, Smith PA, Eyre DR, Marini JC. 2007. Prolyl 3-hydroxylase 1 deficiency causes a recessive metabolic bone disorder resembling lethal/severe osteogenesis imperfecta. Nat Genet 39:359–365.

Cohen-Solal L, Bonaventure J, Maroteaux P. 1991. Dominant mutations in familial lethal and severe osteogenesis imperfecta. Hum Genet 87: 297–301.

Cohen-Solal L, Zylberberg L, Sangalli A, Gomez Lira M, Mottes M. 1994. Substitution of an aspartic acid for glycine 700 in the alpha 2(I) chain of type I collagen in a recurrent lethal type II osteogenesis imperfecta dramatically affects the mineralization of bone. J Biol Chem 269: 14751–14758.

Cohn DH, Starman BJ, Blumberg B, Byers PH. 1990. Recurrence of lethal osteogenesis imperfecta due to parental mosaicism for a dominant mutation in a human type I collagen gene (COL1A1). Am J Hum Genet 46:591–601.

Constantinou CD, Pack M, Young SB, Prockop DJ. 1990. Phenotypic heterogeneity in osteogenesis imperfecta: The mildly affected mother of a proband with a lethal variant has the same mutation substituting cysteine for alpha 1-glycine 904 in a type I procollagen gene (COL1A1). Am J Hum Genet 47:670–679.

Lapunzina P, Aglan M, Temtamy S, Caparrós-Martín JA, Valencia M, Letón R, Martínez-Glez V, Elhossini R, Amr K, Vilaboa N, Ruiz-Perez VL. 2010. Identification of a frameshift mutation in Osterix in a patient with recessive osteogenesis imperfecta. Am J Hum Genet 87:110–114.

Morello R, Bertin TK, Chen Y, Hicks J, Tonachini L, Monticone M, Castagnola P, Rauch F, Glorieux FH, Vranka J, Bächinger HP, Pace JM, Schwarze U, Byers PH, Weis M, Fernandes RJ, Eyre DR, Yao Z, Boyce BF, Lee B. 2006. CRTAP is required for prolyl 3- hydroxylation and mutations cause recessive osteogenesis imperfecta. Cell 127:291–304.

Mottes M, Gomez Lira MM, Valli M, Scarano G, Lonardo F, Forlino A, Cetta G, Pignatti PF. 1993. Paternal mosaicism for a COL1A1 dominant mutation (alpha 1 Ser-415) causes recurrent osteogenesis imperfecta. Hum Mutat 2:196–204.

van Dijk FS, Nesbitt IM, Zwikstra EH, Nikkels PG, Piersma SR, Fratantoni SA, Jimenez CR, Huizer M, Morsman AC, Cobben JM, van Roij MH, Elting MW, Verbeke JI, Wijnaendts LC, Shaw NJ, Högler W, McKeown C, Sistermans EA, Dalton A, Meijers-Heijboer H, Pals G. 2009. PPIB mutations cause severe osteogenesis imperfecta. Am J Hum Genet 85:521–527.

Wallis GA, Starman BJ, Zinn AB, Byers PH. 1990. Variable expression of osteogenesis imperfecta in a nuclear family is explained by somatic mosaicism for a lethal point mutation in the alpha 1(I) gene (COL1A1) of type I collagen in a parent. Am J Hum Genet 46:1034–1040.

Wijsman EM. 1991. Recurrence risk of a new dominant mutation in children of unaffected parents. Am J Hum Genet 48:654–661.

Novel Insights from Clinical Practice

Fetal Diagnosis and Therapy

Fetal Diagn Ther 2012;32:216–220
DOI: 10.1159/000335687

Received: July 13, 2011
Accepted after revision: December 7, 2011
Published online: February 18, 2012

A Case of Boomerang Dysplasia with a Novel Causative Mutation in Filamin B: Identification of Typical Imaging Findings on Ultrasonography and 3D-CT Imaging

Seiji Tsutsumi[a] Ayako Maekawa[a] Miyuki Obata[a] Timothy Morgan[b]
Stephen P. Robertson[b] Hirohisa Kurachi[a]

[a]Department of Obstetrics and Gynecology, Yamagata University Faculty of Medicine, Yamagata, Japan;
[b]Department of Paediatrics and Child Health, Dunedin School of Medicine, University of Otago, Dunedin, New Zealand

Established Facts

- Boomerang dysplasia is a rare lethal osteochondrodysplasia characterized by disorganized mineralization of the skeleton, leading to complete nonossification of some limb bones and vertebral elements and a boomerang-like aspect to some of the long tubular bones.

Novel Insights

- Demonstration of the characteristic bent bone morphology in the limbs by 3D-CT adds diagnostic certainty and facilitates prognostication and genetic counseling for parents.
- The mutation observed in this patient, c.605T>C, is the third causative mutation described in this disorder and, like the other two mutations, leads to substitution of an amino acid residue in the actin-binding domain of filamin B.

Key Words
Boomerang dysplasia · Fetal imaging · Filamin B

Abstract
Boomerang dysplasia is a rare lethal osteochondrodysplasia characterized by disorganized mineralization of the skeleton, leading to complete nonossification of some limb bones and vertebral elements, and a boomerang-like aspect to some of the long tubular bones. Like many short-limbed skeletal dysplasias with accompanying thoracic hypoplasia, the potential lethality of the phenotype can be difficult to ascertain prenatally. We report a case of boomerang dysplasia prenatally diagnosed by use of ultrasonography and 3D-CT imaging, and identified a novel mutation in the gene encoding the cytoskeletal protein filamin B *(FLNB)* postmortem. Findings that aided the radiological diagnosis of this condition in utero included absent ossification of two out of three long bones in each limb and elements of the vertebrae and a boomerang-like shape to the ulnae. The identified mutation is the third described for this disorder and is predicted to lead to amino acid substitution in the actin-binding domain of the filamin B molecule.

KARGER

Fax +41 61 306 12 34
E-Mail karger@karger.ch
www.karger.com

1015–3837/12/0323–0216$38.00/0

Accessible online at:
www.karger.com/fdt

Seiji Tsutsumi
Department of Obstetrics and Gynecology
Yamagata University Faculty of Medicine
2-2-2 Iida-Nishi, Yamagata 990-9585 (Japan)
Tel. +81 23 628 5393, E-Mail stsutsumi@med.id.yamagata-u.ac.jp

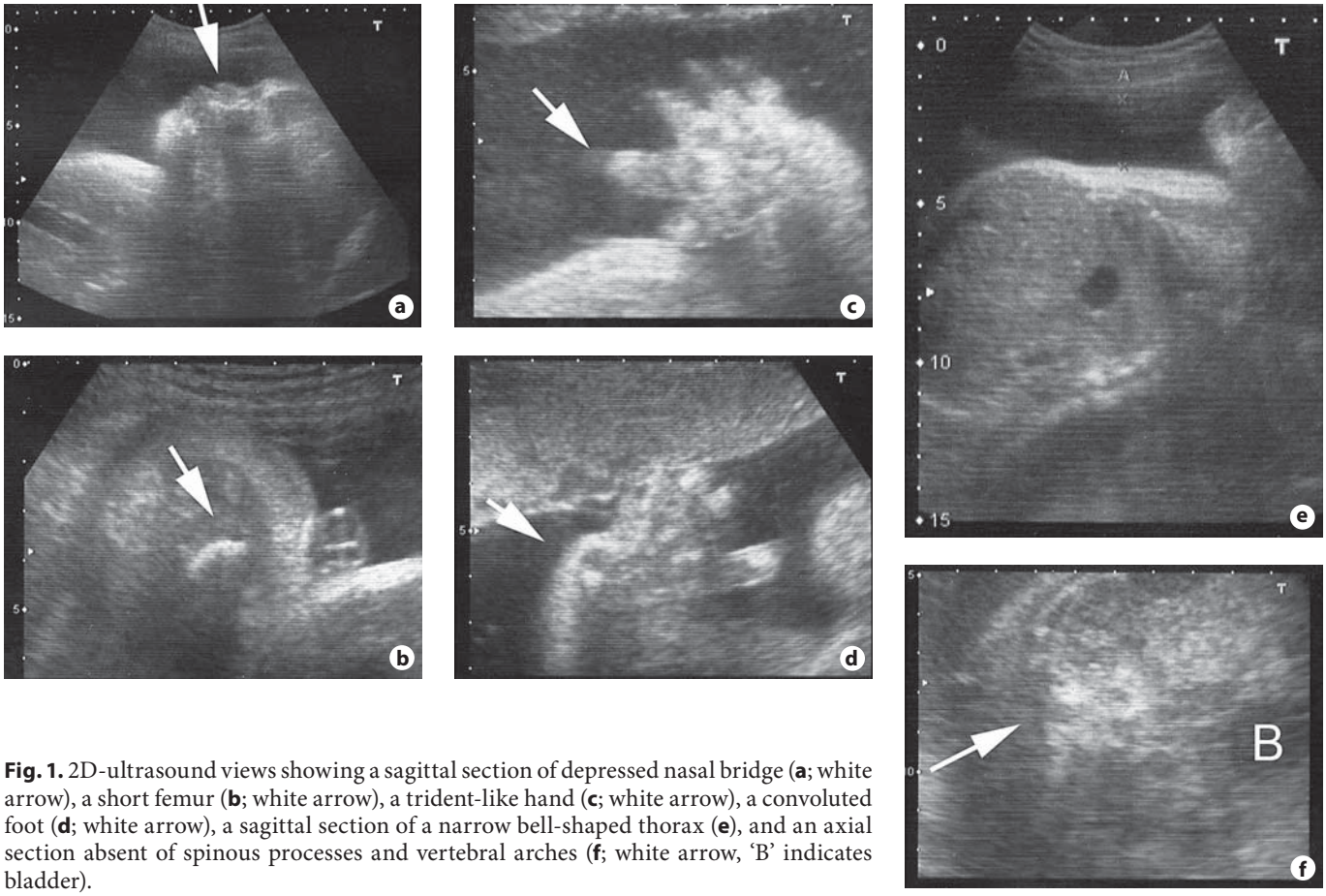

Fig. 1. 2D-ultrasound views showing a sagittal section of depressed nasal bridge (**a**; white arrow), a short femur (**b**; white arrow), a trident-like hand (**c**; white arrow), a convoluted foot (**d**; white arrow), a sagittal section of a narrow bell-shaped thorax (**e**), and an axial section absent of spinous processes and vertebral arches (**f**; white arrow, 'B' indicates bladder).

Clinical Report

This was the second pregnancy of unrelated healthy parents. The family history is noncontributory. At the time of conception the mother was 30 years old and the father 29. Routine ultrasound investigation in the 33rd week of gestation revealed severe fetal malformations, leading to referral to our hospital for prenatal diagnosis. Sonographic evaluation showed a fetus with severe micromelia. At the 33rd week of gestation, the fetal biparietal diameter was 84.8 mm (–0.3 SD), fetal trunk area was 5,808 mm^2 (–1.0 SD) and femur length was 18.2 mm (–14.8 SD). Only one of the three tubular bones was present in each limb, and the elbows and knees were indiscernible. The hands were trident and ossifications of the metacarpal bones were diminished. The bridge of the nose was flattened. The thorax was hypoplastic and had a bell-shaped appearance. The spinous processes and vertebral arches were not ossified (fig. 1). 3D-CT imaging showed the boomerang-like-shaped ulna, and the segment-shaped femur (fig. 2). In view of the typical skeletal abnormalities, including micromelia, and the absence of ossification of some but not all of the long tubular bones, the tentative diagnosis of boomerang dysplasia was made. After genetic counseling, the parents preferred not to resuscitate postpartum in view of the severity of the phenotype.

The fetus was born in the 38th week of gestation, and soon died from respiratory insufficiency. The bridge of the nose was defective (fig. 3) and a cleft palate was recognized. X-ray imaging confirmed the findings as demonstrated on the prenatal 3D-CT. Mutation analysis of the filamin B *(FLNB)* gene was undertaken on DNA extracted from umbilical cord blood after informed consent was obtained from the parents. All exons and exon-intron boundaries of *FLNB* were amplified using polymerase chain reaction as described previously [1], and amplified DNA was subjected to denaturing high-performance liquid chromatography with amplicons exhibiting anomalous waveforms subsequently sequenced on an ABI3100 sequencer. A novel mutation, c.605T>C, in exon 3 was identified, which is predicted to lead to the substitution of p.Met202Thr of the FLNB protein. This substitution occurs in the calponin homology 2 region of the actin-binding domain of FLNB.

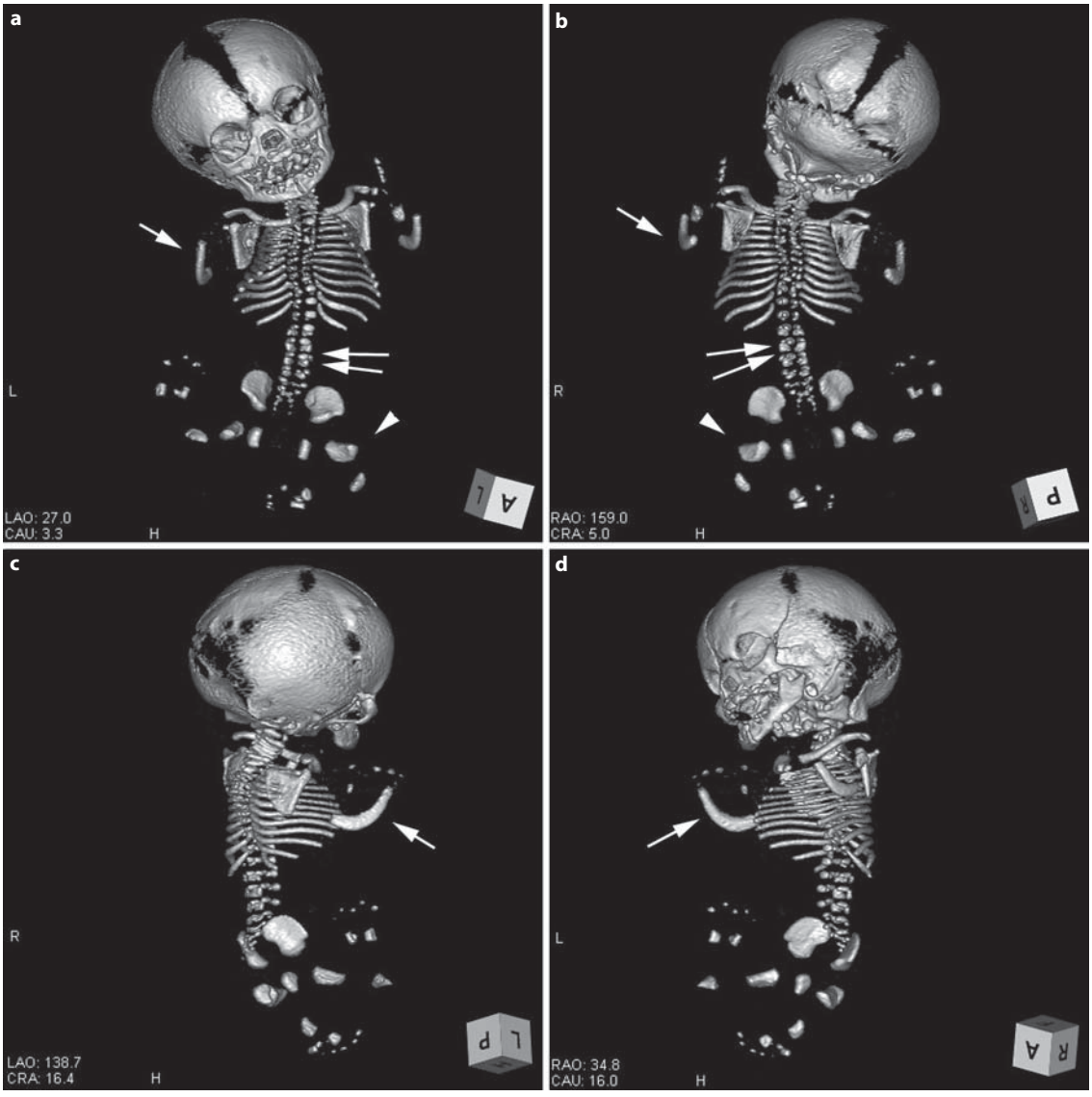

Fig. 2. 3D-CT views showing the boomerang-like shaped ulna (white arrow), the segment shaped femur (white arrow head) and zipper-like shaped spine (double arrows). The humerus and radius were absent: front view (**a**), rear view (**b**), right side view (**c**) and left side view (**d**).

Discussion

Boomerang dysplasia is a rare osteochondrodysplasia characterized by a boomerang-like aspect of the long tubular bones [2, 3]. It belongs to a family of skeletal dysplasias of varying severity, all caused by mutations in the same gene, *FLNB* [4, 5]. These related conditions in order of diminishing severity include atelosteogenesis type I and III [4] and Larsen syndrome [6]. Boomerang dysplasia is difficult to diagnose prenatally. All cases of this condition described in the literature thus far have been characterized by lethality, although instances of the phenotypically similar allelic condition, atelosteogenesis III, have been reported in conjunction with survivorship [7]. In this report we show that helical 3D-CT is a useful adjunct to obtain specific images of the skeletal abnormalities manifest in this condition.

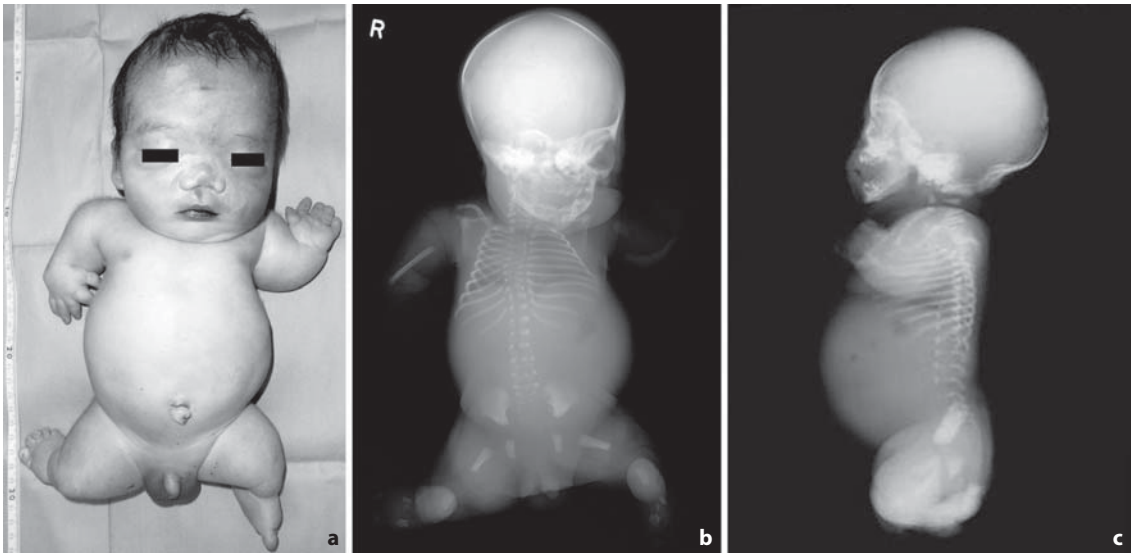

Fig. 3. The postmortem images of the patient. The nasal bridge was flattened, and the extremities were short and flexed: macroscopic front view (**a**), X-ray front view (**b**) and X-ray rear side view (**c**).

The key findings that facilitated the diagnosis of boomerang dysplasia in this instance included the absence of two of the three long bones in each limb, underossification of some components of the vertebrae and disordered ossification of the metacarpals. These findings can also be observed in atelosteogenesis type I, an observation that reflects the close phenotypic relatedness of these two conditions. Importantly, however, the milder potentially survivable condition, atelosteogenesis III, does not feature nonossification of the long bones of the limbs [4, 7]. In this instance demonstration of the characteristic bent bone morphology in the limbs by 3D-CT added diagnostic certainty and facilitated prognostication and genetic counseling for the parents. This was possible because the images obtained by 3D-CT enabled the visualization of some additional details of the fetal skeleton which were not clearly recognized in the ultrasonographic evaluation. Furthermore, the reconstructed 3D-CT enabled visualization of the whole fetal skeleton without contamination from maternal anatomy [8, 9].

The mutation observed in this patient, c.605T>C is the third causative mutation described in this disorder, and like the other two known mutations (p.Leu171Arg, p.Ser235Pro) leads to substitution of an amino acid residue in the actin-binding domain of FLNB [5]. Reflecting their close relatedness, a previously reported mutation, c.604A>G, occurring at the same codon predicts the substitution p.Met202Val and results in an atelosteogenesis I phenotype. The parents of our patient did not give permission to perform their own genetic analysis to check whether the change is de novo. However, this substitution (p.Met202Thr) changes polarity and hydrophilic property of the amino acid residue. Therefore, it might be pathogenic due to the potential of protein structural and functional change. Similar mutations leading to atelosteogenesis I and Larsen syndrome leads to an increased avidity of FLNB for cytoskeletal actin [10], but the mechanism by which this impacts on skeletogenesis and ossification of bone is not understood.

Acknowledgement

This article is supported by a Grant-in-Aid for Scientific Research from the Ministry of Health, Labour and Welfare of Japan (H23-Nanchi-Ippan-123).

References

1 Krakow D, Robertson SP, King LM, et al: Mutations in the gene encoding filamin B disrupt vertebral segmentation, joint formation and skeletogenesis. Nature Genet 2004; 36:405–410.

2 Kozlowski K, Sillence D, Cortis-Jones R, et al: Boomerang dysplasia. Br J Radiol 1985;58: 369–371.

3 Nishimura G, Horiuchi T, Kim OH, et al: Atypical skeletal changes in otopalatodigital syndrome type II: phenotypic overlap among otopalatodigital syndrome type II, boomerang dysplasia, atelosteogenesis type I and type III, and lethal male phenotype of Melnick-Needles syndrome. Am J Med Genet 1997;73:132–138.

4 Farrington-Rock C, Firestein MH, Bicknell LS, et al: Mutations in two regions of FLNB result in atelosteogenesis I and III. Hum Mutat 2006;27:705–710.

5 Bicknell LS, Morgan T, Bonafe L, et al: Mutations in FLNB cause boomerang dysplasia. J Med Genet 2005;42:e43.

6 Bicknell LS, Farrington-Rock C, Shafeghati Y, et al: A molecular and clinical study of Larsen syndrome caused by mutations in FLNB. J Med Genet 2007;44:89–98.

7 Schultz C, Langer LO, Laxova R, et al: Atelosteogenesis type III: long term survival, prenatal diagnosis, and evidence for dominant transmission. Am J Med Genet 1999;83:28–42.

8 Cassart M: Suspected fetal skeletal malformations or bone disease: how to explore. Pediatr Radiol 2010;40:1046–1051.

9 Ulla M, Aiello H, Cobos MP, et al: Prenatal diagnosis of skeletal dysplasias: contribution of three-dimensional computed tomography. Fetal Diagn Ther 2011;29:238–247.

10 Sawyer GM, Clark AR, Robertson SP, et al: Disease-associated substitutions in the filamin B actin binding domain confer enhanced actin binding affinity in the absence of major structural disturbance: insights from the crystal structures of filamin B actin binding domains. J Mol Biol 2009;390:1030–1047.

RESEARCH LETTER

AMERICAN JOURNAL OF medical genetics PART A

Mosaic upd(7)mat in a Patient With Silver–Russell Syndrome

Tomoko Fuke-Sato,[1,2] Kazuki Yamazawa,[1] Kazuhiko Nakabayashi,[3] Keiko Matsubara,[1] Kentaro Matsuoka,[4] Tomonobu Hasegawa,[2] Kazushige Dobashi,[5] and Tsutomu Ogata[1,6]*

[1]Department of Molecular Endocrinology, National Research Institute for Child Health and Development, Tokyo, Japan

[2]Department of Pediatrics, Keio University School of Medicine, Tokyo, Japan

[3]Department of Maternal-Fetal Biology, National Research Institute for Child Health and Development, Tokyo, Japan

[4]Division of Pathology, National Medical Center for Children and Mothers, Tokyo, Japan

[5]Department of Pediatrics, Showa University School of Medicine, Tokyo, Japan

[6]Department of Pediatrics, Hamamatsu University School of Medicine, Hamamatsu, Japan

Received 10 March 2011; Accepted 9 November 2011

TO THE EDITOR:

Silver–Russell syndrome (SRS) is a congenital developmental disorder characterized by pre- and post-natal growth failure, relative macrocephaly, triangular face, hemihypotrophy, and 5th finger clinodactyly [Russell, 1954; Silver et al., 1953]. Recent studies have shown that hypomethylation (epimutation) of the paternally derived differentially methylated region (DMR) in the upstream of *H19* (*H19*-DMR) on chromosome 11p15 and maternal uniparental disomy for chromosome 7 (upd(7)mat) account for ~45% and ~5–10% of SRS patients, respectively [Eggermann, 2010; Binder et al., 2011]. Furthermore, consistent with the involvement of imprinted genes in both body and placental growth [for review, Coan et al., 2005], epimutations of the *H19*-DMR and upd(7)mat are known to result in placental hypoplasia [Yamazawa et al., 2008]. Here, we report on a Japanese boy with mosaic upd(7)mat)mat who was identified through genetic screenings in 120 patients with SRS-like phenotype.

This Japanese boy was conceived naturally to a 41-year-old father and a 36-year-old mother. The parents were non-consanguineous and healthy. The paternal height was 165 cm (−0.9 SD), and the maternal height 155 cm (−0.6 SD).

At 35 weeks of gestation, he was delivered by a cesarean because of fetal distress. At birth, his length was 37.4 cm (−3.1 SD), his weight 1.28 kg (−3.1 SD), and his head circumference 29.0 cm (−1.3 SD). The placenta weighed 400 g (−0.6 SD [Kagami et al., 2008]). Shortly after birth, he was found to have ventricular septal defect, hydronephrosis, and abnormal external genitalia (hypospadias, bifid scrotum, and bilateral cryptorchidism). He received orchidopexy at $1^{10}/_{12}$ years of age and genitoplasty at $2^{4}/_{12}$ years of age. He exhibited feeding difficulty and speech delay.

At $5^{1}/_{12}$ years of age, he was referred because of short stature. His height was 87.9 cm (−4.3 SD), weight was 10.4 kg (−2.9 SD), and his head circumference 49.0 cm (−0.7 SD). Physical examination showed relative macrocephaly, abnormal teeth, 5th finger clinodactyly, and underdeveloped muscles. There was no hemihypotrophy. Endocrine studies for short stature yielded normal results, as did radiological examinations. His karyotype was 46,XY in all the 50 lymphocytes examined. He was clinically diagnosed as having SRS, and molecular studies were performed after obtaining the approval from the Institutional Review Board Committee at National Center for Child Health and Development and the written informed consent from the parents.

We first performed methylation analysis of the *MEST*-DMR on chromosome 7q32.2 using leukocyte genomic DNA by the previously described methods [Yamazawa et al., 2008b], because this patient showed relatively mild SRS-phenotype with speech delay

How to Cite this Article:
Fuke-Sato T, Yamazawa K, Nakabayashi K, Matsubara K, Matsuoka K, Hasegawa T, Dobashi K, Ogata T. 2011. Mosaic upd(7)mat in a patient with Silver–Russell syndrome. Am J Med Genet Part A 9999:1–4.

Grant sponsor: Japan Society for the Promotion of Science (JSPS); Grant number: 22249010; Grant sponsor: Ministry of Health, Labor and Welfare; Grant number: H21-005; Grant sponsor: Grant of National Center for Child Health and Development; Grant number: 23A-1.

*Correspondence to:
Tsutomu Ogata, M.D., Department of Pediatrics, Hamamatsu University School of Medicine, Hamamatsu 431-3192, Japan.
E-mail: tomogata@hama-med.ac.jp

Published online 00 Month 2011 in Wiley Online Library (wileyonlinelibrary.com).
DOI 10.1002/ajmg.a.34404

and feeding difficulty characteristic of upd(7)mat [Hitchins et al., 2001; Kotzot, 2008]. The methylation analysis showed a major peak for methylated clones and a minor peak for unmethylated clones in this patient (Fig. 1A). We also examined the *H19*-DMR and other multiple DMRs on various chromosomes by the bio-COBRA (combined bisulfite restriction analysis) method, as reported previously [Yamazawa et al., 2010]. The *GRB10*-DMR on chromosome 7p12.1 and the *PEG10*-DMR on chromosome 7q21.3 exhibited skewed methylation patterns consistent with the predominance of maternally derived clones, as did the *MEST*-DMR (Fig. 1B). By

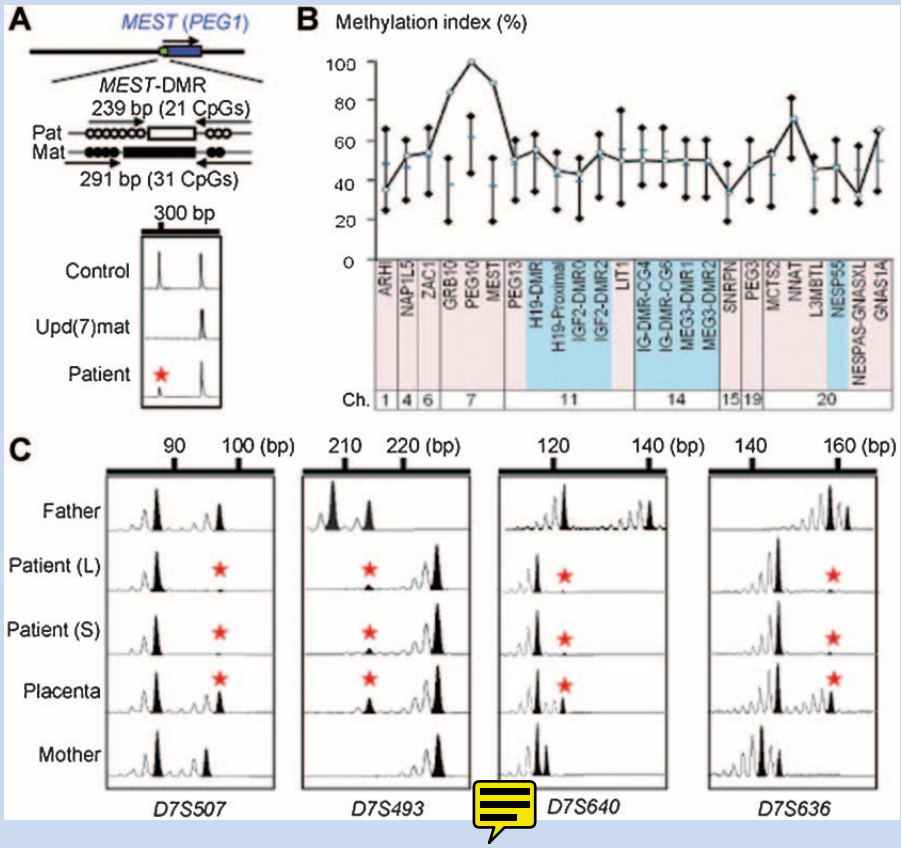

FIG. 1. Representative molecular results. A: Methylation analysis for the *MEST*-DMR. The methylated and unmethylated allele-specific primers were designed to yield PCR products of different sizes, and the PCR products were visualized on the 2100 Bioanalyzer (Agilent, Santa Clara, CA). Both methylated and unmethylated alleles are amplified in a control subject, and the methylated allele only is identified in a previously reported patient with upd(7)mat [Yamazawa et al., 2008b]. In this patient, a major peak for the methylated allele and a minor peak for the unmethylated allele (a red asterisk) are delineated. B: Methylation indices of 24 DMRs examined by the bio-COBRA. The PCR products were digested with methylation sensitive restriction enzymes, and the methylation indices (the ratios of methylated clones) were calculated using peak heights of digested and undigested fragments on the 2100 Bioanalyzer using 2100 expert software. The black vertical bars indicate the reference data in 20 normal control subjects (maximum − minimum). The DMRs highlighted in blue and pink are methylated after paternal and maternal transmissions, respectively.
C: Microsatellite analysis. Major peaks of maternal origin and minor peaks of paternal origin (red asterisks) are identified in this patient. The minor peaks of paternal origin are more obvious in the placenta than in the leukocytes (L) and salivary cells (S). Calculation of the mosaic ratio using the *D7S507* data, under the assumption of no trisomic cells. For this locus, the patient is considered to be heterozygous with the major 87 bp peak of maternal origin and a minor 97 bp peak of paternal origin. The father is also heterozygous with the two peaks of the same sizes, and the area under curve (AUC) is larger for the short 87 bp peak than for the long 97 bp peak. This unequal amplification is consistent with short products being more easily amplified than long products. In this patient, the AUC ratio between the major 87 bp peak and the minor 97 bp peak is obtained as 1.0:0.043 for leukocytes, 1.0:0.044 for salivary cells, and 1.0:0.803 in placental tissue, after compensation of the unequal amplification between the two peaks using the paternal data. Here, let "XL" represent the frequency of the upid(7)mat cells in leukocytes (thus, (1 − XL) denotes the frequency of normal cells in leukocytes). Then, the paternally derived 97 bp peak is generated by one paternally derived chromosome in the normal cells, that is, (1 − XL), and the maternally derived 87 bp peak is formed by the products from two maternally derived homologous chromosomes in the upid(7)mat cells and one maternally derived chromosome in the normal cells, that is, {2XL + (1 − XL)} = (XL + 1). Thus, the AUC ratio between the two peaks is represented as (XL + 1):(1 − XL) = 1.0:0.043, and "XL" is calculated as 0.92 (92%). Similarly, when "XS" and "XP" represent the frequency of the upid(7)mat cells in salivary cells and placental tissue, respectively, "XS" is obtained as 0.91 (91%) and "XP" as 0.11 (11%). Furthermore, when "XB" represents the frequency of the upid(7)mat cells in buccal epithelium cells, "XB" is obtained as 0.91 (91%), on the basis of the previous report that salivary cells comprises ~40% of buccal epithelium cells and ~60% of leukocytes [Thiede et al., 2000].

TABLE I. The Results of Microsatellite Analysis

Locus	Position	Father	Patient (L)	Patient (S)	Placenta	Mother	Assessment
D7S517	7p22.2	254/258	(254)/258	(254)/258	(254)/258	256/258	Maternal Iso-D[a]/biparental
D7S507	7p15–21	87/97	87/(97)	87/(97)	87/(97)	87/95	Maternal Iso-D[a]/biparental
D7S493	7p15.3	208/214	(214)/226	(214)/226	(214)/226	226	Maternal D[b]/biparental
D7S484	7p14–15	96/100	(96)/98	(96)/98	(96)/98	98/100	Maternal Iso-D/biparental
D7S502	7q11.12	298	294/(298)	294/(298)	294/(298)	294/304	Maternal Iso-D/biparental
D7S669	7q11.2	116/126	(116)/124	(116)/124	(116)/124	124	Maternal D[b]/biparental
D7S515	7q21–22	169/173	171/(173)	171/(173)	171/(173)	169/171	Maternal Iso-D/biparental
D7S640	7q21.1–31.2	122/140	116/(122)	116/(122)	116/(122)	116/118	Maternal Iso-D/biparental
D7S684	7q34	169/179	177/(179)	177/(179)	177/(179)	177/179	Not informative
D7S636	7q35–36	158/162	146/(158)	146/(158)	146/(158)	142/146	Maternal Iso-D/biparental
D7S798	7q36	73/79	(79)/83	(79)/83	(79)/83	73/83	Maternal Iso-D/biparental

L, leukocytes; S, salivary cells; D, disomy.
The Arabic numbers denote the PCR product sizes in bp.
The minor peaks are indicated in parentheses.
[a]On the basis of the results of other informative loci, the major peaks are considered to be of maternal origin.
[b]Because of the maternal homozygosity, disomic status (isodisomy or heterodisomy) is unknown for these loci.

contrast, other DMRs including the *H19*-DMR showed normal methylation patterns.

We next performed microsatellite analysis for 11 loci on various parts of chromosome 7, using genomic DNA from leukocytes of the patient and the parents, from salivary cells of the patient, and from formalin-fixed and paraffin-embedded placental tissue. Major peaks consistent with maternal uniparental isodisomy and minor peaks of paternal origin were unequivocally identified for *D7S484*, *D7S502*, *D7S515*, *D7S640*, *D7S636*, and *D7S798*; furthermore, similar patterns were also detected for *D7S517*, *D7S507*, *D7S669*, and *D7S493*, although the results were not informative for *D7S684* (Fig. 1C and Table I). The minor peaks of paternal origin were similar between leukocytes and salivary cells and more evident in placental tissue. These findings, together with the normal karyotype in lymphocytes, indicated mosaic full maternal isodisomy for chromosome 7 (upid(7)mat) in this patient. Furthermore, since such a condition is frequently associated with mosaicism for trisomy 7 [Petit et al., 2011], we performed fluorescence in situ hybridization (FISH) analysis for stocked lymphocyte pellets, using a CEP7 probe for *D7Z1* (Abbott[Q3]). The FISH analysis identified two normal signals in 995 of 1,000 interphase nuclei examined, with no trace of trisomic nuclei; while a single signal was delineated in the remaining five nuclei, this was regarded as a false-positive finding. Thus, assuming no trisomic cells, the frequency of the full upid(7)mat cells was calculated as 92% in leukocytes, using the results of *D7S507* (Fig. 1C). In addition, similarly assuming no trisomic cells in other tissues, the frequency of the full upid(7)mat cells was calculated as 91% salivary cells (and in buccal cells) and 11% in placental tissue, although we could not perform FISH analysis in buccal cells and placental cells.

These results imply that this patient had an abnormal cell lineage with full upid(7)mat and a normal cell lineage with biparentally inherited chromosome 7 homologs at least in lymphocytes, and these had no trisomy 7. It is likely that mitotic non-disjunction and subsequent trisomy rescue (loss of the paternally derived chromosome 7 from a trisomic cell) took place in the post-zygotic developmental stage, resulting in the production of the mosaic full upid(7)mat (Fig. 2). While full upid(7)mat can also be produced by monosomy rescue (duplication of a single maternally derived chromosome 7 in a zygote), this mechanism is predicted to cause non-mosaic rather than mosaic upid(7)mat [Miozzo et al., 2001]. Although it remains to be clarified why trisomic cells mediating the production of full upid(7)mat cells were apparently absent in lymphocytes of this patient, there might be a negative selection against lymphocytes with trisomy 7.

However, the presence or absence of demonstrable trisomic cells was studied only in lymphocytes. In this regard, trisomic cells have been identified more frequently in skin fibroblasts and amniocytes than in blood cells in patients with mosaic trisomy 7 [Chen et al., 2010; Petit et al., 2011], and they are usually more frequently detected in the placental tissue than in the body tissue, as has been demonstrated by confined placental trisomy [Kalousek et al., 1991]. These findings would argue for the possible presence of trisomic cells in several tissues including placenta of this patient.

The full upid(7)mat cells were assessed to account for the majority of the leukocytes and salivary cells (buccal cells) and the minority of the placental tissue, under the assumption of no

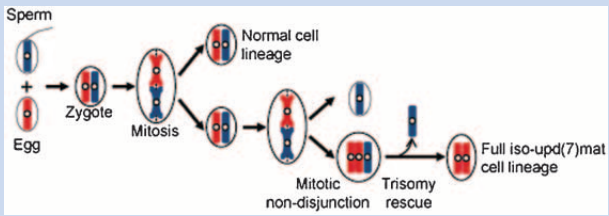

FIG. 2. Schematic representation of the generation of the mosaic upid(7)mat. The maternally and paternally derived chromosome 7 homologs are shown in red and blue, respectively. In this figure, mitotic non-disjunction is assumed at the second mitosis.

trisomic cells. In this regard, if trisomic cells may be present in a certain fraction of buccal cells and placental tissue, the full upid(7)mat cells would still account for a relatively major fraction of buccal cells and a relatively minor fraction of the placental cells. While such a variation in the frequency of the full upid(7)mat cells among different tissues would primarily be a stochastic event, it should be pointed out that human genetic studies are usually performed for leukocytes. Indeed, if the upid(7)mat cells were barely present in leukocytes, the mosaic upid(7)mat would not have been detected. Such a bias in human studies would more or less be relevant to the relative predominance of the full upid(7)mat cells in leukocytes.

Two findings are noteworthy with regard to clinical features of this patient. First, this patient had relatively mild SRS phenotype with speech delay and feeding difficulty. Since such clinical features are grossly consistent with those of patients with upd(7)mat [Hitchins et al., 2001; Kotzot, 2008], it is inferred that the upid(7)mat cells accounted for a considerable fraction of body cells relevant to the development of SRS phenotype. Second, the placental size remained within the normal range. This would be consistent with the relative paucity of the upid(7)mat cells in the placenta.

In summary, we observed mosaic upid(7)mat in a patient with SRS. Further studies will identify mosaic upd(7)mat with or without demonstrable trisomy 7 in patients with relatively mild SRS-like phenotype.

ACKNOWLEDGMENTS

This work was supported by the Grant-in-Aid for Scientific Research (A) (22249010) from the Japan Society for the Promotion of Science (JSPS), by the Grants for Health Research on Children, Youth, and Families (H21-005) from the Ministry of Health, Labor and Welfare, and by the Grant of National Center for Child Health and Development (23A-1).

REFERENCES

Binder G, Begemann M, Eggermann T, Kannenberg K. 2011. Silver-Russell syndrome. Best Pract Res Clin Endocrinol Metab 25:153–160.

Chen CP, Su YN, Chern SR, Hwu YM, Lin SP, Hsu CH, Tsai FJ, Wang TY, Wu PC, Lee CC, Chen YT, Chen LF, Wang W. 2010. Mosaic trisomy 7 at amniocentesis: Prenatal diagnosis and molecular genetic analyses. Taiwan J Obstet Gynecol 49:333–340.

Coan PM, Burton GJ, Ferguson-Smith AC. 2005. Imprinted genes in the placenta: A review. Placenta 26:S10–S20.

Eggermann T. 2010. Russell–Silver syndrome. Am J Med Genet Part C 154C:355–364.

Hitchins MP, Stanier P, Preece MA, Moore GE. 2001. Silver-Russell syndrome: A dissection of the genetic aetiology and candidate chromosomal regions. J Med Genet 38:810–819.

Kagami M, Yamazawa K, Matsubara K, Matsuo N, Ogata T. 2008. Placentomegaly in paternal uniparental disomy for human chromosome 14. Placenta 29:760–761.

Kalousek DK, Howard-Peebles PN, Olson SB, Barrett IJ, Dorfmann A, Black SH, Schulman JD, Wilson RD. 1991. Confirmation of CVS mosaicism in term placentae and high frequency of intrauterine growth retardation association with confined placental mosaicism. Prenat Diagn 11:743–750.

Kotzot D. 2008. Maternal uniparental disomy 7 and Silver–Russell syndrome—Clinical update and comparison with other subgroups. Eur J Med Genet 51:444–451.

Miozzo M, Grati FR, Bulfamante G, Rossella F, Cribiù M, Radaelli T, Cassani B, Persico T, Cetin I, Pardi G, Simoni G. 2011. Post-zygotic origin of complete maternal chromosome 7 isodisomy and consequent loss of placental *PEG1/MEST* expression. Placenta 22:813–821.

Petit F, Holder-Espinasse M, Duban-Bedu B, Bouquillon S, Boute-Benejean O, Bazin A, Rouland V, Manouvrier-Hanu S, Delobel B. 2011. Trisomy 7 mosaicism prenatally misdiagnosed and maternal uniparental disomy in a child with pigmentary mosaicism and Russell–Silver syndrome. Clin Genet [Epub ahead of print], PHID: 21204802.

Russell A. 1954. A syndrome of intra-uterine dwarfism recognizable at birth with cranio-facial dysostosis, disproportionately short arms and other anomalies. Proc R Soc Med 47:1040–1044.

Silver HK, Kiyasu W, George J, Deamer WC. 1953. Syndrome of congenital hemihypertrophy, shortness of stature, and elevated urinary gonadotrophins. Pediatrics 12:368–375.

Thiede C, Prange-Krex G, Freiberg-Richter J, Bornhäuser M, Ehninger G. 2000. Buccal swabs but not mouthwash samples can be used to obtain pretransplant DNA fingerprints from recipients of allogeneic bone marrow transplants. Bone Marrow Transplant 25:575–577.

Yamazawa K, Kagami M, Nagai T, Kondoh T, Onigata K, Maeyama K, Hasegawa T, Hasegawa Y, Yamazaki T, Mizuno S, Miyoshi Y, Miyagawa S, Horikawa R, Matsuoka K, Ogata T. 2008a. Molecular and clinical findings and their correlations in Silver-Russell syndrome: Implications for a positive role of IGF2 in growth determination and differential imprinting regulation of the *IGF2-H19* domain in bodies and placentas. J Mol Med 86:1171–1181.

Yamazawa K, Kagami M, Ogawa M, Horikawa R, Ogata T. 2008b. Placental hypoplasia in maternal uniparental disomy for chromosome 7. Am J Med Genet Part A 146A:514–516.

Yamazawa K, Nakabayashi K, Kagami M, Sato T, Saitoh S, Horikawa R, Hizuka N, Ogata T. 2010. Parthenogenetic chimaerism/mosaicism with a Silver-Russell syndrome-like phenotype. J Med Genet 47:782–785.

AUTHOR QUERY FORM

JOURNAL: AMERICAN JOURNAL OF MEDICAL GENETICS PART A
Article: ajma_34404

Dear Author,

During the copyediting of your paper, the following queries arose. Please respond to these by annotating your proofs with the necessary changes/additions.

- If you intend to annotate your proof electronically, please refer to the E-annotation guidelines.
- If you intend to annotate your proof by means of hard-copy mark-up, please refer to the proof mark-up symbols guidelines. If manually writing corrections on your proof and returning it as a scanned pdf via email, do not write too close to the edge of the paper. Please remember that illegible mark-ups may delay publication.

Whether you opt for hard-copy or electronic annotation of your proofs, we recommend that you provide additional clarification of answers to queries by entering your answers on the query sheet, in addition to the text mark-up.

Query No.	Query	Remark
Q1	Please check the grant sponsors.	
Q2	Please check the change made in the reference citation (Silver et al., 1953).	
Q3	Please give address information for this manufacturer: city, state (if applicable), and country.	
Q4	Please provide the volume number and page range.	

European Journal of Human Genetics (2012) 20, 928–932

www.nature.com/ejhg

EJHG Open

ARTICLE

Relative frequency of underlying genetic causes for the development of UPD(14)pat-like phenotype

Masayo Kagami[1], Fumiko Kato[1], Keiko Matsubara[1], Tomoko Sato[1], Gen Nishimura[2] and Tsutomu Ogata*[,1,3]

Paternal uniparental disomy 14 (UPD(14)pat) results in a unique constellation of clinical features, and a similar phenotypic constellation is also caused by microdeletions involving the *DLK1-MEG3* intergenic differentially methylated region (IG-DMR) and/or the *MEG3*-DMR and by epimutations (hypermethylations) affecting the DMRs. However, relative frequency of such underlying genetic causes remains to be clarified, as well as that of underlying mechanisms of UPD(14)pat, that is, trisomy rescue (TR), gamete complementation (GC), monosomy rescue (MR), and post-fertilization mitotic error (PE). To examine this matter, we sequentially performed methylation analysis, microsatellite analysis, fluorescence *in situ* hybridization, and array-based comparative genomic hybridization in 26 patients with UPD(14)pat-like phenotype. Consequently, we identified UPD(14)pat in 17 patients (65.4%), microdeletions of different patterns in 5 patients (19.2%), and epimutations in 4 patients (15.4%). Furthermore, UPD(14)pat was found to be generated through TR or GC in 5 patients (29.4%), MR or PE in 11 patients (64.7%), and PE in 1 patient (5.9%). Advanced maternal age at childbirth (≥35 years) was predominantly observed in the MR/PE subtype. The results imply that the relative frequency of underlying genetic causes for the development of UPD(14)pat-like phenotype is different from that of other imprinting disorders, and that advanced maternal age at childbirth as a predisposing factor for the generation of nullisomic oocytes through non-disjunction at meiosis 1 may be involved in the development of MR-mediated UPD(14)pat.
European Journal of Human Genetics (2012) **20,** 928–932; doi:10.1038/ejhg.2012.26; published online 22 February 2012

Keywords: genetic cause; maternal age effect; monosomy rescue; UPD(14)pat subtype

INTRODUCTION

Human chromosome 14q32.2 carries a ~1.2 Mb imprinted region with the germline-derived primary *DLK1-MEG3* intergenic differentially methylated region (IG-DMR) and the post-fertilization-derived secondary *MEG3*-DMR, together with multiple imprinted genes.[1,2] Both DMRs are methylated after paternal transmission and unmethylated after maternal transmission in the body, whereas in the placenta the IG-DMR alone remains as a DMR and the *MEG3*-DMR is rather hypomethylated irrespective of the parental origin.[2,3] Furthermore, it has been shown that the unmethylated IG-DMR and *MEG3*-DMR of maternal origin function as the imprinting centers in the placenta and the body, respectively, and that the IG-DMR acts as an upstream regulator for the methylation pattern of the *MEG3*-DMR in the body but not in the placenta.[3]

As a result of the presence of the imprinted region, paternal uniparental disomy 14 (UPD(14)pat) (OMIM #608149) causes a unique constellation of body and placental phenotypes such as characteristic face, bell-shaped small thorax, abdominal wall defect, polyhydramnios, and placentomegaly.[2,4,5] Furthermore, consistent with the essential role of the DMRs in the imprinting regulation, microdeletions and epimutations affecting the IG-DMR or both DMRs of maternal origin result in UPD(14)pat-like phenotype in both the body and the placenta, whereas a microdeletion involving the maternally inherited *MEG3*-DMR alone leads to UPD(14)pat-like phenotype in the body, but not in the placenta.[2,3]

Of the three underlying genetic causes for UPD(14)pat-like phenotype (UPD(14)pat, microdeletions, and epimutations), UPD(14)pat is primarily generated by four mechanisms, that is, trisomy rescue (TR), gamete complementation (GC), monosomy rescue (MR), and post-fertilization mitotic error (PE).[6] TR refers to a condition in which chromosome 14 of maternal origin is lost from a zygote with trisomy 14 formed by fertilization between a disomic sperm and a normal oocyte. GC results from fertilization of a disomic sperm with a nullisomic oocyte. MR refers to a condition in which chromosome 14 of paternal origin is replicated in a zygote with monosomy 14 formed by fertilization between a normal sperm and a nullisomic oocyte. PE is an event after formation of a normal zygote. In this regard, a nullisomic oocyte specific to GC and MR is produced by non-disjunction at meiosis 1 (M1) or meiosis 2 (M2), and non-disjunction at M1 is known to increase with maternal age, probably because of a long-term (10–50 years) meiotic arrest at prophase 1.[7]

However, relative frequency of the genetic causes for UPD(14)pat-like phenotype remains to be determined, as well as that of underlying mechanisms for the generation of UPD(14)pat. Here, we report our data on this matter, and discuss the difference in the relative frequency

[1]Department of Molecular Endocrinology, National Research Institute for Child Health and Development, Tokyo, Japan; [2]Department of Radiology, Tokyo Metropolitan Children's Medical Center, Fuchu, Japan; [3]Department of Pediatrics, Hamamatsu University School of Medicine, Hamamatsu, Japan
*Correspondence: Professor T Ogata, Department of Pediatrics, Hamamatsu University School of Medicine, Hamamatsu 431-3192, Japan. Tel: +81 53 435 2310; Fax: +81 53 435 2312; E-mail: tomogata@hama-med.ac.jp
Received 23 May 2011; revised 10 November 2011; accepted 26 December 2011; published online 22 February 2012

among imprinted disorders and the possible maternal age effect on the relative frequency.

PATIENTS AND METHODS

Patients

This study comprised 26 patients with UPD(14)pat-like phenotype (9 male patients and 17 female patients) (Table 1). Of the 26 patients, 18 patients have been reported previously; they consisted of nine sporadic patients with full UPD(14)pat,[4,5] one sporadic patient with segmental UPD(14)pat,[4] the proband of sibling cases and four sporadic patients with different patterns of microdeletions involving the unmethylated DMRs of maternal origin,[2,3] and three patients with epimutations (hypermethylations) of the two normally unmethylated DMRs of maternal origin.[2] The remaining eight patients were new sporadic cases.

Phenotypic findings of the 26 patients are summarized in Supplementary Table 1; detailed clinical features of patients 6 and 16–25 are as described previously,[2–4] and those of the eight new patients 3, 5, 10–14, and 26 are shown in Supplementary Table 2, together with those of patients 1, 2, 4, 7–9, and 15 in whom detailed phenotypes were not described in the previous report.[5] All the 26 patients were identified shortly after birth because of the unique bell-shaped thorax with coat-hanger appearance of the ribs on roentgenograms obtained because of asphyxia. Subsequent clinical analysis revealed that 25 of the 26 patients exhibited both body and placental UPD(14)pat-like phenotype, whereas the remaining one previously reported patient (patient 22) manifested body, but not placental, UPD(14)pat-like phenotype.[3] The karyotype was found to be normal in 25 patients, although cytogenetic analysis was not performed in one previously reported patient who died of respiratory failure at 2 h of age (patient 6).[4] One patient (patient 15) was conceived by *in vitro* fertilization-embryo transfer.[5] This study was approved by the Institute Review Board Committee at the National Center for Child Health and Development, and performed after obtaining written informed consent.

Analysis of underlying genetic causes in patients with UPD(14)pat-like phenotype

We sequentially performed methylation analysis, microsatellite analysis, and fluorescence *in situ* hybridization (FISH), using leukocyte genomic DNA samples and lymphocyte metaphase spreads of all the 26 patients with UPD(14)pat-like phenotype. The detailed methods were as reported previously.[2,3] In brief, methylation analysis was performed for the IG-DMR (CG4 and CG6) and the *MEG3*-DMR (CG7 and the CTCF-biding sites C and D) by combined bisulfite restriction analysis and bisulfite sequencing. Microsatellite analysis was performed for multiple loci on chromosome 14, by determining the sizes of PCR products obtained with fluorescently labeled forward primers and unlabeled reverse primers. FISH analysis was carried out for the IG-DMR and the *MEG3*-DMR using 5104-bp and 5182-bp long PCR products, respectively, together with the RP11-566I2 probe for 14q12 utilized as an internal control.

In this study, furthermore, oligonucleotide array-based comparative genomic hybridization (CGH) was also performed for the imprinted region of non-UPD(14)pat patients, using a custom-build oligo-microarray containing 12 600 probes for 14q32.2–q32.3 encompassing the imprinted region and ~10 000 reference probes for other chromosomal region (4×180K format, Design ID 032112) (Agilent Technologies, Palo Alto, CA, USA). The procedure was as described in the manufacturer's instructions.

Analysis of subtypes in patients with UPD(14)pat

UPD(14)pat subtype was determined by microsatellite analysis.[8,9] In brief, heterodisomy for at least one locus was regarded as indicative of TR- or GC-mediated UPD(14)pat (TR/GC subtype), whereas isodisomy for all the informative microsatellite loci was interpreted as indicative of MR- or PE-mediated UPD(14)pat (MR/PE subtype) (for details, see Supplementary Figure S1). Here, while heterodisomy and isodisomy for a pericentromeric region in the TR/GC subtype imply a disomic sperm generation through M1

Table 1 Summary of patients examined in this study

Patient	*Genetic cause*	*UPD(14)pat subtype*	*Maternal age at childbirth (years)*	*Paternal age at childbirth (years)*	*Remark*	*Reference*
1	UPD(14)pat	TR/GC [M1]	31	35		5
2	UPD(14)pat	TR/GC [M1]	28	29		5
3	UPD(14)pat	TR/GC [M1]	29	38		This report
4	UPD(14)pat	TR/GC [M1]	36	41		5
5	UPD(14)pat	TR/GC [M2]	30	30		This report
6	UPD(14)pat	MR/PE	42	Unknown		4,5
7	UPD(14)pat	MR/PE	31	28		5
8	UPD(14)pat	MR/PE	32	33		5
9	UPD(14)pat	MR/PE	26	35		5
10	UPD(14)pat	MR/PE	38	38		This report
11	UPD(14)pat	MR/PE	26	32		This report
12	UPD(14)pat	MR/PE	41	36		This report
13	UPD(14)pat	MR/PE	30	28		This report
14	UPD(14)pat	MR/PE	39	34		This report
15	UPD(14)pat	MR/PE	42	37	Born after IVF-ET	5
16	UPD(14)pat	MR/PE	36	36		4,5
17	UPD(14)pat-seg.	PE	27	24	Segmental isodisomy	4,5
18	Microdeletion		31	34		2
19	Microdeletion		33	36		2
20	Microdeletion		28	27		2
21	Microdeletion		27	37	IG-DMR alone	3
22	Microdeletion		25	25	*MEG3*-DMR alone	3
23	Epimutation		35	36		2
24	Epimutation		28	26		2
25	Epimutation		27	30		2
26	Epimutation		33	33		This report

Abbreviation: IVF-ET, *in vivo* fertilization-embryo transfer using parental gametes.
The microdeletions in patients 18–22 are different in size.

and M2 non-disjunction respectively,[9] such discrimination between M1 and M2 non-disjunctions is impossible for the development of a nullisomic oocyte. Furthermore, it is usually impossible to discriminate between TR and GC, although the presence of trisomic cells is specific to TR. Similarly, it is also usually impossible to discriminate between MR and PE, although identification of segmental isodisomy or mosaicism is unique to PE (PE subtype).

Analysis of parental ages

We examined parental ages at childbirth in patients of different underlying causes and different UPD(14)pat subtypes. Statistical significance of the relative frequency was examined by the Fisher's exact probability test, and that of the median age by the Mann–Whitney's *U*-test. $P<0.05$ was considered significant.

RESULTS

Analysis of underlying causes in patients with UPD(14)pat-like phenotype

For the eight new sporadic patients, methylation analysis invariably revealed hypermethylation of both DMRs, and microsatellite analysis showed UPD(14)pat in seven patients and biparentally inherited homologs of chromosome 14 in the remaining one patient (patient 26). FISH analysis for patient 26 identified two signals for the two DMRs, and subsequently performed array CGH analysis showed no evidence for genomic rearrangements (Supplementary Figure S2). Thus, patient 26 was assessed to have an epimutation affecting the two DMRs. Furthermore, the results of array CGH analysis confirmed the presence of microdeletions in patients 18–21 and the absence of a discernible microdeletion in patients 23–25 (Supplementary Figure S2) (array CGH analysis was not performed in patient 22 with a 4303-bp microdeletion[3] because of the lack of DNA sample available). Thus, together with our previous data, all the 26 patients with UPD(14)pat-like phenotype had genetic alteration involving the imprinted region on chromosome14q32.2.

Consequently, the 26 patients with UPD(14)pat-like phenotype were classified as follows: (1) 16 sporadic patients with full UPD(14)pat and 1 sporadic patient with segmental UPD(14)pat (UPD(14)pat group); (2) the proband of the sibling cases and two sporadic patients with different patterns of microdeletions involving the two DMRs, one sporadic patient with a microdeletion involving the IG-DMR alone in whom the *MEG3*-DMR was epimutated, and one patient with a microdeletion involving the *MEG3*-DMR alone (deletion group); and (3) four patients with epimutations (hypermethylations) of both DMRs (epimutation group) (Figure 1 and Table 1).

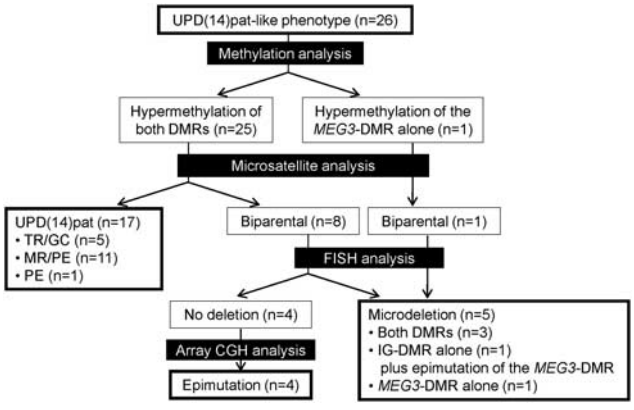

Figure 1 Classification of 26 patients with UPD(14)pat-like phenotype.

Analysis of subtypes in patients with UPD(14)pat

Heterozygosity for at least one locus indicative of TR/GC subtype was identified in five patients (patients 1–5), and the disomic pattern of pericentromeric region indicated M1 non-disjunction in patients 1–4 and M2 non-disjunction in patient 5. Full isodisomy consistent with MR/PE subtype was detected in 11 patients (patients 6–16), and segmental isodisomy unique to PE subtype was revealed in 1 patient (patient 17) (Table 1, Figure 1, and Supplementary Figure S3).

Analysis of parental ages

The distribution of parental ages at childbirth is shown in Figure 2. The advanced maternal age at childbirth ($\geq$35 years) was predominantly observed in the MR/PE subtype of UPD(14)pat. Furthermore, while the relative frequency of aged mothers ($\geq$35 years) did not show a significant difference between the MR/PE subtype of UPD(14)pat (6/11) and (i) other subtypes of UPD(14)pat (1/6) (P=0.159), (ii) deletion group (0/5) (P=0.057), and (iii) epimutation group (1/4) (P=0.338), it was significantly different between the MR/PE subtype and the sum of other subtypes of UPD(14)pat, deletion group, and epimutation group (2/15) (P=0.034). Similarly, while the median maternal age did not show a significant difference between the MR/PE subtype of UPD(14)pat (36 years) *vs* (i) other subtypes of UPD(14)pat (29.5 years) (P=0.118), (ii) deletion type (28 years) (P=0.088), and (iii) epimutation type (30.5 years) (P=0.295), it was significantly different between the MR/PE subtype of UPD(14)pat and the sum of other subtypes of UPD(14)pat, deletion group, and epimutation group (29 years) (P=0.045).

The paternal ages were similar irrespective of the genetic causes and the UPD(14)pat subtypes. In addition, the median paternal age was comparable between the TR/GC subtype of UPD(14)pat that postulates the production of a disomic sperm (35.0 years) and the sum of other subtypes of UPD(14)pat, deletion group, and epimutation group that assumes the production of a normal sperm (33.5 years) (P=0.322).

DISCUSSION

This study revealed that the UPD(14)pat-like phenotype was caused by UPD(14)pat in 65.4% of patients, by microdeletions in 19.2% of patients, and by epimutations in 15.4% of patients. Although the relative frequency of underlying genetic factors for the development of UPD(14)pat-like phenotype has been reported previously,[10] most data are derived from our previous publications. Thus, the present results are regarded as the updated and extended data on the relative frequency. For the relative frequency, it is notable that 25 of the 26 patients were confirmed to have normal karyotype, although chromosome analysis was not performed in patient 6. Thus, while Robertsonian translocations involving chromosome 14 is known to be a

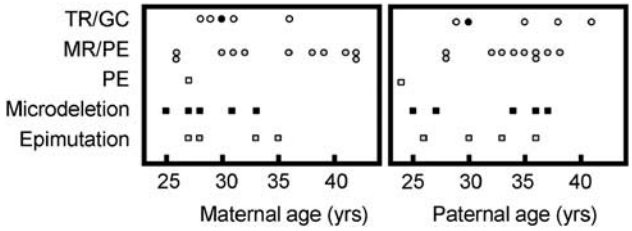

Figure 2 The distribution of parental ages at childbirth according to the underlying genetic causes for the development of UPD(14)pat-like phenotype and UPD(14)pat subtypes. Of the five plots for the TR/GC subtype, open and black circles indicate the TR/GC subtype due to non-disjunction at paternal M1 and M2, respectively.

predisposing factor for the occurrence of UPD(14)pat,[11–16] such a possible chromosomal effect has been excluded in nearly all patients examined in this study.

The relative frequency of underlying causes has also been reported in other imprinting disorders.[8,17–19] The data are summarized in Table 2 (a similar summary has also been reported recently by Hoffmann *et al*).[10] In particular, the results in patients with normal karyotype are available in Prader–Willi syndrome (PWS).[8] Furthermore, PWS is also known to be caused by UPD, microdeletions, and epimutations affecting a single imprinting region,[8,19] although Silver–Russell syndrome and Beckwith–Wiedemann syndrome (BWS) can result from perturbation of at least two imprinted regions,[17,18] and BWS and Angelman syndrome can occur as a single gene disorder.[17,19] Thus, it is notable that the relative frequency of underlying causes is quite different between patients with UPD(14)pat-like phenotype and those with PWS.[8,19] This would primarily be due to the presence of low copy repeats flanking the imprinted region on chromosome 15, because chromosomal deletions are prone to occur in regions harboring such repeat sequences.[20] Indeed, two types of microdeletions mediated by such low copy repeats account for a vast majority of microdeletions in patients with PWS,[21] whereas the microdeletions identified in patients with UPD(14)pat-like phenotype are different to each other. This would explain why microdeletions are less frequent and UPD and epimutations are more frequent in patients with UPD(14)pat-like phenotype than in those with PWS.

Advanced maternal age at childbirth was predominantly observed in the MR/PE subtype. This may imply the relevance of advanced maternal age to the development of MR-mediated UPD(14)pat, because the generation of nullisomic oocytes through M1 non-disjunction is a maternal age-dependent phenomenon.[22] Although no paternal age effect was observed, this is consistent with the previous data indicating no association of advanced paternal age with a meiotic error.[23] For the maternal age effect, however, several matters should be pointed out: (1) the number of analyzed patients is small, although it is very difficult to collect a large number of patients in this extremely rare disorder; (2) of the MR/PE subtype, the advanced maternal age is a risk factor for the generation of MR-mediated UPD(14)pat, but not for the development of PE-mediated UPD(14)pat; (3) it is impossible to discriminate between maternal age-dependent M1 non-disjunction and maternal age-independent M2 non-disjunction in the MR and GC subtypes (however, GC must be extremely rare, because it requires the concomitant occurrence of a nullisomic oocyte and a disomic sperm); (4) of the TR/GC subtype, the advanced maternal age is a risk factor for the generation of GC-mediated UPD(14)pat, but not for the development of TR-mediated UPD(14)pat; and (5) if a cryptic recombination(s) might remain undetected in some patients with apparently full isodisomy, this argues that such patients actually have TR- or GC-mediated UPD(14)pat rather than MR- or PE-mediated UPD(14)pat. Thus, further studies are required to examine the maternal age effect on the generation of MR-mediated UPD(14)pat. In addition, while a relationship is unlikely to exist between advanced maternal age and microdeletions and epimutations, this notion would also await further investigations.

Such a maternal age effect is also expected in the TR/GC subtype maternal UPDs after M1 non-disjunction, because the generation of disomic oocytes through M1 non-disjunction is also a maternal age-dependent phenomenon.[7] Indeed, such a maternal age effect has been shown for PWS patients with normal karyotype; the maternal age at childbirth was significantly higher in patients with heterodisomy for a very pericentromeric region indicative of TR/GC subtype UPD(15)mat after M1 non-disjunction than in those with other genetic causes.[8,9] For various chromosomes other than chromosome 15, furthermore, since maternal age at childbirth is higher in patients with maternal heterodisomy than in those with maternal isodisomy,[24] this would also argue for maternal age effect on the development of maternal UPDs. However, in the previous studies on maternal UPDs other than UPD(15)mat, the available data are quite insufficient to assess the maternal age effect. For example, although a relatively large number of patients with UPD(14)mat phenotype have been reported in the literature (reviewed in reference Hoffmann *et al*),[10] we could identify only six UPD(14)mat patients with normal karyotype in whom maternal age at childbirth was documented and microsatellite analysis was performed.[25–30] Furthermore, the microsatellite data are insufficient to identify the subtype of UPD(14)mat and to distinguish between M1 and M2 non-disjunction in the TR/GC subtype. Thus, while the maternal age at childbirth may be advanced in five patients with apparently TR/GC-mediated UPD(14)mat (27, 35, 37, 41, and 44 years)[25–27,29,30] (the maternal age at childbirth in the remaining one

Table 2 Relative frequency of genetic mechanisms in imprinting disorders

	UPD(14)pat-like phenotype	*BWS*	*SRS*	*AS*	*PWS*
Uniparental disomy	65.4%	16%	10%	3–5%	25% (25%)
	UPD(14)pat	UPD(11)pat (mosaic)	UPD(7)mat	UPD(15)pat	UPD(15)mat
Cryptic deletion	19.2%	Rare	—	70%	70% (72%)
Cryptic duplication	—	—	Rare	—	—
Epimutation					
Hypermethylation	15.4%	9%	—	—	2–5% (2%)
Affected DMR	IG-DMR/*MEG3*-DMR	*H19*-DMR	—	—	*SNRPN*-DMR
Hypomethylation	—	44%	>38%	2–5%	—
Affected DMR		KvDMR1	*H19*-DMR	*SNRPN*-DMR	
Gene mutation	—	5%	—	10-15%	—
Mutated gene		*CDKN1C*		*UBE3A*	
Unknown		25%	>40%	10%	
Reference	This study	17	18	19	8, 19

Abbreviations: AS, Angelman syndrome; BWS, Beckwith–Wiedemann syndrome; PWS, Prader–Willi syndrome; SRS, Silver–Russell syndrome.
Patients with abnormal karyotypes are included in BWS and AS, and not included in SRS. In PWS, the data including patients with abnormal karyotypes are shown, and those from patients with normal karyotype alone are depicted in parentheses.

patient with apparently MR/PE-mediated UPD(14)mat is 40 years),[28] the notion of a maternal age effect awaits further investigations for UPD(14)mat.

Finally, it appears to be worth pointing out that methylation analysis invariably revealed hypermethylated DMR(s) in all the 26 patients who were initially ascertained because of bell-shaped thorax with coat-hanger appearance of the ribs. This indicates that methylation analysis of the DMRs can be utilized for a screening of this condition, and that the constellation of clinical features in the UPD(14)pat-like phenotype, especially the bell-shaped thorax with coat-hanger appearance of the ribs, is highly unique to patients with UPD(14)pat-like phenotype.

In summary, this study confirms the relative frequency of underlying genetic causes for the UPD(14)pat phenotype and reveals the relative frequency of UPD(14)pat subtypes. Furthermore, the results emphasize the difference in the relative frequency of underlying genetic causes among imprinted disorders, and may support a possible maternal age effect on the generation of the nullisomic oocyte mediated UPD(14)pat. Further studies will permit a more precise assessment on these matters.

CONFLICT OF INTEREST

The authors declare no conflict of interest.

ACKNOWLEDGEMENTS

We thank Drs Kenji Kurosawa, Michiko Hayashidani, Toshio Takeuchi, Shinya Tanaka, Mika Noguch, Kouji Masumoto, Takeshi Utsunomiya, Yumiko Komatsu, Hirofumi Ohashi, Maureen J O'Sullivan, Andrew J Green, Yoshiyuki Watabe, Tsuyako Iwai, Hitoshi Kawato, Miho Torikai, Akiko Yamamoto, Nobuhiro Suzumori, Makoto Kuwajima, Hiroshi Yoshihashi, Yoriko Watanabe, and Jin Nishimura for material sampling and phenotype assessment. This work was supported by Grants for Research on Intractable Diseases (H22-161) and for Health Research on Children, Youth and Families (H21-005) from the Ministry of Health, Labor and Welfare, by Grants-in-Aid for Scientific Research (A) (22249010) and (B) (21028026) from the Japan Society for the Promotion of Science (JSPS), by Grants from Takeda Science Foundation and from Kanehara Foundation, and by the Grant for National Center for Child Health and Development (23A-1).

1 da Rocha ST, Edwards CA, Ito M, Ogata T, Ferguson-Smith AC: Genomic imprinting at the mammalian Dlk1-Dio3 domain. *Trends Genet* 2008; **24**: 306–316.
2 Kagami M, Sekita Y, Nishimura G *et al*: Deletions and epimutations affecting the human 14q32.2 imprinted region in individuals with paternal and maternal upd(14)-like phenotypes. *Nat Genet* 2008; **40**: 237–242.
3 Kagami M, O'Sullivan MJ, Green AJ *et al*: The IG-DMR and the MEG3-DMR at human chromosome 14q32.2: hierarchical interaction and distinct functional properties as imprinting control centers. *PLoS Genet* 2010; **6**: e1000992.
4 Kagami M, Nishimura G, Okuyama T *et al*: Segmental and full paternal isodisomy for chromosome 14 in three patients: narrowing the critical region and implication for the clinical features. *Am J Med Genet A* 2005; **138A**: 127–132.
5 Kagami M, Yamazawa K, Matsubara K, Matsuo N, Ogata T: Placentomegaly in paternal uniparental disomy for human chromosome 14. *Placenta* 2008; **29**: 760–761.
6 Shaffer LG, Agan N, Goldberg JD, Ledbetter DH, Longshore JW, Cassidy SB: American College of Medical Genetics statement of diagnostic testing for uniparental disomy. *Genet Med* 2001; **3**: 206–211.
7 Jones KT: Meiosis in oocytes: predisposition to aneuploidy and its increased incidence with age. *Hum Reprod Update* 2008; **14**: 143–158.
8 Matsubara K, Murakami N, Nagai T, Ogata T: Maternal age effect on the development of Prader-Willi syndrome resulting from upd(15)mat through meiosis 1 errors. *J Hum Genet* 2011; **56**: 566–571.
9 Robinson WP, Christian SL, Kuchinka BD *et al*: Somatic segregation errors predominantly contribute to the gain or loss of a paternal chromosome leading to uniparental disomy for chromosome 15. *Clin Genet* 2000; **57**: 349–358.
10 Hoffmann K, Heller R: Uniparental disomies 7 and 14. *Best Pract Res Clin Endocrinol Metab* 2011; **25**: 77–100.
11 Wang JC, Passage MB, Yen PH, Shapiro LJ, Mohandas TK: Uniparental heterodisomy for chromosome 14 in a phenotypically abnormal familial balanced 13/14 Robertsonian translocation carrier. *Am J Hum Genet* 1991; **48**: 1069–1074.
12 Papenhausen PR, Mueller OT, Johnson VP, Sutcliffe M, Diamond TM, Kousseff BG: Uniparental isodisomy of chromosome 14 in two cases: an abnormal child and a normal adult. *Am J Med Genet* 1995; **59**: 271–275.
13 Cotter PD, Kaffe S, McCurdy LD, Jhaveri M, Willner JP, Hirschhorn K: Paternal uniparental disomy for chromosome 14: a case report and review. *Am J Med Genet* 1997; **70**: 74–79.
14 Yano S, Li L, Owen S, Wu S, Tran T: A further delineation of the paternal uniparental disomy (UPD14): the fifth reported liveborn case. *Am J Hum Genet* 2001; **69** (Suppl): A739.
15 Kurosawa K, Sasaki H, Sato Y *et al*: Paternal UPD14 is responsible for a distinctive malformation complex. *Am J Med Genet A* 2002; **110**: 268–272.
16 McGowan KD, Weiser JJ, Horwitz J *et al*: The importance of investigating for uniparental disomy in prenatally identified balanced acrocentric rearrangements. *Prenat Diagn* 2002; **22**: 141–143.
17 Sasaki K, Soejima H, Higashimoto K *et al*: Japanese and North American/European patients with Beckwith-Wiedemann syndrome have different frequencies of some epigenetic and genetic alterations. *Eur J Hum Genet* 2007; **15**: 1205–1210.
18 Eggermann T: Epigenetic regulation of growth: lessons from Silver-Russell syndrome. *Endocr Dev* 2009; **14**: 10–19.
19 Gurrieri F, Accadia M: Genetic imprinting: the paradigm of Prader-Willi and Angelman syndromes. *Endocr Dev* 2009; **14**: 20–28.
20 Pujana MA, Nadal M, Guitart M, Armengol L, Gratacos M, Estivill X: Human chromosome 15q11-q14 regions of rearrangements contain clusters of LCR15 duplicons. *Eur J Hum Genet* 2002; **10**: 26–35.
21 Varela MC, Kok F, Setian N, Kim CA, Koiffmann CP: Impact of molecular mechanisms, including deletion size, on Prader-Willi syndrome phenotype: study of 75 patients. *Clin Genet* 2005; **67**: 47–52.
22 Pellestor F, Andreo B, Anahory T, Hamamah S: The occurrence of aneuploidy in human: lessons from the cytogenetic studies of human oocytes. *Eur J Med Genet* 2006; **49**: 103–116.
23 Sloter E, Nath J, Eskenazi B, Wyrobek AJ: Effects of male age on the frequencies of germinal and heritable chromosomal abnormalities in humans and rodents. *Fertil Steril* 2004; **81**: 925–943.
24 Kotzot D: Advanced parental age in maternal uniparental disomy (UPD): implications for the mechanism of formation. *Eur J Hum Genet* 2004; **12**: 343–346.
25 Fokstuen S, Ginsburg C, Zachmann M, Schinzel A: Maternal uniparental disomy 14 as a cause of intrauterine growth retardation and early onset of puberty. *J Pediatr* 1999; **134**: 689–695.
26 Hordijk R, Wierenga H, Scheffer H, Leegte B, Hofstra RM, Stolte-Dijkstra I: Maternal uniparental disomy for chromosome 14 in a boy with a normal karyotype. *J Med Genet* 1999; **36**: 782–785.
27 Sanlaville D, Aubry MC, Dumez Y *et al*: Maternal uniparental heterodisomy of chromosome 14: chromosomal mechanism and clinical follow up. *J Med Genet* 2000; **37**: 525–528.
28 Towner DR, Shaffer LG, Yang SP, Walgenbach DD: Confined placental mosaicism for trisomy 14 and maternal uniparental disomy in association with elevated second trimester maternal serum human chorionic gonadotrophin and third trimester fetal growth restriction. *Prenat Diagn* 2001; **21**: 395–398.
29 Aretz S, Raff R, Woelfle J *et al*: Maternal uniparental disomy 14 in a 15-year-old boy with normal karyotype and no evidence of precocious puberty. *Am J Med Genet A* 2005; **135**: 336–338.
30 Mitter D, Buiting K, von Eggeling F *et al*: Is there a higher incidence of maternal uniparental disomy 14 [upd(14)mat]? Detection of 10 new patients by methylation-specific PCR. *Am J Med Genet A* 2006; **140**: 2039–2049.

Supplementary Information accompanies the paper on European Journal of Human Genetics website (http://www.nature.com/ejhg)

RESEARCH LETTER

AMERICAN JOURNAL OF medical genetics PART A

FOP in China and Japan: An Overview From Domestic Literatures

Shuang Jiao,[1] Yasu Zhang,[1] Wenhao Ma,[2] and Nobuhiko Haga[1]*

[1]Department of Rehabilitation Medicine, Graduate School of Medicine, The University of Tokyo, Hongo, Bunkyo-ku, Tokyo, Japan

[2]School of Acupuncture Moxibustion and Tuina, Beijing University of Chinese Medicine, Beijing, China

Manuscript Received: 11 April 2012; Manuscript Accepted: 11 October 2012

TO THE EDITOR:

FOP is an autosomal dominant disorder, characterized by progressive ectopic ossification leading to devastating physical disabilities and malformation of the great toe and occasionally of the thumb. It is known that an activating mutation of *ACVR1* is responsible for FOP. FOP is a rare disorder with incidence of 1/2,000,000 [Connor and Evans, 1982a,b]. China has a population of more than 1.3 billion, and Japan has about 0.13 billion people. Although the FOP case reports published in China and Japan might provide valuable information for this rare disease considering their large populations, most cases were published in medical journals of their own respective languages. In order to obtain the information of FOP patients reported in Chinese and Japanese, we summarized the FOP case reports published in China and Japan and analyzed the similarities and differences of the Chinese and Japanese patients to compare their characteristics with those of reports published in international journals.

Literature search was made by using relevant key words in three Chinese and one Japanese electronic databases (Fig. 1). The case reports on FOP published in Chinese or Japanese were included in this research. All references of the identified articles were screened and the relevant articles were also retrieved (see Supporting Information online). Similar case reports were confirmed by telephone to the original author and duplicate publications were excluded.

A total of 86 Chinese patients (46 males and 40 females) and 41 Japanese patients (21 males and 20 females) were included. The median age of onset was defined as the age of first flare-up leading to heterotopic ossification. The clinical information of all patients including age of onset, age of diagnosis, site of heterotopic ossification, malformation, and interventions were extracted (Table I). A total of 32% Chinese and 83% Japanese patients were reported as having spinal deformities such as scoliosis, lordosis, or kyphosis. Unfortunately, 11 Chinese and 19 Japanese patients underwent surgical intervention, but the percentage of patients who underwent surgeries decreased in recent 10 years for both Chinese and Japanese patients. Medical intervention included administration of steroid hormones, non-steroidal anti-inflammatory drugs (including cyclooxygenase-2 inhibitor drugs), and diphosphonates-EHDP.

How to Cite this Article:
Jiao S, Zhang Y, Ma W, Haga N. 2013. FOP in China and Japan: An overview from domestic literatures.
Am J Med Genet Part A 161A:892–893.

It was reported in earlier articles that almost all FOP patients had characteristic malformations of the great toes [Connor and Evans, 1982a,b; Kitterman et al., 2005; Janati et al., 2007]. However in several recent studies, normal great toes and late onset heterotopic ossification were reported with patients with FOP variants [Bocciardi et al., 2009; Kaplan et al., 2009; Barnett et al., 2011]. The classic FOP (with the characteristic features of great toe malformations and progressive heterotopic ossification), FOP-plus (classic defining features of FOP plus one or more atypical features) and FOP variants (major variations in one or both of the two classic defining features of FOP) were reported as having different types of *ACVR1* mutation which showed correlations with the age of onset of heterotopic ossification or malformations [Kaplan et al., 2009]. In this study, 7% of the Chinese patients and 2% of the Japanese patients were reported as having normal toes. In a previous research, 59% of FOP patients were reported as having malformed thumbs [Connor and Evans, 1982a,b]. While in this study, only 21% of the Chinese and 12% of the Japanese patients were reported as having malformed thumb. Because the exact

Additional supporting information may be found in the online version of this article.

Grant sponsor: JSPS Postdoctoral Fellowship; Grant numbers: FY2010, P10714; Grant sponsor: Health and Labor Sciences Grants; Grant sponsor: Ministry of Health Labor and Welfare.
Conflict of interest: None.

Shuang Jiao and Yasu Zhang contributed equally to this work.

*Correspondence to:
Nobuhiko Haga, M.D., Ph.D., Department of Rehabilitation Medicine, Graduate School of Medicine, The University of Tokyo, 7-3-1 Hongo, Bunkyo-ku, 113-8655 Tokyo, Japan. E-mail: hagan-reh@h.u-tokyo.ac.jp

Article first published online in Wiley Online Library (wileyonlinelibrary.com): 26 February 2013
DOI 10.1002/ajmg.a.35771

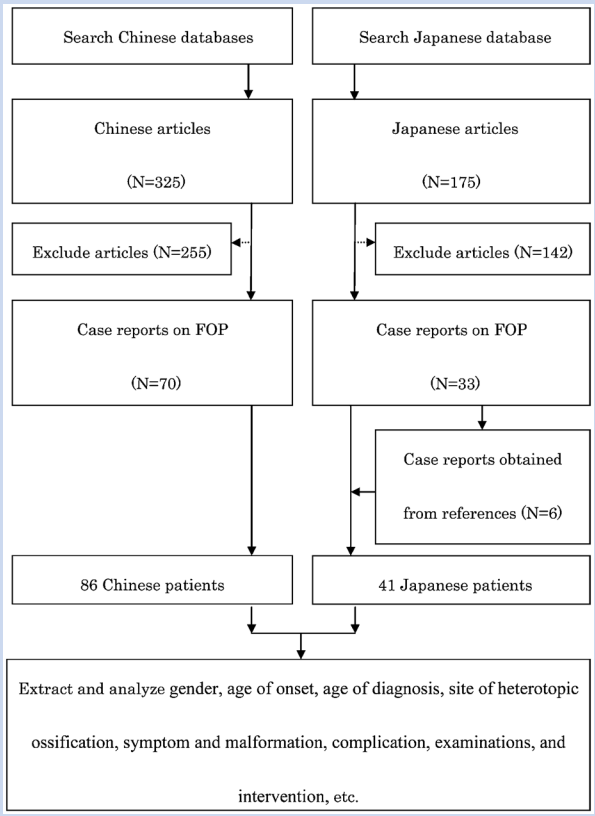

FIG. 1. Three Chinese electronic databases, including China National Knowledge Infrastructure (CNKI), Chinese Scientific Journal Databases (VIP), and Wanfang data were searched with the terms "jin xing xing gu hua xing xian wei fa yu bu liang (fibrodysplasis ossificans progressiva, FOP)" and "jin xing xing gu hua xing ji yan (myositis ossificans progressiva, MOP)" in the full text. The Japanese electronic database, Ichushi WEB, was searched with the terms "sinkousei kokkasei seniikeiseisyou (FOP)," "sinkousei kokkasei kin'en (MOP)," "sinkousei kakotusei kin'en (MOP)," "fibrodysplasis ossificans progressiva," and "myositis ossificans progressiva" in full text. After exclusion of duplicate case reports and addition of reports obtained from references, 86 Chinese and 41 Japanese patients remained for analyses.

TABLE I. Contrast of Chinese and Japanese Patients With FOP

	Chinese	Japanese
Age of onset (year): median (range)*	3.0 (0–38)	3.0 (0–16)
Age of diagnosis (year): median (range)**	10.5 (0–53)	7.0 (0–27)
Site of heterotopic ossification (%)		
At onset	Neck (30) > trunk (27) > head (13)	Neck (42) > trunk (24) > head (17)
When reported	Trunk (94) > neck (64) > shoulder (62)	Trunk (85) > neck (76) > shoulder (71)
Great toe (%): Mal/nor/no info[a]	51/7/42	73/2/24
Thumb (%): Mal/nor/no info[a]	21/9/72	12/5/83

[a]Mal/nor/no info stands for malformation/normal/no information.
*By Kolmogorov–Smirnov nonparametric test, $P = 0.532$, grand median = 3.0.
**By Kolmogorov–Smirnov nonparametric test, $P = 0.027$, grand median = 9.0.

reason for less reported percentage of malformed great toe and thumb is unknown, the ethical or racial differences of FOP subtypes and the *ACVR1* mutations with their genotype–phenotype should also be explored in future research.

Common anomalies associated with FOP such as short, broad femoral necks and metaphysical widening [Deirmengian et al., 2008] or typical complications such as baldness [Connor and Evans, 1982a,b] were not reported in these Chinese and Japanese reports. The fact may be attributed to selection-bias, because earlier reports might come from orthopedic surgeons. Lack of long-term follow up may have precluded identification of these rare onset associations.

ACKNOWLEDGMENTS

This research was supported by FY2010 JSPS Postdoctoral Fellowship for Foreign Researchers (ID No.: P10714) provided by the Japan Society for the Promotion of Science (JSPS) and the Health and Labor Sciences Grants on Intractable Diseases from the Ministry of Health, Labor, and Welfare.

REFERENCES

Barnett CP, Dugar M, Haan EA. 2011. Late-onset variant fibrodysplasia ossificans progressiva leading to misdiagnosis of ankylosing spondylitis. Am J Med Genet Part A 155A:1492–1495.

Bocciardi R, Bordo D, Di Duca M, Di Rocco M, Ravazzolo R. 2009. Mutational analysis of the ACVR1 gene in Italian patients affected with fibrodysplasia ossificans progressiva: Confirmations and advancements. Eur J Hum Genet 17:311–318.

Connor JM, Evans DA. 1982. Fibrodysplasia ossificans progressiva. The clinical features and natural history of 34 patients. J Bone Joint Surg Br 64:76–83.

Connor JM, Evans DA. 1982. Genetic aspects of fibrodysplasia ossificans progressiva. J Med Genet 19:35–39.

Deirmengian GK, Hebela NM, O'Connell M, Glaser DL, Shore EM, Kaplan FS. 2008. Proximal tibial osteochondromas in patients with fibrodysplasia ossificans progressiva. J Bone Joint Surg Am 90:366–374.

Janati J, Aghighi Y, Tofighi A, Akhavan A, Behrouzan O. 2007. Radiologic findings in seven patients with fibrodysplasia ossificans progressiva. Arch Iran Med 10:88–90.

Kaplan FS, Xu M, Seemann P, Connor JM, Glaser DL, Carroll L, Delai P, Fastnacht-Urban E, Forman SJ, Gillessen-Kaesbach G, Hoover-Fong J, Köster B, Pauli RM, Reardon W, Zaidi SA, Zasloff M, Morhart R, Mundlos S, Groppe J, Shore EM. 2009. Classical and atypical FOP phenotypes are caused by mutations in the BMP type I receptor ACVR1. Hum Mutat 30:379–390.

Kitterman JA, Kantanie S, Rocke DM, Kaplan FS. 2005. Iatrogenic harm caused by diagnostic errors in fibrodysplasia ossificans progressiva. Pediatrics 116:654–661.

Journal of Human Genetics (2013), 1–4

www.nature.com/jhg

SHORT COMMUNICATION

Exome sequencing identifies a novel *INPPL1* mutation in opsismodysplasia

Aritoshi Iida[1,9], Nobuhiko Okamoto[2,9], Noriko Miyake[3,9], Gen Nishimura[4], Satoshi Minami[5], Takuya Sugimoto[6], Mitsuko Nakashima[3], Yoshinori Tsurusaki[3], Hirotomo Saitsu[3], Masaaki Shiina[7], Kazuhiro Ogata[7], Shigehiko Watanabe[8], Hirofumi Ohashi[8], Naomichi Matsumoto[3] and Shiro Ikegawa[1]

Opsismodysplasia is an autosomal recessive skeletal disorder characterized by facial dysmorphism, micromelia, platyspondyly and retarded bone maturation. Recently, mutations in the gene encoding inositol polyphosphate phosphatase-like 1 (INPPL1) are found in several families with opsismodysplasia by a homozygosity mapping, followed by whole genome sequencing. We performed an exome sequencing in two unrelated Japanese families with opsismodysplasia and identified a novel *INPPL1* mutation, c.1960_1962delGAG, in one family. The mutation is predicted to result in an in-frame deletion (p.E654del) within the central catalytic 5-phosphate domain. Our results further support that *INPPL1* is the disease gene for opsismodysplasia and that opsismodysplasia has genetic heterogeneity.
Journal of Human Genetics advance online publication, 4 April 2013; doi:10.1038/jhg.2013.25

Keywords: exome sequencing; INPPL1; opsismodysplasia

INTRODUCTION

Opsismodysplasia (OMIM 258480) is a rare skeletal dysplasia identifiable at birth. Its clinical features are rhizomelic micromelia and facial dysmorphism, including prominent brow, large fontanels, depressed nasal bridge and small anteverted nose with long philtrum, as well as short feet and hands with sausage-like fingers.[1] Its main radiological features include retarded bone maturation, marked shortness of the bones of hands and feet with concave metaphyses and thin, lamellar vertebral bodies. Some patients show severe phosphate wasting. Autosomal recessive inheritance is the most likely mode of inheritance; to date, at least three consanguineous families with opsismodysplasia are reported.[2–4]

Recently, Below *et al.*[5] performed a homozygosity mapping coupled with whole genome sequencing in a consanguineous family with opsismodysplasia, and identified *INPPL1* (inositol polyphosphate phosphatase-like 1) as a causative gene for opsismodysplasia. They first identified a homozygous missense mutation, p.Pro659Leu, in the consanguineous family, and then found *INPPL1* mutations in additional five unrelated families with opsismodysplasia. We performed a whole exome sequencing for two patients from two unrelated families and identified a homozygous in-frame deletion of *INPPL1* in one family.

SUBJECTS AND METHODS

Subjects and DNA samples

Two families with clinical diagnosis of opsismodysplaisa were included in the study. Family 1 consisted of parents and affected sibs (Figure 1a), and Family 2 consisted of parents and a patient. Genomic DNA was extracted by standard procedures from peripheral blood of the patients and their family members after informed consent. The study was approved by the ethical committee of RIKEN, Yokohama City University, and participating institutions.

Exome sequencing

Six individuals in the two families were analyzed by the whole exome sequence as described previously.[6] Briefly, 3 μg of genomic DNA was sheared by Covaris 2S system (Covaris, Woburn, MA, USA) and partitioned using SureSelect Human All Exon V4 (Agilent technology, Santa Clara, CA, USA) according to the manufacturer's instructions. The exon-enriched DNA libraries were sequenced using HiSeq2000 (Illumina, San Diego, CA, USA) with a 101-bp paired-end reads and a 7-bp index reads. Four samples (2.5 pM each, with different index) were run in one lane. HiSeq Control Software/Real-Time Analysis and CASAVA1.8.2 (Illumina) were used for image analysis and base calling. The mapping was performed to human genome hg19 using Novoalign (http://www.novocraft.com/main/page.php?s=novoalign). The aligned reads were processed by Picard to remove the polymerase chain reaction (PCR) duplicate (http://picard.sourceforge.net). The variants were called

[1]Laboratory for Bone and Joint Diseases, Center for Genomic Medicine, RIKEN, Tokyo, Japan; [2]Department of Medical Genetics, Osaka Medical Center and Research Institute for Maternal and Child Health, Osaka, Japan; [3]Department of Human Genetics, Yokohama City University Graduate School of Medicine, Yokohama, Japan; [4]Department of Pediatric Imaging, Tokyo Metropolitan Children's Medical Center, Fuchu, Japan; [5]Department of Gynecology and Obstetrics, Shingu Municipal Medical Center, Shingu, Japan; [6]Department of Pediatrics Shingu Municipal Medical Center, Shingu, Japan; [7]Department of Biochemistry, Yokohama City University Graduate School of Medicine, Yokohama, Japan and [8]Division of Medical Genetics, Saitama Children's Medical Center, Saitama, Japan
[9]These authors contributed equally to this work.
Correspondence: Professor S Ikegawa, Laboratory for Bone and Joint Diseases, Center for Genomic Medicine, RIKEN, 4-6-1 Shirokanedai, Minato-ku, Tokyo 108-8639, Japan.
E-mail: sikegawa@ims.u-tokyo.ac.jp
Received 5 January 2013; revised 6 March 2013; accepted 9 March 2013

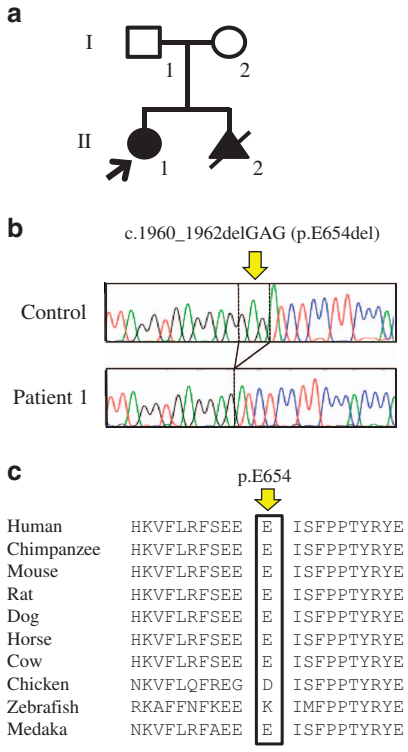

Figure 1 *INPPL1* mutation in a Japanese family with opsismodysplasia. (**a**) Pedigree, (**b**) an in-frame deletion c.1960_1962delGAG (p.E654del) within exon 17 and (**c**) conservation of p.E654 in INPPL1 among different species.

by Genome Analysis Toolkit 1.6-5 (GATK; http://www.broadinstitute.org/gsa/wiki/index.php/Main_Page) with the best practice variant detection with the GAKT v.3 (http://www.broadinstitute.org/gsa/wiki/index.php/Best_Practice_Variant_Detection_with_the_GATK_v3) and annotated by ANNOVAR (23 February 2012) (http://www.openbioinformatics.org/annovar/). Through this flow, common variants registered in dbSNP135 (minor allele frequeny $\geqslant 0.01$) (http://genome.ucsc.edu/cgi-bin/hgTrackUi?hgsid=316787363&g=snp135Common&hgTracksConfigPage=configure) were removed.

Priority scheme

On the basis of the hypothesis that opsismodysplasia is inherited in an autosomal recessive manner, variants were filtered by following conditions using the script created by BITS (Tokyo, Japan). For the homozygous mutation model: (1) variant allele frequency (variant alleles/total alleles) in probands $\geqslant 0.8$, (2) variant allele frequency in parents $\leqslant 0.8$, (3) excluding synonymous changes and (4) excluding the variants observed in our in-house database ($n = 429$). For the compound heterozygous mutation model: (1) mutation allele frequency in probands: 0.2–0.8, (2) variant allele frequency in parents $\leqslant 0.8$, (3) excluding synonymous changes, (4) excluding the variants observed in our in-house database ($n = 429$) and (5) selecting genes with compound heterozygous change. After combining variants selected by both models, genes commonly found in the two families were searched.

Sanger sequencing

We performed Sanger sequencing to confirm the deletion identified in the proband of Family 1 by the exome sequencing. We amplified exon 17 by PCR using primer sequences, 5′-AAGCACAAGGTCTTCCTTCGATTCA-3′ and 5′-CCATACCCTTGACCCAAATTCTTGAT-3′. We directly sequenced the PCR product using an Applied Biosystems 3730xl DNA analyzer (Life Technologies, Forster City, CA, USA). For the patient in Family 2, we screened 28 exons of *INPPL1* and exon–intron boundaries by direct sequencing of PCR products from genome DNA. The primer sequences are available on request.

Evaluation of polymorphism

We used the invader assay coupled with PCR[7] to exclude the possibility of polymorphism in 188 Japanese general populations. The deletion was evaluated by databases, PROVEAN v.1.1 (http://provean.jcvi.org/genome_submit.php), dbSNP (http://www.ncbi.nlm.nih.gov/projects/SNP/) and 1000 genomes (http://www.1000genomes.org/). We used Evola website to investigate the conservation of p.E654 of INPPL1 (http://www.h-invitational.jp/hinv/ahg-db/index.jsp).

RESULTS

Exome sequencing

By the whole exome sequencing, 3.8–5.1 Gb sequences uniquely mapped to all human RefSeq coding region were obtained. For all subjects, at least 95.9% of all coding regions were covered in five reads depth and more (Supplementary Table 1). No candidate genes that had mutations in the two families were identified.

Because *INPPL1* mutations have recently been identified in opsismodysplasia,[5] we checked *INPPL1* mutations in the exome sequence data. Five or more reads covered 100% of its coding regions (Supplementary Table 1). A homozygous deletion, c.1960_1962 (p.E654del), was found in the proband of Family 1 (Figure 1a). However, this deletion had been excluded as a candidate mutation because no *INPPL1* variant likely to be a mutation was detected in Family 2.

Confirmation and evaluation of c.1960_1962delGAG

We confirmed the deletion by direct sequence of PCR product from genomic DNA in the proband of Family 1 (Figure 1b). Next, we performed the invader assay coupled with PCR in the family. The parents were compound heterozygous for the deletion and the affected sibs were homozygous for it. The deletion was not found in 188 Japanese controls and in the public databases. The E654 is conserved between different species (Figure 1c). It is within the central catalytic 5-phosphate domain, but located at the position far from active site (25 amino acids) and within a loop region, which is thought to have structural flexibility in general. Inositol polyphosphate 5-phosphatase domain (ipp5c) of yeast synaptojanin in complex with inositol (1,4)-bisphosphate and calcium ion (PDB ID 1i9z) is the most analogous structure to the human INPPL1 catalytic domain among the currently available structures; however, its sequence identity with the human INPPL1 catalytic domain is low (26%). These make the structural assessment of the mutation equivocal. The PROVEAN database showed that p.E654del had a deleterious function against the gene product (score: −12.1).

Mutation screening of *INPPL1* in Family 2

We screened the *INPPL1* mutation in the patient of Family 2 by direct sequencing of the entire coding exons and their flanking regions. A total of nine SNPs were found, but no mutation was found in the patient.

Clinical information of the patients with the *INPPL1* mutation

The proband of Family 1 (II-1 in Figure 1a) was a 9-year-old girl born to non-consanguineous healthy parents. Family history was unremarkable. She was referred to one of us because fetal echogram revealed short extremities. She was born at 40 weeks' of gestation. Her birth weight was 2119 g (<3 percentile), length 38.0 cm (<3 percentile) and head circumference 35.1 cm (<3 percentile). She had a wide fontanelle, widely patent sutures, frontal bossing, flat nasal

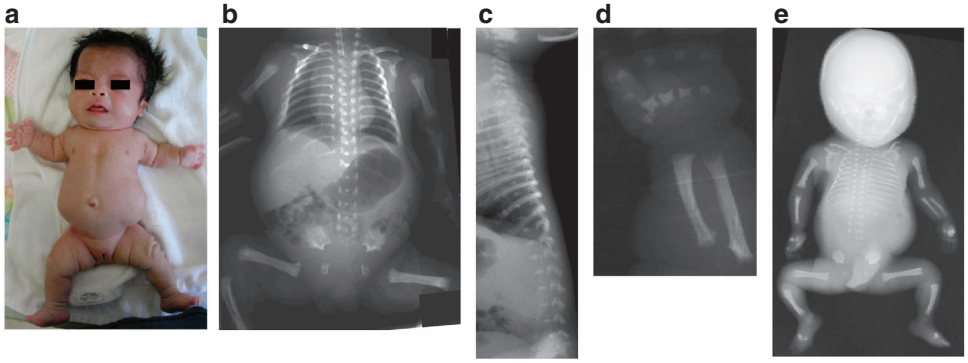

Figure 2 Phenotype of patients in Family 1. (**a**) Appearance of the proband in Family 1. Rhizomelic micromelia, frontal bossing, flat nasal bridge, low set ears, anteverted nostrils, micrognathia, narrow thorax and distended abdomen were noted. Radiographs of the proband (II-1) at birth (**b**–**d**) and the aborted fetus (II-2) (**e**). Characteristics of opsismodysplasia including retarded bone maturation, shortness of the bones of hands and feet, concave metaphyses and thin, lamellar vertebral bodies were noted.

bridge, low set ears, anteverted nostrils, micrognathia, narrow thorax and distended abdomen, and her extremities were remarkably short (Figure 2a). Her respiratory activity was weak and inspiratory wheezing was noted. Tracheal intubation became necessary 4 h after birth. Radiological investigations of her skeleton showed characteristics of opsisimodysplasia (Figures 2b–d). She was repeatedly admitted because of respiratory insufficiency due to infections. At 2 years of age, tracheotomy was performed to care for respiratory problems. She was noticed to show low serum phosphate levels at around 1 year and since then had been treated on phosphate supplements and/or alfacalcidol (1α-OH-D_3). At age 9 years, her height was 65 cm (<–6 s.d.) and weight 9 kg (–4 s.d). Her intellectual development was normal and was attending an elementary school.

In the second pregnancy, similar conditions were found by a fetal echogram. Artificial abortion was carried out. The post-mortem radiograph showed skeletal findings similar to the proband (Figure 2e).

DISCUSSION

Below *et al*.[5] examined *INPPL1* in a total of 12 unrelated families with opsismodysplasia and found its mutations in seven families. The list of mutation includes missense, nonsense and splicing mutations; all are predicted to be loss of function mutations. In one family, we also found a deletion mutation in *INPPL1* that is predicted to be a loss of function mutation, but in another family, we could not detect an *INPPL1* mutation. These results further support the results of the previous study that *INPPL1* is the disease gene for opsismodysplasia and that opsismodysplasia has genetic heterogeneity.[5] In retrospect, the patient of Family 2 showed significant platyspondyly, yet some of the radiographic features for opsismodysplasia that include hypoplasia of the base of the skull on lateral views and lateral spikes of the acetabular roof were absent. Further, the fragmented epiphyses and coning of the distal femora are not characteristically seen in opsismodysplasia. This case is also different from the other cases with an opsismodysplasia phenotype that do not have *INPPL1* mutations (Prof. Debora Krakow, personal communication). Further collection of *INPPL1* mutation-proven cases would help in defining the phenotype of opsismodysplasia. While we were preparing the manuscript, another study reporting the identification of *INPPL1* as the cause of opsismodysplasia was published.[8] It reports identification of the *INPPL1* mutation in all 10 families examined.

INPPL1 (also known as SHIP2) is a member of the inositol 5′-phosphatase family that hydrolyzes phosphatidylinositol 3,4,5-triphosphate (PtdIns(3,4,5)P_3) and generates phosphatidylinositol 3,4-bisphosphate (PtdIns(3,4)P_2).[9] *INPPL1* encodes a 142-kDa protein with a variety of protein interaction domains, including an N-terminal SH2 domain, a central catalytic 5-phosphatase domain, a C-terminal proline-rich domain, an NPXY site and a sterile a motif domain in the C-terminal region.[10] At least 12 proteins of binding partners for INPLL1, such as Shc, APS, filamin and EphA2, have been identified.[10] The genes for these binding partners are good candidates for the disease gene for the opsismodysplasia-like phenotype.

Biological roles of INPPL1 remain unclear. *INPPL1* expression is particularly high in heart, skeletal muscle and placenta.[11,12] Its proposed roles are cell adhesion and spreading, actin cytoskeletal remodeling and receptor internalization. INPPL1 negatively regulates insulin signaling through its catalytic PtdIns(3,4,5) P_3 5-phosphatase activity.[9] The *INPPL1*$^{-/-}$ mice show a shortened snout and grow more slowly than wild-type littermates.[13] After 6 weeks of age, they showed a substantial reduced body length and body weight; however, radiographic analysis showed no gross skeletal deficit. Further studies are necessary to clarify the role of *INPPL1* in skeletal development and homeostasis.

ACKNOWLEDGEMENTS

We thank the patients and their family for their help to the study. We also thank the Japanese Skeletal Dysplasia Consortium. This study is supported by research grants from the Ministry of Health, Labor and Welfare (23300101 to SI and NMat.; 23300201 to SI), by Grants-in-Aid for Young Scientists (23689052 to NMiy.) from the Japan Society for the Promotion of Science; by Research on intractable diseases, Health and Labour Sciences Research Grants, H23-Nanchi-Ippan-123 (SI) and by grants from the Japan Science and Technology Agency, the Strategic Research Program for Brain Sciences (11105137 to NMat.), a Grant-in-Aid for Scientific Research on Innovative Areas (Transcription Cycle) from the Ministry of Education, Culture, Sports, Science and Technology of Japan (12024421 to NMat.), a Grant-in-Aid for Scientific Research from the Japan Society for the Promotion of Science (12020465 to NMat.) and the Takeda Science Foundation (to N Miy. and N Mat.). We thank Professors Debora Krakow and Michael Bamshad for their comments on the patients' phenotypes. We also thank Ms Tomoko Kusadokoro for technical assistance.

1 Cormier-Daire, V., Delezoide, A. L., Philip, N., Marcorelles, P., Casas, K., Hillion, Y. *et al.* Clinical, radiological, and chondro-osseous findings in opsismodysplasia: survey of a series of 12 unreported cases. *J. Med. Genet.* **40,** 195–200 (2003).
2 Beemer, F. A. & Kozlowski, K. S Additional case of opsismodysplasia supporting autosomal recessive inheritance. *Am. J. Med. Genet.* **49,** 344–347 (1994).
3 Santos, H. G. & Saraiva, J. M Opsismodysplasia: another case and literature review. *Clin. Dysmorphol.* **4,** 222–226 (1995).
4 Tyler, K., Sarioglu, N. & Kunze, J Five familial cases of opsismodysplasia substantiate the hypothesis of autosomal recessive inheritance. *Am. J. Med. Genet.* **83,** 47–52 (1999).
5 Below, J. E., Earl, D. L., Shively, K. M., McMillin, M. J., Smith, J. D., Turner, E. H. *et al.* Whole-genome analysis reveals that mutations in inositol polyphosphate phosphatase-like 1 cause opsismodysplasia. *Am. J. Hum. Genet.* **92,** 137–143 (2013).
6 Miyake, N., Elcioglu, N. H., Iida, A., Isguven, P., Dai, J., Murakami, N. *et al.* PAPSS2 mutations cause autosomal recessive brachyolmia. *J. Med. Genet.* **49,** 533–538 (2012).
7 Ohnishi, Y., Tanaka, T., Ozaki, K., Yamada, R., Suzuki, H. & Nakamura, Y A high-throughput SNP typing system for genome-wide association studies. *J. Hum. Genet.* **46,** 471–477 (2001).
8 Huber, C., Faqeih, E. A., Bartholdi, D., Bole-Feysot, C., Borochowitz, Z., Cavalcanti, D. P. *et al.* Exome sequencing identifies INPPL1 mutations as a cause of opsismodysplasia. *Am. J. Hum. Genet.* **92,** 144–149 (2013).
9 Dyson, J. M., Kong, A. M., Wiradjaja, F., Astle, M. V., Gurung, R. & Mitchell, C. A The SH2 domain containing inositol polyphosphate 5-phosphatase-2: SHIP2. *Int. J. Biochem. Cell. Biol.* **37,** 2260–2265 (2005).
10 Suwa, A., Kurama, T. & Shimokawa, T. SHIP2 and its involvement in various diseases. *Expert Opin. Ther. Targets* **14,** 727–737 (2010).
11 Hejna, J. A., Saito, H., Merkens, L. S., Tittle, T. V., Jakobs, P. M., Whitney, M. A. *et al.* Cloning and characterization of a human cDNA (INPPL1) sharing homology with inositol polyphosphate phosphatases. *Genomics* **29,** 285–287 (1995).
12 Pesesse, X., Deleu, S., De Smedt, F., Drayer, L. & Erneux, C Identification of a second SH2-domain-containing protein closely related to the phosphatidylinositol polyphosphate 5-phosphatase SHIP. *Biochem. Biophys. Res. Commun.* **239,** 697–700 (1997).
13 Sleeman, M. W., Wortley, K. E., Lai, K. M., Gowen, L. C., Kintner, J., Kline, W. O. *et al.* Absence of the lipid phosphatase SHIP2 confers resistance to dietary obesity. *Nat. Med.* **11,** 199–205 (2005).

Supplementary Information accompanies the paper on Journal of Human Genetics website (http://www.nature.com/jhg)

ORIGINAL ARTICLE

PAPSS2 mutations cause autosomal recessive brachyolmia

Noriko Miyake,[1] Nursel H Elcioglu,[2] Aritoshi Iida,[3] Pinar Isguven,[4] Jin Dai,[3] Nobuyuki Murakami,[5] Kazuyuki Takamura,[6] Tae-Joon Cho,[7] Ok-Hwa Kim,[8] Tomonobu Hasegawa,[9] Toshiro Nagai,[5] Hirofumi Ohashi,[10] Gen Nishimura,[11] Naomichi Matsumoto,[1] Shiro Ikegawa[3]

[1]Department of Human Genetics, Yokohama City University Graduate School of Medicine, Yokohama, Japan
[2]Department of Pediatric Genetics, Marmara University Pendik Hospital, Istanbul, Turkey
[3]Laboratory for Bone and Joint Diseases, Center for Genomic Medicine, RIKEN, Tokyo, Japan
[4]Department of Pediatrics and Pediatric Endocrinology, Medeniyet University Goztepe Hospital, Istanbul, Turkey
[5]Department of Pediatrics, Dokkyo Medical University Koshigaya Hospital, Koshigaya, Japan
[6]Department of Orthopaedic Surgery, Fukuoka Children's Hospital, Fukuoka, Japan
[7]Division of Pediatric Orthopaedics, Seoul National University Children's Hospital, Seoul, Korea
[8]Department of Radiology, Ajou University Hospital, Suwon, Korea
[9]Department of Pediatrics, Keio University School of Medicine, Tokyo, Japan
[10]Division of Medical Genetics, Saitama Children's Medical Center, Saitama, Japan
[11]Department of Pediatric Imaging, Tokyo Metropolitan Children's Medical Center, Futyu, Japan

Correspondence to
Noriko Miyake, Department of Human Genetics, Yokohama City University Graduate School of Medicine, 3-9, Fukuura, Kanazawa-ku, Yokohama 236-0004, Japan; nmiyake@yokohama-cu.ac.jp or Shiro Ikegawa, Laboratory of Bone and Joint Diseases, Center for Genomic Medicine, RIKEN 4-6-1 Shirokanedai, Minato-ku, Tokyo 108-8639, Japan; sikegawa@ims.u-tokyo.ac.jp

NM, NHE and AI contributed equally to this work.

Received 8 May 2012
Revised 8 June 2012
Accepted 10 June 2012

ABSTRACT

Background Brachyolmia is a heterogeneous group of skeletal dysplasias that primarily affects the spine. Clinical and genetic heterogeneity have been reported; at least three types of brachyolmia are known. *TRPV4* mutations have been identified in an autosomal dominant form of brachyolmia; however, disease genes for autosomal recessive (AR) forms remain totally unknown. We conducted a study on a Turkish family with an AR brachyolmia, with the aim of identifying a disease gene for AR brachyolmia.

Methods and results We examined three affected individuals of the family using exon capture followed by next generation sequencing and identified its disease gene, *PAPSS2* (phosphoadenosine-phosphosulfate synthetase 2). The patients had a homozygous loss of function mutation, c.337_338insG (p.A113GfsX18). We further examined three patients with similar brachyolmia phenotypes (two Japanese and a Korean) and also identified loss of function mutations in *PAPSS2*; one patient was homozygous for IVS3+2delT, and the other two were compound heterozygotes for c.616-634del19 (p.V206SfsX9) and c.1309-1310delAG (p.R437GfsX19), and c.480_481insCGTA (p.K161RfsX6) and c.661delA (p.I221SfsX40), respectively. The six patients had short-trunk short stature that became conspicuous during childhood with normal intelligence and facies. Their radiographic features included rectangular vertebral bodies with irregular endplates and narrow intervertebral discs, precocious calcification of rib cartilages, short femoral neck, and mildly shortened metacarpals. Spinal changes were very similar among the six patients; however, epiphyseal and metaphyseal changes of the tubular bones were variable.

Conclusions We identified *PAPSS2* as the disease gene for an AR brachyolmia. *PAPSS2* mutations have produced a skeletal dysplasia family, with a gradation of phenotypes ranging from brachyolmia to spondylo-epi-metaphyseal dysplasia.

INTRODUCTION

Brachyolmia is a heterogeneous group of skeletal dysplasias that primarily affects the spine. The name comes from the Greek for 'short trunk'; patients with brachyolmia have short stature due to a short trunk.[1] Conceptually, skeletal lesions of brachyolmia are limited to the spine; however, it is generally thought that pure brachyolmia (spine-only dysplasia) does not exist and that metaphyseal and/or epiphyseal involvements may be minimal and scattered, but are always present along with spinal involvements in cases labelled brachyolmia.[2]

Clinical and genetic heterogeneity have been reported in brachyolmia. At least three relatively well defined types of brachyolmia are known: type 1 that includes the Hobaek (OMIM 271530) and Toledo (OMIM 271630) forms; type 2 (OMIM 613678) referred to as the Maroteaux type; and type 3 (OMIM 113500). The former two types are autosomal recessive (AR) traits, while the latter is an autosomal dominant trait. Type 1 is characterised by scoliosis, platyspondyly with rectangular and elongated vertebral bodies, overfaced pedicles, and irregular and narrow intervertebral spaces. The Toledo form is distinguished from the Hobaek form by the presence of corneal opacity and precocious calcification of the costal cartilage.[3 4] Type 2 is distinguished by rounded vertebral bodies, less overfaced pedicles, minor facial anomalies, and precocious calcification of the falx cerebri.[1] Type 3 is characterised by severe kyphoscoliosis and flattened, irregular cervical vertebrae. Heterozygous mutations in the *TRPV4* (transient receptor potential vanilloid 4) gene (OMIM 605427) have been identified in several patients with type 3, autosomal dominant brachyolmia;[5 6] however, disease genes for recessive forms of brachyolmia remain totally unknown.

To identify novel disease genes from a limited number of subjects, exome sequencing (exon capture followed by next generation sequencing) is a promising approach. This approach sometimes presents us with unusual and unexpected connection between genes and phenotypes, thereby opening a new window for biology and medicine. We experienced a family with an AR form of brachyolmia harbouring three affected individuals. By performing exome sequencing for the family, we have identified the disease gene for the recessive brachyolmia, *PAPSS2* (phosphoadenosine-phosphosulfate synthetase 2). The discovery was confirmed by identification of *PAPSS2* mutations in three sporadic patients with different ethnic backgrounds but similar brachyolmia phenotypes. All patients had loss of function mutations of *PAPSS2* in both chromosomes.

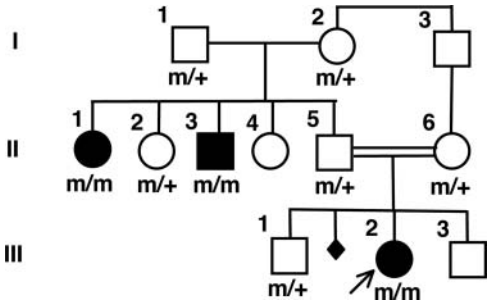

Figure 1 The pedigree of family 1 and co-segregation of the *PAPSS2* mutation (c.337_338insG) in the family. m: mutation allele, +: wild type allele.

MATERIALS AND METHODS

Subjects

P1-3 (family 1)

The proband (P1; III-2 in figure 1) was a Turkish girl referred to one of us (NHE) for genetic evaluation at the age of 8 years 4 months. She has been followed up for her spinal deformity and lumber pain elsewhere for 5 years. She was the result of a consanguineous (first cousin) marriage. A paternal uncle (P2; II-3 in figure 1) and aunt (P3; II-1 in figure 1) had the similar disease (table 1). The paternal grandparents originated from a small area and could be related. The inheritance of the disease was consistent with AR mode. Her birth length was 49 cm and weight 2800 g. She did not gain well after birth and was investigated for short stature at the age of 1 year. Her back deformity was noticed at around 3 years of age. On examination, she had short-trunk short stature. Her height was 109 cm (−3.2 SD), weight 29 kg (+0.38 SD) and head circumference 51 cm (−0.6 SD). She was mentally normal with no hearing or vision problems. She had widened wrists, bulbous proximal interphalangeal joints, clinodactyly of the fifth finger, and bowing deformity in her left lower leg. Serum DHEA-S (dehydroepiandrosterone-sulfate) was under the detection limit (<15.0 μg/dl).

Repeated skeletal surveys showed definite spondylodysplasia with minimal epiphyseal and metaphyseal changes, which was compatible with brachyolmia (table 1 and figure 2). Vertebral bodies were flat, particularly in thoracic spines. Endplates were irregular and intervertebral disc spaces were narrowed. The acetabular roof was horizontal. Femoral necks were slightly short. Metaphyses of the distal tibias had striation. Metacarpals were mildly shortened with mild metaphyseal changes. The bone age was advanced; 6 years 10 months at chronological age 5 years 8 months, and 10 years at chronological age 8 years 2 months (Greulich-Pyle method). MRIs and CTs showed no calcification of the falx cerebri.

At her last visit (10 years 4 months old), she had increasing back deformity and pain. Her height was 121 cm (−3.4 SD), arm span 119 cm, and sitting/standing height ratio was 0.53.

Table 1 Clinical and radiographic phenotypes of autosomal recessive brachyolmina harbouring *PAPSS2* mutation (in comparison to those in spondylo-epi-metaphyseal dysplasia Pakistani type)

Patient ID	P1	P2	P3	P4	P5	P6	
Family	Family 1						Patient reported by Noordam *et al*
Intra-family ID	III-2	II-3	II-1	Family 2	Family 3	Family 4	
Country of origin	Turkey			Japan	Japan	Korea	Turkey
Sex	Female	Male	Female	Female	Female	Male	Female
Age at first presentation	8 years 4 months	29 years	40 years	11 years 4 months	8 years 8 months	12 years 7 months	8 years
Birth length (cm)	49	NA	NA	46	47	50	NA
Birth weight (g)	2800	NA	NA	3340	2676	3100	NA
Consanguinity of the parents	+	Probably +	Probably +	(−)	(−)	(−)	(−)
Clinical feature							
Normal intelligence	+	+	+	+	+	+	NA
Normal facies	+	+	+	+	+	+	NA
Short-trunk short stature	+	+	+	+	+	+	+
Spinal deformity	Kyphosis	(−)	Kyphosis, lumbar scoliosis	Kyphosis	(−)	(−)	Lumbar scoliosis
Leg deformity	Bil genu varum and internal rotation	(−)	Bil genu varum and internal rotation	(−)	Right genu valgum	Bil genu varum	NA
Androgen excess sign	(−)	(−)	(−)	(−)	(−)	(−)	+
Radiographic feature							
Rectangular vertebra	+	+	+	+	+	+	+
Irregular endplate	+	+	+	+	+	+	+
Narrowed disc	+	+	+	+	+	+	+
Precocious calcification of costal cartilage	(−)	+	+	+	(−)	(−)	NA
Delayed ossification of hip and knee epiphyses	(−)	NA	NA	(−)	(−)	(−)	(−)
Early osteoarthritic change	(−)*	(−)	(−)	(−)	(−)*	(−)*	(−)*
Short femoral neck	+	+	+	+	+	+	+
Metaphyseal abnormality†	Dist tibia	Prox tibia	Prox tibia	(−)	(−)	Prox tibia	(−)
Mild brachymetacarpia	+	+	+	+	+	+	+
Advanced bone age	+	NA	NA	+	+	+	+

*May be too young to be evaluated.
†Other than short femoral neck and fingers.
Bil, bilateral; Dist, distal; NA, not available or assessed; Prox, proximal.

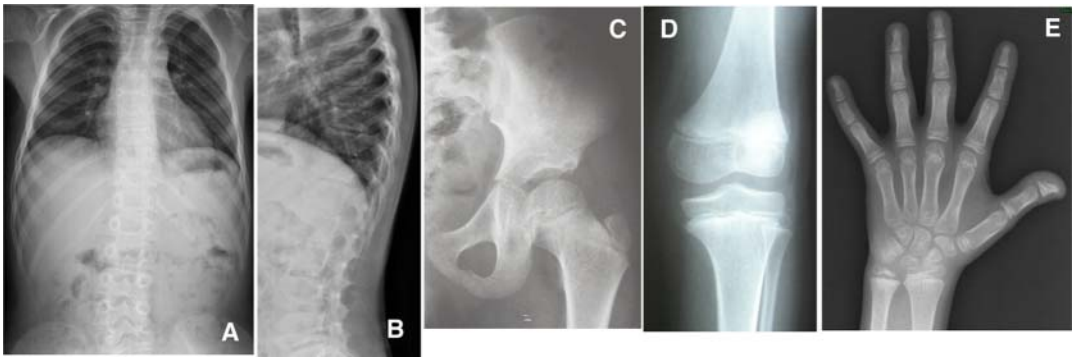

Figure 2 Radiographs of P1 (III-2 in family 1) at age 8.5 years. (A) Spine anteroposterior (AP). Mildly overfaced vertebra. (B) Lateral spine. Mild flattening of vertebral bodies and irregular endplates. (C) Left hip AP. Almost normal epiphysis. (D) Left knee AP. Epiphyseal and metaphyseal abnormalities are unremarkable. (E) Left hand AP. Metacarpals are mildly shortened with mild irregularity of the growth plates. Epiphyses of the distal radius and ulna show mild dysplasia. The bone age is advanced.

Breast development was Tanner 2–3, pubic hair Tanner 1. There had been no sign of androgen excess (acne, hirsutism, etc).

P4-6 (sporadic cases)

After we found *PAPSS2* mutations in family 1, we reviewed the patient registry of the Japanese Skeletal Dysplasia Consortium and found two Japanese patients (P4-5) and one Korean patient (P6) who had similar phenotypes to those of the Turkish family (table 1 and figure 3); all three were sporadic cases from normal, non-consanguineous parents and were *TRPV4* mutation negative.

DNA sample

Genomic DNA was extracted by standard procedures from peripheral blood of the patients and/or their family members after informed consent. The study was approved by the ethical committee of RIKEN, Yokohama City University, and participating institutions.

Exome sequencing

Three affected individuals of family 1 (II-1, II-3 and III-2) were analysed by whole exome sequencing as previously reported (see supplementary online table S1).[7 8] In brief, 3 μg of genomic DNA was sheared by Covaris S2 system (Covaris, Woburn, Massachusetts, USA) and processed using a SureSelect Human All Exon 50 Mb Kit (Agilent Technologies, Santa Clara, California, USA) according to the manufacturer's instructions. DNAs were captured by the kit and were sequenced by GAIIx (Illumina, San Diego, California, USA) with 108 pair-ends reads. Each sample was run in one lane. Image analysis and base calling were performed by sequence control software 2.9 and real time analysis 1.9 (Illumina), and CASAVA software V.1.8.1 (Illumina). The quality-controlled (path-filtered) reads were mapped to human genome reference hg19 with Mapping and Assembly with Qualities (MAQ, http://maq.sourceforge.net/) and NextGENe software V.2.00 (SoftGenetics, State College, Pennsylvania, USA). The variants from MAQ were annotated by SeattleSeq annotation 131 (http://snp.gs.washington.edu/SeattleSeqAnnotation131/).

Priority scheme

Variants were filtered by the following conditions using the script created by BITS (Tokyo, Japan): (1) variants only annotated on human autosomes and chromosome X; (2) variants not in dbSNP131, dbSNP134, the 1000 Genomes database (http://www.1000genomes.org/), and in-house exome data of normal Japanese controls (n=66); (3) variants that were non-synonymous and intronic changes (±20 bp from exon/intron boundaries) called in common by NextGENe and MAQ, and variants of insertion/deletion with a NextGENe score ≥10. The variant numbers in each category are shown in supplementary online table S1.

Sanger sequencing and evaluation of mutations

To confirm the sequence change identified in P1-3 by the exome sequencing, exon 3 of *PAPSS2* and its flanking intronic sequences (The GenBank reference sequence: NM_001015880) were amplified by PCR from genomic DNA. To examine *PAPSS2* mutation in P4-6, all exons of *PAPSS2* and its flanking intronic sequences were amplified by PCR from genomic DNA. Primer sequences and PCR conditions were as previously described.[9] PCR products were directly sequenced using ABI Prism automated sequencers 3730 (PE Biosystems, Foster City, CA, USA).

To evaluate the possibility of polymorphisms, identified sequence changes were genotyped in 93 ethnically matched controls using the invader assay coupled with PCR as described previously.[10] The sequence changes were evaluated by public databases including OMIM (http://www.ncbi.nlm.nih.gov/omim) and dbSNP (http://www.ncbi.nlm.nih.gov/projects/SNP/).

RESULTS

Exome sequencing

A total of 90 964 194 (II-1), 90 508 738 (II-3) and 90 223 680 (III-2) reads were mapped to the whole human genome in pairs by MAQ. Considering the consanguinity of the family, we focused on the same homozygous mutations shared by the three affected individuals. After filtering, a total of 37 homozygous variants remained as candidates (23 missense, 11 intronic, and three insertion changes) (see supplementary online table S1). Among them, one base pair insertion, c.337_338insG in exon 3 of *PAPSS2*, was highlighted because it is a causative gene for SEMD, Pakistani type (OMIM 612847), that has overlapping features with the phenotypes of the three patients.

The insertion sequence was confirmed by direct sequence of PCR products from genomic DNA. Direct sequencing of nine family members showed co-segregation of the mutation with the disease phenotype (figure 1). The insertion mutation was

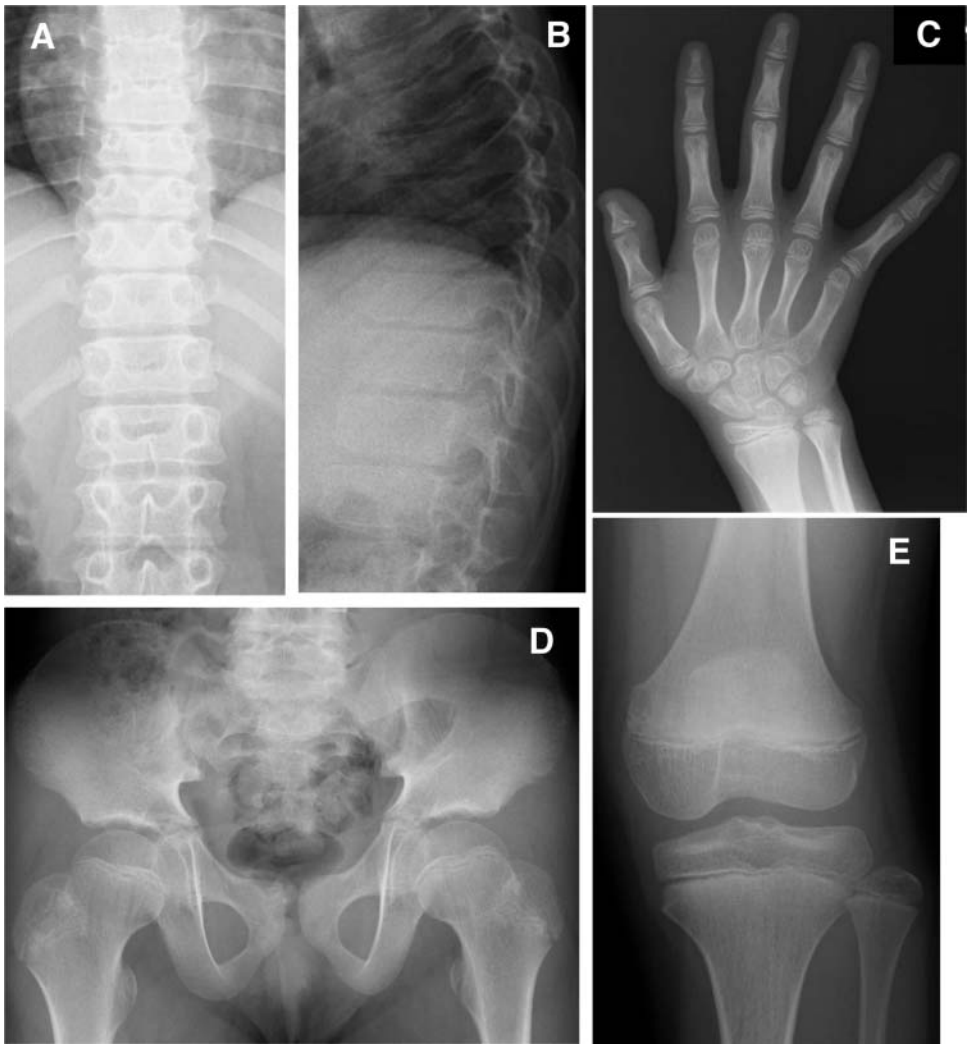

Figure 3 Radiographs of P5 at age 8 years 8 months. (A) Spine anteroposterior (AP). Platyspondyly. Over-faced pedicle is not so distinct. (B) Spine lateral. Flattened vertebral bodies and narrow disc spaces. (C) The right hand AP. Slightly short metacarpals. Phalanges are not so short. The bone age is advanced (12 years by the Greulich-Pyle method). (D) Pelvis AP. Short femoral neck and horizontal acetabulum. Proximal epiphyses are normal. (E) The right knee AP. Unremarkable changes. No fibula overgrowth.

predicted to create a premature stop codon (p.A113GfsX18), thereby most probably resulting in a null allele due to nonsense mutation mediated RNA decay (NMD).[11] The mutation was not found in the public mutation database and sequence variation database. Also, it was not found in 93 ethnically matched controls examined by Invader assay.[10]

Identification of *PAPSS2* mutations in sporadic cases

We screened for *PAPSS2* mutations in P4-6 by direct sequencing as previously described.[9] We found *PAPSS2* mutations in both chromosomes of all subjects (table 2). All mutations are predicted to create premature stop codons before the second last exon of the gene. Therefore, they are most likely to result in null alleles due to NMD. P5 was a homozygote, and P4 and P6 were heterozygotes for the mutations. Compound heterozygosity of the subjects was confirmed by sequencing of the parents' genomic DNA. All these mutations were not found in 93 ethnically matched controls examined by Invader assay[10] nor in public databases.

Phenotypes of the patients with *PAPSS2* mutations

Clinical features of our six patients were short-trunk short stature with short neck (table 1). The short stature was noticeable early in life, but not always at birth; it usually became definite after age 5–6 years. All patients had normal intelligence and facies. Corneal opacity was not found. Kyphosis and/or scoliosis were found in three subjects. Bone age was advanced in all (4/4) cases evaluated. No clinical sign of androgen excess was noted in all (6/6) patients and their family members. The main radiographic feature was pronounced flattening of spine (rectangular vertebral body), particularly in the thoracic spine, which accompanied irregular

Table 2 *PAPSS2* mutations in autosomal recessive brachyolmia

Family	Exon	Nucleotide change	Amino acid change
1	3	c.337_338insG (homozygous)	p.A113GfsX18
2	5	c.616-634del19	p.V206SfsX9
	11	c.1309-1310delAG	p.R437GfsX19
3	3	IVS3+2delT (homozygous)	p.L50SfsX2
4	4	c.480_481insCGTA	p.K161RfsX6
	6	c.661delA	p.I221SfsX40

The nucleotide changes are shown with respect to *PAPSS2* mRNA sequence (NM_001015880). The corresponding predicted amino acid changes are numbered from the initiating methionine residue. Exons are numbered sequentially 1–13.

endplates and narrow disc spaces. Mild shortening of the femoral neck and metacarpals were common features. The costal cartilages showed precocious calcification in the adult subjects (3/3). Epiphyseal and metaphyseal dysplasias were very mild, if present. From these features of spine predominant dysplasia, our patients can be diagnosed as having brachyolmia. Among known types of brachyolmias, characteristics of the Hobaek and Toledo types are mixed.[1 4]

DISCUSSION

PAPSS2 mutation has been reported to be responsible for two other overlapping, but distinct, phenotypes. The first is SEMD Pakistani type; Ahmad *et al*[12] described a large consanguineous Pakistani family with a distinct form of SEMD with autosomal inheritance. Its clinical features include short stature evident at birth, short and bowed lower limbs, mild brachydactyly, kyphoscoliosis, enlarged knee joints, and precocious osteoarthropathy. Radiographic features are platyspondyly with irregular endplates and narrowed joint spaces, delayed epiphyseal ossification at the hips and knees, diffuse early osteoarthritic changes primarily in the spine and hands, and mild brachydactyly. Metaphyseal abnormalities are seen predominantly in the hips and knees. This disease is differentiated from other forms of SEMD by its mild degree of metaphyseal involvement, type of brachydactyly, and the absence of loose joints or other clinical findings. A homozygous nonsense mutation of *PAPSS2* (S438X) is identified in all affected individuals in the family.[13] Many of the characteristics of SEMD Pakistani type, including enlarged joints with deformity, delayed epiphyseal ossification at the hips and knees, and precocious osteoarthritic changes of the large and small joints, are absent in our cases (table 1).

PAPSS2 mutations have also been found in a patient with a different phenotype, spondylodysplasia and premature pubarche.[9] A Turkish girl with premature pubarche, hyperandrogenic anovulation, short stature, and skeletal dysplasia showed a compound heterozygosity for a missense and a nonsense mutation in *PAPSS2*: the former was a 143C>G transversion resulting in a T48R substitution at a conserved residue in the adenosine 5-prime-phosphosulfate kinase domain, and the latter was a 985C>T transition resulting in R329X. Their functional assays revealed no detectable activity for R329X, and only minor residual activity for T48R (6% of the wild type activity). The mother who carried the R329X mutation had normal pubarche and menarche, but developed obesity, oligomenorrhoea, and hirsutism in her fourth decade, while the father who carried the T48R mutation showed normal growth and pubertal development. The skeletal changes in this patient are more similar to those of our cases than SEMD Pakistani type (table 1).

Among our patients, spinal changes were very similar, but epiphyseal and metaphyseal changes were considerably variable (table 1). P4 and P5, similar to the case reported by Noordam *et al*,[9] showed minimal epiphyseal and metaphyseal dysplasias. P6 had considerable epi-metaphyseal changes in the long bones of the lower extremities; they were more severe than those in family 1 (P1-3), but were far milder than those in SEMD Pakistani type. The differential diagnosis includes AR spondyloepiphyseal dysplasia tarda[14] because of late manifestation, AR inheritance, and relatively mild spondyloepiphyseal dysplasia with flat vertebral bodies with irregular endplates. In the disorder, overfaced vertebral bodies is absent and the capital femoral epiphyses are severely affected.[14]

In a form of autosomal dominant brachyolmia, heterozygous *TRPV4* mutation has been identified.[5 6] Notably, the *TRPV4* mutation presents a wide phenotypic gradation from brachyolmia at its most mild, through spondylometaphyseal dysplasia type Kozlowski, spondyloepiphyseal dysplasia type Maroteaux, and metatropic dysplasia, to parastremmatic dysplasia and fetal akinesia at its most severe.[5 15–17] *PAPSS2* mutations might also present a phenotype gradation from brachyolmia to spondylo-epiphyseal and spondylo-epimetaphyseal dysplasia like SEMD Pakistani type. Further investigation of *PAPSS2* mutations in brachyolmia and skeletal dysplasias with overlapping phenotypes to our cases as well as other cases with *PAPSS2* mutations[9 14] would provide further answers.

An additional supplementary table is published online only. To view this file please visit the journal online (http://jmg.bmj.com)

Acknowledgements We thank the patients and their family for their help to the study. We also thank the Japanese Skeletal Dysplasia Consortium.

Contributors NM performed the exome experiments, analysed the data, wrote the paper, and is guarantor. NE and PI collected family samples and evaluated their phenotypes. AI performed the sequence experiments, analysed the data, and wrote the paper. JD performed the experiments. NoM, KM, TC, OK, and TN collected samples and evaluated their clinical and radiographic phenotypes. TH and GN analysed the clinical data. HO collected and controlled the experimental samples. NaM performed the experiments and analysed the data. SI analysed the data, wrote the paper, and is also guarantor. All authors have critically revised the paper.

Funding This study is supported by research grants from the Ministry of Health, Labour and Welfare (23300101: S Ikegawa and N Matsumoto; 23300102: T Hasegawa; 23300201: S Ikegawa), by a Grant-in-Aid for Young Scientists from the Japan Society for the Promotion of Science (N Miyake), and by Research on intractable diseases, Health and Labour Sciences Research Grants, H23-Nanchi-Ippan-123 (S Ikegawa).

Patient consent Obtained.

Ethics approval This study was performed under the approval of the ethical committee of RIKEN, Yokohama City University, and participating institutions.

Provenance and peer review Not commissioned; externally peer reviewed.

Data sharing statement Additional unpublished data on mutation examination are available on request to researchers.

REFERENCES

1. **Shohat M,** Lachman R, Gruber HE, Rimoi DL. Brachyolmia: radiographic and genetic evidence of heterogeneity. *Am J Med Genet* 1989;**33**:209–19.
2. **Kozlowski K,** Beemer FA, Bens G, Dijkstra PF, Iannaccone G, Emons D, Lopez-Ruiz P, Masel J, van Nieuwenhuizen O, Rodriguez-Barrionuevo C. Spondylo-Metaphyseal Dysplasia (Report of 7 cases and essay of classification). *Prog Clin Biol Res* 1982;**104**:89–101.
3. **McKusick VA.** Medical genetics. A 40-year perspective on the evolution of a medical specialty from a basic science. *JAMA* 1993;**270**:2351–6.
4. **Hoo JJ,** Oliphant M. Two sibs with brachyolmia type Hobaek: five year follow-up through puberty. *Am J Med Genet A* 2003;**116A**:80–4.
5. **Rock MJ,** Prenen J, Funari VA, Funari TL, Merriman B, Nelson SF, Lachman RS, Wilcox WR, Reyno S, Quadrelli R, Vaglio A, Owsianik G, Janssens A, Voets T, Ikegawa S, Nagai T, Rimoin DL, Nilius B, Cohn DH. Gain-of-function mutations in TRPV4 cause autosomal dominant brachyolmia. *Nat Genet* 2008;**40**:999–1003.
6. **Dai J,** Cho TJ, Unger S, Lausch E, Nishimura G, Kim OH, Superti-Furga A, Ikegawa S. TRPV4-pathy, a novel channelopathy affecting diverse systems. *J Hum Genet* 2010;**55**:400–2.
7. **Doi H,** Yoshida K, Yasuda T, Fukuda M, Fukuda Y, Morita H, Ikeda S, Kato R, Tsurusaki Y, Miyake N, Saitsu H, Sakai H, Miyatake S, Shiina M, Nukina N, Koyano S, Tsuji S, Kuroiwa Y, Matsumoto N. Exome sequencing reveals a homozygous SYT14 mutation in adult-onset, autosomal-recessive spinocerebellar ataxia with psychomotor retardation. *Am J Hum Genet* 2011;**89**:320–7.
8. **Tsurusaki Y,** Okamoto N, Ohashi H, Kosho T, Imai Y, Hibi-Ko Y, Kaname T, Naritomi K, Kawame H, Wakui K, Fukushima Y, Homma T, Kato M, Hiraki Y, Yamagata T, Yano S, Mizuno S, Sakazume S, Ishii T, Nagai T, Shiina M, Ogata K, Ohta T, Niikawa N, Miyatake S, Okada I, Mizuguchi T, Doi H, Saitsu H, Miyake N, Matsumoto N. Mutations affecting components of the SWI/SNF complex cause Coffin-Siris syndrome. *Nat Genet* 2012;**44**:376–8.
9. **Noordam C,** Dhir V, McNelis JC, Schlereth F, Hanley NA, Krone N, Smeitink JA, Smeets R, Sweep FC, Claahsen-van der Grinten HL, Arlt W. Inactivating PAPSS2 mutations in a patient with premature pubarche. *N Engl J Med* 2009;**360**:2310–18.

10. **Ohnishi Y,** Tanaka T, Ozaki K, Yamada R, Suzuki H, Nakamura Y. A high-throughput SNP typing system for genome-wide association studies. *J Hum Genet* 2001;**46**:471–7.
11. **Holbrook JA,** Neu-Yilik G, Hentze MW, Kulozik AE. Nonsense-mediated decay approaches the clinic. *Nat. Genet* 2004;**36**:801–8.
12. **Ahmad M,** Haque MF, Ahmad W, Abbas H, Haque S, Krakow D, Rimoin DL, Lachman RS, Cohn DH. Distinct, autosomal recessive form of spondyloepimetaphyseal dysplasia segregating in an inbred Pakistani kindred. *Am J Med Genet* 1998;**78**:468–73.
13. **Faiyaz ul Haque M,** King LM, Krakow D, Cantor RM, Rusiniak ME, Swank RT, Superti-Furga A, Haque S, Abbas H, Ahmad W, Ahmad M, Cohn DH. Mutations in orthologous genes in human spondyloepimetaphyseal dysplasia and the brachymorphic mouse. *Nat Genet* 1998;**20**:157–62.
14. **Leroy JG,** Leroy BP, Emmery LV, Messiaen L, Spranger JW. A new type of autosomal recessive spondyloepiphyseal dysplasia tarda. *Am J Med Genet A* 2004;**125A**:49–56.
15. **Krakow D,** Vriens J, Camacho N, Luong P, Deixler H, Funari TL, Bacino CA, Irons MB, Holm IA, Sadler L, Okenfuss EB, Janssens A, Voets T, Rimoin DL, Lachman RS, Nilius B, Cohn DH. Mutations in the gene encoding the calcium-permeable ion channel TRPV4 produce spondylometaphyseal dysplasia, Kozlowski type and metatropic dysplasia. *Am J Hum Genet* 2009;**84**:307–15.
16. **Nishimura G,** Dai J, Lausch E, Unger S, Megarbané A, Kitoh H, Kim OH, Cho TJ, Bedeschi F, Benedicenti F, Mendoza-Londono R, Silengo M, Schmidt-Rimpler M, Spranger J, Zabel B, Ikegawa S, Superti-Furga A. Spondylo-epiphyseal dysplasia, Maroteaux type (pseudo-Morquio syndrome type 2), and parastremmatic dysplasia are caused by TRPV4 mutations. *Am J Med Genet A* 2010;**152A**:1443–9.
17. **Unger S,** Lausch E, Stanzial F, Gillessen-Kaesbach G, Stefanova I, Di Stefano CM, Bertini E, Dionisi-Vici C, Nilius B, Zabel B, Superti-Furga A. Fetal akinesia in metatropic dysplasia: The combined phenotype of chondrodysplasia and neuropathy? *Am J Med Genet A* 2011;**155A**:2860–4.

OPEN ACCESS Freely available online

PLOS ONE

Molecular and Clinical Studies in 138 Japanese Patients with Silver-Russell Syndrome

Tomoko Fuke[1,2], Seiji Mizuno[3], Toshiro Nagai[4], Tomonobu Hasegawa[2], Reiko Horikawa[5], Yoko Miyoshi[6], Koji Muroya[7], Tatsuro Kondoh[8], Chikahiko Numakura[9], Seiji Sato[10], Kazuhiko Nakabayashi[11], Chiharu Tayama[11], Kenichiro Hata[11], Shinichiro Sano[1,12], Keiko Matsubara[1], Masayo Kagami[1], Kazuki Yamazawa[1], Tsutomu Ogata[1,12]*

1 Department of Molecular Endocrinology, National Research Institute for Child Health and Development, Tokyo, Japan, **2** Department of Pediatrics, Keio University School of Medicine, Tokyo, Japan, **3** Department of Pediatrics, Central Hospital, Aichi Human Service Center, Aichi, Japan, **4** Department of Pediatrics, Dokkyo Medical University Koshigaya Hospital, Saitama, Japan, **5** Division of Endocrinology and Metabolism, National Center for Child Health and Development, Tokyo, Japan, **6** Department of Pediatrics, Osaka University Graduate School of Medicine, Suita, Japan, **7** Department of Endocrinology and Metabolism, Kanagawa Children's Medical Center, Kanagawa, Japan, **8** Division of Developmental Disability, Misakaenosono Mutsumi Developmental, Medical, and Welfare Center, Isahaya, Japan, **9** Department of Pediatrics, Yamagata University School of Medicine, Yamagata, Japan, **10** Department of Pediatrics, Saitama Municipal Hospital, Saitama, Japan, **11** Department of Maternal-Fetal Biology, National Research Institute for Child Health and Development, Tokyo, Japan, **12** Department of Pediatrics, Hamamatsu University School of Medicine, Hamamatsu, Japan

Abstract

Background: Recent studies have revealed relative frequency and characteristic phenotype of two major causative factors for Silver-Russell syndrome (SRS), i.e. epimutation of the *H19*-differentially methylated region (DMR) and uniparental maternal disomy 7 (upd(7)mat), as well as multilocus methylation abnormalities and positive correlation between methylation index and body and placental sizes in *H19*-DMR epimutation. Furthermore, rare genomic alterations have been found in a few of patients with idiopathic SRS. Here, we performed molecular and clinical findings in 138 Japanese SRS patients, and examined these matters.

Methodology/Principal Findings: We identified *H19*-DMR epimutation in cases 1–43 (group 1), upd(7)mat in cases 44–52 (group 2), and neither *H19*-DMR epimutation nor upd(7)mat in cases 53–138 (group 3). Multilocus analysis revealed hyper- or hypomethylated DMRs in 2.4% of examined DMRs in group 1; in particular, an extremely hypomethylated *ARHI*-DMR was identified in case 13. Oligonucleotide array comparative genomic hybridization identified a ~3.86 Mb deletion at chromosome 17q24 in case 73. Epigenotype-phenotype analysis revealed that group 1 had more reduced birth length and weight, more preserved birth occipitofrontal circumference (OFC), more frequent body asymmetry and brachydactyly, and less frequent speech delay than group 2. The degree of placental hypoplasia was similar between the two groups. In group 1, the methylation index for the *H19*-DMR was positively correlated with birth length and weight, present height and weight, and placental weight, but with neither birth nor present OFC.

Conclusions/Significance: The results are grossly consistent with the previously reported data, although the frequency of epimutations is lower in the Japanese SRS patients than in the Western European SRS patients. Furthermore, the results provide useful information regarding placental hypoplasia in SRS, clinical phenotypes of the hypomethylated *ARHI*-DMR, and underlying causative factors for idiopathic SRS.

Citation: Fuke T, Mizuno S, Nagai T, Hasegawa T, Horikawa R, et al. (2013) Molecular and Clinical Studies in 138 Japanese Patients with Silver-Russell Syndrome. PLoS ONE 8(3): e60105. doi:10.1371/journal.pone.0060105

Editor: Monica Miozzo, Università degli Studi di Milano, Italy

Received September 7, 2012; **Accepted** February 21, 2013; **Published** March 22, 2013

Funding: This work was funded by Grants-in-Aid for Scientific Research (A) (22249010) and Research (B) (21028026) from the Japan Society for the Promotion of Science (http://www.jsps.go.jp/english/index.html), by Grant for Research on Rare and Intractable Diseases (H24-042) from the Ministry of Health, Labor and Welfare (http://www.mhlw.go.jp/english/), and by Grant for National Center for Child Health and Development (23A-1) (http://www.ncchd.go.jp/English/Englishtop.htm). The funders had no role in study design, data collection and analysis, decision to publish, or preparation of the manuscript.

Competing Interests: The authors have declared that no competing interests exist.

* E-mail: tomogata@hama-med.ac.jp

Introduction

Silver-Russell syndrome (SRS) is a rare congenital developmental disorder characterized by pre- and postnatal growth failure, relative macrocephaly, triangular face, hemihypotrophy, and fifth-finger clinodactyly [1]. Recent studies have shown that epimutation (hypomethylation) of the paternally derived differentially methylated region (DMR) in the upstream of *H19* (*H19*-DMR) on chromosome 11p15.5 and maternal uniparental disomy for chromosome 7 (upd(7)mat) account for ~45% and 5−10% of SRS patients, respectively [1,2]. In this regard, phenotypic assessment has suggested that birth length and weight are more reduced and characteristic body features are more frequent in patients with *H19*-DMR epimutation than in those with upd(7)mat, whereas developmental delay tends to be more

frequent in patients with upd(7)mat than in those with *H19*-DMR epimutation [3,4]. Furthermore, consistent with the notion that imprinted genes play an essential role in placental growth and development [5], placental hypoplasia has been found in both *H19*-DMR epimutation and upd(7)mat [4,6], although comparison of placental weight has not been performed between *H19*-DMR hypomethylation and upd(7)mat. In addition, multilocus hypo- or hypermethylation and positive correlation between methylation index (MI, the ratio of methylated clones) and body and placental sizes have been reported in patients with *H19*-DMR epimutation [4,7–9], and several types of rare genomic alterations have been identified in a few of SRS patients [1,10–12].

Here, we report on molecular and clinical findings in 138 Japanese SRS patients, and discuss on the results obtained in this study.

Patients and Methods

Ethics statement

This study was approved by the Institutional Review Board Committee at the National Center for Child Health and Development. The parents of the affected children and the adult patients who can express an intention by themselves have given written informed consent to participate in this study and to publish their molecular and clinical data.

Patients

This study consisted of 138 Japanese patients (66 males and 72 females) with SRS phenotype aged 0–30 years (median 4.1 years), including 64 previously reported patients (20 patients with variable degrees of *H19*-DMR epimutation, three patients with upd(7)mat, one patient with 46,XY/46,XY,upd(7)mat mosaicism in whom upd(7)mat cells accounted for 91–92% of leukocytes and salivary cells and for 11% of placental tissue, and 40 patients of unknown cause) [4,6,13]. The 138 patients had a normal karyotype in all the ≥50 lymphocytes examined, and satisfied the selection criteria proposed by Netchine et al. [14], i.e., birth length and/or birth weight ≤ –2 standard deviation score (SDS) for gestational age as a mandatory criteria plus at least three of the following five features: (i) postnatal short stature (≤ –2 SDS) at 2 year of age or at the nearest measure available, (ii) relative macrocephaly at birth, i.e., SDS for birth length or birth weight minus SDS for birth occipitofrontal circumference (OFC) ≤ –1.5, (iii) prominent forehead during early childhood, (iv) body asymmetry, and (v) feeding difficulties during early childhood. Birth and present length/height, weight, and OFC were assessed by the gestational/postnatal age- and sex-matched Japanese reference data from the Ministry of Health, Labor, and Welfare and the Ministry of Education, Science, Sports and Culture. Placental weight was assessed by the gestational age-matched Japanese reference data [15]. Clinical features were evaluated by clinicians at different hospitals who participated in this study, using the same clinical datasheet. The SRS patients were classified into three groups by the molecular studies, i.e., those with *H19*-DMR hypomethylation (epimutation) (group 1), those with upd(7)mat (group 2), and the remaining patients (group 3).

Primers and samples

Primers utilized in this study are shown in Table S1. Leukocyte genomic DNA samples were examined in this study.

Methylation analysis

We performed pyrosequencing analysis for the *H19*-DMR encompassing the 6th CTCF (CCCTC-binding factor) binding site that functions as the primary regulator for the monoallelic *IGF2* and *H19* expressions [16–18], using bisulfite treated leukocyte genomic DNA samples of all the 138 patients. The procedure was as described in the manufacturer's instructions (Qiagen, Valencia, CA, USA). In brief, a 279 bp region was PCR-amplified with a primer set (PyF and PyR) for both methylated and unmethylated clones, and a sequence primer (SP) was hybridized to a single-stranded PCR products. Subsequently, the MIs were obtained for four CpG dinucleotides (CG5–CG7 and CG9), using PyroMark Q24 (Qiagen) (the MI for CG8 was not obtained, because the "C" residue of CG8 constitutes a C/T SNP) (Figure 1A). The PyF/PyR and SP were designed by PyroMark Assay Design Software Ver2.0. While the PyF sequence contains a SNP (*rs11564736*) with a mean minor allele frequency of 5% in multiple populations, the minor allele frequency is 0% in the Japanese as well as in the Asian populations (http://browser.1000genomes.org/Homo_sapiens/Variation/Population?db = core;r = 11:2020801–2021801;v = rs11564736;vdb = variation;vf = 7864021). Thus, we utilized this PyF.

We also carried out combined bisulfite restriction analysis (COBRA) for the *H19*-DMR. The methods were as described previously [4]. In short, a 435 bp region was PCR-amplified with a primer set (CoF and CoR) that hybridize to both methylated and unmethylated clones, and MIs were obtained for two CpG dinucleotides (CG5 and CG16) after digestion of the PCR products with methylated allele-specific restriction enzymes (*Hpy*188I and *Afl*III) (Figure 1A).

Thus, we could examine CG5 by both pyrosequencing and COBRA. While we also attempted to analyze CG16 by both methods, it was impossible to design an SP for the analysis of CG16 (although we could design an SP between CG11 and CG12, clear methylation data were not obtained for CG16, probably because of the distance between the SP and CG16).

In addition, we performed COBRA for the KvDMR1 in all the 138 patients (Figure S1A) because of the possibility that epimutation of the KvDMR1 could lead to SRS phenotype via some mechanism(s) such as overexpression of a negative growth regulator *CDKN1C* [19], and for multiple DMRs on various chromosomes in patients in whom relatively large amount of DNA samples were available, as reported previously [4,20,21]. To define the reference ranges of MIs (minimum ~ maximum), 50 control subjects were similarly studied with permission.

To screen upd(7)mat, PCR amplification was performed for the *MEST*-DMR on chromosome 7q32.2 in all the 138 patients, using methylated and unmethylated allele-specific PCR primer sets, as reported previously [6] (Figure 2A). In addition, bisulfite sequencing and direct sequencing for the primer binding sites for the *ARHI*-DMR analysis were performed in a patient (case 13) with an extremely low MI for the *ARHI*-DMR.

Microsatellite analysis

Microsatellite analysis was performed for four loci within a ~4.5 Mb telomeric 11p region (*D11S2071*, *D11S922*, *D11S1318*, and *D11S988*) in patients with hypomethylated *H19*-DMR, to examine the possibility of upd(11p)mat involving the *H19*-DMR. Microsatellite analysis was also carried out for nine loci widely dispersed on chromosome 7 (Table S2) in patients with abnormal methylation patterns of the *MEST*-DMR, to examine the possibility of upd(7)mat and to infer the underlying causes for upd(7)mat, i.e., trisomy rescue, gamete complementation, monosomy rescue, and post-fertilization mitotic error [22]. The methods have been reported previously [4,6].

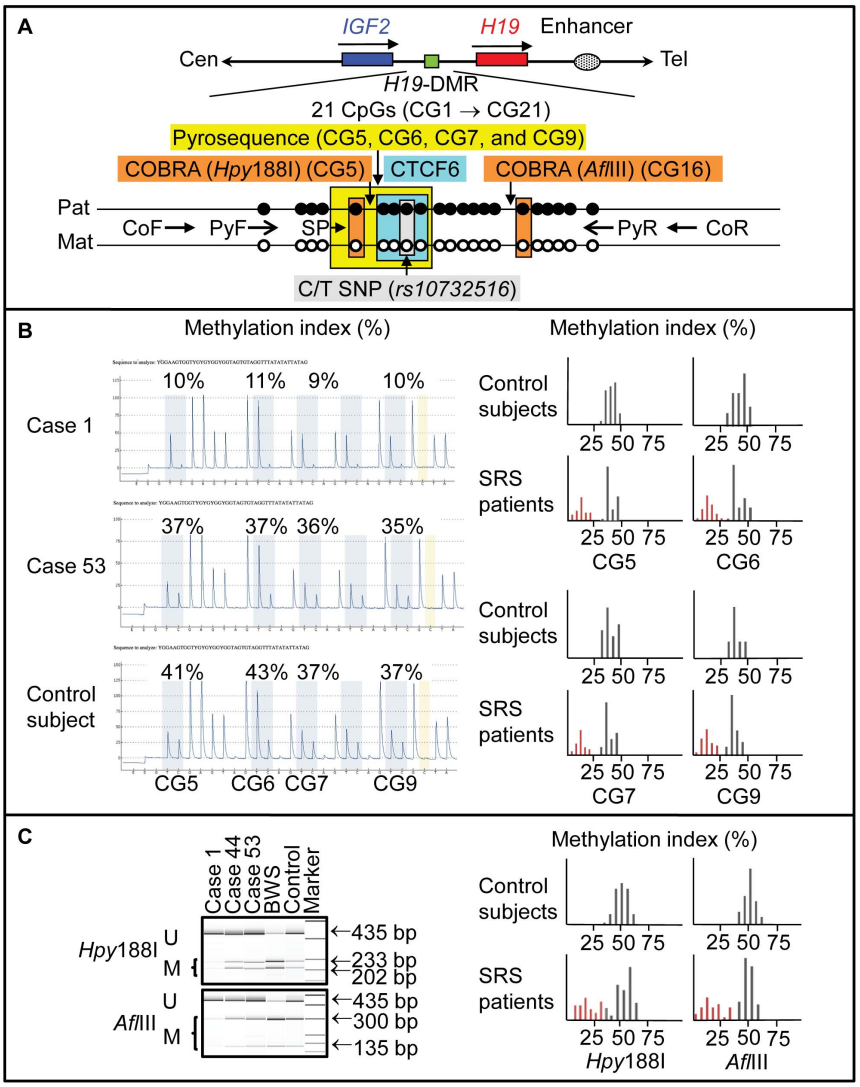

Figure 1. Methylation analysis of the *H19*-DMR, using bisulfite-treated genomic DNA. A. Schematic representation of a segment encompassing 21 CpG dinucleotides (CG1→CG21) within the *H19*-DMR. The cytosine residues at the CpG dinucleotides are usually methylated after paternal transmission (filled circles) and unmethylated after maternal transmission (open circles). The CTCF binding site 6 (CTCF6) is indicated with a blue rectangle; the cytosine residue at CG8 constitutes a C/T SNP (indicated with a gray rectangle). For pyrosequencing analysis, a 279 bp segment was PCR-amplified with PyF & PyR primers, and a sequence primer (SP) was hybridized to a single-stranded PCR products. Subsequently, the MIs were obtained for four CpG dinucleotides (CG5–CG7 and CG9) (indicated with a yellow rectangle). For COBRA, a 435 bp region was PCR-amplified with CoF & CoR primers, and the PCR product was digested with methylated allele-specific restriction enzymes to examine the methylation pattern of CG5 ands CG16 (the PCR products is digested with *Hpy*188I when the cytosine residue at CG5 is methylated and with *Afl*III when the cytosine residue at CG16 is methylated) (indicated with orange rectangles). *IGF2* is a paternally expressed gene, and *H19* is a maternally expressed gene. The stippled ellipse indicates the enhancer for *IGF2* and *H19*. B. Pyrosequencing data. Left part: Representative results indicating the MIs for CG5– CG7 and CG9. CG5– CG7 and CG9 are hypomethylated in case 1, and similarly methylated between case 53 and a control subject. Right part: Histograms showing the distribution of the MIs (the horizontal axis: the methylation index; and the vertical axis: the patient number). Forty-three SRS patients with low MIs are shown in red. C. COBRA data. Left part: Representative findings of PCR products loaded onto a DNA 1000 LabChip (Agilent, Santa Clara, CA, USA) after digestion with *Hpy*188I or *Afl*III. U: unmethylated clone specific bands; M: methylated clone specific bands; and BWS: Beckwith-Wiedemann syndrome patient with upd(11p15)pat. Right part: Histograms showing the distribution of the MIs.
doi:10.1371/journal.pone.0060105.g001

Oligoarray comparative genomic hybridization (CGH)

We performed oligoarray CGH in the 138 SRS patients, using a genomewide 4×180K Agilent platform catalog array and a custom-build high density oligoarray for the 11p15.5, 7p12.2, 12q14, and 17q24 regions where rare copy number variants have been identified in several SRS patients [1,10–12] as well as for the 7q32–qter region involved in the segmental upd(7)mat in four SRS patients [23–25]. The custom-build high density oligoarray contained 3,214 probes for 7p12.2, 434 probes for 7q32, 23,162 probes for 12q14, and 39,518 probes for 17q24, together with ~10,000 reference probes for other chromosomal region (Agilent Technologies, Palo Alto, CA, USA). The procedure was as described in the manufacturer's instructions.

Statistical analysis

After examining normality by χ^2 test, the variables following the normal distribution were expressed as the mean±SD, and those not following the normal distribution were expressed with the

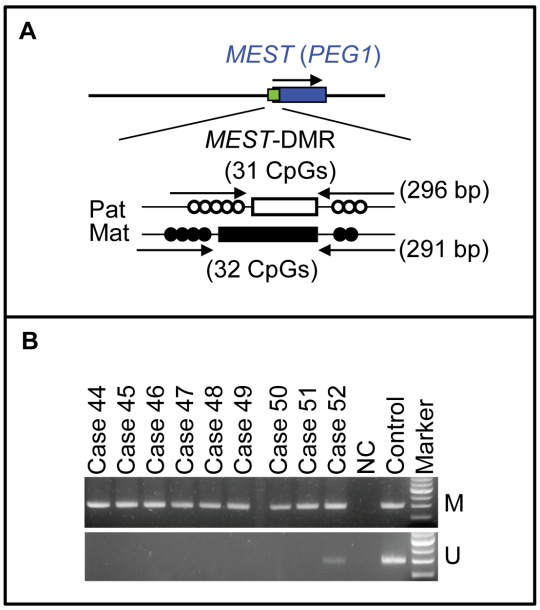

Figure 2. Methylated and unmethylated allele-specific PCR analysis for the *MEST*-DMR. A. Schematic representation of the *MEST*-DMR. The cytosine residues at the CpG dinucleotides are usually unmethylated after paternal transmission (open circles) and methylated after maternal transmission (filled circles). The PCR primers have been designed to hybridize either methylated or unmethylated clones. B. The results of methylation analysis with methylated and unmethylated allele-specific primers.
doi:10.1371/journal.pone.0060105.g002

median and range. Statistical significance of the mean was analyzed by Student's *t*-test or Welch's *t*-test after comparing the variances by *F* test, that of the median by Mann-Whitney's *U*-test, that of the frequency by Fisher's exact probability test, and that of the correlation by Pearson's correlation coefficient after confirming the normality of the variables. $P<0.05$ was considered significant.

Results

Identification of *H19*-DMR hypomethylation

Representative findings are shown in Figure 1B and 1C, and the MIs are summarized in Table 1. Overall, the MIs obtained by the pyrosequencing analysis tended to be lower and distributed more narrowly than those obtained by the COBRA. Despite such difference, the MIs obtained by the pyrosequencing analysis for CG5–CG7 and CG9 and by the COBRA for CG5 and CG16 were invariably below the normal range in the same 43 patients (cases 1–43) (group 1). By contrast, the MIs were almost invariably within the normal range in the remaining 95 patients, while the MIs obtained by the pyrosequencing analysis slightly (1–2%) exceeded the normal range in the same three patients (cases 136–138).

In the 43 cases of group 1, microsatellite analysis for four loci at the telomeric 11p region excluded maternal upd in 14 cases in whom parental DNA samples were available; in the remaining 29 cases, microsatellite analysis identified two alleles for at least one locus, excluding maternal uniparental isodisomy for this region. Furthermore, oligoarray CGH for the chromosome 11p15.5 region showed no copy number alteration such as duplication of maternally derived *H19*-DMR and deletion of paternally derived *H19*-DMR. For the KvDMR1, the MIs of the 138 patients remained within the reference range (Fig. S1B and C).

Table 1. The methylation indices (%) for the *H19*-DMR.

	Cases 1−43	Cases 44−138	Control subjects
Pyrosequencing analysis			
CG5	4–24	35−50	33−48
CG6	5–26	36−53	34−51
CG7	4–24	35−49	30−47
CG9	5–23	34−48	30−46
COBRA			
CG5 (*Hpy*188I)	3.3−35.1	37.8−60.8	36.2−58.5
CG16 (*Afl*III)	4.1−35.0	43.0−59.4	38.7−60.0

The position of examined CpG dinucleotides (CG5–7, CG9, and CG16) is shown in Figure 1A.
COBRA: combined bisulfite restriction analysis.
doi:10.1371/journal.pone.0060105.t001

Identification of upd(7)mat

Methylation analysis for the *MEST*-DMR revealed that unmethylated bands were absent from eight patients and remained faint in a single patient (cases 44–52) (group 2) (Figure 2B). Subsequent microsatellite analysis confirmed upd(7)mat in the eight patients and mosaic upd(7)mat in the remaining one patient, and indicated trisomy rescue or gamete complementation type upd(7)mat in cases 44–48, monosomy rescue or post-fertilization mitotic error type upd(7)mat in cases 49–51, and post-fertilization mitotic error type mosaic upd(7)mat in case 52 (Table S2).

Multiple DMR analysis

We examined 17 autosomal DMRs other than the *H19*-DMR in 14 patients in group 1, four patients in group 2, and 20 patients in group 3, and the *XIST*-DMR in eight female patients in group 1, one female patient in group 2, and five female patients in group 3 (Table S3). The MIs outside the reference ranges were identified in five of 14 examined cases (35.7%) and six of a total of 246 examined DMRs (2.4%) in group 1. In particular, a single case with the mean MI value of 23 obtained by the pyrosequencing analysis for CG5–CG7 and CG9 had an extremely low MI for the *ARHI*-DMR (case 13 of group 1). This extreme hypomethylation was confirmed by bisulfite sequencing, and direct sequencing showed normal sequences of the primer-binding sites, thereby excluding the possibility that such an extremely low MI could be due to insufficient primer hybridization because of the presence of a nucleotide variation within the primer-binding sites (Figure 3). Furthermore, no copy number variation involving the *ARHI*-DMR was identified by CGH analysis using a genomewide catalog array. Consistent with upd(7)mat, three DMRs on chromosome 7 were extremely hypermethylated in four examined cases of group 2. Only a single DMR was mildly hypermethylated in a total of 345 examined DMRs in group 3. The abnormal MIs, except for those for the *H19*-DMR in group 1 and for the three DMRs on chromosome 7 in group 2, were confirmed by three times experiments.

Oligonucleotide array CGH

A ~3.86 Mb deletion at chromosome 17q24 was identified in a single patient (case 73 of group 3) (Figure 4).

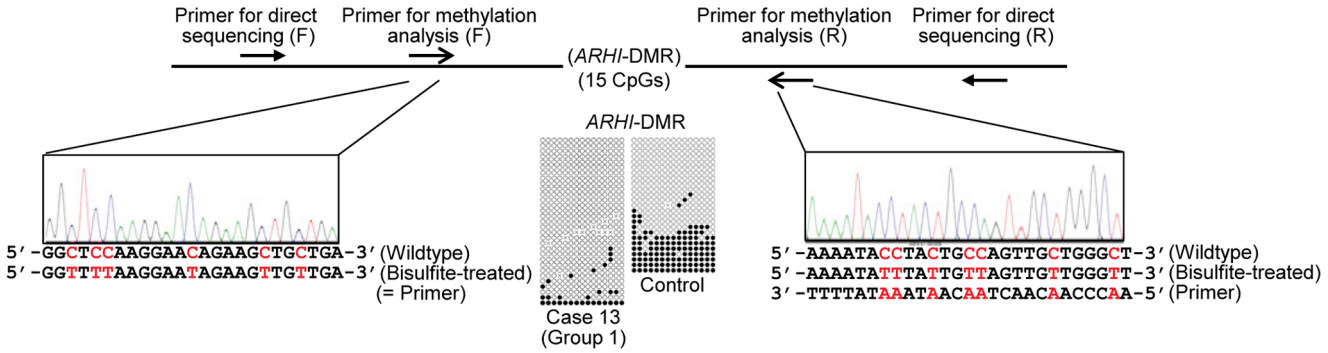

Figure 3. Analysis of the *ARHI*-DMR in case 13. For bisulfite sequencing, each line indicates a single clone, and each circle denotes a CpG dinucleotide; the cytosine residues at the CpG dinucleotides are usually unmethylated after paternal transmission (open circles) and methylated after maternal transmission (filled circles). Electrochromatograms delineate the sequences of the primer binding sites utilized for the methylation analysis.
doi:10.1371/journal.pone.0060105.g003

Epigenotype-phenotype analysis

Clinical findings of SRS patients in groups 1–3 are summarized in Table 2. All the patients met the mandatory criteria, and most patients in each group had severely reduced birth length and weight (both≤–2 SDS). For the five clinical features utilized as scoring system criteria, while 23.2% of patients in group 1 and 22.2% of patients in group 2 exhibited all the five features, there was no patient in group 3 who was positive for all the five features. By contrast, while 39.5% of patients in group 1 and 33.3% of patients in group 2 manifested just three of the five features, 77.6% of patients in group 3 were positive for just three features. In particular, the frequencies of relative macrocephaly at birth and body asymmetry were low in group 3, while those of the remaining three scoring system criteria including prominent forehead during early childhood were similar among groups 1–3.

Phenotypic comparison between groups 1 and 2 revealed that birth length and weight were more reduced and birth OFC was more preserved in group 1 than in group 2, despite comparable gestational age. In the postnatal life, present height and weight became similar between the two groups, whereas present OFC became significantly smaller in group 1 than in group 2. Body asymmetry and brachydactyly were more frequent and speech delay was less frequent in group 1 than in group 2. Placental weight was similar between the two groups, and became more similar after excluding case 52 with mosaic upd(7)mat (see legends for Table 2). Parental age at childbirth was also similar between the two groups. In group 2, placental weight was grossly similar among examined cases, as was parental age at childbirth (see legends for Table 2).

Case 13 with an extremely low MI for the *ARHI*-DMR and case 73 with a cryptic deletion at chromosome 17q24 had no specific phenotype other than SRS-like phenotype (Table S4). However, of the five clinical features utilized as scoring system criteria, all the five features were exhibited by case 13 and just three features were

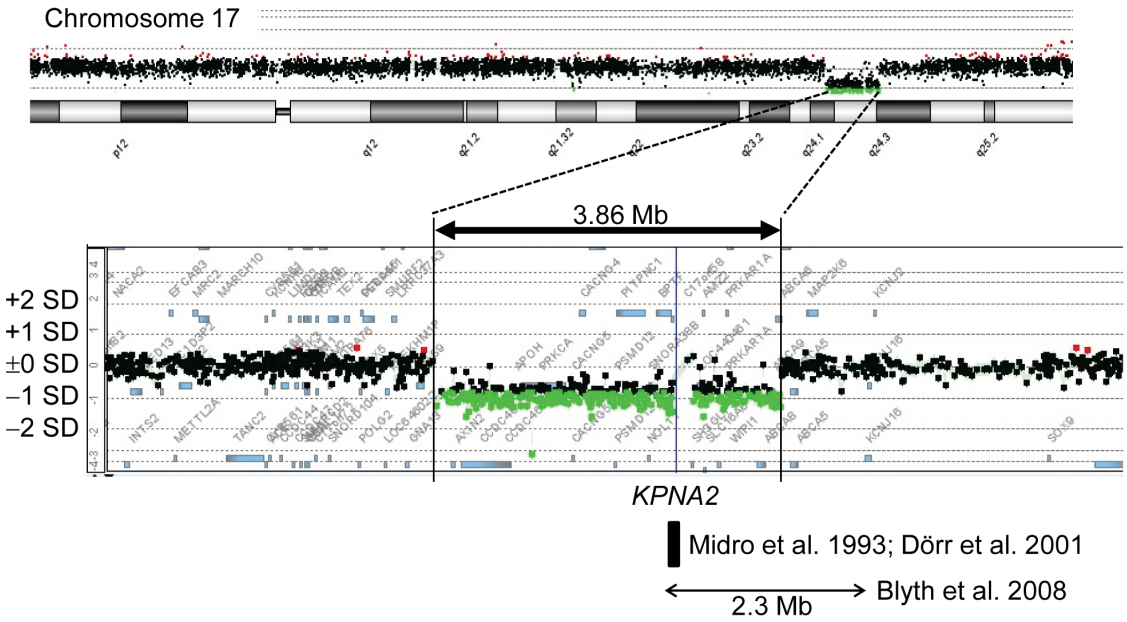

Figure 4. Oligonucleotide array CGH in case 73, showing a ~3.86 Mb deletion at chromosome 17q24. The black, the red, and the green dots denote signals indicative of the normal, the increased(>+0.5), and the decreased (< –1.0) copy numbers, respectively. The horizontal bar with arrowheads indicates a ~2.3 Mb deletion identified in a patient with Carney complex and SRS-like phenotype [44], and the black square represent a ~65 kb segment harboring the breakpoint of a *de novo* translocation 46,XY,t(1;17)(q24;q23–q24) identified in a patient with SRS phenotype [45,46].
doi:10.1371/journal.pone.0060105.g004

Table 2. Phenotypic comparison in three groups of patients with Silver-Russell syndrome.

	H19-DMR hypomethylation	Upd(7)mat	Unknown	*P*-value		
	(Group 1)	(Group 2)	(Group 3)	G1 vs. G2	G1 vs. G3	G2 vs. G3
Patient number	43 (31.2%)	9 (6.5%)	85 (62.0%)			
Mandatory criteria	43/43 (100%)	9/9 (100%)	85/85 (100%)	1.000	1.000	1.000
Scoring system criteria (5/5)	10/43 (23.2%)	2/9 (22.2%)	0/85 (0.00%)	0.965	**1.52×10^{-4}**	**2.58×10^{-2}**
Scoring system criteria (4/5)	16/43 (37.2%)	4/9 (44.4%)	19/85 (22.4%)	0.792	**1.45×10^{-2}**	0.145
Scoring system criteria (3/5)	17/43 (39.5%)	3/9 (33.3%)	66/85 (77.6%)	0.821	**7.17×10^{-4}**	0.161
Gestational age (weeks:days)	38:0 (34:3∼40:0) (n = 36)	38:0 (34:4∼40:0) (n = 9)	37:6 (27:1∼41:4) (n = 65)	0.877	0.120	0.450
BL (SDS)	−4.13±2.01 (n = 31)	−3.18±1.16 (n = 9)	−2.93±1.43 (n = 60)	**2.67×10^{-2}**	**6.69×10^{-5}**	0.619
BW (SDS)	−3.50±0.85 (n = 42)	−2.90±0.64 (n = 9)	−2.71±1.14 (n = 64)	**3.28×10^{-2}**	**5.87×10^{-4}**	0.640
BL≤−2 SDS and/or BW≤−2 SDS*	43/43 (100%)	9/9 (100%)	85/85 (100%)	1.000	1.000	1.000
BL≤−2 SDS and BW≤−2 SDS	39/43 (90.7%)	7/9 (77.8%)	76/85 (89.4%)	0.474	0.821	0.304
BOFC (SDS)	−0.54±1.22 (n = 29)	−1.44±0.47 (n = 9)	−1.92±1.09 (n = 48)	**3.74×10^{-2}**	**1.52×10^{-6}**	0.202
BL (SDS) − BOFC (SDS)	−3.70±2.02 (n = 27)	−1.73±1.20 (n = 9)	−0.943±1.48 (n = 43)	**1.02×10^{-2}**	**3.40×10^{-9}**	0.111
BW (SDS) − BOFC (SDS)	−3.21±1.20 (n = 27)	−1.53±0.57 (n = 9)	−1.04±1.55 (n = 48)	0.326	**7.38×10^{-9}**	0.331
Relative macrocephaly at birth† BL or BW (SDS) − BOFC (SDS)≤−1.5	29/29 (100%)	7/9 (77.8%)	16/45 (35.6%)	0.341	**3.67×10^{-8}**	**2.05×10^{-2}**
Present age (years:months)	4.1 (0:6∼30:6) (n = 31)	4.8 (2:4∼25:2) (n = 9)	4.3 (0:1∼18:6) (n = 60)	0.437	0.813	0.335
PH (SDS)	−3.58±1.65 (n = 35)	−3.77±1.13 (n = 9)	−3.17±1.50 (n = 61)	0.757	0.218	0.253
PH≤−2 SDS (≥2 years)†	29/35 (82.5%)	8/9 (88.9%)	52/61 (85.2%)	0.760	0.758	0.772
PW (SDS)	−3.15±1.16 (n = 32)	−2.77±0.76 (n = 9)	−2.77±1.34 (n = 59)	0.362	0.144	0.968
POFC (SDS)	−1.16±1.18 (n = 21)	−0.01±0.91 (n = 9)	−1.81±1.57 (n = 35)	**2.01×10^{-3}**	0.107	**3.08×10^{-3}**
PH (SDS) − POFC (SDS)	−2.47±1.63 (n = 16)	−3.62±1.38 (n = 8)	−1.55±1.82 (n = 35)	0.103	**4.39×10^{-2}**	**1.64×10^{-2}**
PW (SDS) − POFC (SDS)	−2.84±1.31 (n = 21)	−2.69±1.36 (n = 9)	−1.08±1.71 (n = 35)	0.782	**2.54×10^{-2}**	**1.90×10^{-4}**
Relative macrocephaly at present PH or PW (SDS) − POFC (SDS)≤−1.5	20/21 (95.2%)	8/8 (100%)	29/43 (67.4%)	0.223	**4.77×10^{-3}**	0.156
Triangular face during early childhood	42/43 (97.7%)	8/9 (88.9%)	65/65 (100%)	0.442	0.0773	**5.98×10^{-3}**
Prominent forehead during early childhood†	31/37 (83.8%)	7/9 (100%)	41/53 (77.4%)	0.200	0.456	0.978
Ear anomalies	14/35 (40.0%)	3/9 (33.3%)	15/55 (27.3%)	0.717	0.290	0.823
Irregular teeth	12/26 (46.2%)	4/9 (44.4%)	12/45 (26.7%)	0.930	0.0968	0.291
Body asymmetry†	30/37 (81.1%)	3/9 (33.3%)	19/59 (32.2%)	**4.77×10^{-3}**	**3.51×10^{-6}**	0.947
Clinodactyly	29/37 (78.4%)	5/9 (55.6%)	50/58 (86.2%)	0.167	0.323	**2.68×10^{-2}**
Brachydactyly	30/38 (78.9%)	2/9 (22.2%)	34/56 (60.7%)	1.16×10^{-3}	0.0642	**3.24×10^{-2}**
Syndactyly	3/36 (8.3%)	0/9 (0.00%)	3/52 (5.77%)	0.375	0.641	0.464
Simian crease	4/26 (15.4%)	2/7 (28.6%)	6/49 (12.2%)	0.429	0.705	0.252
Muscular hypotonia	17/32 (53.1%)	5/9 (55.6%)	12/50 (24.0%)	0.898	**7.49×10^{-3}**	0.0564
Developmental delay	18/37 (48.6%)	6/9 (66.7%)	25/54 (46.3%)	0.337	0.826	0.262
Speech delay	8/31 (25.8%)	6/9 (66.7%)	18/43 (41.9%)	**2.55×10^{-2}**	0.156	0.179
Feeding difficulty†	16/34 (47.1%)	6/9 (66.7%)	25/51 (49.0%)	0.301	0.860	0.333
Placental weight (SDS)	−2.10±0.74 (n = 14)	−1.72 ± 0.74 (n = 6)[a]	−1.02±0.86 (n = 18)	0.312	**4.12×10^{-3}**	**8.24×10^{-3}**
Paternal age at childbirth (years:months)	32:0 (19:0∼52:0) (n = 24)	35:0 (27:0∼48:0) (n = 9)	32:0 (25:0∼46:0) (n = 45)	0.223	1.00	0.105
Maternal age at childbirth (years:months)	32:0 (19:0∼43:0) (n = 25)	33:0 (25:0∼42:0) (n = 9)[b]	30:0 (22:0∼43:0) (n = 46)	0.275	0.765	0.117

BL: birth length; BW: birth weight; BOFC: birth occipitofrontal circumference; PH: present height; PW: present weight; POFC: present occipitofrontal circumference, and SDS: standard deviation score.

For body features, the denominators indicate the number of patients examined for the presence or absence of each feature, and the numerators represent the number of patients assessed to be positive for that feature.

*Mandatory criteria and †five clinical features utilized as selection criteria for Silver-Russell syndrome proposed by Netchine et al. [14].

Significant *P*-values(<0.05) are boldfaced.

[a]Placental weight SDS is −1.68, −2.55, −2.24, −1.12, −2.14 and −0.60 in case 46, 47, 49, 50, 51 and 52, respectively; the placental weight SDS is −1.95±0.57 in five cases except for case 52 with mosaic upd(7)mat.

[b]Maternal childbearing age is 32, 32, 33, 42, 32, 34, 33, 25 and 36 years in case 44–52, respectively.

doi:10.1371/journal.pone.0060105.t002

manifested by case 73. In addition, cases 136–138 with slightly elevated MIs for CG5–CG7 and CG9, and cases with multilocus methylation abnormalities, had no particular phenotype other than SRS-compatible clinical features.

Correlation analysis

In group 1, the mean value of the MIs for CG5–CG7 and CG9 obtained by pyrosequencing analysis was positively correlated with the birth length and weight, the present height and weight, and the placental weight, but with neither the birth nor the present OFC (Table 3). Such correlations with the growth parameters were grossly similar but somewhat different for the MIs obtained by COBRA (Table S5). Furthermore, the placental weight was positively correlated with the birth weight and length, but not with the birth OFC. Such positive correlations were not found in groups 2 and 3.

Discussion

The present study identified hypomethylation of the *H19*-DMR and upd(7)mat in 31.2% and 6.5% of 138 Japanese SRS patients, respectively. In this regard, the normal KvDMR1 methylation patterns indicate that the aberrant methylation in 43 cases of group 1 is confined to the *H19*-DMR. Furthermore, oligoarray CGH excludes copy number variants involving the *H19*-DMR, and microsatellite analysis argues against segmental maternal isodisomy that could be produced by post-fertilization mitotic error [26]. These findings imply that the *H19*-DMR hypomethylation is due to epimutation (hypomethylation of the normally methylated *H19*-DMR of paternal origin).

The frequency of epimutations detected in this study is lower than that reported in Western European SRS patients [1,2,14], although the frequency of upd(7)mat is grossly similar between the two populations [2,11,14,27,28]. In this context, it is noteworthy that, of the five scoring system criteria, the frequencies of relative macrocephaly at birth and body asymmetry were low in group 3, while those of the remaining three scoring system criteria were similar among groups 1–3. Since relative macrocephaly and body asymmetry are characteristic of *H19*-DMR epimutation, the lack of these two features in a substantial fraction of cases in group 3 would primarily explain the low frequency of *H19*-DMR epimutations in this study. In group 3, furthermore, the low prevalence of relative macrocephaly at birth appears to be discordant with the high prevalence of prominent forehead during early childhood. Since relative macrocephaly was evaluated by an objective method (SDS for birth length or birth weight minus SDS for birth OFC$\leq$–1.5) and prominent forehead was assessed by a subjective impression of different clinicians, it is recommended to utilize relative macrocephaly as a more important and reliable feature in the scoring system than prominent forehead. In addition, the difference in the ethnic group might also be relevant to the low frequency of *H19*-DMR epimutations in this study.

Table 3. Correlation analyses in patients with *H19*-DMR hypomethylations.

Parameter 1	Parameter 2	*r*	*P*-value
Methylation index (%)* vs.	Birth length (SDS)	0.647	**6.70×10^{-3}**
	Birth weight (SDS)	0.590	**7.80×10^{-3}**
	Birth OFC (SDS)	0.190	0.498
	Present height (SDS)	0.612	**5.33×10^{-3}**
	Present weight (SDS)	0.605	**7.81×10^{-3}**
	Present OFC (SDS)	–0.166	0.647
	Placental weight (SDS)	0.809	**8.30×10^{-3}**
Placental weight (SDS) vs.	Birth weight (SDS)	0.717	**8.64×10^{-3}**
	Birth length (SDS)	0.636	**2.63×10^{-2}**
	Birth OFC (SDS)	0.400	0.198

SDS: standard deviation score; and OFC: occipitofrontal circumference.
*The mean value of MIs for CG5, CG6, CG7, and CG9 obtained by pyrosequencing analysis.
Significant *P*-values($<$0.05) are boldfaced.
doi:10.1371/journal.pone.0060105.t003

Epigenotype-phenotype correlations in this study are grossly similar to those previously reported in Western European SRS patients [1–3]. Cases 1–43 in group 1 with *H19*-DMR epimutation had more reduced birth weight and length, more preserved birth OFC and more reduced present OFC, more frequent body features, and less frequent speech delay than case 44–52 in group 2 with upd(7)mat, although the difference in the prevalence of somatic features appears to be less remarkable in this study than in the previous studies [3,4]. This provides further support for the presence of relatively characteristic clinical features in *H19*-DMR epimutation and upd(7)mat [1–3]. In this context, previous studies have indicated biallelic *IGF2* expression in the human fetal choroid plexus, cerebellum, and brain, and monoallelic *IGF2* expression in the adult brain, while the precise brain tissue(s) with such a unique expression pattern remains to be clarified [29,30,31]. This may explain why the birth OFC is well preserved and the present OFC is reduced in group 1. However, since the difference in present OFC between groups 1 and 2 is not necessarily significant in the previous studies [32], the postnatal OFC growth awaits further investigations.

Placental weight was similarly reduced in groups 1 and 2. Thus, placental weight is unlikely to represent an indicator for the discrimination between the two groups, although the present data provide further support for imprinted genes being involved in placental growth, with growth-promoting effects of *PEGs* and growth-suppressing effects of *MEGs* [5,6]. It should be pointed out, however, that the placental hypoplasia could be due to some other genetic or environmental factor(s). In particular, while placental weight was apparently similar among cases of group 2, possible confined placental mosaicism [33,34] with trisomy for chromosome 7 may have exerted some effects on placental growth in cases with trisomy rescue type upd(7)mat.

Correlation analysis would imply that the *IGF2* expression level, as reflected by the MI of the *H19*-DMR, plays a critical role in the determination of pre- and postnatal body (stature and weight) and placental growth in patients with *H19*-DMR epimutation. Since the placental weight was positively correlated with the birth length and weight, the reduced *IGF2* expression level appears to have a similar effect on the body and the placental growth. Furthermore, the lack of correlations between the MI and birth and present OFC and between placental weight and birth OFC would be compatible with the above mentioned *IGF2* expression pattern in the central nervous system [29]. Although the MI would also reflect the *H19* expression level, this would not have a major growth effect. It has been implicated that *H19* functions as a tumor suppressor [35,36].

Multilocus analysis revealed co-existing hyper- and hypomethylated DMRs predominantly in cases of group 1, with frequencies of 35.7% of examined patients and 2.4% of examined DMRs. The results are grossly consistent with the previous data indicating that co-existing abnormal methylation patterns of DMRs are almost exclusively identified in patients with *H19*-DMR epimutation with frequencies of 9.5$\sim$30.0% of analyzed patients and 1.8$\sim$5.2% of a

total of analyzed DMRs [7–9]. Notably, the co-existing methylation abnormalities were predominantly observed as mild hypermethylations of maternally methylated DMRs and were restricted to a single DMR or two DMRs in patients with multilocus abnormalities. Such findings are obviously inexplicable not only by assuming a *ZFP57* mutation that is known to cause severely abnormal methylation patterns of multiple DMRs or a *ZAC1* mutation that may affect methylation patterns of multiple DMRs [37–39], but also by assuming defective maintenance of methylation in the postzygotic period [7]. Thus, some factor(s) susceptible to the co-occurrence of hypomethylation of the *H19*-DMR and hypermethylation of other DMR(s) might be operating during a gametogenic or postzygotic period in cases with *H19*-DMR epimutation.

The patients with multilocus methylation abnormalities had no specific clinical features other than SRS-compatible phenotype. Previous studies have also indicated grossly similar SRS-like phenotype between patients with monolocus and multilocus hypomethylations [7], although patients with multilocus hypomethylation occasionally have apparently severe clinical phenotype [7]. These findings would argue for the notion that the *H19*-DMR epimutation has an (epi)dominant clinical effect. Indeed, *H19*-DMR hypomethylation has led to SRS-like phenotype in a patient with parthenogenetic chimerism/mosaicism [21], whereas *H19*-DMR hypermethylation has resulted in Beckwith-Wiedemann syndrome-like phenotype in patients with androgenetic mosaicism [40].

An extremely hypomethylated *ARHI*-DMR was found in case 13. In this regard, it is known that *ARHI* with a potentially cell growth suppressor function is normally expressed from paternally inherited chromosome with unmethylated *ARHI*-DMR [41]. Indeed, hypermethylation of the *ARHI*-DMR, which is predicted to result in reduced expression of *ARHI*, has been identified as a tumorigenic factor for several cancers with an enhanced cell growth function [42,43]. Thus, it is possible that hypomethylation of the *ARHI*-DMR has led to overexpression of *ARHI*, contributing to the development of typical SRS phenotype in the presence of a low but relatively preserved MI of the *H19*-DMR in case 13.

Oligonucleotide array CGH identified a ~3.86 Mb deletion at chromosome 17q24 in case 73 of group 3. This provides further support for the presence of rare copy number variants in several SRS patients and the relevance of non-imprinted gene(s) to the development of SRS [10]. Interestingly, the microdeletion overlap with that identified in a patient with Carney complex and SRS-like features [44], and the overlapping region encompasses a ~65 kb segment defining the breakpoint of a *de novo* reciprocal translocation involving 17q23–q24 in a patient with SRS-like phenotype (Figure 4) [45,46]. Furthermore, the translocation breakage has affected *KPNA2* involved in the nuclear transport of proteins [46–48]. Thus, *KPNA2* has been regarded as a candidate gene for SRS, although mutation analysis of *KPNA2* has failed to detect a disease-causing mutation in SRS patients [49].

Lastly, it would be worth discussing on the comparison between pyrosequencing analysis and COBRA. Since the same 43 patients were found to have low MIs by both analyses, this implies that both methods can be utilized as a diagnostic tool. While the distribution of the MIs was somewhat different between the two methods, this would primarily be due to the difference in the employed methods such as the hybridization efficiency of utilized primers. Importantly, pyrosequencing analysis was capable of studying plural CpG dinucleotides at the CTCF6 binding site, whereas COBRA examined only single CpG dinucleotides outside the CTCF6 binding site. Thus, the MIs obtained by pyrosequencing analysis would be more accurate than those obtained by COBRA in terms of *IGF2* expression levels, and this would underlie the reasonable correlations of MIs yielded by pyrosequencing analysis with body and placental growth parameters.

In summary, the present study provides useful information for the definition of molecular and clinical findings in SRS. However, several matters still remain to be elucidated, including underlying mechanisms in SRS patients with no *H19*-DMR epimutation or upd(7)mat and the DMR(s) and imprinted gene(s) responsible for the development of SRS in patients with upd(7)mat. Furthermore, while advanced maternal age at childbirth has been shown to be a predisposing factor for the development of upd(15)mat because of increased non-disjunction at meiosis 1 [50], such studies remain fragmentary for upd(7)mat, primarily because of the relative paucity of upd(7)mat. Further studies will permit a better characterization of SRS.

Supporting Information

Figure S1 Methylation analysis of the KvDMR1 using COBRA. A. Schematic representation of the KvDMR1. A 326 bp region harboring 24 CpG dinucleotides was studied. The cytosine residues at the CpG dinucleotides are usually methylated after paternal transmission (filled circles) and unmethylated after maternal transmission (open circles); after bisulfite treatment, this region is digested with *Hpy*188I when the cytosine at the 5th CpG dinucleotide (indicated with a green rectangle) is methylated and with *Eci*I when the cytosines at the 22nd CpG dinucleotide (indicated with a pink rectangle) is methylated. *KCNQ1OT1* is a paternally expressed gene, and *KCNQ1* and *CDKN1C* are maternally expressed genes. B. Representative COBRA results. U: unmethylated clone specific bands; M: methylated clone specific bands; and BWS: Beckwith-Wiedemann syndrome patient with upd(11p15)pat. C. Histograms showing the distribution of the MIs (the horizontal axis: the methylation index; and the vertical axis: the patient number).
(TIF)

Table S1 Primers utilized in the methylation analysis and microsatellite analysis.
(XLS)

Table S2 The results of microsatellite analysis.
(XLSX)

Table S3 Methylation indices for multiple differetially methylated resions (DMRs) obtained by COBRA in 38 patients with Silver-Russell syndrome.
(XLSX)

Table S4 Clinical findings in two unique patients.
(DOC)

Table S5 Correlation analyses in patients with H19-DMR hypomethylations.
(DOC)

Acknowledgments

We would like to thank the following doctors for providing us with blood samples and clinical data: Toshio Yamazaki, Yukihiro Hasegawa, Daisuke Ariyasu, Michiko Hayashidani, Hiroshi Yoshihashi, Tomoki Kosho, Rika Kosaki, Yasuhiro Naiki, Hideki Fujita, Aya Yamashita, Katsuhiro Maeyama, Sayu Omori, Takashi Koike, Makoto Ono, Sachiko Kitanaka, Jun Mori, Shinichiro Miyagawa, Masamichi Ogawa, Toshiaki Tanaka, Naomi Hizuka, Yoko Fujimoto, Zenro Kizaki, Fumio Katsushima, Takashi Iwamoto, Wakako Yamamoto, Hotaka Kamasaki, Shun Soneda, Takahiro Tajima, Yoriko Watanabe, Kanako Ishii, Noriko Kinoshita, Tohjyu Tanaka, Eriko Nishi, Tohru Yorifuji, Yoshio Makita, Yoshinobu Honda, Junko Tsubaki, Yoko Shimabukuro, Yoko Hiraki, Kazushige

Dobashi, Kazumichi Onigata, Hisaaki Kabata, Shigeki Ishii, Kimiko Taniguchi, and Masaoki Sugita. We are also grateful to Drs. Kyoko Tanabe and Kentaro Matsuoka for their technical assistance.

Author Contributions

Conceived and designed the experiments: TF KY TO. Performed the experiments: TF KN CT S. Sano K. Matsubara MK KY. Analyzed the data: TF KN KH KY. Contributed reagents/materials/analysis tools: SM TN TH RH YM K. Muroya TK CN S. Sato TO. Wrote the paper: TO.

References

1. Eggermann T (2010) Russell-Silver syndrome. Am J Med Genet C Semin Med Genet 154C: 355–364.
2. Binder G, Begemann M, Eggermann T, Kannenberg K (2011) Silver-Russell syndrome. Best Pract Res Clin Endocrinol Metab 25: 153–160.
3. Wakeling EL, Amero SA, Alders M, Bliek J, Forsythe E, et al. (2010) Epigenotype-phenotype correlations in Silver-Russell syndrome. J Med Genet 47: 760–768.
4. Yamazawa K, Kagami M, Nagai T, Kondoh T, Onigata K, et al. (2008) Molecular and clinical findings and their correlations in Silver-Russell syndrome: implications for a positive role of IGF2 in growth determination and differential imprinting regulation of the IGF2-H19 domain in bodies and placentas. J Mol Med (Berl) 86: 1171–1181.
5. Fowden AL, Sibley C, Reik W, Constancia M (2006) Imprinted genes, placental development and fetal growth. Horm Res 65 Suppl 3: 50–58.
6. Yamazawa K, Kagami M, Ogawa M, Horikawa R, Ogata T (2008) Placental hypoplasia in maternal uniparental disomy for chromosome 7. Am J Med Genet A 146A: 514–516.
7. Azzi S, Rossignol S, Steunou V, Sas T, Thibaud N, et al. (2009) Multilocus methylation analysis in a large cohort of 11p15-related foetal growth disorders (Russell Silver and Beckwith Wiedemann syndromes) reveals simultaneous loss of methylation at paternal and maternal imprinted loci. Hum Mol Genet 18: 4724–4733.
8. Turner CL, Mackay DM, Callaway JL, Docherty LE, Poole RL, et al. (2010) Methylation analysis of 79 patients with growth restriction reveals novel patterns of methylation change at imprinted loci. Eur J Hum Genet 18: 648–655.
9. Hiura H, Okae H, Miyauchi N, Sato F, Sato A, et al. (2012) Characterization of DNA methylation errors in patients with imprinting disorders conceived by assisted reproduction technologies. Hum Reprod 27: 2541–2548.
10. Abu-Amero S, Monk D, Frost J, Preece M, Stanier P, et al. (2008) The genetic aetiology of Silver-Russell syndrome. J Med Genet 45: 193–199.
11. Hitchins MP, Stanier P, Preece MA, Moore GE (2001) Silver-Russell syndrome: a dissection of the genetic aetiology and candidate chromosomal regions. J Med Genet 38: 810–819.
12. Spengler S, Schönherr N, Binder G, Wollmann HA, Fricke-Otto S, et al. (2010) Submicroscopic chromosomal imbalances in idiopathic Silver-Russell syndrome (SRS): the SRS phenotype overlaps with the 12q14 microdeletion syndrome. J Med Genet 47: 356–360.
13. Fuke-Sato T, Yamazawa K, Nakabayashi K, Matsubara K, Matsuoka K, et al. (2012) Mosaic upd(7)mat in a patient with Silver-Russell syndrome. Am J Med Genet A 158A: 465–468.
14. Netchine I, Rossignol S, Dufourg MN, Azzi S, Rousseau A, et al. (2007) 11p15 imprinting center region 1 loss of methylation is a common and specific cause of typical Russell-Silver syndrome: clinical scoring system and epigenetic-phenotypic correlations. J Clin Endocrinol Metab 92: 3148–3154.
15. Kagami M, Yamazawa K, Matsubara K, Matsuo N, Ogata T (2008) Placentomegaly in paternal uniparental disomy for human chromosome 14. Placenta 29: 760–761.
16. Bell AC, Felsenfeld G (2000) Methylation of a CTCF-dependent boundary controls imprinted expression of the Igf2 gene. Nature 405: 482–485.
17. Hark AT, Schoenherr CJ, Katz DJ, Ingram RS, Levorse JM, et al. (2000) CTCF mediates methylation-sensitive enhancer-blocking activity at the H19/Igf2 locus. Nature 405: 486–489.
18. Takai D, Gonzales FA, Tsai YC, Thayer MJ, Jones PA (2001) Large scale mapping of methylcytosines in CTCF-binding sites in the human H19 promoter and aberrant hypomethylation in human bladder cancer. Hum Mol Genet 10: 2619–2626.
19. Fisher AM, Thomas NS, Cockwell A, Stecko O, Kerr B, et al. (2002) Duplications of chromosome 11p15 of maternal origin result in a phenotype that includes growth retardation. Hum Genet 111: 290–296.
20. Brena RM, Auer H, Kornacker K, Hackanson B, Raval A, et al. (2006) Accurate quantification of DNA methylation using combined bisulfite restriction analysis coupled with the Agilent 2100 Bioanalyzer platform. Nucleic Acids Res 34: e17.
21. Yamazawa K, Nakabayashi K, Kagami M, Sato T, Saitoh S, et al. (2010) Parthenogenetic chimaerism/mosaicism with a Silver-Russell syndrome-like phenotype. J Med Genet 47: 782–785.
22. Shaffer LG, Agan N, Goldberg JD, Ledbetter DH, Longshore JW, et al. (2001) American College of Medical Genetics statement on diagnostic testing for uniparental disomy. Genet Med 3: 206–211.
23. Hannula K, Lipsanen-Nyman M, Kontiokari T, Kere J (2001) A narrow segment of maternal uniparental disomy of chromosome 7q31-qter in Silver-Russell syndrome delimits a candidate gene region. Am J Hum Genet 68: 247–253.
24. Eggermann T, Schonherr N, Jager S, Spaich C, Ranke MB, et al. (2008) Segmental maternal UPD(7q) in Silver-Russell syndrome. Clin Genet 74: 486–489.
25. Begemann M, Spengler S, Kordass U, Schroder C, Eggermann T (2012) Segmental maternal uniparental disomy 7q associated with DLK1/GTL2 (14q32) hypomethylation. Am J Med Genet A 158A: 423–428.
26. Yamazawa K, Ogata T, Ferguson-Smith AC (2010) Uniparental Disomy and Human Disease: An Overview. Am J Med Genet C 154C: 329–334.
27. Gicquel C, Rossignol S, Cabrol S, Houang M, Steunou V, et al. (2005) Epimutation of the telomeric imprinting center region on chromosome 11p15 in Silver-Russell syndrome. Nat Genet 37: 1003–1007.
28. Bliek J, Terhal P, van den Bogaard MJ, Maas S, Hamel B, et al. (2006) Hypomethylation of the H19 gene causes not only Silver-Russell syndrome (SRS) but also isolated asymmetry or an SRS-like phenotype. Am J Hum Genet 78: 604–614.
29. Ulaner GA, Yang Y, Hu JF, Li T, Vu TH, et al. (2003) CTCF binding at the insulin-like growth factor-II (IGF2)/H19 imprinting control region is insufficient to regulate IGF2/H19 expression in human tissues. Endocrinology 144: 4420–4426.
30. Pham NV, Nguyen MT, Hu JF, Vu TH, Hoffman AR (1998) Dissociation of IGF2 and H19 imprinting in human brain. Brain Res 810: 1–8.
31. Albrecht S, Waha A, Koch A, Kraus JA, Goodyer CG, et al. (1996) Variable imprinting of H19 and IGF2 in fetal cerebellum and medulloblastoma. J Neuropathol Exp Neural 55: 1270–1276.
32. Kotzot D (2008) Maternal uniparental disomy 7 and Silver-Russell syndrome - clinical update and comparison with other subgroups. Eur J Med Genet 51: 444–451.
33. Kotzot D, Balmer D, Baumer A, Chrzanowska K, Hamel BC, et al. (2000) Maternal uniparental disomy 7-review and further delineation of the phenotype. Eur J Pediatr 159: 247–256.
34. Robinson WP (2000) Mechanisms leading to uniparental disomy and their clinical consequences. Bioessays 22: 452–459.
35. Hao Y, Crenshaw T, Moulton T, Newcomb E, Tycko B (1993) Tumour-suppressor activity of H19 RNA. Nature 365: 764–767.
36. Juan V, Crain C, Wilson C (2000) Evidence for evolutionarily conserved secondary structure in the H19 tumor suppressor RNA. Nucleic Acids Res 28: 1221–1227.
37. Arima T, Kamikihara T, Hayashida T, Kato K, Inoue T, et al. (2005) ZAC, LIT1 (KCNQ1OT1) and p57KIP2 (CDKN1C) are in an imprinted gene network that may play a role in Beckwith-Wiedemann syndrome. Nucleic Acids Res 33: 2650–2660.
38. Varrault A, Gueydan C, Delalbre A, Bellmann A, Houssami S, et al. (2006) Zac1 regulates an imprinted gene network critically involved in the control of embryonic growth. Dev Cell 11: 711–722.
39. Quenneville S, Verde G, Corsinotti A, Kapopoulou A, Jakobsson J, et al. (2011) In embryonic stem cells, ZFP57/KAP1 recognize a methylated hexanucleotide to affect chromatin and DNA methylation of imprinting control regions. Mol Cell 44: 361–372.
40. Yamazawa K, Nakabayashi K, Matsuoka K, Masubara K, Hata K, et al. (2011) Androgenetic/biparental mosaicism in a girl with Beckwith-Wiedemann syndrome-like and upd(14)pat-like phenotypes. J Hum Genet 56: 91–93.
41. Huang J, Lin Y, Li L, Qing D, Teng XM, et al. (2009) ARHI, as a novel suppressor of cell growth and downregulated in human hepatocellular carcinoma, could contribute to hepatocarcinogenesis. Mol Carcinog 48: 130–140.
42. Feng W, Marquez RT, Lu Z, Liu J, Lu KH, et al. (2008) Imprinted tumor suppressor genes ARHI and PEG3 are the most frequently down-regulated in human ovarian cancers by loss of heterozygosity and promoter methylation. Cancer 112: 1489–1502.
43. Tang HL, Hu YQ, Qin XP, Jazag A, Yang H, et al. (2012) Aplasia ras homolog member I is downregulated in gastric cancer and silencing its expression promotes cell growth in vitro. J Gastroenterol Hepatol 27: 1395–1404.
44. Blyth M, Huang S, Maloney V, Crolla JA, Karen Temple I (2008) A 2.3 Mb deletion of 17q24.2-q24.3 associated with 'Carney Complex plus'. Eur J Med Genet 51: 672–678.
45. Midro AT, Debek K, Sawicka A, Marcinkiewicz D, Rogowska M (1993) Second observation of Silver-Russel syndrome in a carrier of a reciprocal translocation with one breakpoint at site 17q25. Clin Genet 44: 53–55.
46. Dörr S, Midro AT, Farber C, Giannakudis J, Hansmann I (2001) Construction of a detailed physical and transcript map of the candidate region for Russell-Silver syndrome on chromosome 17q23-q24. Genomics 71: 174–181.
47. Cuomo CA, Kirch SA, Gyuris J, Brent R, Oettinger MA (1994) Rch1, a protein that specifically interacts with the RAG-1 recombination-activating protein. Proc Natl Acad Sci U S A 91: 6156–6160.

48. Weis K, Mattaj IW, Lamond AI (1995) Identification of hSRP1 alpha as a functional receptor for nuclear localization sequences. Science 268: 1049–1053.
49. Dörr S, Schlicker M, Hansmann I (2001) Genomic structure of karyopherin alpha2 (KPNA2) within a low-copy repeat on chromosome 17q23-q24 and mutation analysis in patients with Russell-Silver syndrome. Hum Genet 109: 479–486.
50. Matsubara K, Murakami N, Nagai T, Ogata T (2011) Maternal age effect on the development of Prader-Willi syndrome resulting from upd(15)mat through meiosis 1 errors. J Hum Genet 56: 566–571.

ARTICLE

ABSTRACT

Fibrodysplasia ossificans progressiva (FOP) is a rare disease characterized by postnatal heterotopic ossification (HO). When HO affects the masticatory muscles, mouth opening becomes restricted. This paper presents the changes in facial morphology and occlusion of a patient with FOP who was followed from the age of 8 to age 21. At the initial examination, he had a severely protruded maxilla and Angle Class II Division 1 malocclusion. His mouth opening was restricted (5.0 mm). He had a large overjet and this enabled him to clean his teeth and to eat. Orthodontic correction was not planned, and his facial growth was closely followed with attention to his oral hygiene. The maxillary protrusion and a low mandibular plane angle became more prominent as the patient aged. His mandible rotated in a counterclockwise direction. His molars had delayed eruption or were impacted and seven were extracted. His mouth opening increased slightly and his oral hygiene improved to excellent.

KEY WORDS: fibrodysplasia ossificans progressiva (FOP), heterotopic ossification, facial morphology, occlusion, growth

Facial morphology and occlusion of a patient with fibrodysplasia ossificans progressiva (FOP): a case report

Takafumi Susami, DDS, PhD;[1]* Yoshiyuki Mori, DDS, PhD;[1] Kazumi Tamura;[2] Kazumi Ohkubo, DDS, PhD;[3] Kouhei Nagahama, DDS, PhD;[4] Naoko Takahashi, DDS;[4] Natsuko Uchino, DDS;[4] Kiwako Uwatoko, DDS;[4] Nobuhiko Haga, MD, PhD;[5] Tsuyoshi Takato, MD, PhD[6]

[1]Associate Professor; [2]Oral Hygienist; [3]Assistant Professor; [4]Orthodontist—Department of Oral-Maxillofacial Surgery, Dentistry and Orthodontics; [5]Professor, Department of Rehabilitation Medicine; [6]Professor, Department of Oral-Maxillofacial Surgery, Dentistry and Orthodontics—The University of Tokyo Hospital, Tokyo, Japan.
*Corresponding author e-mail: susami-ora@h.u-tokyo.ac.jp

Spec Care Dentist 32(4): 165-170, 2012

Introduction

Fibrodysplasia ossificans progressiva (FOP) is an autosomal dominant disorder characterized by postnatal heterotopic ossification (HO).[1,2] The disorder is caused by a gene mutation in the activin A receptor type I (ACVR1), which is responsible for bone morphogenetic protein (BMP) activity.[3,4] The incidence of FOP is quite rare, affecting an estimated one in 2 million people. HO is usually not apparent at birth; congenital malformation of the great toes is a sign for early diagnosis of the disorder. HO often appears within the first decade of life, after swelling with sensation of heat and pain (flare-up) of the soft tissues such as the skeletal muscles, tendons, and ligaments. When HO occurs in tissues surrounding joints, their mobility is lost.[1,2,5-7] In the maxillofacial region, the temporomandibular joint (TMJ) and masticatory muscles are common sites of involvement and this results in restricted mouth opening.[5,8-14] Surgical treatment for the restricted mouth opening in patients with FOP often results in relapse and worsening of HO and is generally not recommended.[1,15-18] HO in growing children affects facial growth and occlusion. Although there are a few reports about occlusion,[19,20] little is known about the facial morphology and occlusion of patients with FOP. In this paper, we present a longitudinal record of facial morphology and occlusion (from 8 to 21 years of age) in a patient with FOP, and discuss the dental care for children with FOP.

Case report

The patient first visited the University of Tokyo Hospital at the age of 8 years and 9 months. He had severe maxillary protrusion in the mixed dentition with a large overjet (9.5 mm) and a deep overbite (5.0 mm). The molar relationship was Angle Class II (Angle Classification Class II, Division 1). His mouth opening was severely restricted and the maximum opening was 5.0 mm (Figure 1). Evaluation of the patient's panoramic radiograph revealed the presence of all permanent teeth, widening of the right coronoid process, and elongation of the left coronoid process; mild flattening of the bilateral condylar heads was suspected

doi: 10.1111/j.1754-4505.2012.00260.x

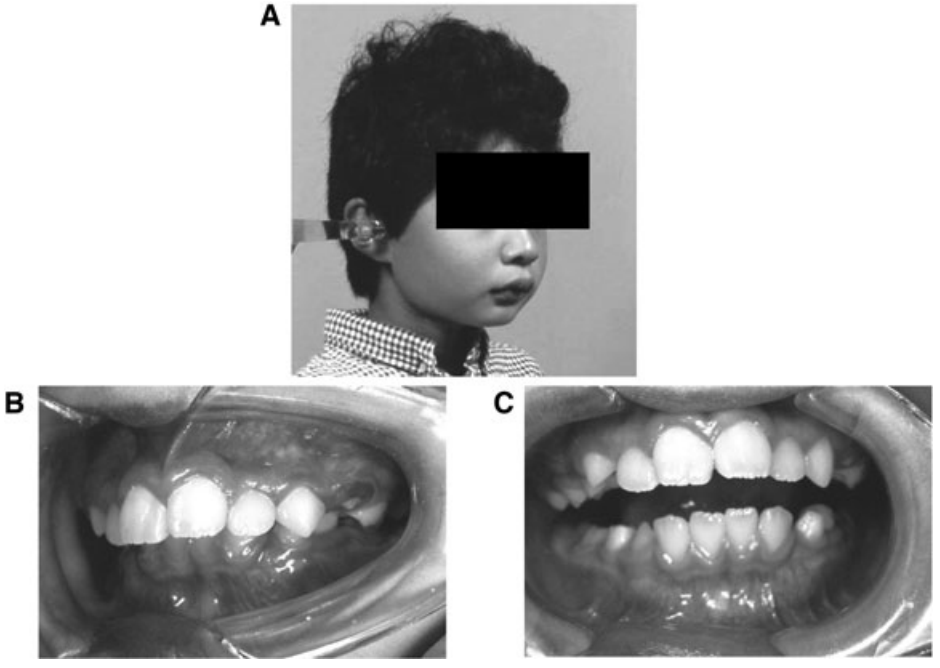

Figure 1. Facial appearance and occlusion at the initial visit (age 8 years, 9 months). (A) Face. (B) Occlusion at closed position. (C) Maximum opening. The occlusion showed severe maxillary protrusion and the amount of maximum mouth opening was 5.0 mm.

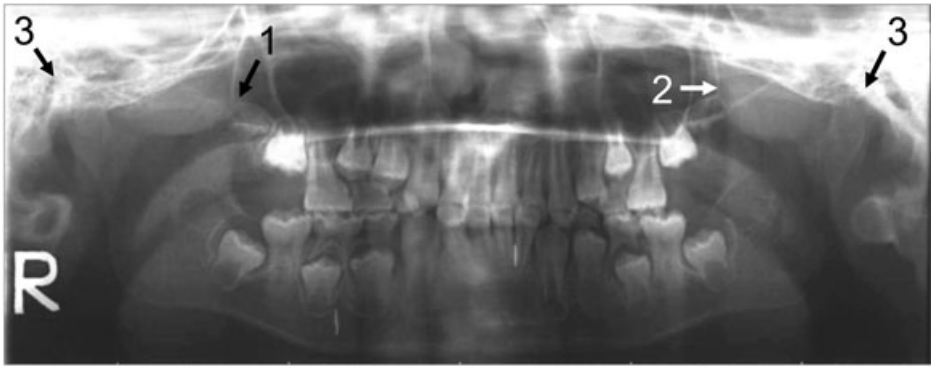

Figure 2. Panoramic radiograph at the initial visit (age 8 years, 9 months). Widening of the right coronoid process (arrow 1) and elongation of the left coronoid process (arrow 2) were seen. Mild flattening of the bilateral condylar heads was suspected (arrows 3).

(Figure 2). The lateral cephalogram showed a severe Class II facial skeleton (SNA: 85.4°, SNB: 75.6°, ANB: 9.8°) (Figure 3, Table 1). The maxilla was protruded and the mandible had normal anteroposterior development. Both maxillary and mandibular incisors were proclined and fusion of cervical vertebrae was also noted in the cephalogram. At that time, the spinal deformity in the coronal plane (scoliosis) was mild (Figure 4A).

The patient had received surgical correction of bilateral hallux valgus at the age of 1 year and was diagnosed with FOP in another hospital at 5 years of age. As the large overjet enabled his teeth to be cleaned and for him to eat, orthodontic correction was not planned and it was decided to follow his facial growth carefully and to maintain his oral hygiene at the highest level.

At 12 years of age, the patient had pain in his right hip joint, which affected

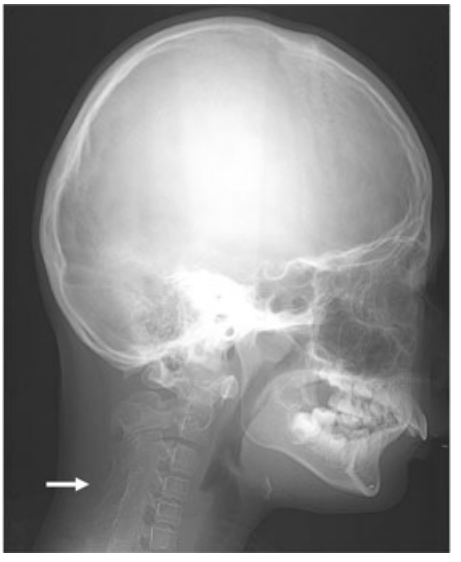

Figure 3. Lateral cephalogram at the initial visit (age 8 years, 9 months). The patient had severe Angle Class II facial skeleton. Fusion of cervical vertebrae was seen (arrow).

his movement. From 13 years of age, HO in the ligaments surrounding the vertebral column progressed, and scoliosis and tilting of the head became more prominent (Figures 4B and 5). At 16 years of age, the last cephalogram was made; as it was impossible thereafter because of his vertebral deformation. The superimposition of cephalogram tracings at ages 8 and 16 showed greater forward growth of both the maxilla and mandible relative to the anterior cranial base. The mandible showed counterclockwise rotation and both maxillary and mandibular incisors were proclined further (Figure 6, Table 1). The computed tomography (CT) made at 16 years of age clearly depicted deformation of bilateral condylar heads, widening of the right coronoid process, and elongation of the left coronoid process. HO was found at the anterior edge of the right coronoid process, but it was not fused with the upper bones of the skull (Figure 7). These findings suggested that the restricted mouth opening was caused by the mechanical interference between the coronoid processes and upper bones, and not because there was a bony fusion. Between 16 and 17 years of age, the patient experienced acute

Table 1. Cephalogram measurements.

Parameters	Age		Japanese adult male norm:
	8 years, 10 months	16 years, 4 months	Mean (SD)
SNA	85.4[a]	93.5[c]	81.8 (3.1)
SNB	75.6	81.4	78.6 (3.1)
ANB	9.8[b]	12.1[c]	3.3 (2.7)
MP-FH	19.6[a]	11.8[b]	26.3 (6.3)
U1-FH	117.9[a]	126.4[c]	108.9 (5.6)
L1-MP	123.3[c]	129.5[c]	94.7 (7.2)

MP-FH: Mandibular plane–Frankfurt plane Angle; U1-FH: Upper incisor–Frankfurt plane Azngle; L1-MP: Lower incisor-Frankfurt plane Angle; SD: Standard deviation.
Deviation from the mean value [a]between 1 and 2 SD, [b]between 2 and 3 SD, [c]more than 3 SD.
Japanese norm is from Izuka and Ishikawa[25]

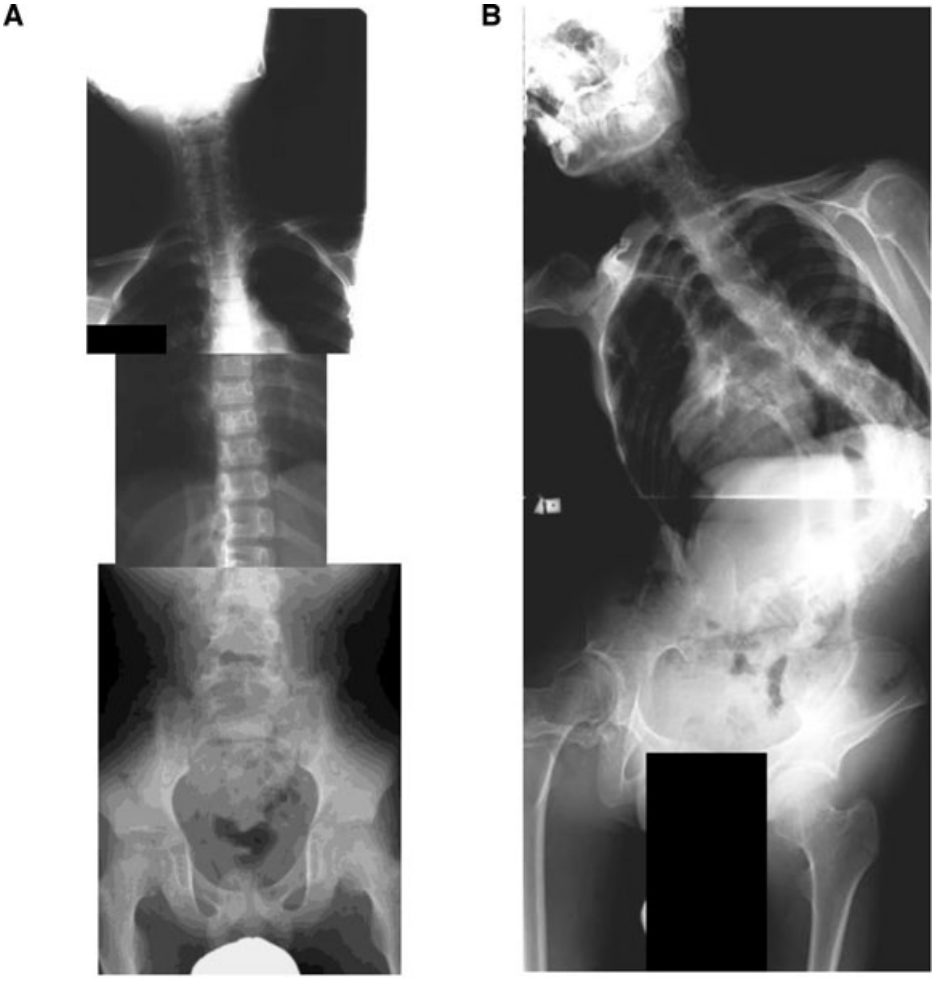

Figure 4. Integrated radiographic films of the vertebral column. (A) At the initial visit (age 8 years, 9 months). (B) At 18 years and 3 months of age, lateral curvature of the vertebral column had become severe.

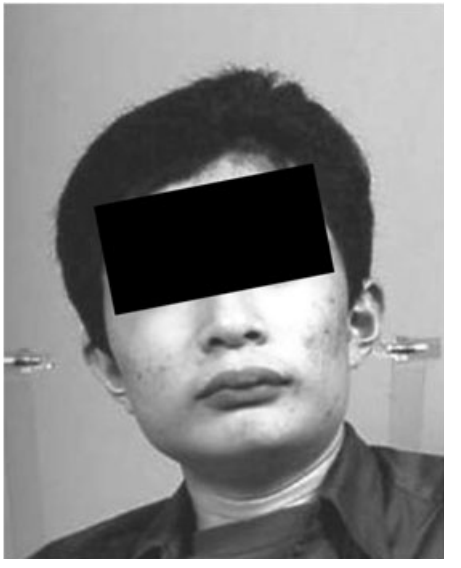

Figure 5. Facial appearance at age 15 years and 4 months. Tilting of the head had become prominent and standardization using ear rods was impossible.

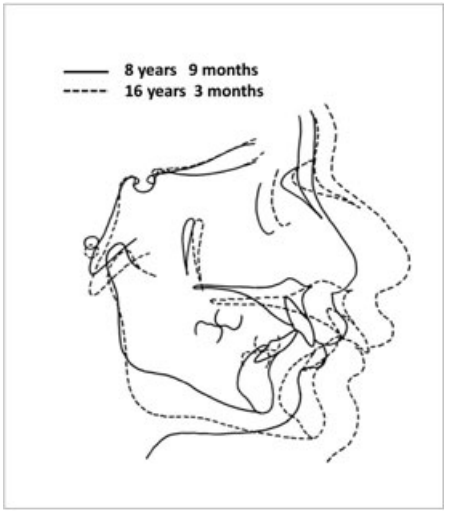

Figure 6. Superimposition of lateral cephalograms. Large forward growths of both maxilla and mandible were found. The mandible showed counterclockwise rotation and both maxillary and mandibular incisors were proclined further.

submandibular swelling (flare-up) twice and antibiotics and a bisphosphonate were administered. He also experienced swelling in the right elbow and forearm during that period.

At 19 years of age, the maxillary protrusion had increased. The overjet and overbite had increased to 12.0 and

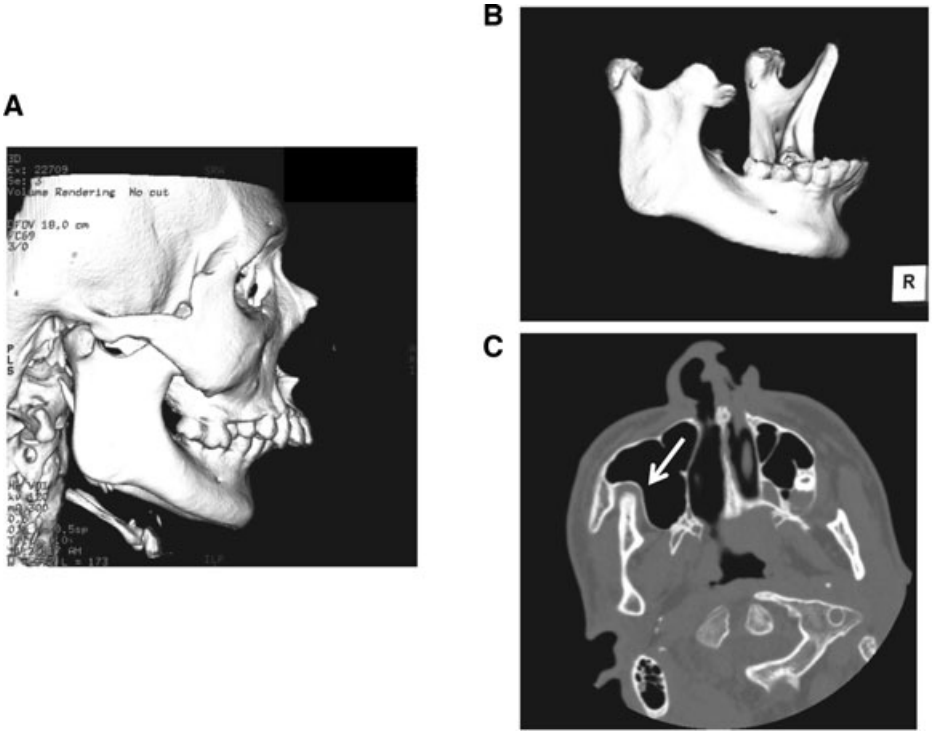

Figure 7. CT made at age 16 years and 3 months. (A) 3-D lateral facial view. (B) Extracted mandible. (C) 2-D view showing HO at the front edge of the right coronoid process. Deformation of bilateral condylar heads, widening of the right coronoid process, and elongation of left coronoid process were observed. HO was found at the anterior edge of the right coronoid process, but it was not fused with upper bones.

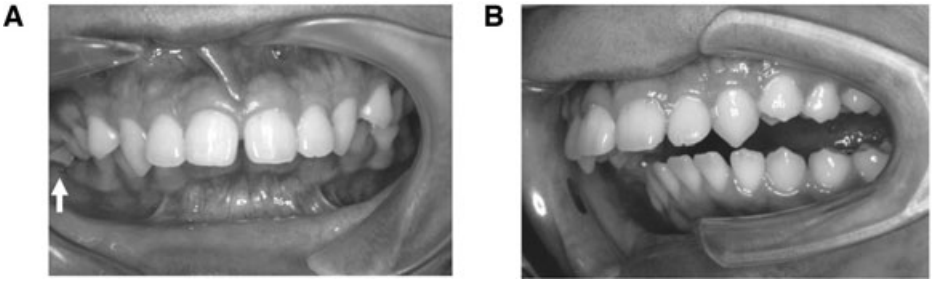

Figure 8. Occlusion at age 19 years and 4 months. (A) In occlusion. Upper right second molar had erupted buccally, showing a scissor bite (arrow). (B) Maximum opening. The maxillary protrusion deteriorated but the amount of mouth opening had slightly improved (6.0 mm).

6.0 mm, respectively. The premolars had erupted normally, but molars had delayed eruption or impaction (Figures 8 and 9). However, the amount of maximum opening slightly improved (6.0 mm). To prevent acute inflammation and subsequent swelling (flare-up) caused by dental caries or periodontal disease, seven molars were extracted under local or general anesthesia. The details of the surgical extraction of the six molars under general anesthesia have been reported previously.[21] The last examination of the patient for this report was at 21 years of age. Bone healing was good at the extraction sites and there was no further deterioration of HO in the facial region. His oral hygiene was excellent and we continue to provide periodic care.

Discussion

Signs or symptoms of FOP are usually not apparent at birth except for the congenital malformation of the great toes; HO often appears within the first decade of life after flare-ups in the soft tissues.[1,2,5,6] When joints are affected by HO, they lose their mobility, and when the vertebral column is affected, it often results in lateral curvature of the column.[1,2,7,12] TMJ and masticatory muscles are also commonly affected, resulting in restricted mouth opening.[5,8-14] The involvement of these tissues occurs relatively late in comparison with other joints, but restricted mouth opening occurs in about half of patients by the age of 20.[7] HO in oral regions appears after trauma or infection, but inadequate dental treatment and acute exacerbation of caries or periodontal disease have also been reported as causative factors.[10,14]

In growing children, HO seems to affect facial growth and occlusion. According to Nussbaum *et al.*,[19] there was a high incidence of mandibular hypoplasia and large overjet in patients with FOP. Renton *et al.*[22] reported flattening of the condylar heads which was found even in patients without restricted mouth opening. However, there are no detailed reports on facial morphology and occlusion, including changes with growth.

Our patient exhibited a skeletal Class II relationship with protrusion of the maxillary alveolar process. The mandible showed normal anteroposterior growth as measured by SNB angle at the age of 8 and 16 years. Flattening of condylar heads was suspected at the first examination and it was clearly seen later in the evaluation of the CT of the head and neck. The restricted mouth opening (5.0 mm) was already recorded at the initial visit. The patient's mother recalled that he had difficulty opening his mouth beginning in infancy. The widening of the right condylar process found at the initial examination was considered to be the cause of the restricted mouth opening. Evaluation of the CT scans made later revealed HO at the front edge of the coronoid process, though the coronoid process was not fused with upper facial

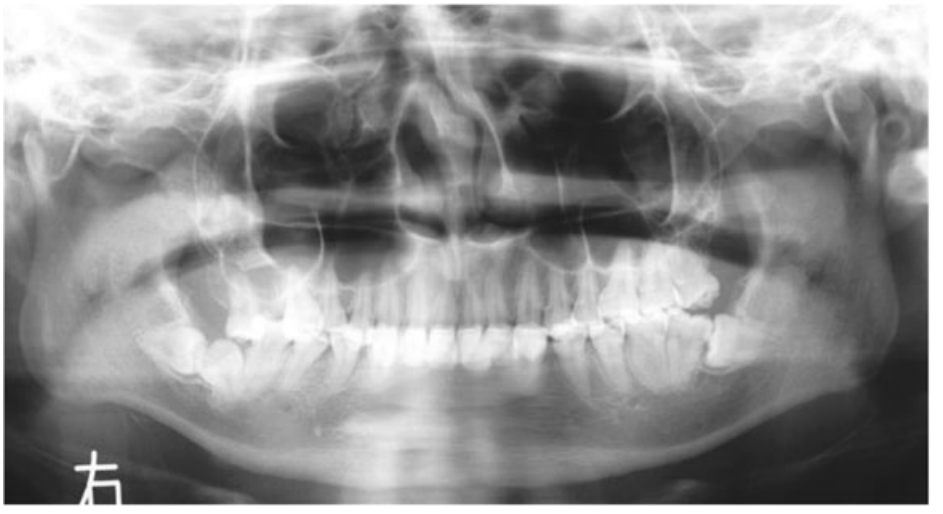

Figure 9. Panoramic radiograph at age 19 years and 5 months. Molars showed abnormal eruption or impaction. Seven molars were later extracted under local or general anesthesia.

bones (Figure 7). This suggested that the restriction was not caused by bone fusion but by mechanical interference of bones on mouth opening as pointed out by Connor and Evans[8] and Nunnelly and Yussen.[9]

Our patient had severe maxillary protrusion with Angle Class II Division 1 occlusion. As Nussbaum *et al.*[19] reported in some of their patients with FOP, this malocclusion seemed to be helpful for cleaning the oral cavity and for eating, as mouth opening was restricted in these patients. If our patient had a normal overjet, the mouth opening would have been smaller. The proclination of maxillary incisors might be caused by forces exerted during masticatory movement.

During follow-up of our patient, the mouth opening did not decrease but rather increased slightly (6.0 mm). Analysis of the cephalogram found that both the maxilla and mandible had greater forward growth than did the anterior cranial base. The ANB angle changed from 9.8° to 12.1° and the overjet changed from 9.5 to 12.0 mm. The forward inclination of both maxillary and mandibular incisors was also increased (Figure 6, Table 1). These changes indicate a probable influence on upper incisor inclination from his hyperactive lower lip as it tried to make an anterior seal during swallowing, and was also influenced by the movement of the tongue on the lower incisors as it thrusts forward to achieve an anterior seal during swallowing. Although the premolars had erupted without problem, the molars were delayed or impacted. This seemed to be due to the lack of eruption space in the posterior region of the mandibular arch. As these molars are more susceptible to dental caries and periodontal disease, seven molars were extracted under local or general anesthesia.[21] After extraction, oral hygiene maintenance became easier than before. At present, a slender toothbrush and an interdental brush are being used for oral cleaning and the patient's oral hygiene is excellent.

The guidelines for dental management of patients with FOP, such as the treatment of caries, tooth extraction, orthodontic treatment, and oral hygiene maintenance, have been proposed by several authors.[19,23] Restricted mouth opening is the main problem, but surgical release of HO has been reported to cause flare-ups and aggravate the HO further.[15] Since it is difficult to carry out dental treatment on these patients, good oral hygiene must be maintained to prevent dental caries and periodontal disease.[19,23,24] Patients should be aware of the problems with oral care methods before the onset of HO and should receive preventive or early interceptive dental treatment. However, even normal opening of the mouth during dental treatment might be traumatic for patients with FOP, and dentists caring for these patients must be aware of this problem.

Maxillary protrusion seems to be common in patients with FOP and orthodontic treatment would be safe.[10] However, the space for cleaning the mouth and eating needs be taken into consideration. If the child shows severe crowding of anterior teeth, orthodontic treatment will be helpful for maintenance of oral hygiene. However, an orthodontic appliance increases the risk of dental caries and gingivitis. Problems with posterior teeth may occur with facial growth similar to our patient, so early and regular dental examination by dentists knowledgeable about FOP is recommended. If abnormal eruption of posterior teeth is found, extraction of the teeth should be considered to prevent dental caries or periodontal disease and to avoid flare-ups and HO.

Conclusion

The patient in this case report had a severely restricted mouth opening caused by HO. He had a Class II facial skeleton and Angle Class II Division 1 occlusion. His maxilla protruded severely but his mandible showed normal anteroposterior development. He also had an abnormally low mandibular plane angle. Orthodontic treatment was not considered because the large overjet enabled him to clean his mouth and to eat. Facial growth was closely monitored over time. As the patient grew, the maxillary protrusion became more prominent and the mandible rotated counterclockwise between the ages of 8 and 16 years. However, the restricted mouth opening did not worsen. The patient's molars had delayed eruption or were impacted, and were extracted under local and general anesthesia. The patient's oral hygiene is currently excellent.

In children with FOP, involvement of the TMJ occurs rather late in comparison with other joints. If FOP is diagnosed at an early age, efforts should be made to

prevent the onset of HO. Oral hygiene maintenance and early preventive or interceptive dental treatment are necessary before the onset of HO. Orthodontic treatment to correct crowding might be helpful for oral hygiene maintenance, but the space for food intake should be taken into consideration if there is restricted mouth opening.

References

1. Kaplan FS, Le Merrer M, Glaser DL, *et al*. Fibrodysplasia ossificans progressiva. *Best Pract Res Clin Rheumatol* 2008;22:191-205.
2. Shore EM, Kaplan FS. Insights from a rare genetic disorder of extra-skeletal bone formation, fibrodysplasia ossificans progressiva (FOP). *Bone* 2008;43:427-33.
3. Shore EM, Xu M, Feldman GJ, *et al*. A recurrent mutation in the BMP type I receptor ACVR1 causes inherited and sporadic fibrodysplasia ossificans progressiva. *Nat Genet* 2006;38:525-7.
4. Kaplan FS, Xu M, Seemann P, *et al*. Classic and atypical fibrodysplasia ossificans progressiva (FOP) phenotypes are caused by mutations in the bone morphogenetic protein (BMP) type I receptor ACVR1. *Hum Mutat* 2009;30:379-90.
5. Rocke DM, Zasloff M, Peeper J, Cohen RB, Kaplan FS. Age- and joint-specific risk of initial heterotopic ossification in patients who have fibrodysplasia ossificans progressiva. *Clin Orthop Relat Res* 1994;301:243-8.
6. Kaplan FS, Xu M, Glaser DL, *et al*. Early diagnosis of fibrodysplasia ossificans progressiva. *Pediatrics* 2008;121:e1295-300.
7. Nakashima Y, Haga N, Kitoh H, *et al*. Deformity of the great toe in fibrodysplasia ossificans progressiva. *J Orthop Sci* 2010;15:804-9.
8. Connor JM, Evans DA. Extra-articular ankylosis in fibrodysplasia ossificans progressiva. *Br J Oral Surg* 1982;20: 117-21.
9. Nunnelly JF, Yussen PS. Computed tomographic findings in patients with limited jaw movement due to myositis ossificans progressiva. *J Oral Maxillofac Surg* 1986;44:818-21.
10. Luchetti W, Cohen RB, Hahn GV, *et al*. Severe restriction in jaw movement after routine injection of local anesthetic in patients who have fibrodysplasia ossificans progressive. *Oral Surg Oral Med Oral Pathol Oral Radiol Endod* 1996;81:21-5.
11. Janoff HB, Zasloff MA, Kaplan FS. Submandibular swelling in patients with fibrodysplasia ossificans progressiva. *Otolaryngol Head Neck Surg* 1996;114: 599-604.
12. Smith R. Fibrodysplasia (myositis) ossificans progressiva. Clinical lessons from a rare disease. *Clin Orthop Relat Res* 1998;346:7-14.
13. van der Meij EH, Becking AG, van der Waal I. Fibrodysplasia ossificans progressiva. An unusual cause of restricted mandibular movement. *Oral Dis* 2006;12:204-7.
14. Sendur OF, Gurer G. Severe limitation in jaw movement in a patient with fibrodysplasia ossificans progressiva: a case report. *Oral Surg Oral Med Oral Pathol Oral Radiol Endod* 2006;102:312-7.
15. Crofford LJ, Brahim JS, Zasloff MA, Marini JC. Failure of surgery and isotretinoin to relieve jaw immobilization in fibrodysplasia ossificans progressiva: report of two cases. *J Oral Maxillofac Surg* 1990;48:204-8.
16. Herford AS, Boyne PJ. Ankylosis of the jaw in a patient with fibrodysplasia ossificans progressiva. *Oral Surg Oral Med Oral Pathol Oral Radiol Endod* 2003;96:680-4.
17. Wadenya R, Fulcher M, Grunwald T, Nussbaum B, Grunwald Z. A description of two surgical and anesthetic management techniques used for a patient with fibrodysplasia ossificans progressiva. *Spec Care Dentist* 2010;30:106-9.
18. Duan Y, Zhang H, Bu R. Intraoral approach technique for treating trismus caused by fibrodysplasia ossificans progressiva. *J Oral Maxillofac Surg* 2010;68:1408-10.
19. Nussbaum BL, Grunwald Z, Kaplan FS. Oral and dental health care and anesthesia for persons with fibrodysplasia ossificans progressiva. *Clin Rev Bone Miner Metab* 2005;3:239-42.
20. Carvalho DR, Pinnola GC, Ferreira DR, *et al*. Mandibular hypoplasia in fibrodysplasia ossificans progressiva causing obstructive sleep apnea with pulmonary hypertension. *Clin Dysmorphol* 2010;19:69-72.
21. Mori Y, Susami T, Haga N, *et al*. Extraction of 6 molars under general anesthesia in patient with fibrodysplasia ossificans progressiva. *J Oral Maxillofac Surg* 2011;69:1905-10.
22. Renton P, Parkin SF, Stamp TC. Abnormal temporomandibular joints in fibrodysplasia ossificans progressiva. *Br J Oral Surg* 1982; 20:31-8.
23. Nussbaum BL, O'Hara I, Kaplan FS. Fibrodysplasia ossificans progressiva: report of a case with guidelines for pediatric dental and anesthetic management. *ASDC J Dent Child* 1996;63:448-50.
24. Young JM, Diecidue RJ, Nussbaum BL. Oral management in a patient with fibrodysplasia ossificans progressiva. *Spec Care Dentist* 2007;27:101-4.
25. Izuka T, Ishikawa F. Normal standards for various cephalometric analyses in Japanese adults. *J Jpn Orthod Soc* 1957;16:4-12.

表2　骨系統疾患国際分類（2010）和訳（Warmanら[4]より引用、改変）

グループ / 疾患名（原文）	グループ / 疾患名（和訳）	遺伝形式	MIM番号	遺伝子座	遺伝子	タンパク	注釈
1. FGFR3 chondrodysplasia group	**1. FGFR3 軟骨異形成症グループ**						
Thanatophoric dysplasia type 1 (TD1)	タナトフォリック骨異形成症1型（TD1）	AD	187600	4p16.3	*FGFR3*	FGFR3	以前のSan Diego型を含む
Thanatophoric dysplasia type 2 (TD2)	タナトフォリック骨異形成症2型（TD2）	AD	187601	4p16.3	*FGFR3*	FGFR3	
Severe achondroplasia with developmental delay and acanthosis nigricans (SADDAN)	重症軟骨無形成症・発達遅滞・黒色表皮腫（SADDAN）	AD	187600を参照	4p16.3	*FGFR3*	FGFR3	
Achondroplasia	軟骨無形成症	AD	100800	4p16.3	*FGFR3*	FGFR3	
Hypochondroplasia	軟骨低形成症	AD	146000	4p16.3	*FGFR3*	FGFR3	
Camptodactyly, tall stature and hearing loss syndrome (CATSHL)	屈指・高身長・難聴症候群（CATSHL）	AD	187600	4p16.3	*FGFR3*	FGFR3	不活性化変異
Hypochondroplasia–like dysplasia(s)	軟骨低形成症様異形成症	AD, SP					軟骨低形成症に類似するがFGFR3と非連鎖であり，おそらく異質性．診断基準は不確定
グループ39のFGFR3関連の表現型を示すLADD症候群同様，グループ33のFGFR3変異と関連する頭蓋骨癒合症候群も参照							
2. Type 2 collagen group and similar disorders	**2. 2型コラーゲングループおよび類似疾患**						
Achondrogenesis type 2 (ACG2; Langer-	軟骨無発生症2型（ACG2: Langer–Saldino型）	AD	200610	12q13.1	*COL2A1*	Type 2 collagen	
Platyspondylic dysplasia, Torrance type	扁平椎異形成症，Torrance型	AD	151210	12q13.1	*COL2A1*	Type 2 collagen	重症脊椎異形成症（グループ14）も参照
Hypochondrogenesis	軟骨低発生症	AD	200610	12q13.1	*COL2A1*	Type 2 collagen	
Spondyloepiphyseal dysplasia congenita (SEDC)	先天性脊椎骨端異形成症（SEDC）	AD	183900	12q13.1	*COL2A1*	Type 2 collagen	
Spondyloepimetaphyseal dysplasia (SEMD) Strudwick type	脊椎骨端骨幹端異形成症（SEMD）Strudwick型	AD	184250	12q13.1	*COL2A1*	Type 2 collagen	
Kniest dysplasia	Kniest骨異形成症	AD	156550	12q13.1	*COL2A1*	Type 2 collagen	
Spondyloperipheral dysplasia	脊椎末梢異形成症	AD	271700	12q13.1	*COL2A1*	Type 2 collagen	
Mild SED with premature onset arthrosis	早発性関節症を伴う軽症脊椎骨端異形成症	AD		12q13.1	*COL2A1*	Type 2 collagen	p.R719Cとp.G474S変異にしばしば関係
SED with metatarsal shortening (formerly Czech dysplasia)	中足骨短縮を伴う脊椎骨端異形成症（以前のCzech異形成症）	AD	609162	12q13.1	*COL2A1*	Type 2 collagen	R275C変異にしばしば関係
Stickler syndrome type 1	Stickler症候群1型	AD	108300	12q13.1	*COL2A1*	Type 2 collagen	
Stickler-like syndrome(s)	Stickler様症候群						COL2A1，COL11A1，COL11A2のいずれにも非連鎖．劣性型はCOL9A1も参照
3. Type 11 collagen group	**3. 11型コラーゲングループ**						
Stickler syndrome type 2	Stickler症候群2型	AD	604841	1p21	*COL11A1*	Type 11 collagen alpha-1 chain	
Marshall syndrome	Marshall症候群	AD	154780	1p21	*COL11A1*	Type 11 collagen alpha-1 chain	
Fibrochondrogenesis	線維性軟骨発生症	AR	228520	1p21	*COL11A1*	Type 11 collagen alpha-1 chain	
Otospondylomegaepiphyseal dysplasia (OSMED), recessive type	耳脊椎巨大骨端異形成症（OSMED），劣性型	AR	215150	6p21.3	*COL11A2*	Type 11 collagen alpha-2 chain	
Otospondylomegaepiphyseal dysplasia (OSMED), dominant type (Weissenbacher-Zweymüller syndrome, Stickler syndrome type 3)	耳脊椎巨大骨端異形成症（OSMED），優性型（Weissenbacher–Zweymüller症候群，Stickler症候群3型）	AD	215150	6p21.3	*COL11A2*	Type 11 collagen alpha-2 chain	
グループ2のStickler症候群1型も参照.							
4. Sulphation disorders group	**4. 硫酸化障害グループ**						
Achondrogenesis type 1B (ACG1B)	軟骨無発生症1B型（ACG1B）	AR	600972	5q32-33	*DTDST*	SLC26A2 sulfate transporter	以前はFraccaro型軟骨無発生症として知られていた
Atelosteogenesis type 2 (AO2)	骨発生不全症2型（AO2）	AR	256050	5q32-33	*DTDST*	SLC26A2 sulfate transporter	de la Chapelle骨異形成症，McAlister骨異形成症，"新生児骨異形成症"を含む
Diastrophic dysplasia (DTD)	捻曲性骨異形成症（DTD）	AR	222600	5q32-33	*DTDST*	SLC26A2 sulfate transporter	
MED, autosomal recessive type (rMED; EDM4)	多発性骨端異形成症，常染色体劣性型（rMED; EDM4）	AR	226900	5q32-33	*DTDST*	SLC26A2 sulfate transporter	多発性骨端異形成症および偽性軟骨無形成症グループ（グループ10）も参照
SEMD, PAPSS2 type	脊椎骨端骨幹端異形成症，PAPSS2型	AR	603005	10q23-q24	*PAPSS2*	PAPS-Synthetase 2	以前の"Pakistan型"．脊椎骨端骨幹端異形成症グループ（グループ13）も参照

グループ / 疾患名（原文）	グループ / 疾患名（和訳）	遺伝形式	MIM番号	遺伝子座	遺伝子	タンパク	注釈
Chondrodysplasia with congenital joint dislocations, CHST3 type (recessive Larsen	先天性関節脱臼を伴う軟骨異形成症, CHST3型（劣性Larsen症候群）	AR	608637	10q22.1	*CHST3*	Carbohydrate sulfotransferase 3; chondroitin 6-sulfotransferase	劣性型Larsen症候群，上腕−脊椎異骨症，脊椎骨端異形成症 Oman型を含む
Ehlers-Danlos syndrome, CHST14 type ("musculo-skeletal variant")	Ehlers−Danlos症候群, CHST14型（"筋骨格型"）	AR	601776	15q14	*CHST14*	Carbohydrate sulfotransferase 14; dermatan 4-sulfotransferase	内転母指−内反足症候群を含む
グループ7およびグループ20の多発性脱臼を伴う他の疾患も参照.							
5. Perlecan group	**5. Perlecanグループ**						
Dyssegmental dysplasia, Silverman-Handmaker	分節異常骨異形成症, Silverman−Handmaker型	AR	224410	1q36-34	*PLC (HSPG2)*	Perlecan	
Dyssegmental dysplasia, Rolland-Desbuquois	分節異常骨異形成症, Rolland−Desbuquois型	AR	224400	1q36-34	*PLC (HSPG2)*	Perlecan	
Schwartz-Jampel syndrome (myotonic chondrodystrophy)	Schwartz−Jampel症候群（筋ミオトニー軟骨異栄養症）	AR	255800	1q36-34	*PLC (HSPG2)*	Perlecan	軽症型および重症型．以前のBurton骨異形成症を含む
6. Aggrecan group	**6. Aggrecanグループ**						
SED, Kimberley type	脊椎骨端異形成症, Kimberley型	AD	608361	15q26	*AGC1*	Aggrecan	
SEMD, Aggrecan type	脊椎骨端骨幹端異形成症, Aggrecan型	AR	612813	15q26	*AGC1*	Aggrecan	
Familial osteochondritis dissecans	家族性離断性骨軟骨炎	AD	165800	15q26	*AGC1*	Aggrecan	
7. Filamin group and related disorders	**7. Filaminグループと関連疾患**						
Frontometaphyseal dysplasia	前頭骨幹端異形成症	XLD	305620	Xq28	*FLNA*	Filamin A	明らかにFLNA変異を欠く例がある
Osteodysplasty Melnick-Needles	異形成骨症Melnick−Needles型	XLD	309350	Xq28	*FLNA*	Filamin A	
Otopalatodigital syndrome type 1 (OPD1)	耳口蓋指症候群1型（OPD1）	XLD	311300	Xq28	*FLNA*	Filamin A	
Otopalatodigital syndrome type 2 (OPD2)	耳口蓋指症候群2型（OPD2）	XLD	304120	Xq28	*FLNA*	Filamin A	
Terminal osseous dysplasia with pigmentary defects (TODPD)	色素異常を伴う末端骨異形成症（TODPD）	XLD	300244	Xq28	*FLNA*	Filamin A	
Atelosteogenesis type 1 (AO1)	骨発生不全症1型（AO1）	AD	108720	3p14.3	*FLNB*	Filamin B	ブーメラン骨異形成症，Piepkorn骨異形成症，脊椎上腕大腿骨（巨細胞）異形成症を含む
Atelosteogenesis type 3 (AO3)	骨発生不全症3型（AO3）	AD	108721	3p14.3	*FLNB*	Filamin B	
Larsen syndrome (dominant)	Larsen症候群（優性）	AD	150250	3p14.3	*FLNB*	Filamin B	
Spondylo-carpal-tarsal dysplasia	脊椎・手根骨・足根骨異形成症	AR	272460	3p14.3	*FLNB*	Filamin B	
Spondylo-carpal-tarsal dysplasia	脊椎・手根骨・足根骨異形成症	AR	272460				FLNBと非連鎖
Franck - ter Haar syndrome	Franck − ter Haar症候群	AR	249420	5q35.1	*SH3PXD2B*	TKS4	
Serpentine fibula - polycystic kidney syndrome	蛇行腓骨・多嚢胞腎症候群	AD?	600330				
グループ4の劣性型Larsen症候群とグループ20の多発性脱臼の疾患も参照.							
8. TRPV4 group	**8. TRPV4グループ**						
Metatropic dysplasia	変容性骨異形成症	AD	156530	12q24.1	*TRPV4*	Transient receptor potential cation channel, subfamily V, member 4	致死型および非致死型を含む
Spondyloepimetaphyseal dysplasia, Maroteaux type (Pseudo-Morquio syndrome type 2)	脊椎骨端骨幹端異形成症, Maroteaux型（偽性Morquio症候群2型）	AD	184095	12q24.1	*TRPV4*	Transient receptor potential cation channel, subfamily V, member 4	
Spondylometaphyseal dysplasia, Kozlowski type	脊椎骨幹端異形成症, Kozlowski型	AD	184252	12q24.1	*TRPV4*	Transient receptor potential cation channel, subfamily V, member 4	
Brachyolmia, autosomal dominant type	短体幹症，常染色体優性型	AD	113500	12q24.1	*TRPV4*	Transient receptor potential cation channel, subfamily V, member 4	
Familial digital arthropathy with brachydactyly	短指を伴う家族性指関節症	AD	606835	12q24.1	*TRPV4*	Transient receptor potential cation channel, subfamily V, member 4	
9. Short-ribs dysplasias (with or without polydactyly) group	**9. 短肋骨異形成症（多指症を伴う/伴わない）グループ**						
Chondroectodermal dysplasia (Ellis-van Creveld)	軟骨外胚葉性異形成症（Ellis−van Creveld）	AR	225500	4p16	*EVC1*	EvC gene 1	
				4p16	*EVC2*	EvC gene 2	
Short ribs – polydactyly syndrome (SRPS) type 1/3 (Saldino-Noonan/Verma-Naumoff)	短肋骨多指症候群（SRPS）1/3型（Saldino−Noonan/Verma−Naumoff）	AR	263510	11q22.3	*DYNC2H1*	Dynein, cytoplasmic 2, heavy chain 1	

グループ / 疾患名(原文)	グループ / 疾患名(和訳)	遺伝形式	MIM番号	遺伝子座	遺伝子	タンパク	注釈
SRPS type 1/3 (Saldino-Noonan/Verma-Naumoff)	短肋骨多指症候群 1/3型 (Saldino-Noonan/Verma-Naumoff)	AR	263510	3q25.33	*IFT80*	Intraflagellar transport 80 (homolog of)	
SRPS type 1/3 (Saldino-Noonan/Verma-Naumoff)	短肋骨多指症候群 1/3型 (Saldino-Noonan/Verma-Naumoff)	AR	263510				DYNC2H1, IFT80のどちらとも非連鎖
SRPS type 2 (Majewski)	短肋骨多指症候群 2型 (Majewski)	AR	263520				
SRPS type 4 (Beemer)	短肋骨多指症候群 4型 (Beemer)	AR	269860				
Oral-facial-digital syndrome type 4 (Mohr-Majewski)	口・顔面・指症候群4型 (Mohr-Majewski)	AR	258860				
Asphyxiating thoracic dysplasia (ATD; Jeune)	呼吸不全性胸郭異形成症 (ATD; Jeune)	AR	208500	3q25.33	*IFT80*	intraflagellar transport 80 (homolog of)	
Asphyxiating thoracic dysplasia (ATD; Jeune)	呼吸不全性胸郭異形成症 (ATD; Jeune)	AR	208500	11q22.3	*DYNC2H1*	Dynein, cytoplasmic 2, heavy chain 1	
Asphyxiating thoracic dysplasia (ATD; Jeune)	呼吸不全性胸郭異形成症 (ATD; Jeune)	AR	208500				DYNC2H1, IFT80のどちらとも非連鎖
Thoracolaryngopelvic dysplasia (Barnes)	胸郭咽頭骨盤異形成症 (Barnes)	AD	187760				

14 番染色体父性片親性ダイソミーおよび脳・肋骨・下顎症候群も参照.

10. Multiple epiphyseal dysplasia and pseudoachondroplasia group	**10. 多発性骨端異形成症および偽性軟骨無形成症グループ**						
Pseudoachondroplasia (PSACH)	偽性軟骨無形成症 (PSACH)	AD	177170	19p12-13.1	*COMP*	COMP	
Multiple epiphyseal dysplasia (MED) type 1	多発性骨端異形成症 (MED) 1型 (EDM1)	AD	132400	19p13.1	*COMP*	COMP	
Multiple epiphyseal dysplasia (MED) type 2	多発性骨端異形成症 (MED) 2型 (EDM2)	AD	600204	1p32.2-33	*COL9A2*	Collagen 9 alpha-2 chain	
Multiple epiphyseal dysplasia (MED) type 3	多発性骨端異形成症 (MED) 3型 (EDM3)	AD	600969	20q13.3	*COL9A3*	Collagen 9 alpha-3 chain	
Multiple epiphyseal dysplasia (MED) type 5	多発性骨端異形成症 (MED) 5型 (EDM5)	AD	607078	2p23-24	*MATN3*	Matrilin 3	
Multiple epiphyseal dysplasia (MED) type 6	多発性骨端異形成症 (MED) 6型 (EDM6)	AD	120210	6q13	*COL9A1*	Collagen 9 alpha-1 chain	
Multiple epiphyseal dysplasia (MED), other types	多発性骨端異形成症 (MED), 他の型						いくつかの多発性骨端異形成症様症例は既知の遺伝子に非連鎖
Stickler syndrome, recessive type	Stickler症候群, 劣性型	AR	120210	6q13	*COL9A1*	Collagen 9 alpha-1 chain	
Familial hip dysplasia (Beukes)	家族性臼蓋形成不全症 (Beukes)	AD	142669	4q35			
Multiple epiphyseal dysplasia with microcephaly and nystagmus (Lowry-Wood)	小頭症と眼振を伴う多発性骨端異形成症 (Lowry-Wood)	AR	226960				

遠位肢異形成症グループ(グループ15)のASPEDと同様, 硫酸化障害(グループ4)の多発性骨端異形成症, 常染色体劣性型(rMED, EDM4), Aggrecanグループ(グループ6)の家族性離断性骨軟骨炎も参照.

11. Metaphyseal dysplasias	**11. 骨幹端異形成症**						
Metaphyseal dysplasia, Schmid type (MCS)	骨幹端異形成症, Schmid型 (MCS)	AD	156500	6q21-22.3	*COL10A1*	Collagen 10 alpha-1 chain	
Cartilage-hair hypoplasia (CHH; metaphyseal dysplasia, McKusick type)	軟骨・毛髪低形成症 (CHH; 骨幹端異形成症, McKusick型)	AR	250250	9p13	*RMRP*	RNA component of RNAse H	成長抑制性異形成症を含む
Metaphyseal dysplasia, Jansen type	骨幹端異形成症, Jansen型	AD	156400	3p22-21.1	*PTHR1*	PTH/PTHrP receptor 1	活性化変異－Blomstrand骨異形成症(グループ22)も参照
Eiken dysplasia	Eiken異形成症	AR	600002	3p22-21.1	*PTHR1*	PTH/PTHrP receptor 1	活性化変異－Blomstrand骨異形成症(グループ22)も参照
Metaphyseal dysplasia with pancreatic insufficiency and cyclic neutropenia (Shwachman-Bodian-Diamond syndrome,	膵不全, 周期性好中球減少を伴う骨幹端異形成症 (Shwachman-Bodian-Diamond症候群, SBDS)	AR	260400	7q11	*SBDS*	SBDS protein	
Metaphyseal anadysplasia type 1	回復性骨幹端異形成症1型	AD, AR	309645	11q22.2	*MMP13*	Matrix metalloproteinase 13	脊椎骨端骨幹端異形成症 Missouri型を含む。優性と劣性変異の記述あり
Metaphyseal anadysplasia type 2	回復性骨幹端異形成症2型	AR		20q13.12	*MMP9*	Matrix metalloproteinase 9	
Metaphyseal dysplasia, Spahr type	骨幹端異形成症, Spahr型	AR	250400				
Metaphyseal acroscyphodysplasia (various	骨幹端先端杯状異形成症 (種々の型)	AR	250215				
Genochondromatosis (type 1/type 2)	遺伝性軟骨腫症 (1型/2型)	AD/SP	137360				
Metaphyseal chondromatosis with D-2-hydroxyglutaric aciduria	D-2水酸化グルタール酸尿症を伴う骨幹端軟骨腫症	AR/SP	271550を参照				

12. Spondylometaphyseal dysplasias (SMD)	**12. 脊椎骨幹端異形成症 (SMD)**

グループ / 疾患名(原文)	グループ / 疾患名(和訳)	遺伝形式	MIM番号	遺伝子座	遺伝子	タンパク	注釈
Spondyloenchondrodysplasia (SPENCD)	脊椎内軟骨異形成症 (SPENCD)	AR	271550	19p13.2	*ACP5*	Tartrate-resistant acid phosphatase (TRAP)	自己免疫を伴う免疫不全と脊椎骨幹端異形成症(MIM 607944)を含む
Odontochondrodysplasia (ODCD)	歯軟骨異形成症 (ODCD)	AR	184260				
Spondylometaphyseal dysplasia, Sutcliffe type or corner fractures type	脊椎骨幹端異形成症, Sutcliffe型/corner fracture型	AD	184255				
SMD with severe genu valgum	高度外反膝を伴う脊椎骨幹端異形成症	AD	184253				脊椎骨幹端異形成症 Schmidt型と脊椎骨幹端異形成症 Algeria型を含む
SMD with cone-rod dystrophy	錐体・杆体ジストロフィーを伴う脊椎骨幹端異形成	AR	608940				
SMD with retinal degeneration, axial type	網膜変性を伴う脊椎骨幹端異形成症, 体幹型	AR	602271				
Dysspondyloenchondromatosis	異脊椎内軟骨腫症	SP					
Cheiro-spondyloenchondromatosis	手・脊椎内軟骨腫症	SP					グループ29も参照

脊椎骨幹端異形成症 Sedaghatian型 (グループ14)と同様, 脊椎骨幹端異形成症 Kozlowski型 (グループ8, TRPV4), も参照; 脊椎骨幹端異形成症 variantは多くの報告あり.

13. Spondylo-epi-(meta)-physeal dysplasias	**13. 脊椎・骨端(・骨幹端)異形成症 (SE(M)D)**						
Dyggve-Melchior-Clausen dysplasia (DMC)	Dyggve-Melchior-Clausen骨異形成症 (DMC)	AR	223800	18q12-21.1	*DYM*	Dymeclin	Smith-McCort骨異形成症を含む
Immuno-osseous dysplasia (Schimke)	免疫不全性骨異形成症 (Schimke)	AR	242900	2q34-36	*SMARCAL1*	SWI/SNF-related regulator of chromatin subfamily A-like protein 1	
SED, Wolcott-Rallison type	脊椎骨端異形成症, Wolcott-Rallison型	AR	226980	2p12	*EIF2AK3*	Translation initiation factor 2-alpha kinase-3	
SEMD, Matrilin type	脊椎骨端骨幹端異形成症, Matrilin型	AR	608728	2p23-p24	*MATN3*	Matrilin 3	グループ10のmatrillin関連多発性骨端異形成症も参照
SEMD, short limb – abnormal calcification type	脊椎骨端骨幹端異形成症, 短肢・異常石灰化型	AR	271665	1q23	*DDR2*	Discoidin domain receptor family, member 2	グループ21の点状石灰化を伴う他の疾患も参照
SED tarda, X-linked (SED-XL)	遅発性脊椎骨端異形成症, X連鎖 (SED-XL)	XLR	313400	Xp22	*SEDL*	Sedlin	
Spondylo-megaepiphyseal-metaphyseal dysplasia (SMMD)	脊椎・巨大骨端・骨幹端異形成症 (SMMD)	AR	613330	4p16.1	*NKX3-2*	NK3 Homeobox 2	
Spondylodysplastic Ehlers-Danlos syndrome	脊椎異形成Ehlers-Danlos症侯群	AR	612350	11p11.2	*SLC39A13*	Zinc transporter ZIP13	
SPONASTRIME dysplasia	SPONASTRIME骨異形成症	AR	271510				
SEMD with joint laxity (SEMD-JL) leptodactylic or Hall type	関節弛緩を伴う脊椎骨端骨幹端異形成症 (SEMD-JL) 細指型/Hall型	AD	603546				
SEMD with joint laxity (SEMD-JL) Beighton type	関節弛緩を伴う脊椎骨端骨幹端異形成症 (SEMD-JL) Beighton型	AR	271640				
Platyspondyly (brachyolmia) with amelogenesis imperfecta	エナメル質形成不全を伴う扁平椎 (短体幹症)	AR	601216				
Late onset SED, autosomal recessive type	遅発性脊椎骨端異形成症, 常染色体劣性型	AR	609223				
Brachyolmia, Hobaek and Toledo types	短体幹症, Hobaek型・Toledo型	AR	271530, 271630				Hobaek型・Toledo型短体幹症と劣性型遅発性脊椎骨端異形成症との間の疾病分類上の関係は不明確で、現状では明確な区別の基準は

進行性偽性リウマチ様骨異形成症(進行性関節症を伴う脊椎骨端異形成症)(グループ31)と同様, 短体幹症(グループ8), 成熟遅延骨異形成症(グループ14), SMDs(グループ12), グループ27のムコ多糖症 4型(Morquio症侯群)および他の疾患も参照.

14. Severe spondylodysplastic dysplasias	**14. 重症脊椎異形成症**						
Achondrogenesis type 1A (ACG1A)	軟骨無発生症1A型 (ACG1A)	AR	200600	14q32.12	*TRIP11*	Golgi-microtubule-associated protein, 210-KD; GMAP210	
Schneckenbecken dysplasia	蝸牛様骨盤異形成症	AR	269250	1p31.3	*SLC35D1*	solute carrier family 35 member D1; UDP-glucuronic acid/UDP-N-acetylgalactosamine dual transporter	
Spondylometaphyseal dysplasia, Sedaghatian	脊椎骨幹端異形成症, Sedaghatian型	AR	250220				
Severe spondylometaphyseal dysplasia (SMD Sedaghatian-like)	重症脊椎骨幹端異形成症(脊椎骨幹端異形成症 Sedaghatian様)	AR		7q11	*SBDS*	SBDS gene, function still unclear	
Opsismodysplasia	成熟遅延骨異形成症	AR	258480				

タナトフォリック骨異形成症1型・2型(グループ1), 軟骨無発生症2型とTorrance骨異形成症(グループ2), 線維性軟骨発生症(グループ3), 軟骨無発生症1B型(ACG1B, グループ4), 変容性骨異形成症(グループ8)も参照.

15. Acromelic dysplasias	**15. 遠位肢異形成症**

グループ / 疾患名(原文)	グループ / 疾患名(和訳)	遺伝形式	MIM番号	遺伝子座	遺伝子	タンパク	注釈
Trichorhinophalangeal dysplasia types 1/3	毛髪鼻指節異形成症 1型/3 型	AD	190350	8q24	*TRPS1*	Zinc finger transcription factor	
Trichorhinophalangeal dysplasia type 2 (Langer-Giedion)	毛髪鼻指節異形成症 2型 (Langer-Giedion)	AD	150230	8q24	*TRPS1 and EXT1*	Zinc finger transcription factor and Exostosin 1	小欠失症侯群;グループ29の多発性軟骨性外骨腫症も参照
Acrocapitofemoral dysplasia	先端大腿骨頭異形成症	AR	607778	2q33-q35	*IHH*	Indian hedgehog	
Cranioectodermal dysplasia (Levin-Sensenbrenner) type 1	頭蓋外胚葉異形成症 (Levin-Sensenbrenner) 1型	AR	218330	3q21	*IFT122*	Intraflagellar transport 122 (Chlamydomonas, homolog of)	
Cranioectodermal dysplasia (Levin-Sensenbrenner) type 2	頭蓋外胚葉異形成症 (Levin-Sensenbrenner) 2型	AR	613610	2p24.1	*WDR35*	WD repeat-containing protein 35	
Geleophysic dysplasia	幸福顔貌骨異形成症	AR	231050	9q34.2	*ADAMTSL2*	ADAMTS-like protein 2	
Geleophysic dysplasia, other types	幸福顔貌骨異形成症, その他の型	AR					ADAMTSL2と非連鎖
Acromicric dysplasia	先端短肢異形成症	AD	102370				以前Fantasy Island骨異形成症あるいはTattoo骨異形成症として知られていた先端咽頭骨異形成症を含む
Acrodysostosis	先端異骨症	AD	101800				
Angel-shaped phalango-epiphyseal dysplasia (ASPED)	天使形指節骨・骨端異形成症 (ASPED)	AD	105835				短指症C型と関連または対立遺伝子
Saldino-Mainzer dysplasia	Saldino-Mainzer骨異形成症	AR	266920				

短肋骨異形成症グループも参照.

16. Acromesomelic dysplasias	**16. 遠位中間肢異形成症**						
Acromesomelic dysplasia type Maroteaux	遠位中間肢異形成症Maroteaux型 (AMDM)	AR	602875	9p13-12	*NPR2*	Natriuretic peptide receptor 2	
Grebe dysplasia	Grebe骨異形成症	AR	200700	20q11.2	*GDF5*	Growth and Differentiation Factor 5	遠位中間肢異形成症 Hunter-Thompson型を含む。短指症(グループ37)も参照
Fibular hypoplasia and complex brachydactyly (Du Pan)	腓骨低形成複雑短指症 (Du Pan)	AR	228900	20q11.2	*GDF5*	Growth and Differentiation Factor 5	短指症(グループ37)も参照
Acromesomelic dysplasia with genital anomalies	性器異常を伴う遠位中間肢異形成症	AR	609441	4q23-24	*BMPR1B*	Bone morphogenetic protein receptor	
Acromesomelic dysplasia, Osebold-Remondini	遠位中間肢異形成症, Osebold-Remondini型	AD	112910				

17. Mesomelic and rhizo-mesomelic dysplasias	**17. 中間肢・近位肢中間肢異形成症**						
Dyschondrosteosis (Leri- Weill)	異軟骨骨症 (Leri-Weill)	Pseudo-AD	127300	Xpter-p22.32	*SHOX*	Short stature – homeobox gene	Reinhardt-Pfeiffer骨異形成症(MIM 191400)を含む
Langer type (homozygous dyschondrosteosis)	Langer 型 (ホモ接合性異軟骨骨症)	Pseudo-AR	249700	Xpter-p22.32	*SHOX*	Short stature – homeobox gene	
Omodysplasia	肩骨異形成症	AR	258315	13q31-q32	*GPC6*	Glypican 6	「優性型肩骨異形成症」(OMIM 164745)の存在はまだ確認されていない
Robinow syndrome, recessive type	Robinow症候群, 劣性型	AR	268310	9q22	*ROR2*	Receptor tyrosine kinase-like orphan receptor 2	以前のCOVESDEM(中間肢短縮を伴う肋骨・脊椎分節異常)を含む。短指症B型も参照
Robinow syndrome, dominant type	Robinow症候群, 優性型	AD	180700				
Mesomelic dysplasia, Korean type	中間肢異形成症, Korea型	AD		2q24-32		Duplication in HOXD gene cluster	
Mesomelic dysplasia, Kantaputra type	中間肢異形成症, Kantaputra型	AD	156232	2q24-32		Duplications in HOXD gene cluster	
Mesomelic dysplasia, Nievergelt type	中間肢異形成症, Nievergelt型	AD	163400				
Mesomelic dysplasia, Kozlowski-Reardon type	中間肢異形成症, Kozlowski-Reardon型	AR	249710				
Mesomelic dysplasia with acral synostoses (Verloes-David-Pfeiffer type)	先端癒合症を伴う中間肢異形成症 (Verloes-David-Pfeiffer型)	AD	600383	8q13	*SULF1 and SLCO5A1*	Heparan sulfate 6-O-endosulfatase 1 and solute carrier organic anion	2つの隣接遺伝子を含む小欠失症侯群
Mesomelic dysplasia, Savarirayan type (Triangular Tibia-Fibular Aplasia)	中間肢異形成症, Savarirayan型 (三角形脛骨・腓骨無形成)	SP	605274				Nievergelt型骨異形成症と関連がある可能性. 意義不明の2q11.2小欠失を伴う1報告例あり

18. Bent bones dysplasias	**18. 弯曲骨異形成症**						
Campomelic dysplasia (CD)	屈曲肢異形成症 (CD)	AD	114290	17q24.3-25.1	*SOX9*	SRY-box 9	軽症型屈曲肢異形成症 (MIM 602196)と同様, acampomelic campomelic dysplasia (ACD) を含む
Stüve-Wiedemann dysplasia	Stüve-Wiedemann骨異形成症	AR	601559	5p13.1	*LIFR*	Leukemia Inhibitory Factor Receptor	以前の新生児Schwartz-Jampel症候群またはSchwartz-Jampel症候群2型と呼ばれていた疾患を含む

グループ / 疾患名(原文)	グループ / 疾患名(和訳)	遺伝形式	MIM番号	遺伝子座	遺伝子	タンパク	注釈
Kyphomelic dysplasia, several forms	後彎肢異形成症, 各型		211350				おそらく異質性あり
生下時の骨彎曲は, 以下を含む多様な疾患でみられる: 骨形成不全症, Antley-Bixler症候群, 軟骨・毛髪低形成症, Cumming 症候群, 低フォスファターゼ症, 分節異常骨異形成症, タナトフォリック骨異形成症, 呼吸不全性胸郭異形成症, など.							
19. Slender bone dysplasia group	**19. 狭細骨異形成症グループ**						
3-M syndrome (3M1)	3M症候群 (3M1)	AR	273750	6p21.1	*CUL7*	Cullin 7	高脊椎異形成症とYakut低身長症侯群を含む
3-M syndrome (3M2)	3M症候群 (3M2)	AR	612921	2q35	*OBSL1*	Obscurin-like 1	
Kenny-Caffey dysplasia type 1	Kenny-Caffey骨異形成症1型	AR	244460	1q42-q43	*TBCE*	Tubulin-specific chaperone E	
Kenny-Caffey dysplasia type 2	Kenny-Caffey骨異形成症2型	AD	127000				
Microcephalic osteodysplastic primordial dwarfism type 1/3 (MOPD1)	小頭型骨異形成性原発小人症 1型/3型 (MOPD1)	AR	210710	2q			Taybi-Linder頭骨格異形成症を含む
Microcephalic osteodysplastic primordial dwarfism type 2 (MOPD2; Majewski type)	小頭型骨異形成性原発小人症 2型 (MOPD2; Majewski型)	AR	210720	21q	*PCNT2*	Pericentrin 2	
IMAGE syndrome (intrauterine growth retardation, metaphyseal dysplasia, adrenal hypoplasia, and genital anomalies)	IMAGE症候群 (子宮内発育遅延, 骨幹端異形成, 副腎低形成, 性器異常)	XL/AD	300290				異質性がある可能性
Osteocraniostenosis	骨頭蓋狭窄症	SP	602361				同胞発生例の報告あり, 遺伝形式不明
Hallermann-Streiff syndrome	Hallermann-Streiff症侯群	AR	234100				1例のみでGJA1変異の報告
脳・関節・指異形成症を参照.							
20. Dysplasias with multiple joint dislocations	**20. 多発性脱臼を伴う骨異形成症**						
Desbuquois dysplasia (with accessory ossification centre in digit 2)	Desbuquois骨異形成症(第2指に余剰骨化中心を伴う)	AR	251450	17q25.3	*CANT1*		
Desbuquois dysplasia with short metacarpals and elongated phalanges (Kim type)	中手骨短縮と指節骨延長を伴うDesbuquois骨異形成症 (Kim型)	AR	251450	17q25.3	*CANT1*		
Desbuquois dysplasia (other variants with or without accessory ossification centre)	Desbuquois骨異形成症(余剰骨化中心を伴う/伴わない他の変異型)	AR					おそらく遺伝的異質性あり
Pseudodiastrophic dysplasia	偽性捻曲性骨異形成症	AR	264180				
先天性脱臼を伴う軟骨異形成症, CHST3型(グループ4), 骨発生不全症3型とLarsen症候群(グループ7), 関節弛緩を伴う脊椎骨端骨幹端異形成症(グループ13)も参照.							
21. Chondrodysplasia punctata (CDP) group	**21. 点状軟骨異形成症(CDP)グループ**						
CDP, X-linked dominant, Conradi-Hünermann type (CDPX2)	点状軟骨異形成症, X染色体優性, Conradi-Hünermann型 (CDPX2)	XLD	302960	Xp11	*EBP*	Emopamil-binding protein	
CDP, X-linked recessive, brachytelephalangic type (CDPX1)	点状軟骨異形成症, X連鎖性劣性, 末節骨短縮型 (CDPX1)	XLR	302950	Xp22.3	*ARSE*	Arylsulfatase E	
CHILD (congenital hemidysplasia, ichthyosis, limb defects)	CHILD症候群 (先天性片側異形成, 魚鱗癬, 四肢欠損)	XLD	308050	Xp11	*NSDHL*	NAD(P)H steroid dehydrogenase-like protein	
CHILD (congenital hemidysplasia, ichthyosis, limb defects)	CHILD症候群 (先天性片側異形成, 魚鱗癬, 四肢欠損)	XLD	308050	Xq28	*EBP*	Emopamil-binding protein	
Greenberg dysplasia	Greenberg骨異形成症	AR	215140	1q42.1	*LBR*	Lamin B receptor, 3-beta-hydroxysterol delta (14)-reductase	胎児水腫・異所性石灰化・虫食い像骨異形成症 (HEM) およびまだら状骨幹異形成症 を含む
Rhizomelic CDP type 1	近位肢型点状軟骨異形成症 1型	AR	215100	6q22-24	*PEX7*	Peroxisomal PTS2 receptor	
Rhizomelic CDP type 2	近位肢型点状軟骨異形成症 2型	AR	222765	1q42	*DHPAT*	Dihydroxyacetonephosphate	
Rhizomelic CDP type 3	近位肢型点状軟骨異形成症 3型	AR	600121	2q31	*AGPS*	Alkylglycerone-phosphate synthase (AGPS)	
CDP tibial-metacarpal type	点状軟骨異形成症 脛骨・中手骨型	AD/AR	118651				疾病分類が不確実
Astley-Kendall dysplasia	Astley-Kendall骨異形成症	AR?					骨形成不全症やGreenberg骨異形成症との関係が不明確
点状石灰化はZellweger, Smith-Lemli-Opitz, その他いくつかの症候群で生じることに注意. グループ13の脊椎骨端骨幹端異形成症, 短肢・異常石灰化型と同様, デスモステロール症を参照.							
22. Neonatal osteosclerotic dysplasias	**22.新生児骨硬化性異形成症**						
Blomstrand dysplasia	Blomstrand骨異形成症	AR	215045	3p22-21.1	*PTHR1*	PTH/PTHrP receptor 1	劣性の不活性化変異で生じる;Eiken骨異形成症とJansen骨異形成症を参照

グループ / 疾患名(原文)	グループ / 疾患名(和訳)	遺伝形式	MIM番号	遺伝子座	遺伝子	タンパク	注釈
Desmosterolosis	デスモステロール症	AR	602398	1p33-31.1	*DHCR24*	3-beta-hydroxysterol delta-24-reductase	他のステロール代謝に関連する疾患を参照
Caffey disease (including infantile and attenuated forms)	Caffey病 (乳児型・寛解型を含む)	AD	114000	17q21-22	*COL1A1*	Collagen 1, alpha-1 chain	1型コラーゲン遺伝子に関連する骨形成不全症(グループ25)を参照
Caffey disease (severe variants with prenatal	Caffey病 (出生前発症の重症型)	AR	114000				
Raine dysplasia (lethal and non-lethal forms)	Raine骨異形成症 (致死型・非致死型)	AR	259775	7p22	*FAM20C*		致死型と非致死型を含む
グループ21のAstley-Kendall骨異形成症と点状軟骨異形成症も参照.							
23. Increased bone density group (without modification of bone shape)	**23. 骨変形を伴わない骨硬化性疾患グループ**						
Osteopetrosis, severe neonatal or infantile forms (OPTB1)	大理石骨病, 重症新生児型/乳児型 (OPTB1)	AR	259700	11q13	*TCIRG1*	Subunit of ATPase proton pump	
Osteopetrosis, severe neonatal or infantile forms (OPTB4)	大理石骨病, 重症新生児型/乳児型 (OPTB4)	AR	611490	16p13	*CLCN7*	Chloride channel 7	
Osteopetrosis, infantile form, with nervous system involvement (OPTB5)	大理石骨病, 乳児型, 神経系の罹患を伴う (OPTB5)	AR	259720	6q21	*OSTM1*	Grey lethal / Osteopetrosis associated transmembrane protein	
Osteopetrosis, intermediate form, osteoclast-poor (OPTB2)	大理石骨病, 中間型, 破骨細胞減少型 (OPTB2)	AR	259710	13q14.11	*RANKL (TNFSF11)*	Receptor activator of NF-kappa-B ligand (Tumor necrosis factor ligand superfamily, member 11)	
Osteopetrosis, infantile form, osteoclast- poor with immunoglobulin deficiency (OPTB7)	大理石骨病, 乳児型, 免疫グロブリン欠乏を伴う破骨細胞減少型 (OPTB7)	AR	612302	18q21.33	*RANK (TNFRSF11A)*	Receptor activator of NF-kappa-B	骨溶解症グループ(グループ28)の家族性拡張性骨溶解症を参照
Osteopetrosis, intermediate form (OPTB6)	大理石骨病, 中間型 (OPTB6)	AR	611497	17q21.3	*PLEKHM1*	Pleckstrin homology domain-	
Osteopetrosis, intermediate form (OPTA2)	大理石骨病, 中間型 (OPTA2)	AR	259710	16p13	*CLCN7*	Chloride channel pump	
Osteopetrosis with renal tubular acidosis	腎細管性アシドーシスを伴う大理石骨病(OPTB3)	AR	259730	8q22	*CA2*	Carbonic anhydrase 2	
Osteopetrosis, late-onset form type 1 (OPTA1)	大理石骨病, 遅発型1型 (OPTA1)	AD	607634	11q13.4	*LRP5*	Low density lipoprotein receptor-related protein 5	Worth型骨硬化症(MIM 144750)を含む
Osteopetrosis, late-onset form type 2 (OPTA2)	大理石骨病, 遅発型2型 (OPTA2)	AD	166600	16p13	*CLCN7*	Chloride channel 7	
Osteopetrosis with ectodermal dysplasia and immune defect (OLEDAID)	外胚葉異形成と免疫不全を伴う大理石骨病 (OLEDAID)	XL	300301	Xq28	*IKBKG (NEMO)*	Inhibitor of kappa light polypeptide gene enhancer, kinase of	
Osteopetrosis, moderate form with defective leucocyte adhesion (LAD3)	大理石骨病, 白血球接着不全を伴う中等症型 (LAD3)	AR	612840	11q12	*FERMT3 (KIND3)*	Fermitin 3 (Kindlin 3)	
Osteopetrosis, moderate form with defective leucocyte adhesion	大理石骨病, 白血球接着不全を伴う中等症型	AR	612840	11q13	*RASGRP2 (CalDAG-GEF1)*	Ras guanyl nucleotide-releasing protein 2	
Pyknodysostosis	濃化異骨症	AR	265800	1q21	*CTSK*	Cathepsin K	
Osteopoikilosis	骨斑紋症	AD	155950	12q14	*LEMD3*	LEM domain-containing 3	Buschke-Ollendorff症侯群(MIM 166700)を含む
Melorheostosis with osteopoikilosis	骨斑紋症を伴う流蝋骨症	AD	155950	12q14	*LEMD3*	LEM domain-containing 3	混合型骨硬化性異形成症を含む
Osteopathia striata with cranial sclerosis (OSCS)	頭蓋骨硬化を伴う骨線状症 (OSCS)	XLD	300373	Xq11.1	*WTX*	FAM123B	
Melorheostosis	流蝋骨症 (メロレオストーシス)	SP					生殖細胞系列にLEMD3変異は今まで明らかにされていない
Dysosteosclerosis	異骨性骨硬化症	AR	224300				骨硬化性骨幹端異形成症と関連がある可能性
Osteomesopyknosis	骨中間濃化症	AD	166450				
Osteopetrosis with infantile neuroaxonal dysplasia	乳児神経軸索異形成症を伴う大理石骨病	AR?	600329				神経系の罹患を伴う大理石骨病と同じか(上を見よ)?
24. Increased bone density group with metaphyseal and/or diaphyseal involvement	**24. 骨幹端・骨幹罹患を伴う骨硬化性疾患グループ**						
Craniometaphyseal dysplasia, autosomal dominant type	頭蓋骨幹端異形成症, 常染色体優性型	AD	123000	5p15.2-14.2	*ANKH*	Homolog of mouse ANK (ankylosis) gene	機能獲得変異
Diaphyseal dysplasia Camurati-Engelmann	骨幹異形成症 Camurati-Engelmann病	AD	131300	19q13	*TGFbeta1*	Transforming growth factor beta 1	
Hematodiaphyseal dysplasia Ghosal	血液骨幹異形成症 Ghosal	AR	231095	7q34	*TBXAS1*	Thromboxane A synthase 1	
Hypertrophic osteoarthropathy	過形成型骨関節症	AR	259100	4q34-35	*HPGD*	15-alpha-hydroxyprostaglandin dehydrogenase	頭蓋・骨関節症と劣性の皮膚骨膜肥厚症を含む
Pachydermoperiostosis (hypertrophic osteoarthropathy, primary, autosomal dominant)	皮膚骨膜肥厚症 (過形成型骨関節症, 一次性, 常染色体優性)	AD	167100				劣性型(MIM 259100, HPGD欠損)との関係は不明

グループ / 疾患名(原文)	グループ / 疾患名(和訳)	遺伝形式	MIM番号	遺伝子座	遺伝子	タンパク	注釈
Oculodentoosseous dysplasia (ODOD) mild type	眼歯骨異形成症 (ODOD) 軽症型	AD	164200	6q22-23	*GJA1*	Gap junction protein alpha-1	
Oculodentoosseous dysplasia (ODOD) severe	眼歯骨異形成症 (ODOD) 重症型	AR	257850				軽症型ODODのホモ接合の可能性
Osteoectasia with hyperphosphatasia (juvenile Paget disease)	高フォスファターゼ症を伴う骨肥大症 (若年性Paget病)	AR	239000	8q24	*OPG*	Osteoprotegerin	
Sclerosteosis	硬化性骨症	AR	269500	17q12-21	*SOST*	Sclerostin	
Endosteal hyperostosis, van Buchem type	骨内膜性骨増殖症, van Buchem型	AR	239100	17q12-21	*SOST*	Sclerostin	*SOST*の下流の52kb欠失に特異的
Trichodentoosseous dysplasia	毛髪歯骨異形成症	AD	190320	17q21	*DLX3*	Distal-less homeobox 3	
Craniometaphyseal dysplasia, autosomal recessive type	頭蓋骨幹端異形成症, 常染色体劣性型	AR	218400	6q21-22			
Diaphyseal medullary stenosis with bone	骨悪性腫瘍を伴う骨幹部骨髄腔狭窄症	AD	112250	9p21-p22			
Craniodiaphyseal dysplasia	頭蓋骨幹異形成症	AD	122860				
Craniometadiaphyseal dysplasia, Wormian bone	頭蓋骨幹端骨幹異形成症, Worm骨型	AR	--				
Endosteal sclerosis with cerebellar hypoplasia	小脳低形成を伴う骨内膜硬化症	AR	213002				
Lenz-Majewski hyperostotic dysplasia	Lenz-Majewski骨増殖異形成症	SP	151050				
Metaphyseal dysplasia, Braun-Tinschert type	骨幹端異形成症, Braun-Tinschert型	XL	605946				
Pyle disease	Pyle病	AR	265900				
25. Osteogenesis Imperfecta and decreased bone density group	**25. 骨形成不全症と骨密度低下を示すグループ**						
骨形成不全症の分類についての記述は本文を参照のこと							
Osteogenesis imperfecta, non-deforming form	骨形成不全症, 非変形型 (OI1型)	AD			*COL1A1, COL1A2*	COL1A1: Collagen 1 alpha-1 chain, COL1A2: Collagen 1 alpha-2 chain, CRTAP: Cartilage-Associated Protein, LEPRE1: leucine proline-enriched proteoglycan (leprecan) 1, PPIB: peptidylprolyl isomerase B (cyclophilin B), FKBP10: FK506 binding protein 10, SERPINH: serpin peptidase inhibitor clade H 1, SP7: SP7 transcription factor (Osterix)	
Osteogenesis imperfecta, perinatal lethal form (OI type 2)	骨形成不全症, 周産期致死型 (OI 2型)	AD, AR			*COL1A1, COL1A2, CRTAP, LEPRE1, PPIB*		
Osteogenesis imperfecta, progressively deforming type (OI type 3)	骨形成不全症, 変形進行型 (OI 3型)	AD, AR			*COL1A1, COL1A2, CRTAP, LEPRE1, PPIB, FKBP10, SERPINH1*		Bruck 症候群1型も参照(下記)
Osteogenesis imperfecta, moderate form (OI type 4)	骨形成不全症, 中等症型 (OI 4型)	AD, AR			*COL1A1, COL1A2, CRTAP, FKBP10, SP7*		
Osteogenesis imperfecta with calcification of the interosseous membranes and/or hypertrophic callus (OI type 5)	骨間膜石灰化・過形成仮骨を伴う骨形成不全症 (OI 5型)	AD	610967				
Osteogenesis imperfecta, other types	骨形成不全症, その他の型						
Bruck syndrome type 1 (BS1)	Bruck 症候群 (BS1)	AR	259450	17p12	*FKBP10*	FK506 binding protein 10	上記常染色体劣性骨形成不全症を参照; OI3とBS1間には家族内多様性の報告あり
Bruck syndrome type 2 (BS2)	Bruck 症候群 (BS2)	AR	609220	3q23-24	*PLOD2*	Procollagen lysyl hydroxylase 2	
Osteoporosis-pseudoglioma syndrome	骨粗鬆症・偽神経膠腫症候群	AR	259770	11q12-13	*LRP5*	LDL-receptor related protein 5	
Calvarial doughnut lesions with bone fragility	骨脆弱性を伴う頭蓋ドーナッツ様病変	AD	126550				
Idiopathic juvenile osteoporosis	特発性若年性骨粗鬆症	SP	259750				*LRP5*遺伝子内のヘテロ変異も報告あり
Cole-Carpenter dysplasia (bone fragility with craniosynostosis)	Cole-Carpenter骨異形成症 (頭蓋骨癒合症を伴う骨脆弱症)	SP	112240				group33の頭蓋骨癒合症候群も参照
Spondylo-ocular dysplasia	脊椎・眼異形成症	AR	605822				1型コラーゲンと2型コラーゲン遺伝子又は*LRP5*と非連鎖
Osteopenia with radiolucent lesions of the	下顎骨X線透過性病変を伴う骨減少症	AD	166260				
Ehlers-Danlos syndrome, progeroid form	Ehlers-Danlos症候群, 早老型	AR	130070	5q35	*B4GALT7*	Xylosylprotein 4-beta-	
Geroderma osteodysplasticum	骨異形性老人様皮膚症	AR	231070	1q24.2	*GORAB*	SCYL1-binding protein 1	
Cutis laxa, autosomal recessive form, type 2B (ARCL2B)	皮膚弛緩症, 常染色体劣性型, 2B型 (ARCL2B)	AR	612940	17q25.3	*PYCR1*	Pyrroline-5-carboxylate reductase 1	骨格の特徴は早老型EDSや骨異形成性老人様皮膚症と重複あり
Cutis laxa, autosomal recessive form, type 2A (ARCL2A) (Wrinkly skin syndrome)	皮膚弛緩症, 常染色体劣性型, 2A型 (ARCL2A) (皺状皮膚症候群)	AR	278250, 219200	12q24.3	*ATP6VOA2*	ATPase, H+ transporting, lysosomal, V0 subunit A2	骨格の特徴は早老型EDSや骨異形成性老人様皮膚症と重複あり
Singleton-Merten dysplasia	Singleton-Merten骨異形成症	AD	182250				

グループ / 疾患名(原文)	グループ / 疾患名(和訳)	遺伝形式	MIM番号	遺伝子座	遺伝子	タンパク	注釈
26. Abnormal mineralization group	**26. 異常骨石灰化グループ**						
Hypophosphatasia, perinatal lethal and infantile forms	低フォスファターゼ症, 周産期致死性型・乳児型	AR	241500	1p36.1-p34	*ALPL*	Alkaline phosphatase, tissue non-specific (TNSALP)	家族内多様性あり
Hypophosphatasia, adult form	低フォスファターゼ症, 成人型	AD	146300	1p36.1-p34	*ALPL*	Alkaline phosphatase, tissue non-specific (TNSALP)	歯低フォスファターゼ症を含む
Hypophosphatemic rickets, X-linked dominant	低リン血症性くる病, X連鎖性優性	XLD	307800	Xp22	*PHEX*	X-linked hypophosphatemia membrane protease	
Hypophosphatemic rickets, autosomal dominant	低リン血症性くる病, 常染色体優性	AD	193100	12p13.3	*FGF23*	Fibroblast growth factor 23	
Hypophosphatemic rickets, autosomal recessive, type 1 (ARHR1)	低リン血症性くる病, 常染色体劣性, 1型 (ARHR1)	AR	241520	4q21	*DMP1*	Dentin matrix acidic phosphoprotein 1	
Hypophosphatemic rickets, autosomal recessive, type 2 (ARHR2)	低リン血症性くる病, 常染色体劣性, 2型 (ARHR2)	AR	613312	6q23	*ENPP1*	Ectonucleotide pyrophosphatase/phosphodiesterase 1	
Hypophosphatemic rickets with hypercalciuria, X-linked recessive	高カルシウム尿症を伴う低リン血症性くる病, X連鎖劣性	XLR	300554	Xp11.22	*ClCN5*	Chloride channel 5	Dent 病複合体の一部
Hypophosphatemic rickets with hypercalciuria, autosomal recessive (HHRH)	高カルシウム尿症を伴う低リン血症性くる病, 常染色体優性 (HHRH)	AR	241539	9q34	*SLC34A3*	Sodium-phosphate cotransporter	
Neonatal hyperparathyroidism, severe form	新生児上皮小体機能亢進症, 重症型	AR	239200	3q13.3-21	*CASR*	Calcium-sensing receptor	
Familial hypocalciuric hypercalcemia with transient neonatal hyperparathyroidism	一過性新生児上皮小体機能亢進症を伴う家族性低カルシウム尿性高カルシウム血症	AD	145980	3q13.3-21	*CASR*	Calcium-sensing receptor	
Calcium pyrophosphate deposition disease (familial chondrocalcinosis) type 2	カルシウムピロリン酸塩沈着症 (家族性軟骨石灰症)2型	AD	118600	5p15.2-14.2	*ANKH*	Homolog of mouse ANK (ankylosis) gene	機能喪失変異(group24の頭蓋骨幹端異形成症を参照)
Jansen骨異形成症, Eiken骨異形成症も参照.							
27. Lysosomal Storage Diseases with Skeletal Involvement (Dysostosis Multiplex group)	**27. 骨変化を伴うリソソーム蓄積症(多発性異骨症グループ)**						
Mucopolysaccharidosis type 1H / 1S	ムコ多糖症 1H/1S型	AR	607014	4p16.3	*IDA*	Alpha-1-Iduronidase	
Mucopolysaccharidosis type 2	ムコ多糖症 2型	XLR	309900	Xq27.3-28	*IDS*	Iduronate-2-sulfatase	
Mucopolysaccharidosis type 3A	ムコ多糖症 3A型	AR	252900	17q25.3	*HSS*	Heparan sulfate sulfatase	
Mucopolysaccharidosis type 3B	ムコ多糖症 3B型	AR	252920	17q21	*NAGLU*	N-Ac-beta-D-glucosaminidase	
Mucopolysaccharidosis type 3C	ムコ多糖症 3C型	AR	252930	8p11-q13	*HSGNAT*	Ac-CoA: alpha-glucosaminide N-acetyltransferase	
Mucopolysaccharidosis type 3D	ムコ多糖症 3D型	AR	252940	12q14	*GNS*	N-Acetylglucosamine 6-sulfatase	
Mucopolysaccharidosis type 4A	ムコ多糖症 4A型	AR	253000	16q24.3	*GALNS*	Galactosamine-6-sulfate sulfatase	
Mucopolysaccharidosis type 4B	ムコ多糖症 4B型	AR	253010	3p21.33	*GLBI*	beta-Galactosidase	
Mucopolysaccharidosis type 6	ムコ多糖症 6型	AR	253200	5q13.3	*ARSB*	Arylsulfatase B	
Mucopolysaccharidosis type 7	ムコ多糖症 7型	AR	253220	7q21.11	*GUSB*	beta-Glucuronidase	
Fucosidosis	フコシドーシス	AR	230000	1p34	*FUCA*	alpha-Fucosidase	
alpha-Mannosidosis	アルファ・マンノシドーシス	AR	248500	19p13.2-12	*MANA*	alpha-Mannosidase	
beta-Mannosidosis	ベータ・マンノシドーシス	AR	248510	4q22-25	*MANB*	beta-Mannosidase	
Aspartylglucosaminuria	アスパルチルグルコサミン尿症	AR	208400	4q23-27	*AGA*	Aspartyl-glucosaminidase	
GMI Gangliosidosis, several forms	GMIガングリオシドーシス, 各型	AR	230500	3p21-14.2	*GLB1*	beta-Galactosidase	
Sialidosis, several forms	シアリドーシス, 各型	AR	256550	6p21.3	*NEU1*	Neuraminidase (sialidase)	
Sialic acid storage disease (SIASD)	シアル酸蓄積症 SIASD)	AR	269920	6q14-q15	*SLC17A5*	Sialin (sialic acid transporter)	
Galactosialidosis, several forms	ガラクトシアリドーシス, 各型	AR	256540	20q13.1	*PPGB*	beta-Galactosidase protective protein	
Multiple sulfatase deficiency	多種サルファターゼ欠損症	AR	272200	3p26	*SUMF1*	Sulfatase-modifying factor-1	
Mucolipidosis II (I-cell disease), alpha/beta type	ムコ脂質症Ⅱ型 (I-cell 病), アルファ/ベータ型	AR	252500	12q23.2	*GNPTAB*	N-Acetylglucosamine 1-	
Mucolipidosis III (Pseudo-Hurler polydystrophy), alpha/beta type	ムコ脂質症Ⅲ (偽性Hurlerポリジストロフィー), アルファ/ベータ型	AR	252600	12q23.2	*GNPTAB*	N-Acetylglucosamine 1-phosphotransferase, alpha/beta	
Mucolipidosis III (Pseudo-Hurler polydystrophy), gamma type	ムコ脂質症Ⅲ (偽性Hurlerポリジストロフィー), ガンマ型	AR	252605	16p13.3	*GNPTG*	N-Acetylglucosamine 1-phosphotransferase, gamma subunit	

グループ / 疾患名（原文）	グループ / 疾患名（和訳）	遺伝形式	MIM番号	遺伝子座	遺伝子	タンパク	注釈
28. Osteolysis group	**28. 骨溶解症グループ**						
Familial expansile osteolysis	家族性拡張性骨溶解症	AD	174810	18q22.1	*RANK (TNFRSF11A)*		拡張性骨高フォスファターゼ症を含む（MIM602080）
Mandibuloacral dysplasia type A	下顎先端症候群　A型	AD	248370	1q21.2	*LMNA*	Lamin A/C	
Mandibuloacral dysplasia type B	下顎先端症候群　B型	AR	608612	1p34	*ZMPSTE24*	Zinc metalloproteinase	
Progeria, Hutchinson-Gilford type	早老症, Hutchinson-Gilford 型	AD	176670	1q21.2	*LMNA*	Lamin A/C	
Torg-Winchester syndrome	Torg-Winchester 症候群	AR	259600	16q13	*MMP2*	Matrix metalloproteinase 2	結節症・関節症・骨溶解症候群（MIM605156)を含む
Hajdu-Cheney syndrome	Hajdu-Cheney 症候群	AD	102500				
Multicentric carpal-tarsal osteolysis with and without nephropathy	多中心性手根骨・足根骨溶解症（腎症を伴う/伴わない）	AD	166300				
Lipomembraneous osteodystrophy with leukoencephalopathy (presenile dementia with bone cysts; Nasu-Hakola)	白質脳症を伴う脂肪膜性骨異栄養症（骨嚢腫を伴う初老期認知症; Nasu-Hakola）	AR	221770	6p21.2	*TREM2*	Triggering receptor expressed on myeloid cells 2	
Lipomembraneous osteodystrophy with leukoencephalopathy (presenile dementia with bone cysts; Nasu-Hakola)	白質脳症を伴う脂肪膜性骨異栄養症（骨嚢腫を伴う初老期認知症; Nasu-Hakola）	AR	221770	19q13.1	*TYROBP*	Tyro protein tyrosine kinase-binding protein	

濃化異骨症, 鎖骨頭蓋異形成症, Singleton-Merten症候群も参照. 注:いくつかの神経学的状態は先端骨溶解の原因となりうる.

29. Disorganized development of skeletal components group	**29. 骨格成分の発生異常グループ**						
Multiple cartilaginous exostoses 1	多発性軟骨性外骨腫症 1型	AD	133700	8q23-24.1	*EXT1*	Exostosin-1	
Multiple cartilaginous exostoses 2	多発性軟骨性外骨腫症　2型	AD	133701	11p12-11	*EXT2*	Exostosin-2	
Multiple cartilaginous exostoses 3	多発性軟骨整外骨腫症　3型	AD	600209	19p			
Cherubism	ケルビム症	AD	118400	4p16	*SH3BP2*	SH3 domain-binding protein 2	
Fibrous dysplasia, polyostotic form	線維性骨異形成症, 多骨性	SP	174800	20q13	*GNAS1*	Guanine nucleotide-binding protein, alpha-stimulating activity subunit 1	体細胞モザイクやインプリンティング現象; McCune-Albright症候群を含む
Progressive osseous heteroplasia	進行性骨性異形成症	AD	166350	20q13	*GNAS1*	Guanine nucleotide-binding protein, alpha-stimulating activity subunit 1	遺伝子はインプリンティングを生じやすい
Gnathodiaphyseal dysplasia	下顎骨幹異形成症	AD	166260	11p15.1-	*TMEM16E*	Transmembrane protein 16E	
Metachondromatosis	メタコンドロマトーシス	AD	156250	12q24	*PTPN11*	Protein-tyrosine phosphatase nonreceptor-type 11	
Osteoglophonic dysplasia	骨空洞性異形成症	AD	166250	8p11	*FGFR1*	Fibroblast growth factor receptor 1	グループ33の頭蓋骨癒合症候群も参照
Fibrodysplasia ossificans progressiva (FOP)	進行性骨化性線維異形成症	AD, SP	135100	2q23-24	*ACVR1*	Activin A (BMP type 1) receptor	
Neurofibromatosis type 1 (NF1)	神経線維腫症 1型（NF1）	AD	162200	17q11.2	*NF1*	Neurofibromin	
Carpotarsal osteochondromatosis	手根足根骨軟骨腫症	AD	127820				
Cherubism with gingival fibromatosis (Ramon syndrome)	歯肉線維腫症を伴うケルビム症（Ramon症候群）	AR	266270				
Dysplasia epiphysealis hemimelica (Trevor)	片肢性骨端異形成症（Trevor）	SP	127800				
Enchondromatosis (Ollier)	内軟骨腫症（Ollier）	SP	166000				*PTHR1*と*PTPN11*変異が少数例で発見されたのみ, 役割不明
Enchondromatosis with hemangiomata (Maffucci)	血管腫を伴う内軟骨腫症（Maffucci）	SP	166000				*PTPN11*変異が少数例で発見されたのみ, 役割不明

グループ30のProteus 症候群も参照.

30. Overgrowth syndromes with skeletal involvement	**30. 骨格罹患を示す過成長症候群**						
Weaver syndrome	Weaver症候群	SP/AD	277590				*NSD1*変異を伴う報告例あり（Sotos症候群参照）
Sotos syndrome	Sotos症候群	AD	117550	5q35	*NSD1*	Nuclear receptor-binding su-var, enhancer of zeste, and trithorax domain protein 1	症例により*NFIX*変異の可能性あり（Marshall-Smith症候群参照）
Marshall-Smith syndrome	Marshall－Smith症候群	SP	602535	19p13.3	*NFIX*	nuclear factor I/X	Sotos症候群との臨床的重複例あり（上記参照）
Proteus syndrome	Proteus症候群	SP	176920				Proteus様症例は*PTEN*遺伝子に変異を伴うものがある

グループ / 疾患名(原文)	グループ / 疾患名(和訳)	遺伝形式	MIM番号	遺伝子座	遺伝子	タンパク	注釈
Marfan syndrome	Marfan症候群	AD	154700	15q21.1	*FBN1*	Fibrillin 1	
Congenital contractural arachnodactyly	先天性拘縮性くも状指症	AD	121050	5q23.3	*FBN2*	Fibrillin 2	
Loeys-Dietz syndrome types 1A and 2A	Loeys-Dietz 症候群1A型と2A型	AD	609192, 610168,	9q22	*TGFBR1,*	TGFbeta receptor subunit 1	
Loeys-Dietz syndrome types 1B and 2B	Loeys-Dietz 症候群1B型と2B型	AD	608967, 610380	3p22	*TGFBR2*	TGFbeta receptor subunit 2	
Overgrowth syndrome with 2q37 translocations	2q37転座を伴う過成長症候群	SP	--	2q37	*NPPC*	Natriuretic peptide precursor C	過成長はおそらく*NPPC*の過剰発現が原因
Overgrowth syndrome with skeletal dysplasia (Nishimura-Schmidt, endochondral gigantism)	骨異形成を伴う過成長症候群 (Nishimura-Schmidt, 内軟骨性巨人症)	SP?					疾病分類は不明確だがはっきりとした骨格表現型

頭蓋骨癒合グループ(グループ33)のShprintzen-Goldberg 症候群も参照.

31. Genetic inflammatory/rheumatoid-like osteoarthropathies	**31. 遺伝性炎症性/リウマチ様骨関節症**						
Progressive pseudorheumatoid dysplasia (PPRD; SED with progressive arthropathy)	進行性偽性リウマチ様骨異形成症 (PPRD; 進行性関節症を伴う脊椎骨端異形成症)	AR	208230	6q22-23	*WISP3*	WNT1-inducible signaling pathway protein 3	
Chronic infantile neurologic cutaneous articular syndrome (CINCA) / neonatal onset multisystem inflammatory disease (NOMID)	慢性乳児神経皮膚関節症候群 (CINCA)/新生児期発症多系統炎症性疾患 (NOMID)	AD	607115	1q44	*CIAS1*	Cryopyrin	
Sterile multifocal osteomyelitis, periostitis, and pustulosis (CINCA/NOMID-like)	無菌性多巣性骨髄炎、骨膜炎、膿疱症 (CINCA/NOMID様)	AR	147679	2q14.2	*IL1RN*	Interleukin 1 receptor antagonist	
Chronic recurrent multifocal osteomyelitis with congenital dyserythropoietic anemia (CRMO with CDA; Majeed syndrome)	先天性異常赤血球性貧血を伴う慢性再発性多巣性骨髄炎 (CDAを伴うCRMO; Majeed症候群)	AR	609628	18p11.3	*LPIN2*	Lipin 2	
Hyperostosis/hyperphosphatemia syndrome	骨増殖症/高リン血症症候群	AR	610233	2q24-q31;	*GALNT3*	UDP-N-acetyl-alpha-D-	
Infantile systemic hyalinosis/Juvenile hyaline fibromatosis (ISH/JHF)	乳児全身性硝子化症/若年性ヒアリン線維腫症 (ISH/JHF)	AR	236490	4q21	*ANTXR2 (CMG2)*	Anthrax toxin receptor 2	若年性ヒアリン線維腫症(JHF, 228600)およびPuretic症候群を含む
32. Cleidocranial dysplasia and isolated cranial ossification defects group	**32. 鎖骨頭蓋異形成症および単独頭蓋骨骨化障害グループ**						
Cleidocranial dysplasia	鎖骨頭蓋異形成症	AD	119600	6p21	*RUNX2*	Runt related transcription factor 2	
CDAGS syndrome (craniosynostosis, delayed fontanel closure, parietal foramina, imperforate anus, genital anomalies, skin eruption)	CDAGS症候群 (頭蓋骨癒合症, 泉門閉鎖遅延, 頭頂孔, 鎖肛, 性器異常, 発疹)	AR	603116	22q12-q13			
Yunis-Varon dysplasia	Yunis-Varon骨異形成症	AR	216340				
Parietal foramina (isolated)	頭頂孔 (単独型)	AD	168500	11q11.2	*ALX4*	Aristaless-like 4	前頭鼻異形成症I型(グループ34)を参照
Parietal foramina (isolated)	頭頂孔 (単独型)	AD	168500	5q34-35	*MSX2*	Muscle segment homeobox 2	

濃化異骨症, 皺状皮膚症候群, 他を参照.

33. Craniosynostosis syndromes	**33. 頭蓋骨癒合症候群**						
Pfeiffer syndrome (FGFR1-related)	Pfeiffer症候群 (FGFR1関連)	AD	101600	8p12	*FGFR1*	Fibroblast growth factor receptor 1	多くは*FGFR1* P252R変異(FGFR2関連Pfeiffer症候群より一般的に軽い表現型)
Pfeiffer syndrome (FGFR2-related)	Pfeiffer症候群 (FGFR2関連)	AD	101600	10q26.12	*FGFR2*	Fibroblast growth factor receptor 2	*FGFR2*変異(下記参照)によって発症するJackson-Weiss症候群(MIM 123150)とAntley-Bixler症候群変異型を含む
Apert syndrome	Apert症候群	AD	101200	10q26.12	*FGFR2*	Fibroblast growth factor receptor 2	
Craniosynostosis with cutis gyrata (Beare-	脳回状皮膚を伴う頭蓋骨癒合症 (Beare-	AD	123790	10q26.12	*FGFR2*	Fibroblast growth factor receptor 2	
Crouzon syndrome	Crouzon症候群	AD	123500	10q26.12	*FGFR2*	Fibroblast growth factor receptor 2	
Crouzon-like craniosynostosis with acanthosis nigricans (Crouzonodermoskeletal syndrome)	黒色表皮腫を伴うCrouzon様頭蓋骨癒合症 (Crouzon皮膚骨格症候群)	AD	612247	4p16.3	*FGFR3*	Fibroblast growth factor receptor 3	*FGFR3* A391E特異的変異により定義される
Craniosynostosis, Muenke type	頭蓋骨癒合症, Muenke型	AD	602849	4p16.3	*FGFR3*	Fibroblast growth factor receptor 3	*FGFR3* P250R特異的変異により定義される
Antley-Bixler syndrome	Antley-Bixler症候群	AR	201750	7q11.23	*POR*	Cytochrome P450 oxidoreductase	*FGFR2*変異を有する類似症例はPfeiffer症候群(MIM207410)に分類される
Craniosynostosis Boston type	頭蓋骨癒合症, Boston型	AD	604757	5q35.2	*MSX2*	MSX2	1家系でP148Hヘテロ接合変異
Saethre-Chotzen syndrome	Saethre-Chotzen症候群	AD	101400	7p21.1	*TWIST1*	TWIST	

グループ / 疾患名(原文)	グループ / 疾患名(和訳)	遺伝形式	MIM番号	遺伝子座	遺伝子	タンパク	注釈
Shprintzen-Goldberg syndrome	Shprintzen-Goldberg症候群	AD	182212				*FBN1*変異を有する症例の報告あり
Baller-Gerold syndrome	Baller-Gerold症候群	AR	218600	8q24.3	*RECQL4*	RECQ Protein-like 4	すべてのBaller-Gerold症候群が*RECQL4*変異では説明できないかもしれない
Carpenter syndrome	Carpenter症候群	AR	201000		*RAB23*		

グループ25のCole-Carpenter症候群, グループ32のCDAGS症候群, グループ34の頭蓋前頭鼻症候群も参照.

34. Dysostoses with predominant craniofacial involvement	**34. 頭蓋顔面骨罹患を主とする異骨症**						
Mandibulo-facial dysostosis (Treacher Collins, Franceschetti-Klein)	下顎・顔面異骨症 (Treacher Collins, Franceschetti-Klein)	AD	154500	5q32	*TCOF1*	Treacher Collins-Franceschetti syndrome 1	
Mandibulo-facial dysostosis (Treacher-Collins, Franceschetti-Klein)	下顎・顔面異骨症(Treacher Collins, Franceschetti-Klein)	AD	154500	13q12.2	*POLR1D*	Polymerase (RNA) I polypeptide D	
Mandibulo-facial dysostosis (Treacher-Collins, Franceschetti-Klein)	下顎・顔面異骨症 (Treacher Collins, Franceschetti-Klein)	AR	154500	6p21.1	*POLR1C*	Polymerase (RNA) I polypeptide C	
Oral-facial-digital syndrome type I (OFD1)	口・顔面・指症候群1型 (OFD1)	XLR	311200	Xp22.3	*CXORF5*	chr. X open reading frame 5	
Weyer acrofacial (acrodental) dysostosis	Weyer先端顔面 (先端歯) 異骨症	AD	193530	4p16	*EVC1*	Ellis-van Creveld 1 protein	
Endocrine-cerebro-osteodysplasia (ECO)	内分泌・脳・骨異形成症 (ECO)	AR	612651	6p12.3	*ICK*	Intestinal cell kinase	
Craniofrontonasal syndrome	頭蓋前頭鼻症候群	XLD	304110	Xq13.1	*EFNB1*	Ephrin B1	
Frontonasal dysplasia, type 1	前頭鼻異形成症1型	AR	136760	1p13.3	*ALX3*	Aristaless-like-3	
Frontonasal dysplasia, type 2	前頭鼻異形成症2型	AR	613451	11p11.2	*ALX4*	Aristaless-like-4	
Frontonasal dysplasia, type 3	前頭鼻異形成症3型	AR	613456	12q21.3	*ALX1*	Aristaless-like 1	
Hemifacial microsomia	片側顔面形成不全症	SP/AD					Goldenhar症候群と眼・耳・脊椎スペクトラムを含む;おそらく遺伝的異質性を有する
Miller syndrome (postaxial acrofacial dysostosis)	Miller症候群 (軸後性先端顔面異骨症)	AR	263750	16q22	*DHODH*	Dihydroorotate dehydrogenase	
Acrofacial dysostosis, Nager type	先端顔面異骨症, Nager型	AD/AR	154400				
Acrofacial dysostosis, Rodriguez type	先端顔面異骨症, Rodriguez型	AR	201170				

短肋骨異形成症グループの口・顔面・指症候群4型も参照.

35. Dysostoses with predominant vertebral with and without costal involvement	**35. 脊椎罹患(肋骨異常を伴う/伴わない)を主とする異骨症**						
Currarino triad	Currarino三徴症	AD	176450	7q36	*HLXB9*	Homeobox gene HB9	
Spondylocostal dysostosis type 1 (SCD1)	脊椎肋骨異骨症1型 (SCD1)	AR	277300	19q13	*Dll3*	Delta-like 3	
Spondylocostal dysostosis type 2 (SCD2)	脊椎肋骨異骨症2型 (SCD2)	AR	608681	15q26	*MESP2*	Mesoderm posterior (expressed in) 2	
Spondylocostal dysostosis type 3 (SCD3)	脊椎肋骨異骨症3型 (SCD3)	AR?	609813	7p22	*LFNG*	Lunatic fringe	
Spondylocostal dysostosis type 4 (SCD4)	脊椎肋骨異骨症4型 (SCD4)	AR		17p13.1	*HES7*	Hairy-and-enhancer-of-split-7	
Spondylothoracic dysostosis	脊椎胸郭異骨症	AR		15q26	*MESP2*	Mesoderm posterior (expressed in) 2	JarchoとLevinにより最初に記述された病態を含む
Klippel-Feil anomaly with laryngeal malformation	咽頭形態異常を伴うKlippel-Feil異常	AD	148900	8q22.1	*GDF6*	Growth and differentiation factor 6	優性脊椎胸郭異骨症における*GDF6*変異の役割は不明瞭
Spondylocostal/thoracic dysostosis, other forms	脊椎肋骨・胸郭異骨症, 他の型	AD/AR					上述のGDF6を参照
Cerebro-costo-mandibular syndrome (rib gap syndrome)	脳・肋骨・下顎症候群 (rib gap症候群)	AD/AR	117650				
Cerebro-costo-mandibular-like syndrome with vertebral defects	脊椎欠損を伴う脳・肋骨・下顎様症候群	AR	611209	17q25	*COG1*	Component of oligomeric Golgi complex 1	CDGタイプIIgとしても分類される
Diaphanospondylodysostosis	透明脊椎異骨症	AR	608022	7p14	*BMPER*	Bone morphogenetic protein-binding endothelial cell precursor-derived regulator	おそらく坐骨脊椎異骨症とオーバーラップする

グループ7の脊椎手根骨足根骨異形成症とグループ13の脊椎・骨幹端・巨大骨端異形成症も参照.

36. Patellar dysostoses	**36. 膝蓋骨異骨症**						
Ischiopatellar dysplasia (small patella syndrome)	坐骨膝蓋骨異形成症 (小膝蓋骨症候群)	AD	147891	17q21-q22	*TBX4*	T-box gene 4	

グループ / 疾患名(原文)	グループ / 疾患名(和訳)	遺伝形式	MIM番号	遺伝子座	遺伝子	タンパク	注釈
Small patella - like syndrome with clubfoot	内反足を伴う小膝蓋骨様症候群	AD		5q31	*PITX1*	Paired-like homeodomain transcription factor 1 (pituitary homeobox 1)	単独優性家族性内反足を含む
Nail-patella syndrome	爪・膝蓋骨症候群	AD	161200	9q34.1	*LMX1B*	LIM homeobox transcription factor 1	
Genitopatellar syndrome	性器膝蓋骨症候群	AR?	606170				
Ear-patella-short stature syndrome (Meier-	耳・膝蓋骨・低身長症候群 (Meier-Gorlin)	AR	224690				

屈曲肢異形成症の軽症型としての坐骨・恥骨・膝蓋骨異形成症と同様, 膝蓋骨異常を伴う病態の多発性骨端異形成症グループを参照.

37. Brachydactylies (with or without extraskeletal manifestations) **37. 短指症(骨外形態異常を伴う/伴わない)**

Brachydactyly type A1	短指症A1型	AD	112500	2q35-36	*IHH*	Indian Hedgehog	
Brachydactyly type A1	短指症A1型	AD		5p31			
Brachydactyly type A2	短指症A2型	AD	112600	4q23	*BMPR1B*	Bone morphogenetic protein	
Brachydactyly type A2	短指症A2型	AD	112600		*BMP2*	Bone morphogenetic protein type 2	
Brachydactyly type A2	短指症A2型	AD	112600	20q11.2	*GDF5*	Growth and differentiation factor 5	
Brachydactyly type A3	短指症A3型	AD	112700				
Brachydactyly type B	短指症B型	AD	113000	9q22	*ROR2*	Receptor tyrosine kinase-like orphan receptor 2	Robinow症候群/COVESDEMを参照
Brachydactyly type B2	短指症B2型	AD	611377	17q	*NOG*	Noggin	
Brachydactyly type C	短指症C型	AD, AR	113100	20q11.2	*GDF5*	Growth and differentiation factor 5	ASPED(グループ15)と他のGDF5異常症を参照
Brachydactyly type D	短指症D型	AD	113200	2q31	*HOXD13*	Homeobox D13	
Brachydactyly type E	短指症E型	AD	113300	12p11.22	*PTHLH*	Parathyroid hormone-like hormone (parathyroid hormone related peptide, PTHRP)	
Brachydactyly type E	短指症E型	AD	113300	2q31	*HOXD13*	Homeobox D13	
Brachydactyly - mental retardation syndrome	短指症・精神遅滞症候群	AD	600430	2q37.3	*HDAC4*	Histone deacetylase 4	隣接遺伝子に小欠失を有する(2q37欠損症候群)症例もある
Hyperphosphatasia with mental retardation, brachytelephalangy, and distinct face	精神遅滞, 末節骨短縮および特徴的な顔貌を伴う高フォスファターゼ症	AR		1p36.11	*PIGV*	Phosphatidylinositol-glycan biosynthesis class V protein (GPI mannosyltransferase 2)	Mabry症候群としても知られている
Brachydactyly-hypertension syndrome	短指症・高血圧症候群 (Bilginturian)	AD	112410	12p12.2-			おそらくPTHLH
Brachydactyly with anonychia (Cooks syndrome)	爪欠損を伴う短指症 (Cooks症候群)	AD	106995	17q24.3	*SOX9*		調節変異
Microcephaly-oculo-digito-esophageal-duodenal syndrome (Feingold syndrome)	小頭・眼・指・食道・十二指腸症候群 (Feingold症候群)	AD	164280	2p24.1	*MYCN*	nMYC oncogene	
Hand-foot-genital syndrome	手・足・性器症候群	AD	140000	7p14.2	*HOXA13*	Homeobox A13	
Brachydactyly with elbow dysplasia (Liebenberg syndrome)	肘異形成を伴う短指症 (Liebenberg症候群)	AD	186550				
Keutel syndrome	Keutel症候群	AR	245150	12p13.1-	*MGP*	Matrix Gla protein	
Albright hereditary osteodystrophy (AHO)	Albright遺伝性骨異栄養症 (AHO)	AD	103580	20q13	*GNAS1*	Guanine nucleotide binding protein of adenylate cyclase – subunit	グループ29の線維性骨異形成症, 多骨性および進行性骨性異形成症を参照
Rubinstein-Taybi syndrome	Rubinstein-Taybi症候群	AD	180849	16p13.3	*CREBBP*	CREB-Binding Protein	
Rubinstein-Taybi syndrome	Rubinstein-Taybi症候群	AD	180849	22q13	*EP300*	E1A-Binding Protein, 300-KD	
Catel-Manzke syndrome	Catel-Manzke症候群	XLR?	302380				
Brachydactyly, Temtamy type	短指症, Temtamy型	AR	605282				
Christian type brachydactyly	Christian型短指症	AD	112450				
Coffin-Siris syndrome	Coffin-Siris症候群	AR	135900				
Mononen type brachydactyly	Mononen型短指症	XLD?	301940				
Poland anomaly	Poland異常	SP	173800				

末節骨短縮型点状軟骨異形成症と同様, グループ20の短指症を伴う他の病態を参照.

38. Limb hypoplasia – reduction defects group **38. 四肢低形成/欠失グループ**

グループ / 疾患名（原文）	グループ / 疾患名（和訳）	遺伝形式	MIM番号	遺伝子座	遺伝子	タンパク	注釈
Ulnar-mammary syndrome	尺骨・乳房症候群	AD	181450		*TBX3*	T-box gene 3	
de Lange syndrome	de Lange症候群	AD	122470	5p13.1	*NIPBL*	Nipped-B-like	
Fanconi anemia *(see note below)*	Fanconi貧血（下の注を参照）	AR	227650	(several)	*(several)*		いくつかの関連グループと遺伝子
Thrombocytopenia-absent radius (TAR)	血小板減少症・橈骨欠損（TAR）	AR?/AD?	274000	1q21.1	*(several)*		1q21.1の小欠失
Thrombocythemia with distal limb defects	四肢遠位欠損を伴う血小板増加症	AD		3q27	*THPO*	Thrombopoietin	四肢遠位欠損は血管閉塞の結果とされる
Holt-Oram syndrome	Holt–Oram症候群	AD	142900	12q24.1	*TBX5*	T-box gene 5	
Okihiro syndrome (Duane – radial ray anomaly)	Okihiro症候群（Duane–橈骨列異常）	AD	607323	20q13	*SALL4*	SAL-like 4	
Cousin syndrome	Cousin症候群	AR	260660	1p13	*TBX15*	T-box gene 15	
Roberts syndrome	Roberts症候群	AR	268300	8p21.1	*ESCO2*	Homolog of establishment of cohesion - 2	
Split-hand-foot malformation with long bone deficiency (SHFLD1)	長官骨形成障害を伴う裂手・裂足形態異常（SHFLD1）	AD	119100	1q42.2-q43			
Split-hand-foot malformation with long bone deficiency (SHFLD2)	長官骨形成障害を伴う裂手・裂足形態異常（SHFLD2）	AD	610685	6q14.1			
Split-hand-foot malformation with long bone deficiency (SHFLD3)	長官骨形成障害を伴う裂手・裂足形態異常（SHFLD3）	AD	612576	17p13.1			
Tibial hemimelia	脛骨欠損	AR	275220				
Tibial hemimelia-polysyndactyly-triphalangeal	脛骨欠損・多合指症・母指三指節症	AD	188770				
Acheiropodia	欠手足症	AR	200500	7q36	*LMBR1*	Putative receptor protein	LMBR1の部分欠失がソニックヘッジホック（SHH）の発現に影響を与える
Tetra-amelia	無四肢症	XL	301090				
Tetra-amelia	無四肢症	AR	273395	17q21	*WNT3*	Wingless-type MMTV integration site family, member 3	
Ankyloblepharon-ectodermal dysplasia-cleft lip/palate (AEC)	眼瞼癒着・外胚葉異形成・口唇口蓋裂症候群（AEC）	AD	106260	3q27	*P63 (TP63)*	Tumor protein p63	
Ectrodactyly-ectodermal dysplasia cleft-palate syndrome Type 3 (EEC3)	欠指・外胚葉異形成・口蓋裂症候群3型（EEC3）	AD	604292	3q27	*P63 (TP63)*	Tumor protein p63	
Ectrodactyly-ectodermal dysplasia cleft-palate syndrome type 1 (EEC1)	欠指・外胚葉異形成・口蓋裂症候群1型（EEC1）	AD	129900	7q11.2-12.3			
Ectrodactyly-ectodermal dysplasia-macular dystrophy syndrome (EEM)	欠指・外胚葉異形成・黄斑ジストロフィ（EEM）	AR	225280	16q22	*CDH3*	Cadherin 3	
Limb-mammary syndrome (including ADULT syndrome)	四肢・乳房症候群（ADULT症候群を含む）	AD	603273	3q27	*P63 (TP63)*	Tumor protein p63	
Split hand-foot malformation, isolated form, type 4 (SHFM4)	単独型裂手・裂足形態異常4型（SHFM4）	AD	605289	3q27	*P63 (TP63)*	Tumor protein p63	
Split hand-foot malformation, isolated form, type 1 (SHFM1)	単独型裂手・裂足形態異常1型（SHFM）	AD	183600	7q21.3-22.1			
Split hand-foot Malformation, isolated form, type 2 (SHFM2)	単独型裂手・裂足形態異常2型（SHFM2）	XL	313350	Xq26			
Split hand-foot malformation, isolated form, type 3 (SHFM3)	単独型裂手・裂足形態異常3型（SHFM3）	AD	600095	10q24	*FBXW4*	Dactylin	
Split hand-foot malformation, isolated form, type 5 (SHFM5)	単独型裂手・裂足形態異常5型（SHFM5）	AD	606708	2q31			
Al-Awadi Raas-Rothschild limb-pelvis hypoplasia-aplasia	Al–Awadi Raas–Rothschild四肢・骨盤低（無）形成	AR	276820	3p25	*WNT7A*	Wingless-type MMTV integration site family, member 7A	
Fuhrmann syndrome	Fuhrmann症候群	AR	228930	3p25	*WNT7A*	Wingless-type MMTV integration site family, member 7A	
RAPADILINO syndrome	RAPADILINO症候群	AR	266280	8q24.3	*RECQL4*	RECQ protein-like 4	
Adams-Oliver syndrome	Adams–Oliver症候群	AD/AR	100300				
Femoral hypoplasia-unusual face syndrome (FHUFS)	大腿骨低形成・異常顔貌症候群（FHUFS）	SP/AD?	134780				いくつかの表現形は大腿骨・腓骨・尺骨症候群（下記）と重複
Femur-fibula-ulna syndrome (FFU)	大腿骨・腓骨・尺骨症候群（FFU）	SP?	228200				
Hanhart syndrome (Hypoglossia-hypodactylia)	Hanhart症候群（舌低形成・指低形成）	AD	103300				
Scapulo-iliac dysplasia (Kosenow)	肩甲骨・腸骨異形成症（Kosenow）	AD	169550				

グループ / 疾患名（原文）	グループ / 疾患名（和訳）	遺伝形式	MIM番号	遺伝子座	遺伝子	タンパク	注釈
注）ファンコニー貧血とその相補群の特に複雑な遺伝子基盤は知られているがこの分類表ではさらに載せていない．MIMまたは他の特別なレヴューを参考にすること．グループ21のCHILD症候群や中間肢・遠位中間肢異形成症も参照．							
39. Polydactyly-Syndactyly-Triphalangism	**39. 多指・合指・母指三指節症グループ**						
Preaxial polydactyly type 1 (PPD1)	軸前性多指症1型（PPD1）	AD	174400	7q36	*SHH*	Sonic Hedgehog	調節変異
Preaxial polydactyly type 1 (PPD1)	軸前性多指症1型（PPD1）	AD	174400				いくつかの例ではSHHと関連していない
Preaxial polydactyly type 2 (PPD2)/ Triphalangeal thumb (TPT)	軸前性多指症2型（PPD2）/母指三指節症（TPT）	AD	174500	7q36	*SHH*	Sonic Hedgehog	調節変異
Preaxial polydactyly type 3 (PPD3)	軸前性多指症3型（PPD3）	AD	174600				
Preaxial polydactyly type 4 (PPD4)	軸前性多指症4型（PPD4）	AD	174700	7p13	*GLI3*	Gli-Kruppel Family Member 3	
Greig cephalopolysyndactyly syndrome	Greig頭多合指症候群	AD	175700	7p13	*GLI3*	Gli-Kruppel Family Member 3	
Pallister-Hall syndrome	Pallister-Hall症候群	AD	146510	7p13	*GLI3*	Gli-Kruppel Family Member 3	
Synpolydactyly (complex, fibulin1 - associated)	多合指症（fibulin1関連複合）	AD	608180	22q13.3	*FBLN1*	Fibulin 1	
Synpolydactyly	多合指症	AD	186000	2q31	*HOXD13*	Homeobox D13	
Townes-Brocks syndrome (Renal-Ear-Anal-Radial syndrome)	Townes-Brocks症候群（腎・耳・肛門・橈骨症候群）	AD	107480	16q12.1	*SALL1*	SAL-like 1	
Lacrimo-auriculo-dento-digital syndrome (LADD)	涙・耳・歯・指症候群（LADD）	AD	149730	10q26.12	*FGFR2*	Fibroblast growth factor receptor 2	
Lacrimo-auriculo-dento-digital syndrome (LADD)	涙・耳・歯・指症候群（LADD）	AD	149730	4p16.3	*FGFR3*	Fibroblast growth factor receptor 3	
Lacrimo-auriculo-dento-digital syndrome (LADD)	涙・耳・歯・指症候群（LADD）	AD	149730	5p13-p12	*FGF10*	Fibroblast growth factor 10	
Acrocallosal syndrome	先端脳梁症候群	AR	200990	7p13			
Acro-pectoral syndrome	先端・胸症候群	AD	605967	7q36			
Acro-pectoro-vertebral dysplasia (F-syndrome)	先端・胸・椎体異形成症（F症候群）	AD	102510	2q36			
Mirror-image polydactyly of hands and feet (Laurin-Sandrow syndrome)	鏡面像多指趾症（Laurin-Sandrow症候群）	AD	135750	7q36	*SHH*	Sonic Hedgehog	
Mirror-image polydactyly of hands and feet (Laurin-Sandrow syndrome)	鏡面像多指趾症（Laurin-Sandrow症候群）						SHHと非連鎖
Cenani-Lenz syndactyly	Cenani-Lenz 合指症	AR	212780	11p11.2	*LRP4*	low density lipoprotein receptor-	
Cenani-Lenz like syndactyly	Cenani-Lenz様合指症	SP (AD?)		15q13-q14	*GREM1, FMN1*	Gremlin 1, Formin 1	両方の遺伝子座の単一対立遺伝子重複（これまでに1例のみ）
Oligosyndactyly, radio-ulnar synostosis, hearing loss and renal defects syndrome	乏合指・橈尺骨癒合・難聴・無腎症候群	SP (AR?)		15q13-q14	*FMN1*	Formin 1	欠失
Syndactyly, Malik-Percin type	合指症, Malik-Percin型	AD	609432	17p13.3			
STAR syndrome (syndactyly of toes, telecanthus, ano- and renal malformations)	STAR症候群（合趾症・眼角隔離症・肛門・腎形態異常）	XL	300707	Xq28	*FAM58A*		
Syndactyly type 1 (III-IV)	合指症1型（III-IV）	AD	185900	2q34-36			
Syndactyly type 3 (IV-V)	合指症3型（IV-V）	AD	185900	6q21-23	*GJA1*		
Syndactyly type 4 (I-V) Haas type	合指症4型（I-V）Haas型	AD	186200	7q36	*SHH*	Sonic Hedgehog	
Syndactyly type 5 (syndactyly with metacarpal and metatarsal fusion)	合指症5型（中手骨・中足骨癒合を伴う合指症）	AD	186300	2q31	*HOXD13*		
Syndactyly with craniosynostosis (Philadelphia	頭蓋骨癒合症を伴う合指症（Philadelphia型）	AD	601222	2q35-36.3			
Syndactyly with microcephaly and mental retardation (Filippi syndrome)	小頭症・精神発達遅滞を伴う合指症（Filippi症候群）	AR	272440				
Meckel syndrome type 1	Meckel症候群1型	AR	249000	17q23	*MKS1*		
Meckel syndrome type 2	Meckel症候群2型	AR	603194	11q			
Meckel syndrome type 3	Meckel症候群3型	AR	607361	8q21	*TMEM67*		
Meckel syndrome type 4	Meckel症候群4型	AR	611134	12q	*CEP290*		
Meckel syndrome type 5	Meckel症候群5型	AR	611561	16q12.1	*RPGRIP1L*		
Meckel syndrome type 6	Meckel症候群6型	AR	612284	4p15	*CC2D2A*		
注）Smith-Lemli-Opitz症候群は多指症・合指症を合併する．短肋骨多指症候群グループも参照．							
40. Defects in joint formation and synostoses	**40. 関節形成不全・骨癒合症**						
Multiple synostoses syndrome type 1	多発性骨癒合症候群1型	AD	186500	17q22	*NOG*	Noggin	

グループ / 疾患名（原文）	グループ / 疾患名（和訳）	遺伝形式	MIM番号	遺伝子座	遺伝子	タンパク	注釈
Multiple synostoses syndrome type 2	多発性骨癒合症候群2型	AD	186500	20q11.2	*GDF5*	Growth and differentiation factor 5	
Multiple synostoses syndrome type 3	多発性骨癒合症候群3型	AD	612961	13q11-q12	*FGF9*		
Proximal symphalangism type 1	近位指節癒合症1型	AD	185800	17q22	*NOG*	Noggin	
Proximal symphalangism type 2	近位指節癒合症2型	AD	185800	20q11.2	*GDF5*	Growth and differentiation factor 5	
Radio-ulnar synostosis with amegakaryocytic thrombocytopenia	無巨核球性血小板減少を伴う橈尺骨癒合症	AD	605432	7p15-14.2	*HOXA11*	Homeobox A11	

脊椎・手根骨・足根骨異形成症，先端癒合症を伴う中間肢異形成症，他も参照.